UNIVERSITÀ
DEGLI STUDI
DI PADOVA

UNIVERSITA' DEGLI STUDI DI PADOVA

Sede Amministrativa: Università degli Studi di Padova
Dipartimento di BIOLOGIA

SCUOLA DI DOTTORATO DI RICERCA IN: BIOLOGIA E MEDICINA DELLA
RIGENERAZIONE
INDIRIZZO: INGEGNERIA DEI TESSUTI E DEI TRAPIANTI
CICLO XXIII

LOCAL SYNTHESIS AND EFFECT OF SEX STEROIDS IN HUMAN SKIN AND THE HAIR FOLLICLE AND HORMONAL EFFECTS ON THE WOUND HEALING RESPONSE

Direttore della Scuola: Ch.mo Prof. Pier Paolo Parnigotto
Coordinatore d'indirizzo: Ch.mo Prof. Maria Teresa Conconi
Supervisore: Ch.mo Prof. Lorenzo Colombo
Supervisore estero: Dr. M.Julie Thornton
Correlatore: Dott.ssa Luisa Dalla Valle

Dottoranda: Elena Pomari

31 gennaio 2011

Index

Abbreviations

ANPTL4: angiopoietin like 4

bp: base pair

cDNA: complementary DNA

CXCL1: chemokine (C-X-C motif) ligand 1

Cy3: cyanine-3

Cy5: cyanine-5

DEX: dexamethasone

DF: dermal fibroblast

DHEA: dehydroepiandrosterone

DHEA-S: dehydroepiandrosterone-sulfate

DMEM: dulbecco's modified eagle medium

DMSO: dimethylsulfoxide

DNA: deoxyribonucleic acid

dNTP: deoxynucleotide triphosphate

DP: dermal papilla

DS: dermal sheath

DTT: dithiothreitol

EDTA: ethylenediaminetetraacetic acid

EK: epidermal keratinocyte

E2: 17ß-estradiol

FBS: fetal bovine serum

FCS: fetal calf serum

g: gravity force

HF: hair follicle

IPTG: isopropyl ß-D-1-thiogalactopyranoside

LMNB1: lamin b1

LOR: loricrin

$MgCl_2$: magnesium chloride

MIDAS: microarray data analysis system

mRNA: messenger ribonucleic acid

NaCl: sodium chloride

NaOH: sodium hydroxide

OATP2B1: organic anion transporting polypeptide 2B1

O.D.: optical density

PBS: phosphate buffered saline

PCR: polymerase chain reaction

RNA: ribonucleic acid

RNase: ribonuclease

RIN: RNA Integrity Number

rpm: rotations per minute

RPMI: roswell park memorial institute medium

RT: room temperature

RT-PCR: reverse transcription and polymerase chain reaction

S.E.M.: standard error of the mean

SD: standard deviation

SDS: sodium dodecyl sulfate

STS: steroid sulfatase

TAE: tris-Acetate-EDTA

Taq: thermos aquaticus

Tris: trishydroxymethylaminomethane

TST: testosterone

TXNIP: thioredoxin-interacting protein

X-Gal: (5-bromo-4-chloro-3-indolyl-beta-D-galactopyranoside

Abstract

Humans, as others mammals, are able to synthesize steroid hormones from endocrine organs, such as gonads, adrenal gland and placenta. The expression and activity of steroidogenic enzymes in peripheral tissues provide the intracrine production of active androgens and estrogens by transformation of adrenal precursor dehydroepiandrosterone (DHEA). Only human and primates are unique in having large amounts of the inactive adrenal DHEA and especially DHEA-sulfate (DHEA-S). However, adrenal secretion decreases from the age of 30 years in both sexes, thus potentially providing an explanation for part of the mechanisms involved in the pathogenesis of age-related conditions, such as skin aging. In this study, it was determined whether human skin expresses the enzymes required for the local biosynthesis of active sex steroid hormones. Specifically, biopsies of skin and hair follicles (HFs) were collected from female healthy donors, and cultured dermal fibroblasts (DFs) and cultured epidermal keratinocytes (EKs) were established from female and male healthy donors. The mRNA expression of seven key steroidogenic proteins (P450arom, P450scc, P450c17, STS, OATP2B1, 5α-reductase 1 and 5α-reductase 2), and the estrogen receptors (ERα and ERß) and the androgen receptor (AR) were investigated using RT-PCR and qRT-PCR. All samples produced PCR products of the expected size for P450scc, P450c17, STS and 5α-reductase 1. The mRNA expression of 5α-reductase 2 was detected only in HF. EK did not produce the transcript of P450arom and DF did not express OATP2B1. Both ERα and ERß were expressed in EK as well as in DF. In particular, EK showed to strongly express ERß compared to ERα. In contrast, ERα has been detected with higher expression than ERß in DF. Differences in estrogen receptors expression have been demonstrated also in human HFs that have showed strongly expressed ERß in comparison with ERα. On the other hand, all the samples showed AR expression. In order to the possibility of steroids metabolism, a gene array analysis was performed on whole transcriptome of

human HFs and cultured EKs after steroid treatment. Three different hormones were used for 24h of incubation: DHEA-S (10µM), testosterone (TST) (50nM) and 17ß-estradiol (E2) (1nM). The global mRNA expression profiling revealed changes in the expression of a large number of genes. In particular, interesting up-regulation of genes involved in inflammation, cell proliferation and differentiation and structural functions. The analysis on EKs was focused on four genes up-regulated with all three steroids investigated: *CXCL1*, *ANGPTL4*, *TXNIP*, and *LMNB1*. In addition, the *in vitro* scratch wound assay was used to determine the direct effects of E2, DHEA, DHEA-S and TST on the migration of mechanically wounded human DFs and EKs. All steroids stimulated cell migration, although both DHEA and TST were blocked by an aromatase inhibitor (Arimidex) and DHEA-S by the STS inhibitor. These results indicate an important role for local synthesis of E2 in skin from the circulating precursor DHEAS and expression of its action in the wound healing process. To verify the hypothesis of the local synthesis of E2, the activity of the aromatase, which is the enzyme that catalyzes the conversion of androgen to estrogen, was assessed in EKs and DFs using the tritiated water (^3H_2O) assay. Specifically, it was investigated whether the aromatase activity and mRNA expression were modulated in cultured skin cells in response to either dexamethasone or mechanical wounding. The analysis revealed that dexamethasone increased the activity and mRNA expression in particular in DFs, in contrast, the mechanically wounded showed in EKs an increase of the aromatase activity at 24h compared to the non-wounded confluent monolayer cells. All data suggest that human skin and individual cells as target and source of active androgens and estrogens. Further studies are required to understand the role of steroids in inflammation, proliferation and differentiation which have implications for hair growth, skin cancer, aging and wound-healing. In particular, a greater understanding of DHEA signalling may help develop wound-healing therapies, without the risks of estrogen therapy, benefiting the elderly and patients with impaired wound-healing.

Riassunto

Gli umani, come altri mammiferi, sintetizzano ormoni steroidei da organi endocrini come le gonadi, la surrenale e la placenta. L'espressione e attività di enzimi steroidogenici a livello di tessuti periferici provvedono alla formazione intracrina di androgeni ed estrogeni attivi a partire dal precursore deidroepiandrosterone (DHEA). Solamente umani ed alcuni primati secernono alti livelli di DHEA e DHEA-S. Tuttavia con l'età si presenta in entrambi i sessi una riduzione della secrezione adrenalica che si riflette in un notevole declino della produzione periferica di ormoni sessuali. Questa diminuita formazione è potenzialmente correlata alla patogenesi di malattie che incorrono con la vecchiaia tra cui anche alcune condizioni della pelle. Nel presente studio è stata valutata l'espressione dell'mRNA di sette proteine chiave della steroidogenesi (P450arom, P450scc, P450c17, STS, OATP2B1, 5α-riduttasi 1 e 5α-riduttasi 2), oltre che dei recettori di estrogeni (ERα e ERß) ed androgeni (AR), in biopsie di pelle e follicoli piliferi derivati da donatrici donne sane e in fibroblasti dermici e cheratinociti epidermici primari di donatori femmine e un maschio sempre sani. L'analisi condotta con RT-PCR e qRT-PCR ha rilevato in particolare che solo i follicoli esprimono 5α-riduttasi 2, i cheratinociti non presentano espressione dell'aromatasi (P450arom) e i fibroblasti non risultano esprimere il trasportatore OATP2B1. Dall'altra parte, entrambi i recettori ERα e ERß e quello per androgeni sono espressi nelle cellule della pelle e nei follicoli piliferi. In particolare ERß risulta con più forte espressione in cheratinociti e follicoli piliferi rispetto a ERα e il contrario in fibroblasti. In relazione quindi alla possibilità di una locale formazione ed azione di ormoni sessuali nella pelle, è stato investigato l'effetto *in vitro* di tre steroidi sull'espressione genica di follicoli piliferi e cheratinociti ottenuti da pelle facciale di donne sane. L'intero trascrittoma è stato analizzato dopo un'incubazione di 24 ore con DHEA-S (10μM), testosterone (TST) (50nM) e 17ß-estradiolo (E2) (1nM). In particolare sono state individuate modulazioni dell'espressione di geni coinvolti in funzioni

come infiammazione, proliferazione e differenziamento cellulare, e di struttura. L'analisi condotta su cheratinociti è stata focalizzata su quattro geni sovra-espressi da tutti e tre i diversi trattamenti steroidei: *CXCL1*, *ANGPTL4*, TXNPI e *LMNB1*. Dati gli effetti e funzioni implicati dagli ormoni in esame, è stato valutato *in vitro* l'effetto di E2, DHEA, DHEA-S e TST sulla migrazione di fibroblasti e cheratinociti mediante *scratch wound assay*. L'analisi ha rilevato l'accelerazione della migrazione di entrambi i tipi cellulari in presenza di tutti gli steroidi in esame. In particolare, la combinazione di un inibitore dell'aromatasi (Arimidex) e uno della steroide solfatasi (STX64) hanno determinato l'inibizione dell'effetto stimolatorio rispettivamente di DHEA e TST, e di DHEA-S. I risultati suggeriscono un importante ruolo della formazione locale di E2 nella pelle a partire dal precursore DHEA (-S) e della sua azione nel processo di *wound healing*. Per verificare tale ipotesi della sintesi locale di estradiolo, è stata investigata l'attività dell'enzima catalizzante la conversione di androgeno ad estrogeno, l'aromatasi. Le misurazioni dell'attività aromatasica sono state eseguite con il metodo dell'acqua triziata. Specificatamente, l'esame è stato condotto su fibroblasti e cheratinociti umani e individuando l'effetto su attività ed espressione dell'mRNA dell'enzima dopo trattamento con desametasone o eseguendo *mechanical scratch wound*. Nel primo caso, il desametasone ha indotto stimolazione sia di attività che di espressione del trascritto. Mentre nel secondo caso, è stato rilevato un incremento in cheratinociti dopo 24 ore dallo *scratch*. In generale questo studio suggerisce che la pelle umana, oltre che separatamente fibroblasti e cheratinociti, e follicolo pilifero, siano *target* e fonte degli ormoni sessuali. Ulteriori studi saranno necessari per comprendere il ruolo di estrogeni ed androgeni in meccanismi come infiammazione, proliferazione e differenziamento cellulare, che possono avere implicazioni nella crescita del pelo, cancro della pelle, invecchiamento e *wound healing*. In particolare, la comprensione del *signalling* di DHEA aiuterebbe lo sviluppo di terapie per il *wound healing* riducendo i rischi correlati alla somministrazione degli estrogeni.

1. Introduction

1.1 The Structure of Skin

In mammals, the skin is the largest organ of the integumentary system made up of multiple layers of ectodermal tissue. Mammalian skin is composed of three primary layers (Figure 1):

- the epidermis, which provides waterproofing and serves as a barrier;
- the dermis, which serves as a location for the appendages of skin;
- the hypodermis, which is subcutaneous adipose layer.

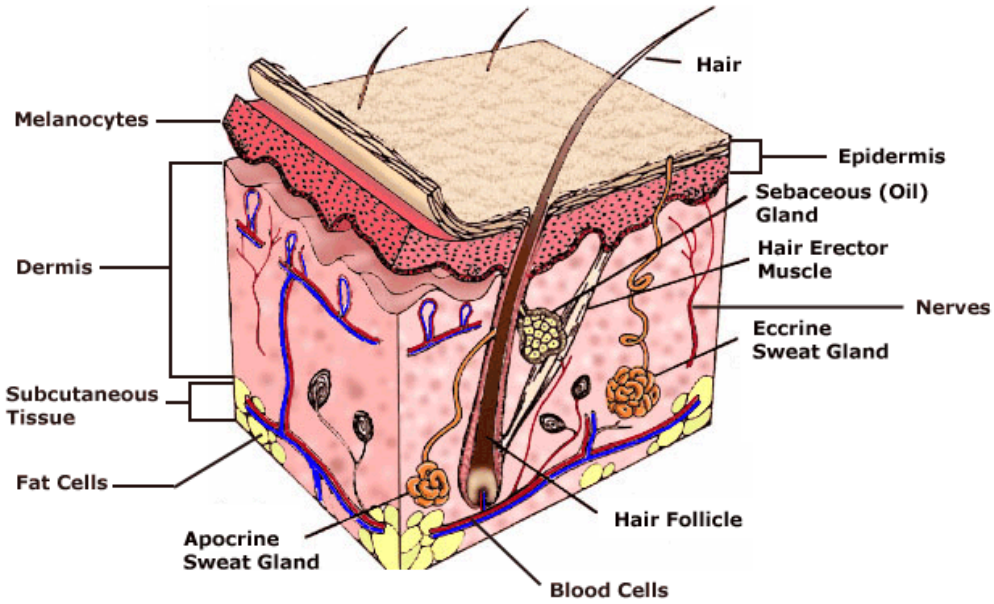

Figure 1. Structure of the skin

The image illustrates the structure of the skin, including the epidermis, dermis and skin appendages (taken from www.americanskin.org).

1.1.1 The Epidermis

The epidermis is a stratified keratinizing epithelium with a resistant surface that is interrupted by HFs and the pores of sweat glands. The physical barrier is localized primarily in the stratum corneum (Elias *et al.* 2003, Taylor, 2002). The epidermis is composed of five layers from deep to superficial: the stratum basale (the germinative layer of keratinocytes), the stratum spinosum, the stratum granulosum, the stratum lucidum and the stratum corneum (Figure 2). The stratum corneum consists of keratinocytes and acts as a barrier to the passage of water and solutes through the skin, defends against the penetration of microorganisms and of toxic substances, and protects against most mechanical injury caused by abrasion, friction, or arthropod bites (Marks, 1991). The epidermis is in a constant state of turnover with a continued epidermal growth and a high proliferative potential. The keratinocytes are the predominant cells within the epidermis and consist of three groups: epidermal stem cells, transit-amplifying cells and post-mitotic cells. Keratinocytes are composed mainly of filamentous proteins known as keratins (Proksch *et al*., 2008). The process of keratinisation (between 26 and 42 days in human skin) involves the detachment of post-mitotic cells from the basement membrane, moving from the basal to the spinous layer, undergoing a gradual transition through a range of histological appearances. Keratinocytes at the stratum basale are attached via hemidesmosomes to a basement membrane which separate them from the dermis. The basement membrane consists of type IV and type VII collagen, laminin and fibronectin (Kanitakis *et al.* 1998). The epidermis also contains populations of three types of dendritic cells: melanocytes, Langerhans cells, and Merkel cells. Melanocytes produce the pigment known as melanin (Fistarol *et al*., 2010). Langerhans cells are specialized cells of the immune system that present and respond to antigens coming in contact with the skin (Stoitzner *et al*., 2010). Merkel cells are neuroendocrine cutaneous cells and primarily localized in the basal layer of the epidermis; they are

concentrated in touch-sensitive areas in glabrous and hairy skin and in some mucosa (Boulais and Misery, 2007).

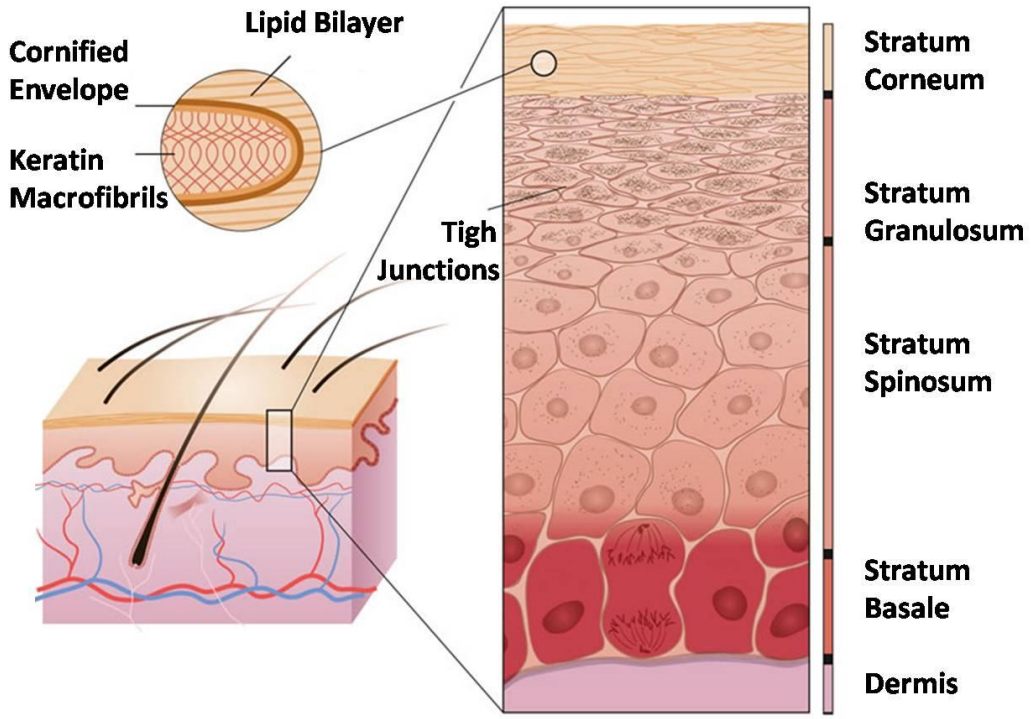

Figure 2. Structure of the epidermis

The image illustrates the layers of the epidermis with stratum corneum, stratum granulosum, stratum spinosum and stratum basale. The stratum lucidum is not seen in this picture (taken from www.genome.gov).

1.1.2 The Dermis

The dermis is a thick, dense fibroelastic connective tissue composed of collagen fibers, elastic fibers, and an interfibrillar gel composed of glycosaminoglycans, salts, and water. It varies in thickness in different parts of the body but is usually 2-4mm thick. The primary cells of the dermis are collagen-rich fibroblasts (Kollias, 1995; Shea and Parrish, 1991). Macrophages, mast cells and lymphocytes are also found within the dermis.

The dermis encloses blood vessels, nerves, sweat glands, and a pilosebaceous complex of HFs and sebaceous glands (Figure 1). The rich vascular supply of the skin is responsible for supplying the needs of the sweat glands, HFs, and rapidly multiplying epidermal cells in the stratum basale. The nerve supply of the skin is highly complex because the skin is a major sensory surface that contains varied types of receptors sending signals to the central nervous system about the external environment and the internal state of the skin (Lynn, 1991; Chu *et al.,* 2003). Numerous hairs, which grow from HFs located in the dermis, are associated with mechanoreceptors and sebaceous glands. Hair performs a range of functions from insulation, to protection against the sun, enhancement of cutaneous sensation to communication of emotion (through piloerection), and ornamentation (Schneider *et al*., 2009).

1.2 The Function of the Skin

The most important function of the skin is to form an effective barrier between the external and internal environment. It also plays a role in sensation, thermoregulation, immunity, and metabolism.

1.2.1 Skin as a physical barrier

The skin forms an effective barrier between the organism and the environment preventing invasion of pathogens and fending off chemical and physical assaults, as well as the unregulated loss of water and solutes (Proksch *et al*., 2008). The presence of a cornified envelope and structural proteins of the stratum corneum makes the epidermis a very durable tissue. Furthermore, melanocytes within the epidermis provide protection against ultraviolet radiation (UVR) by the production of melanin, which will absorb the UVR and reduce the risk of DNA damage (Agar and Young, 2005).

1.2.2 Sensation in the skin

The skin has a variety of nerve receptors and free nerve endings, which can detect pressure, touch, vibration, pain and temperature. Meissner's corpuscles and Merkel's discs are touch receptors found in large numbers in the finger tips, lips and other areas where touch sensation is highly developed. Pacinian corpuscles lie immediately below the skin and are important in detecting rapid movement as in tissue vibration (Guyton, 1996).

1.2.3 Thermoregulation in the skin

The skin plays an essential role in the control of body temperature within a narrow range. This is a complex system that involves the blood vessels, sweat glands and hair (Shibasaki and Crandall, 2010). If core temperature raises, vasodilation increases the blood flow to the skin. Vasoconstriction, in a cold situation leads to the opposite effect. Shivering is another important mechanism to maintain body temperature by increasing heat production. This is usually associated with piloerection. An increasing body temperature also stimulates the sympathetic nervous system to activate the sweat glands. This increases sweat production, mainly from the eccrine glands, and leads to cooling by evaporation (Guyton, 1996).

1.2.4 Immunology in the skin

The skin is one of the primary sites for the protection against pathogenic micro-organisms. Under normal conditions, the protection of the stratum corneum prevents potential pathogens from entering the body, however this is not always possible after physical injury. Langerhans cells within the epidermis are the principal antigen-presenting cells in the skin and provide a first line of defence against invading pathogens. They have the ability to process and present antigens to T lymphocytes thus initiating an antigen specific response (Wood and Bladon, 1985). Macrophages and mast cells

found in the dermis can also phagocytose bacteria or foreign material and help induce an inflammatory response (Adamson, 2009). In addition, keratinocytes play a role in immune response by secreting immunomodulatory cytokines which can regulate many immune responses (Nestle *et al*., 2009).

1.2.5 Metabolism in the skin

The skin plays an important role in Vitamin D production, a hormone essential in calcium metabolism and bone formation. Cholecalciferol is formed in the skin due to the effect of UVR from the sun (Bikle, 2010). In addition, the skin plays a role in the production of androgens and estrogens by the action of the enzymes 5α-reductase and aromatase, respectively (Chen *et al.,* 2002).

1.3 Embryogenesis of human skin

In humans, individual epidermis and dermis is formed within the first two weeks of embryonic life. Thereafter, they continue to develop at dissimilar rates with the dermis lagging behind the epidermis (Hamilton *et al.*, 1972).

1.3.1 The Epidermis

The epidermis is largely formed from the ectoderm. The primitive epidermis is established within seven to eight days and begins to develop its specific features over the next 20 days. It is composed of a basal epidermis layer and an outer layer known as periderm. The basal layer forms the epidermis and epidermal derived appendages proper and differentiates in a sequence similar to that of the adult epidermis (Goldsmith, 1983). Initially, the keratinocytes are loosely attached but, as a second layer develops, they become tightly integrated. By the second trimester further intermediate

layers start to form and these gradually differentiate to become the granular and spinous layers. The first stratum corneum is established towards the end of the second trimester and progressively increases in thickness up until birth. This process of differentiation within layers occurs at different rates in distinct regions of the body. At birth it is a thick as adult stratum corneum. The periderm gradually becomes eratinocyt with the stratum corneum and is then desquamated into the amniotic fluid and together with sebaceous secretions and desquamated stratum corneal cells forms the vernix caseosa (Hamilton, 1972). Human melanocytes develop from the neural crest and migrate to the skin at the second month of gestation. By the third to fifth months they have penetrated the epidermis and progressively increase in number. They are not thought to become functional until the second trimester. Langerhans cells are derived from bone marrow and enter the epidermis toward the end of the first trimester. They are structurally identical to the adult cell. Merkel cells are the last to appear in the epidermis between four and six months. They again have similar morphology to the adult cell (Goldsmith, 1983). During development the human epidermis is closely associated with a basal lamina, although initially it lacks the junctions and contouring of the mature epidermis. As eratinocytes differentiation arises, hemidesmosomes form and gradually assume the structure and number found in adult human skin. Dermal-epidermal ridges start to develop as the skin appendages push downwards from the epidermis to enter the dermis. This occurs first in hair-bearing areas and with gradual development elsewhere up until birth.

1.3.2 The Dermis

The dermis derives from mesenchimal cells of the superficial dermatome segments of somite mesoderm. During the first two months of gestation, the human dermis consists of a network of stellate, mesenchymal cells. The outer layer of the dermis proliferates during the third month of gestation forming the dermal papillae (DP) that protrude into the overlying epidermis. During

the fourth and fifth months the amount of collagen increases and it becomes possible to distinguish between the papillary and reticular dermis. Elastic fibres are ecognized from around the sixth month but this structure also remains immature up until the first or second year of life (Goldsmith, 1983). Therefore at birth, unlike the epidermis, the dermis is not fully developed and thickens progressively throughout infancy and childhood (Champion, 1970).

1.4 Structure and function of hair follicle

In mammals, HFs produce hairs that exert a wide number of functions including thermoregulation, sensory activity, protection against environmental trauma, social communication and mimicry (Botchkarev and Paus, 2003). The adult human body is covered with HFs, except lips, palms of the hands and soles of the feet. The scalp, eyebrows and lashes consist of long, thick and pigmented terminal hair shafts, whereas the rest is covered with short, thin and often unpigmented vellus hairs (Krause and Kerstin, 2006). There are essentially three types of hair: lanugo, vellus and terminal hair. Lanugo hair is very fine, wispy, unpigmented hair and found on the fetus. It is shed inside the womb at about the seventh or eighth month of pregnancy, or soon after birth. Vellus hair covers the body surface after birth and is fine, soft, velvety and unpigmented. Terminal hair is long, coarse and pigmented and can grow to long length (Spearman, 1977). Hair is harboured into the HF, a complex miniorgan of the skin, which constitutes the pilosebaceous unit together with its associated structures, the sebaceous gland, the apocrine gland and the arrector pili muscle (Figure 3 and 4). The mature HF can be divided into an upper part and a lower part, which is continuously emodeled in each hair cycle (Figure 4). The upper part of the HF consists of the infundibulum, which is the opening of the hair canal to the skin surface and the isthmus. The lower and cycling part represents the bulb (Figure 3). At the proximal end, the infundibulum joins the isthmus region of the outer root sheath, where the arrector pili muscle is inserted. The lower

isthmus also harbours epithelial and melanocytic HF stem cells in the called bulge region. Within the hair bulb there is a population of cells with high proliferation rate: the keratinocytes of the hair matrix. These can give rise to the various cell lineages of the hair shaft and the inner root sheath (IRS), while the outer root (ORS) sheath, hair matrix and hair shaft derive from epithelial stem cells in the bulge area, functioning as a pluripotent epithelial stem cell population for the skin. The bulge stem cells posses high proliferative capacity and multipotency to regenerate not only the hair but also sebaceous gland and epidermis (Ohyama, 2007). Mesenchymal stem cells within the tissue sheath serve as a recruitment pool for new DP cells. Apart from mesenchymal stem cells, the HF also contains mast cell precursors and neuronal stem cells, the latter of which can develop into neurons and blood vessels. The large numbers of stem cells make the HF a fascinating organ in the field of stem cell biology (Krause and Kerstin, 2006).

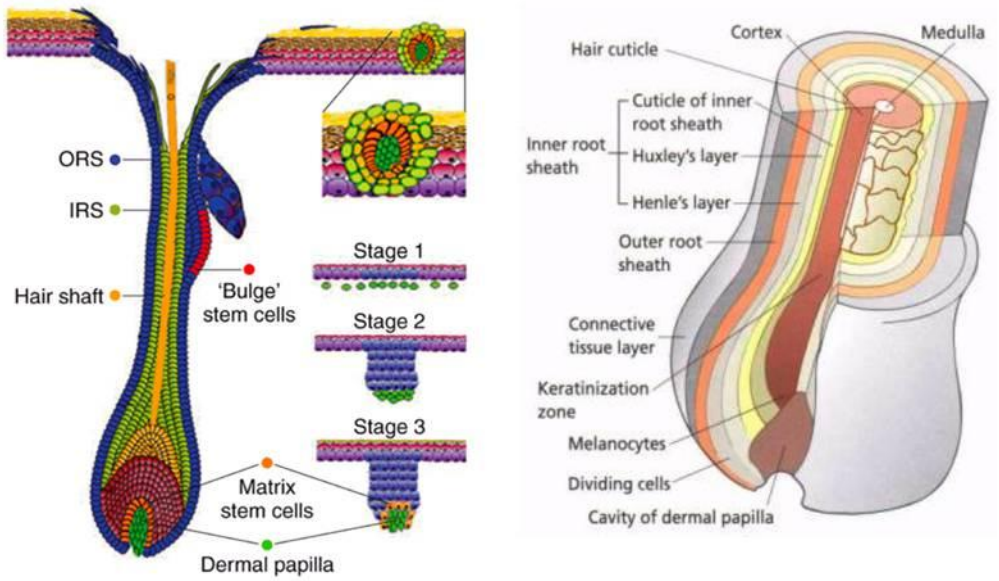

A **B**

Figure 3. The structure of the HF

A mature HF in the anagen and growth phase with its concentric layers of the outer root sheath (ORS, blue), inner root sheath (IRS, drab green) and hair shaft (tan). The IRS and hair shaft are derived from matrix stem cells (orange) at the base of the hair bulb in contact with the DP (bright green). Matrix stem cells are a distinct population from the stem cells of the follicular bulge (red) that regenerate the follicle during the hair cycle. Three successive stages in the development of the follicle are diagrammed at lower right (adapted from Morgan, 2006). **B)** The structure of the hair bulb (adapted from www.texascollaborative.org)

1.4.1 The hair growth cycle

HF generates hairs in a cyclical mechanism through phases anagen, catagen, telogen and exogen. The duration of anagen, the period of hair growth, varies from weeks to several years on different body sites and determines the length of the hair shaft (Krause and Kerstin, 2006). After anagen, the follicle enters a stage of involution (catagen) and then a stage of rest (telogen). The hair remains anchored in the follicle until it is shed during exogen (Figure 4). During anagen, proliferating progenitor cells, derived from HF stem cells, proliferate and differentiate into different cell lines to (re)generate a new hair. This proliferation results in the elongation of the hair shaft. The anagen period ends with a highly controlled involution of the HF. This process, called catagen, consists of cessation of melanin production, apoptosis and terminal differentiation. In telogen, the DP comes to rest immediately below the bulge, which allows direct interactions between bulge stem cells and the DP. The DP is essential for stem cell activation and initiation of a new hair cycle. As the new hair grows in, the old hair is shed during exogen. The duration of each stage varies depending on the type, site, and genetic programming of the follicle (Costarelis, 2006).

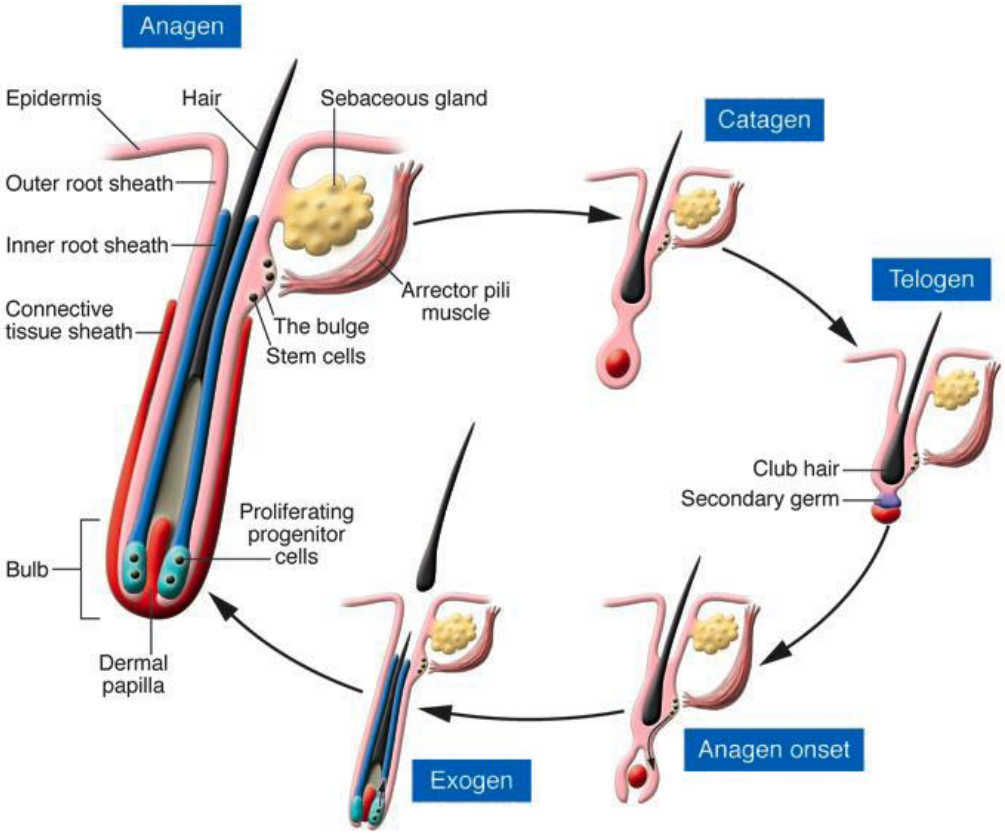

Figure 4. HF cycle

Cyclical changes in the HF growth are divided into different phases: anagen, catagen, telogen, and exogen. HF stem cells are localized within the bulge region at the bottom of the permanent follicle at the site of arrector pili muscle attachment. During anagen, proliferating progenitor cells in the bulb generate the hair and its surrounding inner root sheath. Catagen is characterized by cessation of proliferation and apoptosis of the epithelial cells below the bulge. The mesenchimally derived DP survives catagen and moves upward to be next the lowest portion of the bulge, which then forms the secondary germ at its base, during telogen. As the new hair grows in, the old hair is shed during exogen (taken from Costarelis, 2006).

1.5 Steroid hormones and their biosynthesis

Steroid hormones are all derived from cholesterol (Figure 5). They can be divided into five groups according to their specific receptors and their physiological features:

- **Mineralcorticoids**, are primarily secreted by the adrenal cortex. The major circulating mineralcorticoid is aldosterone, and they are involved in renal excretion of electrolytes.
- **Glucocorticoids**, are primarily synthesized by the adrenal cortex and are so called for modulating the metabolism of carbohydrates. Cortisol is the most important naturally occurring glucocorticoid in humans. Glucocorticoids exert many effects, not only metabolic but also immunosuppressive and anti-inflammatory.
- **Androgens**, are primarily synthesized by the reticularis zone of the adrenal cortex in both sexes (e.g. ehydroepiandrosterone) and testis in the male (e.g. testosterone). They primarily modulate the development and maintenance of male secondary sexual characters.
- **Estrogens**, are principally produced from the ovary in the female and modulate the development and maintenance of female secondary sexual characters, accelerate the metabolism, stimulate the endometrial growth in the female, and modulate the maintenance of vessel and skin.
- **Progestins**, are synthesized from the ovary and are involved in the reproductive function.

Steroid hormones have a similar structure and contain the same cyclopentanophenanthrene ring and atomic numbering system as cholesterol (Miller, 1988). The pathway (Figure 5) by which steroids are synthesized has been studied by focusing on the structure of hormones, steroid-protein interactions, and kinetics and transcriptional regulation of specific enzymes

involved in the conversion of cholesterol to biologically active steroids. These enzymes belong to two main classes: cytochrome P450 heme containing proteins and hydroxysteroid dehydrogenases. The first and rate-limiting step of steroidogenesis is the transfer of cholesterol from the outer mitochondrial membrane to the inner membrane by a protein called steroidogenic acute regulatory protein (StAR) (Thomsom, 2003). Cholesterol is converted to pregnenolone (PRE) by cytocrome P450 side chain cleavage (P450scc) which is a mitochondrial enzyme encoded by a single gene CYP11A located, in human, on chromosome 15q23-q24 (Sparkes *et al*., 1991). PRE then undergoes 17α-hydroxylation to 17α-hydroxypregnenolone by the microsomal enzyme cytocrome P450c17 which is encoded by gene CYP17A1 located on chromosome 10q24-q25 (Sparkes *et al*., 1991). If StAR/P450scc is the quantitative limiting step of biosynthesis of all steroids, P450c17 is the qualitative regulator step. P450c17 is a single enzyme but can exert two activities, 17α-hydroxylase and 17,20-lyase, according to distinct catalytic sites (Sanderson, 2006). The 17α-hydroxylase activity gives rise to glucocorticoid synthesis and the 17,20 lyase activity to sex steroid synthesis. In regards to this, recent data has demonstrated that cytochrome b5 (CytB5) and serine phosphorylation are independently of each other related to P450c17 17,20-lyase function in the human adrenal gland, which is one of the main endocrine organs of the human body. This relationship is probably due to the increasing the interaction between P450c17 and NADPH-cytochrome P450 oxidoreductase (Pandey and Miller, 2005). PRE can undergo another reaction catalyzed by 3ß-hydroxy-Δ^5-steroid dehydrogenase (3ß-HSD) giving rise to progesterone (PROG). Multiple isoforms of 3ß-HSD have been isolated and characterized and they are encoded by distinct genes HSD3B (Payne and Hales, 2004; Simard *et al*., 2005,). Both PRE and PROG can be 17α-hydroxylated to 17-hydroxypregnenolone and 17-hydroxyprogesterone (17OHPROG), respectively. Then these steroids can be 21-hydroxylated by the microsomal enzyme P450c21 which catalyzes the synthesis of precursors of glucocorticoids and mineralcorticoids. PROG and 17OHPROG can also undergo cleavage of the C17,20 carbon by P450c17 to give DHEA and

androstenedione which give rise to the synthesis of androgens such as testosterone (TST) by the action of 3ß-HSD and 17ß-hydroxysteroid dehydrogenase (17ß-HSD), whose multiple isoforms, encoded by distinct genes HSD17B, have been reported (Payne and Hales, 2004). Androstenedione and testosterone can be converted to estrogens by the microsomal enzyme P450arom which is encoded by the CYP19 gene located on chromosome 15q21.1 (Payne and Hales, 2004).

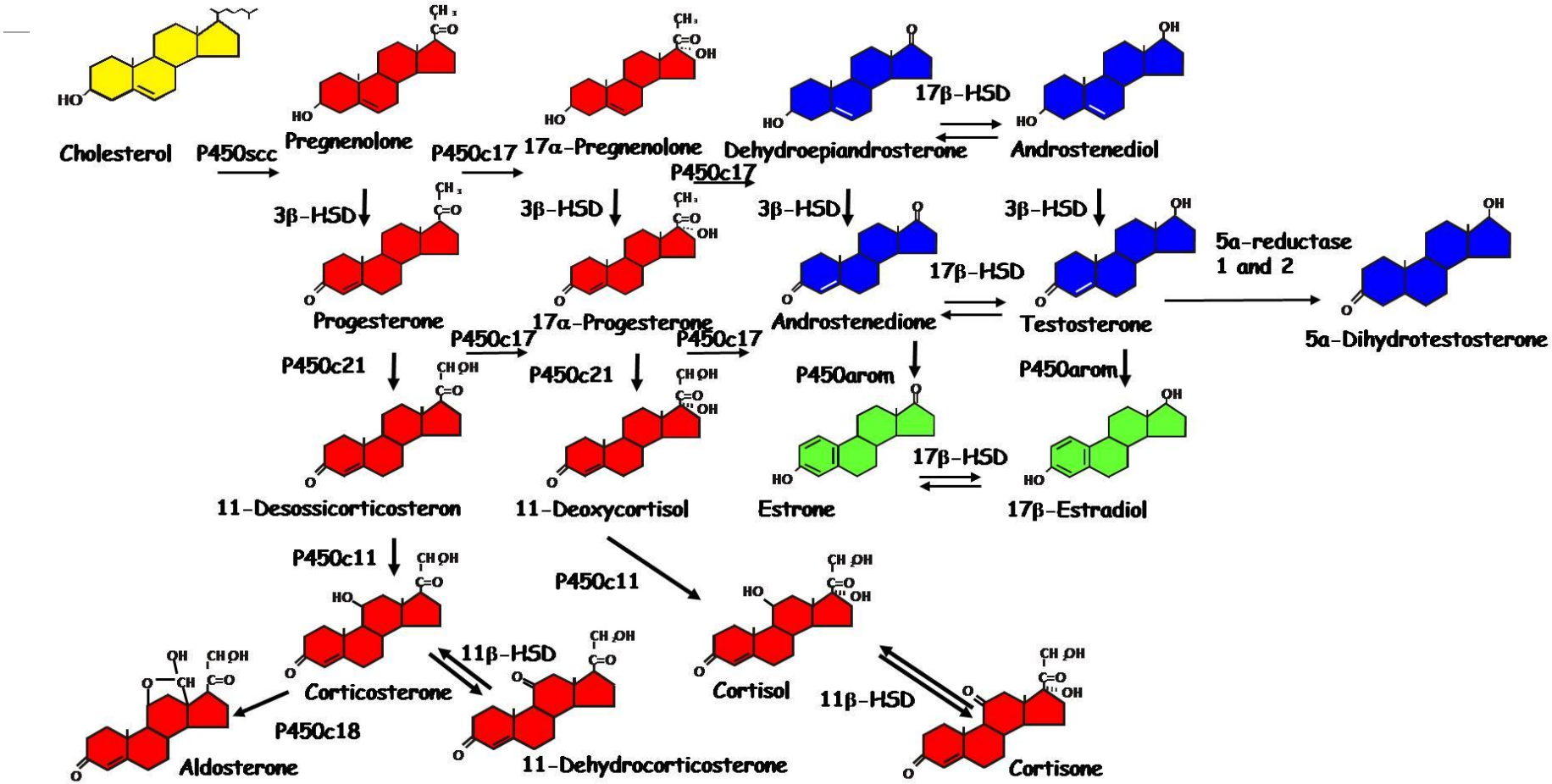

Figure 5. Human steroidogenesis

Steroidogenesis is the biological process by which steroids are generated from cholesterol and transformed into other steroids. **P450arom**: cytochrome P450 aromatase; **P450c11**: cytochrome P450 11 beta-hydroxylase; **P450c17**: cytochrome P450 17α-hydroxylase/17,20 lyase/17,20 desmolase; **P450c18**: cytochrome P450 18-hydroxylase; **P450c21**: cytochrome P450 21-hydroxylase; **P450scc**: cytochrome P450 holesterol side-chain cleavage; **3ß-HSD**: 3-β-hydroxysteroid dehydrogenase/Δ-5-4 isomerase); **11ß-HSD**: 11-beta hydroxysteroid dehydrogenase; **17ß-HSD**: 17β-hydroxysteroid dehydrogenases.

1.5.1 Peripheral synthesis of steroids: intracrinology

Humans, in line with others mammals, are able to synthesize steroid hormones from endocrine organs, such as the gonads (testis in male and ovary in female), the adrenal gland and the placenta (Sanderson, 2006). These endocrine organs are specialized in *de novo* steroid synthesis which is described above and starts with the conversion of cholesterol to pregnenolone by P450scc. However, the expression of steroidogenic enzymes in peripheral tissues can permit the local production of androgens and estrogens by transformation of the adrenal precursors DHEA and androstenedione (4-dione). This is recognized as intracrine transformation of steroids and is defined as the formation of active hormones which exert their action in the same cells where their synthesis took place. In humans and some primates, but not in lower mammals, the adrenal cortex secretes high amounts of the precursor of steroids ehydroepiandrosterone sulfate (DHEA-S) and DHEA, which are converted to 4-dione in both sexes. The adrenal secretion of DHEA-S changes with age with commonly higher circulating levels in men than in women (Rainey and Nakamura, 2008). As shown in Figure 6, fetal levels of DHEA-S increase progressively and following birth decrease rapidly. Prior to puberty, at the age of 6 to 8 years, there is an increment to maximal values that peak between 20 and 30 years. Successively, serum levels of DHEA-S decrease markedly. The reduction of adrenal DHEA-S levels during aging determines a remarkable decline in the production of androgens and estrogens in peripheral target tissues, which could be involved in the pathogenesis of age-related diseases such as insulin resistance and obesity.

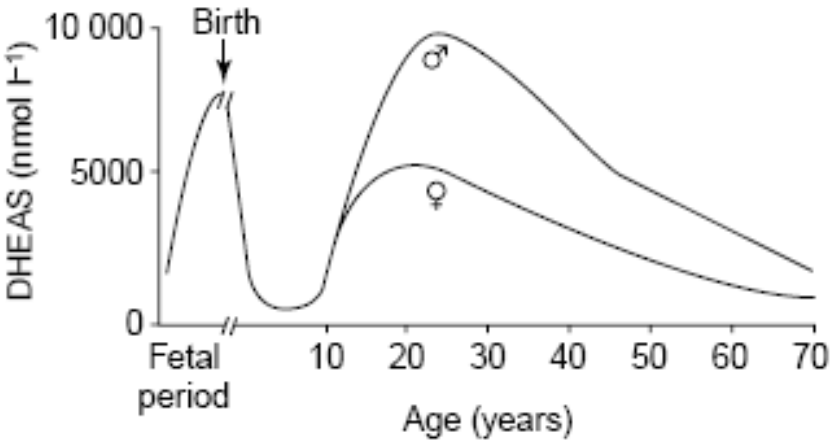

Figure 6. Variation in circulating ehydroepiandrosterone sulfate (DHEA-S) levels throughout human life

During pregnancy, fetal levels of DHEA-S rise progressively to reach a peak at term, and following birth there is a rapid decline. At 5–6 years of age, DHEA-S levels rise again (adrenarche), reach a peak during early adulthood, and decline thereafter. The levels of circulating DHEA-S during adult life also exhibit a gender difference, with higher levels found in men than in women (taken from Rainey and Nakamura, 2008).

Following menopause, with the block of secretion of estrogens by the ovary, women only have adrenal DHEA and DHEA-S as exclusive source of sex steroids for all tissues, except the uterus. However, the decline in the adrenal production of DHEA and its low circulating levels result in a weak source of sex steroids. Several problems are classically associated to the post-menopausal period such as osteoporosis, muscle loss, fat accumulation, vaginal atrophy, skin aging, diabetes and possibly Alzheimer's syndrome. On the other hand, the comparable decrease in serum DHEA levels observed in both sexes has less consequence in men who continue to receive a practically constant supply of testicular sex steroids during their whole life (Labrie *et al*., 2010). In fact, in men the appearance of hormone-deficiency symptoms common to women is observed at a much later age with a lower degree of severity.

1.5.2 Transformation of DHEA in androgens and estrogens

Transformation of the adrenal precursor DHEA-S into androgens and estrogens in peripheral target tissues depends on the presence and activity of specific steroidogenic enzymes. Plasma DHEA-S levels in adult men and women are 100–500 times higher than those of testosterone and 1000–10000 times higher than those of 17ß-estradiol, thus providing a large reservoir of substrate for intracrine conversion into androgens and/or estrogens in peripheral tissues. 50% of total androgens in the prostate of adult men are derived from this adrenal precursor steroid, while 75% before menopause and close to 100% after menopause of estrogens are derived from DHEA-S in peripheral tissues in women (Labrie *et al*., 1998; Labrie *et al*., 2005). As described in section *1.5*, the biosynthesis of DHEA requires two steroidogenic enzymes, P450scc and P450c17, and the StAR protein for transportation of cholesterol into the mitochondria. However, three other proteins – cytochrome b5, DHEA sulfotransferase (SULT2A1) and 3β-hydroxysteroid dehydrogenase type 2 (HSD3B2) – are the main regulators of the adrenal synthesis of DHEA-S (Rainey and Nakamura, 2008). In particular, adrenal production of DHEA-S is correlated with zona reticularis expression of SULT2A1 and CYB5. In contrast, HSD3B2 has an inverse correlation with adrenal androgen production likely due to its unique ability to remove precursors from the pathway leading to DHEA. The half-life of DHEA-S in plasma (10–20 h) is significantly longer than that of un-conjugated DHEA and about 75% of the daily production rate of DHEA-S is converted to DHEA in peripheral tissues (Labrie *et al*., 2003). Here, after transport inside the cell by members of the organic anion transporting polypeptide family (OATPs) such as OATP2B1 (Hagenbuch and Meier, 2003), the enzyme steroid sulfatase (STS) removes the sulfate group and the resulting DHEA can undergo reduction to 4-androstenedione (4-dione) by 3ß-HSD1 (Samson *et al*., 2005) or androstenediol by 17ß-HSD1 (Stanway *et al*., 2007). Both steroids can be converted to TST which can undergo transformation to either 17ß-estradiol

(E2) by aromatase or 5α-dihydrotestosterone (5α-DHT) by 5α-reductase (Figure 7).

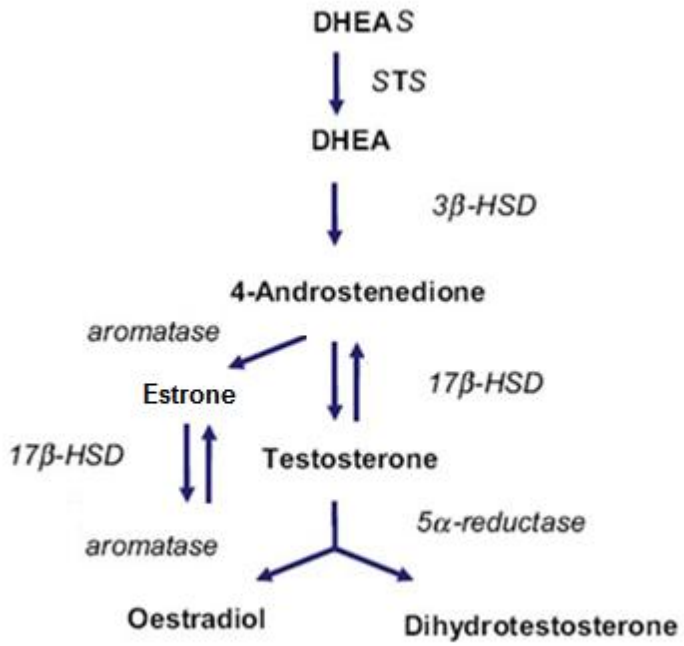

Figure 7. Intracrine formation of sex steroids

Schematic representation of the steps of the intracrine pathways of sex steroids. DHEA (dehydroepiandrosterone), STS (steroid sulfatase), HSD (hydroxysteroid dehydrogenase) (adapted from Luu-The *et al*., 2008).

1.5.3 Human skin: target and source of steroid hormones

Human skin is a target for many chemical molecules including hormones secreted into the blood circulation by endocrine glands. For example, melanocytes respond to polypeptide hormones, such as ACTH released by the pituitary gland that has significant effects on pigmentation and proliferation (Kadecaro *et al*., 2003). The HF and sebaceous gland respond to androgens secreted by the gonads and the adrenal cortex modulating hair growth and intracellular lipid production, respectively (Randall, 2008). Skin can be

described as a functional coordinated district in which cells produce, receive and modulate molecular signals from distant sources (endocrine glands), neighboring cells (paracrine and juxtacrine communication) and themselves (autocrine and intracrine communication). Therefore, the skin is both a target and a source of hormones (Figure 8). In this matter, Thiboutot and colleagues (2003) detected mRNA expression of StAR protein which is essential for cholesterol translocation into the mitochondrial membrane and consequently the beginning of steroidogenesis in human sebocytes. They also demonstrated that normal sebocytes expressed cytochrome P450scc, which catalyses the conversion of cholesterol into pregnenolone, and cytochrome P450c17, giving rise to the precursors of cortisol and DHEA, thus demonstrating that the sebaceous gland can be a steroidogenic tissue. In addition, Fritsch and colleagues (2001) investigated mRNA expression and inhibition of key steroidogenic enzymes in SZ95 sebocytes and HaCat keratinocytes. Both cell lines expressed 3ß-HSDΔ^{5-4}, 17ß-HSD, 5α-reductase type 1 and 3α-HSD indicating the occurrence of androgen metabolism. Indeed, DHEA can be transformed into 4-dione and TST. The latter of which is further activated by its conversion into 5α-DHT by 5α-reductase type 1 or 2. Type 1 is expressed in almost all skin cells but especially in sebocytes, while type 2 is found predominantly in the HF (Chen *et al*., 1998). On the other hand, androgen can be converted to estrogen in DFs which express aromatase and inactivated to androsterone in EKs by 3α-HSD (Zouboulis, 2000). In contrast to *de novo* synthesis of sex steroids, the adrenal DHEA-S can reach the cells of the skin via the bloodstream and undergo intracrine transformation in cells containing the specific regulatory enzymes. As described in section *1.5.2*, the first conversion to DHEA is catalyzed by the key enzyme steroid sulfatase (STS) which has become a valid prognostic and diagnostic factor in hormone dependent tumors (Reed *et al*., 2005). Localization and activity of STS has been detected in skin, in particular in DFs, EKs and the DP of the HF (Chen *et al*., 2002). It has also been reported that human EKs derived from foreskin express both mRNA and OATP2B1 protein (Schiffer *et al*., 2003).

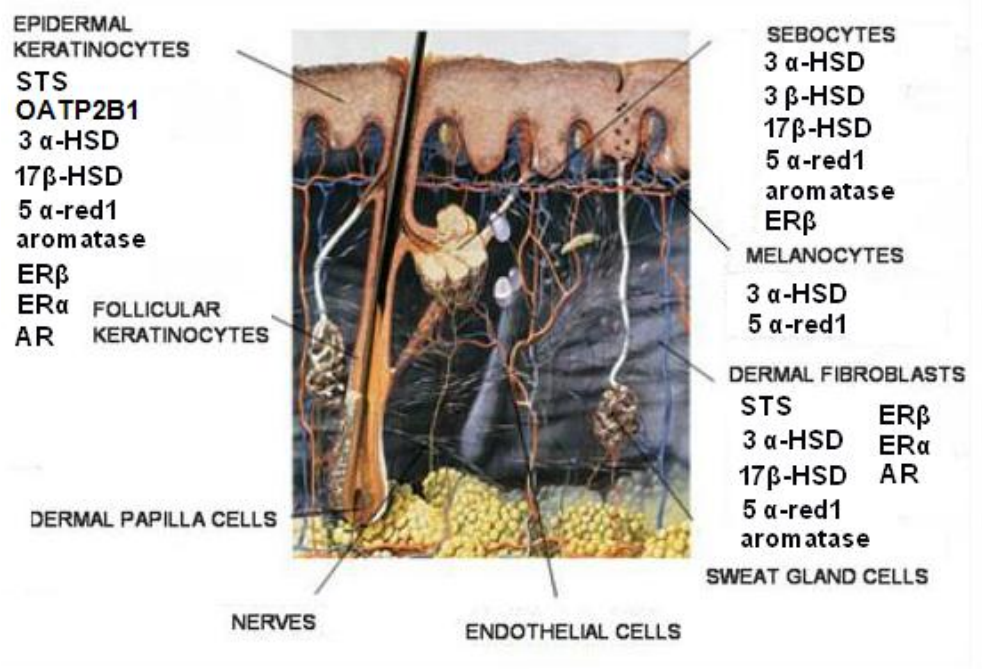

Figure 8. Synthesis of hormones in human skin

The image displays the localization of the proteins involved in steroidogenesis in human skin: aromatase, HSD (hydroxysteroid-dehydrogenase), steroid sulfatase (STS), OATP2B1 (organic anion transporting polypeptide 2B1), and 5α-reductase 1 and 2 (5α-red1 and 2). The skin expresses also estrogen receptor α and ß (ERα and ERß), and the androgen receptor (AR) (adapted from Zouboulis, 2004).

1.5.4 Synthesis of androgens and estrogens in the hair follicle

The literature on normal and pathologic steroid metabolism in the HF is vast. In particular, some pivotal aspects of androgen metabolism are thought to be important for human hair growth (Randall, 2008). It is known that the skin is able to synthesize active androgens, such as DHT, from the systemic precursor DHEA-S. The first step in this pathway is the desulfation of DHEA-S by the enzyme STS. DHEA-S is thought to be involved in the pathogenesis of

hirsutism in hyperandrogenic women (Karrer-Voegeli *et al*., 2009). However, in women an excess of DHEA-S or STS is believed to be involved in several androgen-dependent processes such as acne and androgenetic alopecia (AGA) (Trüeb *et al*., 2004; Birch *et al*., 2002). DHEA-S and DHEA plasma levels also seem to correlate with balding in young men indicating that STS may play a role in the pathogenesis of AGA (Trüeb, 2002). The conversion of DHEA-S to DHEA by human HFs is documented and it has been shown that STS is mainly located within the DP (Hoffmann *et al*., 2001) and is able to convert DHEA-S to DHEA. Another important step in the biosynthesis of androgens and estrogens is catalyzed by 3ß-HSD. The two human 3ß-HSD1 and 3ß-HSD2 are expressed in a tissue-specific manner involving separate mechanisms of regulation (Payne and Hales, 2004). The importance of 3ß-HSD in androgen metabolism and increased activity in AGA warrants further investigation. The DP revealed an intense 3ß-HSD activity resulting in testosterone as an intermediate reaction product and 5α-DHT as the final metabolite (Hoffmann *et al*., 2001). The isoenzymes of 17ß-HSD regulate levels of bioactive androgens and estrogens in a variety of tissues. At present, 11 isoenzymes of 17ß-HSD are known to differ in tissue expression. The potential significance of 17ß-HSD isoenzymes in AGA has so far not been investigated. However, it is underscored by observations of Hodgins et al. (1985) who plucked HFs from young adults not yet expressing AGA, but with a strong family history of baldness, and found two populations, one with high 17ß-HSD activity and one with low enzyme activity. Therefore, linkage of the genes coding for the 17ß-HSD isoenzymes and AGA warrants further investigation. The isoenzyme specific expression pattern in different parts of the HF has so far not been investigated in detail. Only one study described type 1 and 2 17ß-HSD in the epithelial parts of the HF. The authors did not find mRNA for 17ß-HSD in the DP. However, at the protein level, this enzyme is metabolically active within the DP (Hoffmann *et al*., 2003). The microsomal enzyme steroid 5α-reductase is responsible for the conversion of testosterone into the more potent androgen DHT and the conversion of androstenedione to 5α-androstanedione. Interestingly, the observations that

humans have beard and frontal scalp HFs with higher 5α-reductase activity than HFs from the occiput (Itami *et al*., 1999), indicate that the type 2 5α-reductase is crucially involved in the pathogenesis of androgen-dependent hair growth and therefore the inhibition of this isoenzyme is a rational approach for treatment such as topical finasteride administered systemically (Bienová *et al*., 2005). The 5α-reductase inhibitor finasteride blocks the conversion of testosterone to DHT, the androgen responsible for androgenetic alopecia (McClellan and Markham, 1999). Special attention has been paid to the DP, and several authors have tried to localize both isoenzymes 5α-reductase 1 and 2 within the DP. Some authors found considerable 5α-reductase 2 activity in occipital scalp and in beard DP (Itami *et al*., 1990). Provided the DP plays a crucial role during androgen-mediated processes on the HF, the data suggest that the DP might amplify testosterone-driven responses in the human HF via the action of 5α-reductase.

Once formed, DHT is further inactivated via 3α-HSDs to the rather weak steroids androsterone and androstanediol. In theory, the back-conversion of these weak steroids to DHT via oxidative 3α-HSD may promote DHT dependent hair loss. Very recently, it has been demonstrated that such a metabolism is present in the DP of occipital and beard HFs, and theoretically any drug that is able to block this process might be beneficial for AGA. Moreover, the cytochrome P450 aromatase enzyme is required for the conversion of androgens to estrogens. Mutations in the CYP19 gene do rarely occur and result in aromatase deficiency. At puberty, affected females will develop hirsutism due to an androgen excess and in theory females and males might develop early-onset AGA. Women tend to develop AGA later in life and in a milder form than men. With the decline of serum estrogens during menopause, many women show an accelerated progression of AGA. Estrogens may play a protective role against the development of AGA, because pregnant women with high levels of estrogens show a prolonged anagen phase, but lose their hair again post partum (Hoffmann, 2003). Recently, it has been shown that HFs from women with AGA express more aromatase activity as compared to male-derived HFs (Sawaya and Price,

1997), and interestingly those women taking aromatase inhibitors tend to develop AGA rather rapidly (Goss *et al*., 1995). Aromatase has been found mainly expressed within the root sheaths of the HF. However, some cells of the stalk region of the DP also stained for aromatase (Figure 9).

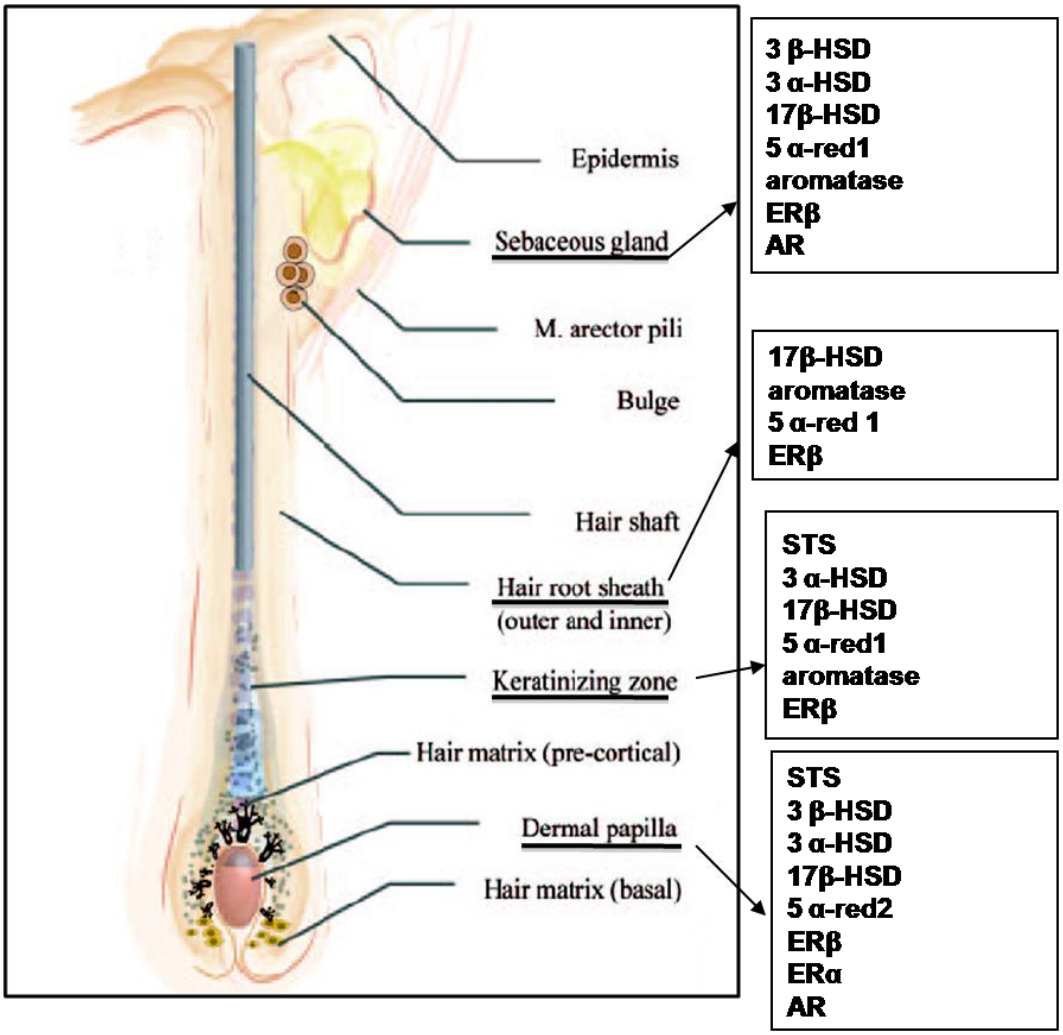

Figure 9. Localization of steroidogenic enzymes and sex steroid receptor in the HF

The image displays the localization of the enzymes involved in the steroidogenesis in the HF: aromatase, hydroxysteroid dehydrogenase (HSD), steroid sulfatase (STS), and 5α-reductase 1 and 2 (5α-red1 and 2). The hair express also the estrogen receptor α and ß (ERα and Erß), and the androgen receptor (AR) (adapted from Ohnemus *et al.*, 2006).

1.6 Localization of receptors of estrogen and androgen in human skin

To better understand the role of sex steroids in development and pathology of human skin, in recent years, the estrogen receptors (ER) and androgen receptor (AR) have been localized in both sexes and different anatomical sites of the human body. In particular, the information on the differential localization of steroid receptors in human skin should be of great help for further investigation into the specific role of specific steroids on human skin and skin appendages.

1.6.1 Estrogen receptor

Two separate intracellular estrogen receptors (ER) have been isolated, cloned and characterized namely Erα and Erß (Greene *et al.*, 1986). These two forms are encoded by separate genes, ESR1 and ESR2 respectively (Klinge, 2001), and located on different chromosomes, 6q25.1 and 14q23.2. Erα and Erß are found in the cytosol and after binding 17ß-estradiol they dimerize and migrate into the nucleus. Here, the receptor acts as a transcription factor that regulates gene expression by binding to specific sequences of DNA called hormone response elements (ERE) (Welboren *et al*., 2007). Hormone-activated estrogen receptors form dimers, and, since the two forms are coexpressed in many cell types, the receptors may form either Erα (αα) or Erβ (ββ) homodimers, or Erαβ (αβ) heterodimers (Matthews and Gustafsson, 2003). Estrogen receptor alpha and beta show significant overall sequence homology, and both are composed of three major functional domains (Klinge, 2001): the N-terminal transactivation domain, the DNA-binding domain (DBD), and the C-terminal ligand-binding domain (LBD) (Figure 10). However, a second different type of estrogen receptor has been discovered. This type is associated with the cell surface membrane and with G protein. Its mechanism of action is non genomic through specific

interactions with signals proteins and action of enzymes which constitute known second messenger pathways such as the mitogen-activated protein kinase (MAPK/ERK) and phosphoinositide 3-kinase (PI3K/AKT) (Simoncini and Genazzani, 2003). Immunohistochemistry has shown that human scalp Eks express Erß but not Erα *in situ* (Thornton *et al*., 2003), with more intense staining in the stratum basale and stratum spinosum than the stratum granulosum. *In vitro* studies have also examined ER expression within individual skin cells. It has been shown using RT-PCR, that Erß and not Erα mRNA was expressed by cultured Eks (Kanda and Watanabe, 2003). The same group have shown that only Erß protein was expressed using Western Blotting. In contrast, Verdier-Sevrain and colleagues (2004) demonstrated that both Erα and Erß were expressed in cultured keratinocytes derived from human foreskin using immunohistochemistry. Erß has also been found in cells of the human dermis, including DFs and blood vessels (Pelletier and Ren, 2004). Human cultured DFs have also been shown to express Erα (Ankrom *et al*., 1998). Within the HF differences in estrogen receptor distribution have been demonstrated. In human scalp skin, anagen HFs have been shown to strongly express Erß compared to Erα *in situ*. Immunohistochemistry has demonstrated that Erβ is the main receptor in human keratinocytes, HFs and sebaceous glands (Thornton *et al.,* 2003); however Erα is predominantly expressed in non-hair bearing skin from the breast and abdomen (Nelson, 2005).

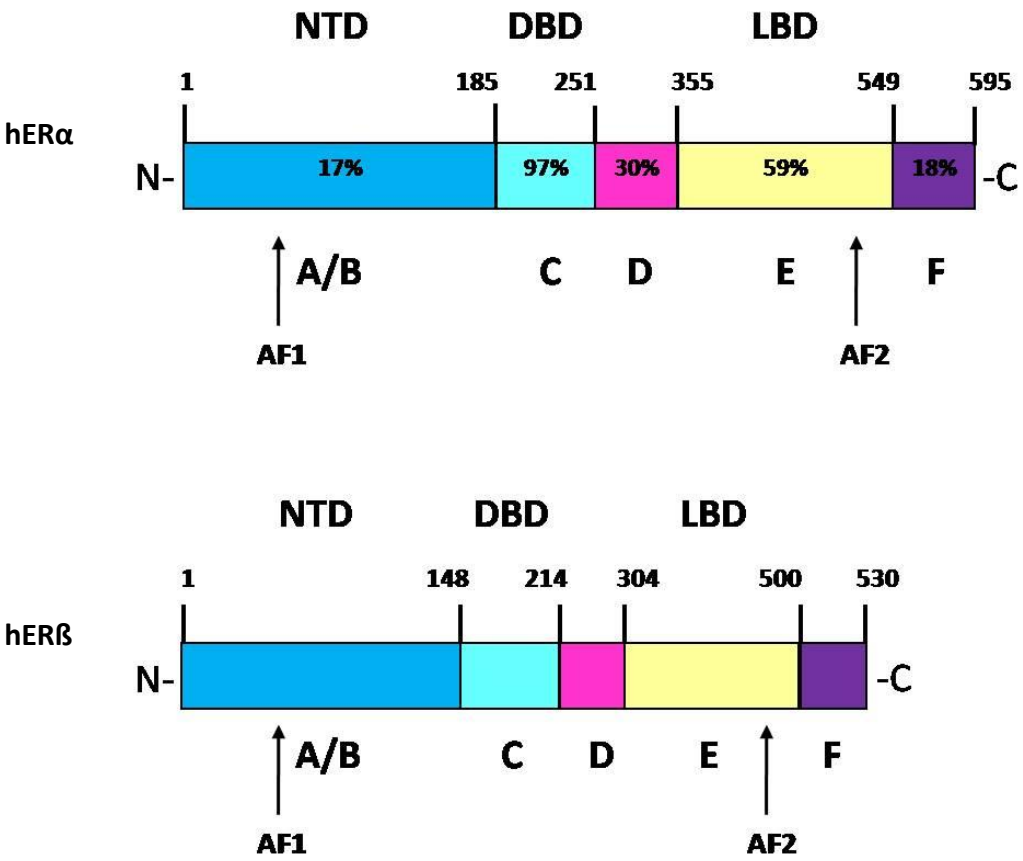

Figure 10. The molecular structure of the estrogen receptors

Three major functional domains exist in each of the estrogen receptors, the amino terminal domain that contains the Activation Function-1 (AF-1), the DNA-binding domain (DBD) and the ligand binding domain (LBD), that contains also Activation Function-2 (AF-2), which is involved in dimerisation and transcriptional activation. Numbers above the bars refer to the amino acid residues which separate the domains starting from the N-terminus (left) to C-terminus (right). The numbers within ERα domains represent the percentage of homology between the two receptors.

1.6.2 The androgen receptor

The androgen receptor (AR) has been cloned and characterized in human tissues (Lubahn *et al*., 1988). The AR is a nuclear receptor and is encoded by a gene located on the X chromosome at Xq12 (Németh *et al*., 2002). Two forms of the androgen receptor (AR-A and AR-B), that differ by the lack of the first 187 amino acids in the N-terminal transactivation domain of AR-A, are expressed in human tissues (Wilson and McPhaul, 1996). Similar to be estrogen receptor, common structural features of the receptor include three major functional domains: the N-terminal transactivation domain, the DNA-binding domain (DBD) and the C-terminal ligand-binding domain (LBD) (Liegibel *et al*., 2003) (Figure 11). AR is activated by the association of androgens TST or 5α-DHT in the cytosol followed by translocation into the nucleus where it binds to androgen response elements (ARE) on the DNA thereby modulating gene expression (Chen *et al.,* 2009). However, recent studies have shown that AR may possibly have a different mechanism of action independently of interaction with DNA: the non genomic mode (Foradori *et al*., 2008). In this case, the AR interacts with specific signal transduction proteins in the cytosol independently of direct effect on gene expression, for example, by phosphorylation of other transcription factors. In the skin the AR has been detected mostly in Eks and keratinocytes within the pilosebaceous duct, indicating that these cells are targets for androgens, for example in the acne process. DFs in the dermis and sebocytes express the AR. In addition, AR has been shown to be expressed in the secretory cells of the eccrine sweat gland and in the DP of HF (Zouboulis, 2004).

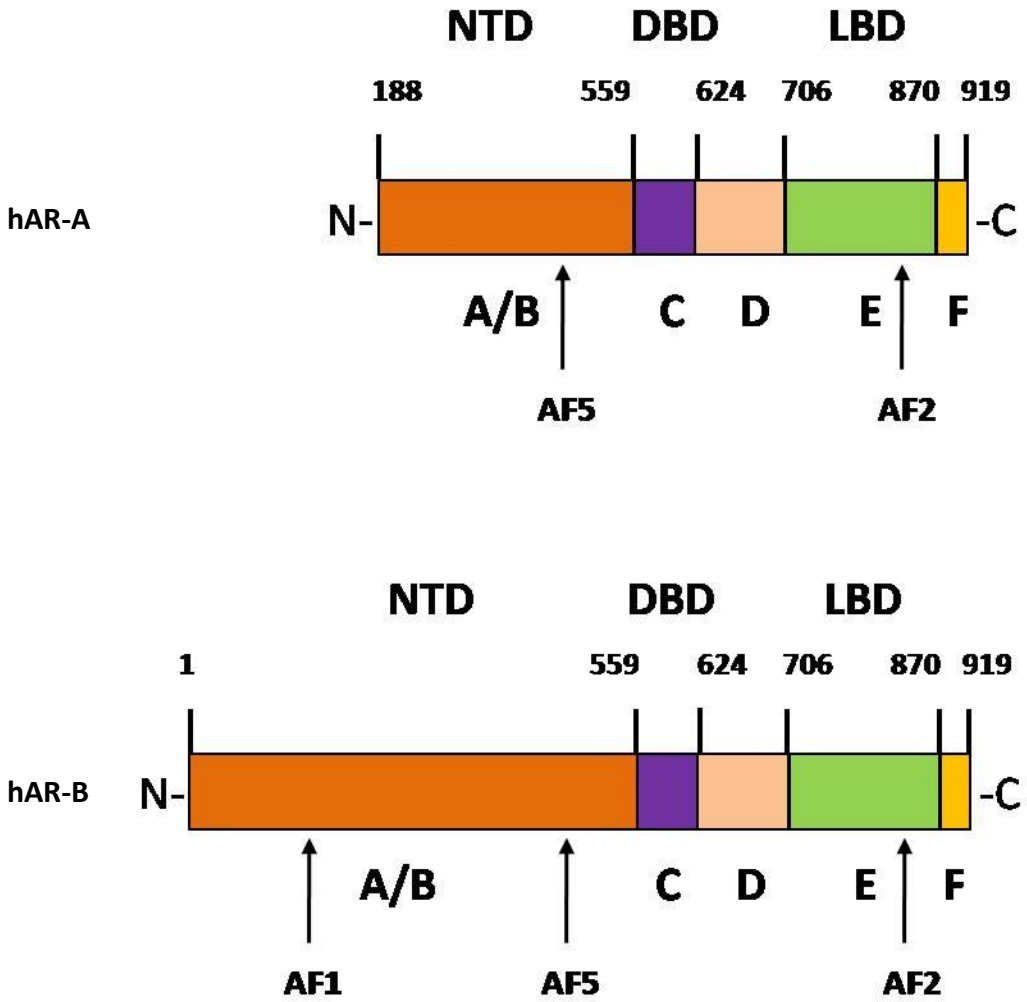

Figure 11. Structural domains of the two androgen receptors (AR-A and AR-B)

Numbers above the bars refer to the amino acid residues which separate the domains starting from the N-terminus (left) to C-terminus (right). NTD = N-terminal domain, DBD = DNA binding domain, LBD = ligand binding domain. AF = activation function.

1.7 Wound Healing

Wound healing is an intricate process in which the skin (or another organ) repairs itself after injury. Different cell types, cytokines and growth factors work simultaneously and in sequence to restore cutaneous continuity. The classic model of wound healing is divided into three sequential, overlapping phases: the inflammatory, proliferative and remodelling phases (Stadelmann *et al*., 1998) (Figure 12).

1.7.1 The inflammatory phase

The inflammatory phase is the first to occur and begins as a consequence of tissue injury. The inflammation is essential for the establishment of cutaneous homeostasis following injury. During this phase, platelet aggregation is followed by infiltration of leukocytes into the wound site. In tissue formation, epithelialisation and newly formed granulation tissue, consisting of endothelial cells, macrophages and fibroblasts, begin to cover and fill the wound area to restore tissue integrity. Immediately after injury extravasated blood constituents form a hemostatic plug. Platelets and polymorphonuclear leukocytes entrapped and aggregated in the blood clot release a wide variety of factors that amplify the aggregation response, initiate a coagulation cascade, and act as chemoattractants for cells involved in the inflammatory phase (Szpaderska *et al*., 2003). The clot acts as a framework for migrating inflammatory cells, fibroblasts and endothelial cells. Platelets fibrinogen, platelet derived growth factor (PDGF), TGF-β, factor V and thromboxane A2 (TXA2), are factors which play a key role in homeostasis, promoting the inflammatory response, fibroblasts proliferation and extracellular matrix synthesis. A few hours post-injury neutrophils in the wound transmigrate across the endothelial cell wall of blood capillaries, which have been activated by proinflammatory cytokines such as IL-1ß, tumor necrosis factor-α (TNF-α), and IFN-γ at the wound site, leading to the

expression of various classes of adhesion molecules essential for leukocyte adhesion and diapedesis. Monocytes often infiltrate the wound within first 24 to 48 hours, following a chemoattractant gradient, before differentiating into macrophages (Clark and Henson, 1988; Eming, 2007b). They remain within the wound site for days to weeks and play an important role in debridement, defense against microbes as well as releasing growth factors and cytokines involved in tissue repair.

1.7.2 The Proliferative Phase

The proliferative phase of wound healing is defined by a number of overlapping processes including re-epithelialisation, formation of granulation tissue, wound contraction and angiogenesis.

1.7.2.1 Re-epithelialisation

Re-epithelialisation involves the migration and proliferation of cells arising from residual epithelium or from epithelial cells within skin appendages such as HFs and sweat glands, at the base of the wound to reform the epithelial barrier and basement membrane. During this process, keratinocytes migration and proliferation depends on the interaction of keratinocytes with DFs and the extracellular matrix (ECM) (Auger *et al*., 2009). The events in re-epithelialisation are regulated by the presence of growth factors such as EGF and transforming growth factor alpha (TGF-α), integrins, which allow for interaction with ECM components and MMPs, which facilitate cell migration (Santoro and Gaudino 2005). After one to two days, cells behind the migrating wound edge start to proliferate and create cells to feed the migrating sheets at the wound margin.

1.7.2.2 Granulation tissue: fibroblast proliferation

DFs play an important role in the initial response to injury. They migrate to the wound site, actively proliferate and produce hyaluronic acid, collagen, fibronectin and proteoglycans, under the control of local factors released by different cell types. Hyaluronic acid, a glycoaminoglycan forms an important element of granulation tissue with a role in promoting cell migration and division (Clark and Henson 1988). It is produced in large amounts in the early phase of wound healing than in normal dermis and increases cell motility by reducing cell-matrix adhesions. Hyaluronic acid also leads to tissue swelling which increases the space between the collagen and cells, facilitating cell movement. Fibronectin is also secreted by fibroblasts and provides a network to which myofibroblasts attach to allow wound contraction. Fibrillar collagen is secreted by fibroblasts during the proliferative phase, within granulation tissue largely in the form of type III collagen, compared to type I collagen. TGF-β, PDGF, FGF and IGF-1 are intimately involved in fibroblast activity in this phase of wound healing. PDGF is a potent activator of fibroblasts and encourages the chemotaxis, proliferation and new gene expression *in vitro* (Pierce *et al*., 1991). TGF-β also stimulates fibroblast migration and proliferation as well as increasing fibronectin and collagen production. IGF also increases DF migration, proliferation, TGF-β1 secretion and ECM secretion (Takehara, 2000).

1.7.2.3 Wound contraction

Wound contraction is a normal physiological part of the wound healing process and acts to assist in wound closure as well as protection against micro-organisms. The key cell thought to be involved in wound contraction is the myofibroblast, a specialised fibroblast within the extra-cellular matrix which has the characteristics of a fibroblast and smooth muscle cell (Desmouliere *et al*., 2005). It is charaterised by the expression of smooth muscle cell markers such as alpha-smooth-muscle actin (α-SMA).

Myofibroblasts act as multicellular units with cell contraction resulting in the rearrangement of the surrounding tissue matrix. Myofibroblasts appear within wounds after 3 days and disappear following the completion of the wound healing process. Shephard *et al.* (2004) demonstrated that TGF-β and fibronectin are regulators of myofibroblast differentiation and α-SMA expression is reduced when TGF-β neutralizing antibodies are added to human DF cell monolayers. Studies have also suggested that DF motion is responsible for providing the force for wound closure, through the movement of individual fibroblasts through the extracellular matrix (Stadelmann *et al*., 1998; Midwood *et al*., 2004). This movement results in the reorganization of connective tissue fibers leading to a smaller unit, pulling the skin in with it. Fibroblasts become denser as the unit decreases in size, and cell-to-cell contact leads to contact inhibition. Fibroblasts then top migrating and proliferating and cytoplasmic stress fibers form. This has lead to the theory that myofibroblasts are actually fibroblasts in a transitional state.

1.7.2.4 Angiogenesis

The formation of new blood vasculature from preexisting vessels, a process called angiogenesis, is essential to wound healing (Folkman and Shing, 1992). Newly formed blood vessels provide nutrition and oxygen to growing tissues. In addition, inflammatory cells require the interaction with and transmigration through the endothelial basement membrane to enter the site of injury (Eming *et al*., 2007a). Matrix metalloproteinases (MMPs) are secreted by endothelial cells which degrade the vascular basement membrane on the side of angiogenic stimulus. Cells then migrate across the degraded basement membrane forming a tubular lumen and new sprouts connect to form a branching network. As new vessels develop, extracellular matrix components form a new basement membrane and endothelial cells become surrounded by a layer of perivascular cells. Angiogenesis, in response to tissue injury, is a dynamic process that is highly regulated by

signals from both serum and surrounding specialicing ECM environment (Risau, 1997). The new vascular network is actively remodeled under the influence of angiogenic factors from the FGF family, TGF-β, PDGF and VEGF, and eventually, capillaries differentiate into arteries and veins (Tonnesen *et al*., 2000).

1.7.3 The Remodelling phase

The last step of normal wound healing is remodelling, also called maturation, during which the ECM components will be modified by the balanced mechanisms of proteolysis and new matrix secretion (Auger *et al.,* 2009). The complete maturation of a wound may take months or even years to complete, depending on its initial extent and various factors that can affect the healing process. DFs play an important role in the remodelling phase of wound healing (Ghalbzouri *et al*., 2004). They are responsible for ECM secretion and continued wound contraction, although fibroblasts gradually show a reduced cell density as connective tissue matrix is consolidated into scar tissue. MMPs degrade amorphous collagen and fibronectin and collagenases cleave fibrillar collagen types I,II and III (Nagase and Woessner 1999). MMPs are involved in remodelling the scar ECM either directly by proteolytic degradation of proteins, such as collagens, or indirectly via their ability to affect cell behavior. Alteration of the ECM is integral to the resolution of wound healing but also has implications in the regulation of inflammation (Gill and Parks, 2008). Thus, MMPs are key regulators of multiple aspects of tissue repair and further study of these enzymes and their interaction with their substrates will provide insight into possible therapies.

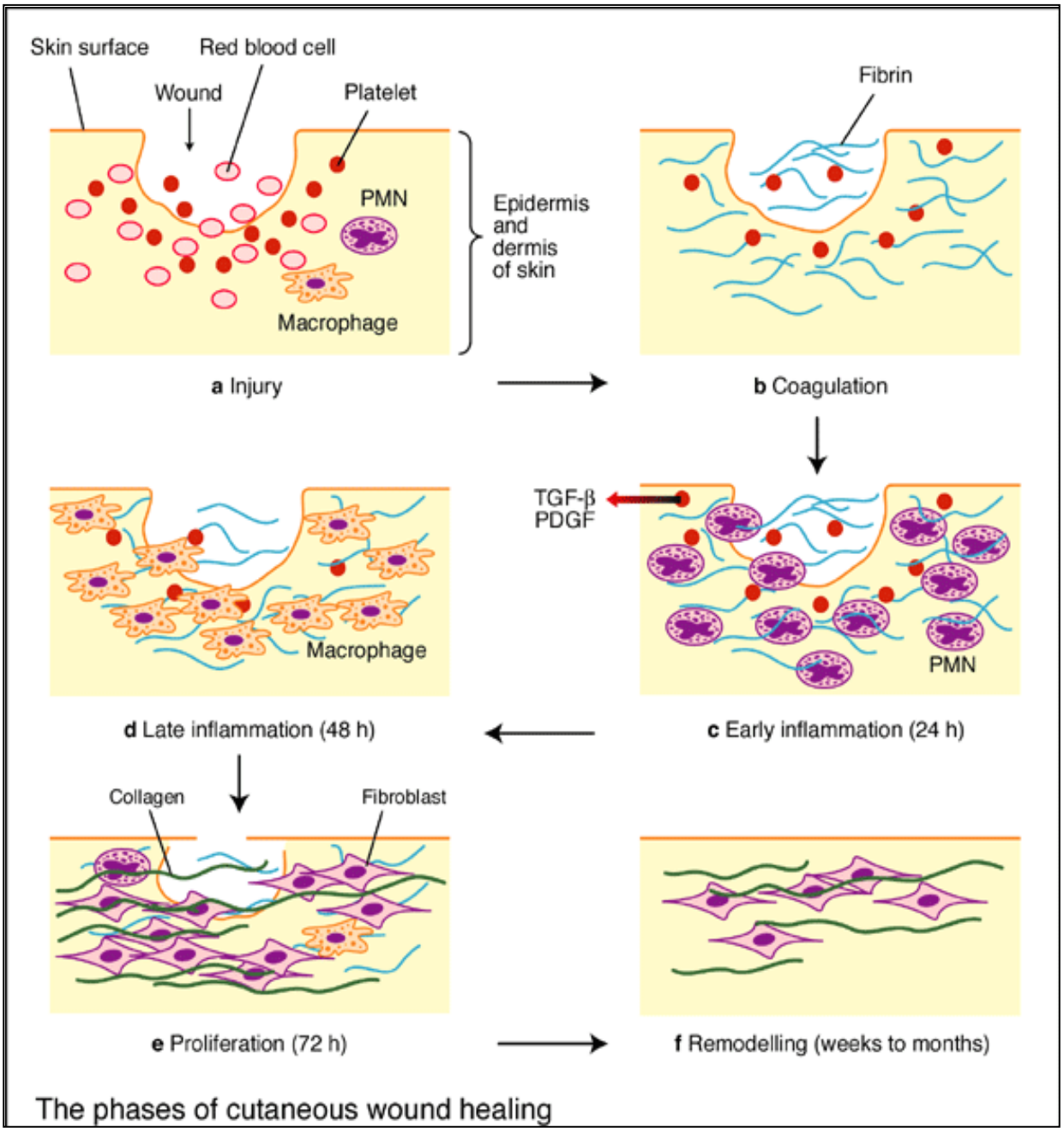

Figure 12. The phases of cutaneous wound healing

Wound healing involves three overlapping phases, the inflammatory, proliferative and remodelling phases. Different cell types, cytokines and growth factors work simultaneously and in sequence to restore cutaneous continuity (taken from Beanes *et al.* 2003, Expert Reviews in Molecular Medicine).

1.8 Estrogens and wound healing

There is strong evidence that estrogens play an important role in skin physiology and wound healing. Reduced estrogen levels have major effects on cellular and tissue responses to injury. These effects include impaired cytokine signal transduction, unchecked inflammation, and altered protein balance, all of which have a major impact on the rate of wound healing (Ashcroft and Ashworth, 2003). The presence of ERs in human EKs, DFs and inflammatory cells in males and females suggests that estrogen may act by modulating the inflammatory response, re-epithelialisation, granulation tissue formation and proteolysis (Calvin, 2000; Ashcroft and Ashworth, 2003). The administration of 17ß-estradiol, either systemically or topically, has been shown to reverse the fundamental repair defects observed in postmenopausal women (Gilliver and Ashcroft, 2007). Estrogen reduces collagen loss in women with higher initial collagen levels (early menopause) and stimulates collagen synthesis in women with lower initial collagen levels (late menopause) (Oh and Phillips, 2006). Additionally, it has been demonstrated that estrogens modulated vascular endothelial cells through ERs. Estradiol has also been shown to influence the dynamics of vascular endothelial progenitor cells and neovascularization in wound's granulation tissue (Xin *et al*., 2009). Various animal and human studies have been conducted *in vitro* and *in vivo* in an attempt to characterize the effects of estrogen on wound repair as well as to elucidate the bio-molecular mechanisms behind these actions.

1.9 DHEA and wound healing

As previously described, DHEA is the predominant adrenal precursor of androgens and estrogens in humans. There are numerous lines of evidence to suggest that high serum DHEA levels have a beneficial effect on longevity and prevent a number of human pathophysiological conditions, such as heart disease and diabetes. DHEA has been shown to exert many of its effects via AR and/or ER after its enzymatic conversion to androgen or estrogen (Labrie

et al., 1998). More recently, DHEA has been shown to act via non steroid receptor non genomic pathways, in vascular endothelial cells (Williams *et al*., 2002; Williams *et al*., 2004), neuroendocrine cells (Charalampopoulos *et al*., 2006a) and human keratinocytes (Alexaki *et al*., 2009). Recently, it has been reported that the acceleration of healing following topical DHEA treatment in mice is associated with a decrease in the local inflammatory response and a reduction in tissue cytokine levels (Mills *et al*., 2005). DHEA has been also shown to accelerate wounded human DF migration *in vitro* (Stevenson *et al*., 2009). DHEA may also have implications for angiogenesis and wound healing via its inhibitory effects on human platelet aggregation *in vitro* and *in vivo* (Jesse *et al*., 1995). Additionally, DHEA can exert stimulator effects on human umbilical vein endothelial cell proliferation *in vitro* (William *et al*., 2002; William *et al.*, 2004). Therefore, DHEA represents an exciting candidate for clinical manipulation.

1.10 Aim of the study

The aim of this study was to determine whether human skin expresses the enzymes required for the local biosynthesis of active sex steroid hormones. Specifically, biopsies of skin, HFs, cultured DFs, and cultured EKs were investigated for the mRNA expression of seven key steroidogenic proteins (P450arom, P450scc, P450c17, STS, OATP2B1, 5α-reductase 1 and 5α-reductase 2), and the ERs and the AR using non quantitative RT-PCR. Absolute qRT-PCR was also performed to measure the gene expression of the seven key steroidogenic proteins of interest in whole skin and HFs. In addition, the response of culturing human skin cells in the presence of androgens or estrogens *in vitro* was also investigated. The changes in the pangenomic profile induced in human EKs treated with E2, TST or DHEA-S were explored by an array gene expression analysis. Migration of DFs and EKs was assessed following mechanical wounding of cell monolayers, as this is a key function during the proliferative and re-modeling phases of wound healing. The *in vitro* scratch wound assay was used to determine the direct

effects of E2, DHEA, DHEA-S and TST on cell migration. In addition, the effect of an aromatase inhibitor (Arimidex) and a steroid sulphatase inhibitor (STX64) were also included to determine whether the observed responses were a result of the intracrine conversion of steroids. Moreover, the activity of the aromatase enzyme was also assessed in keratinocytes and fibroblasts using the tritiated water (^3H_2O) assay to verify the results obtained from the analysis of the expression of both the protein and mRNA for P450arom in human skin cells.

2. Materials and Methods

2.1 Human skin biopsies and hair follicles

The samples were collected from healthy individuals (see appendices 5 and 6) with full consent and ethical approval from Cutech s.r.l. and Orthopaedic Clinic of Ospedale Civile of Padova, Italy and and University of Bradford, UK. Samples (Figure 13) were used for either RNA extraction or isolation of HFs or culture of primary cells such as DFs, EKs, DP and dermal sheath cells (DS). For RNA extraction, each sample was transported in RNA later (Ambion) or frozen in liquid nitrogen. For HF isolation, samples were transported in William's Medium E (Sigma) supplemented with penicillin/streptomycin (100U/ml and 100µg/ml) and amphotericin B (250µl/ml) until used within 24 hours. For cell culture, skin biopsies were kept in Dulbecco Modified Eagle's Medium (DMEM) (GIBCO, Invitrogen), stored at 4°C, and used within 24 hours of surgery.

2.2 Micro-dissection of hair follicles

Micro-dissection was performed using a Leica MZ8 stereomicroscope and Schott KL1500 cool light to isolate HFs from terminal haired skin (Figure 13 and 14). Skin samples were washed in PBS containing penicillin/streptomycin (100U/ml and 100µg/ml) and amphotericin B (250µl/ml) in a 100 mm culture dish. Then, the excess fat was removed using a sterile razor blade, forceps and needles to expose the hair bulb and the dermis was cut from the skin sample. Isolated HFs were either transferred to a 35mm culture dish containing William's Medium E to further separate the different components such as the DP and the DS for the propagation of primary cultures (see section *2.3.3* and *2.3.4*) or were immediately frozen in liquid nitrogen and then stored at -80°C for subsequent extraction of RNA (see section *2.12*).

2.3 Culture of primary skin and hair follicle cells

2.3.1 Epidermal keratinocytes

Non haired skin biopsies from fronto-temporal scalp, breast, abdomen and thigh (see appendices 7 and 8) were washed in phosphate buffered saline (PBS) containing amphotericine B (750µl/ml) for 5 min to remove blood and micro-organisms. Then, each sample was dissected removing excess fat and cut into small pieces of approximately 5x5 mm. Those pieces were placed with enough to cover the surface of a 35mm culture dish and incubated with dispase 2.4 U/ml overnight at 4°C. Then the plate was incubated at 37°C for 1 hour. To isolate the EKs, the sample was dissected to remove the epidermis from the dermis using sterile forceps and needles. The epidermis was washed in PBS with amphotericin B (250µl/ml) and transferred to a 5 ml universal tube containing 1 ml of 0.05 % trypsin/EDTA and incubated at 37° for 5-6 min. The tube was briefly vortexed and the trypsin/EDTA transferred into 10 ml of Keratinocyte-SFM (K-SFM) Medium (Invitrogen) containing 10% FCS. The medium containing the cells was centrifuged at 1,200 x *g* for 5 min. The supernatant was gently removed and then 1 ml of serum free K-SFM supplemented with epidermal growth factor (EGF, 0.05 µg/µl), bovine pituitary extract (BPE, 12.5 mg/ml), L-glutamine (10mM), penicillin/streptomycin (100U/ml and 100µg/ml) and amphotericin B (250µl/ml), was added to resuspend the pellet. The cells were transferred into a T25 culture flask with an additional 3 ml of serum free K-SFM. The medium was changed every 2-3 days until the cells were 70% confluent.

2.3.2 Dermal fibroblasts

Four or five pieces of remaining dermis were placed into a T75 culture flask containing 8 ml of DMEM supplemented with 20% fetal bovine serum (FCS), L-glutamine (10mM), penicillin/streptomycin (100U/ml and 100µg/ml) and amphotericin B (250µl/ml). Each flask was placed in a humidified incubator

at 37°C in 5% CO_2 in air and left undisturbed for 7-10 days to establish DF explants.

2.3.3 Dermal papillae cells

Isolated follicles were cleared of surrounding dermis (Figure 15). Gentle pressure was applied to the base of HF with the tip of a needle, which pushes the hair shaft out the DS. The follicular DP was then dissected from the DS, by making a slit in the DS next to the DP and manipulating the DS with needles to expose the DP. The DP was cut at the base where it joins the DS and transferred to a fresh 35mm dish containing 1ml DMEM growth medium supplemented with 20% FCS. A scratch was made with a needle, longitudinally through the centre of the DP to attach it to the dish and to encourage migration of the DP cells. At least six DPs were transferred into one 35mm dish and placed in groups of three close together to encourage migration of cells. The DPs were incubated undisturbed for 7 days at 37 °C with an atmosphere of 5% CO_2. After 7 days, explants were checked for cell migration and medium was refreshed by gently adding 1ml DMEM supplemented with 20% FCS. Once the cells had reached confluence (usually 2-4 weeks) around the explants (approximately 0.5-1cm in diameter) they were trypsinised (see section *2.7*) and resuspended in fresh growth medium supplemented with 20% FCS and transferred into a 25cm^2 flask. The cells were allowed to attach for 24 hours, before the medium was replaced. Medium was then changed every 2-3 days until the cells were 70% confluent. Thereafter, they were passaged with a split ratio of 1:3, trypsinised and frozen as described in section *2.8*.

2.3.4 Dermal sheath cells

Once the DP had been removed from the DS the individual DS (Figure 15) were transferred to a separate dish containing 1ml DMEM growth medium

supplemented with 20% FCS. Using a blade, a scratch was put through the DS to attach it to the base of the dish; at least six DSs were transferred into each dish. These dishes were incubated at 37°C with an atmosphere of 5% of CO_2 and left undisturbed for 7 days. After 7 days explants were checked for cell migration and the medium was refreshed by gently adding 1ml DMEM supplemented with 20% FCS. Once the cells had reached confluence (approximately 4-8 weeks) around the explant (approximately 0.5-1cm in diameter) they were trypsinised (see section *2.7*) and resuspended in fresh growth medium supplemented with 20% FCS and transferred into a $25cm^2$ flask. Cells were allowed to attach for 24 hours, before the medium was replaced. The medium was then changed every 2-3 days until the cells were 70% confluent. Thereafter, they were passaged with a split ratio of 1:3.

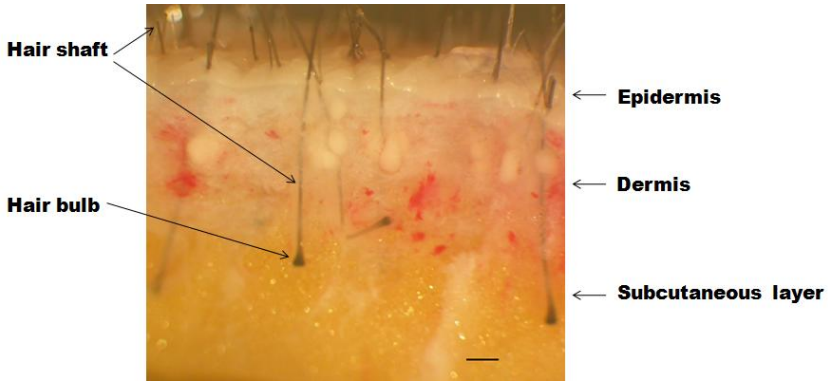

A

B

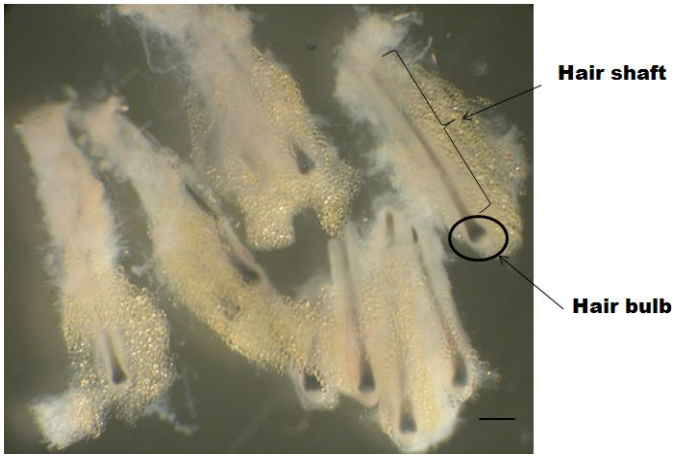

C

Figure 13. Human skin and hair follicle samples

Hairy skin samples were used for isolation of hair follicles (HFs) (A;C), scale bar = 1µm. Non hairy skin (B, scale bar = 1mm) samples were used for RNA extraction or culture of primary cells such as dermal fibroblasts (DFs), epidermal keratinocytes (EKs), dermal papilla (DP) and dermal sheath cells (DS).

Figure 14. Establish of primary cultures

Skin was dissected through the dermis, divided in small pieces (5x5 mm) and left undisturbed one week in a T75 culture flask (A), scale bar = 1mm. Epidermal keratinocytes (B), scale bar = 100µm and dermal fibroblasts (C), scale bar = 100µm were established from skin samples as described in section *2.3*.

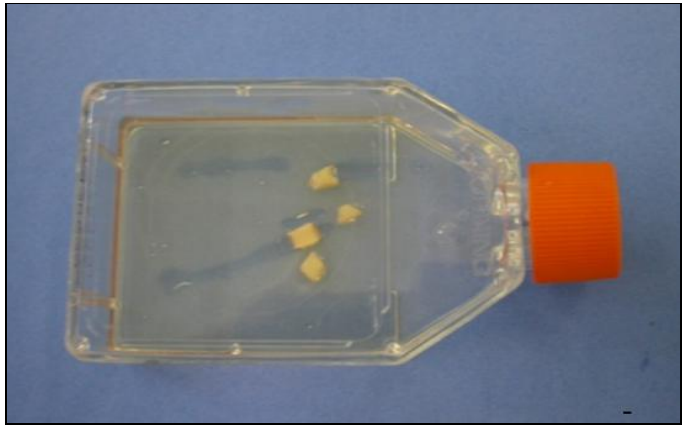

A

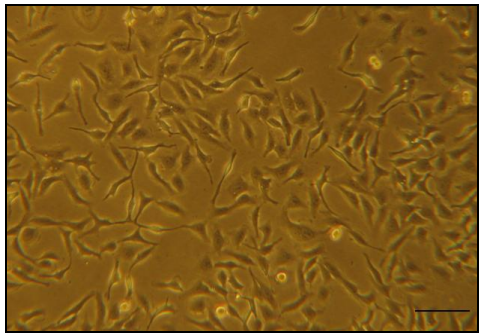

B

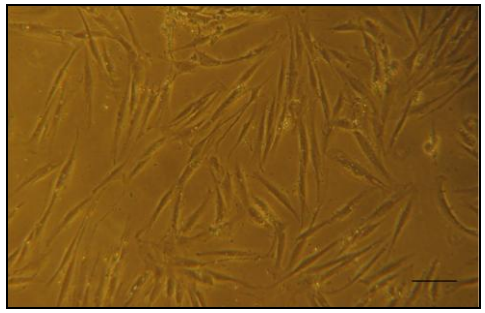

C

A

B

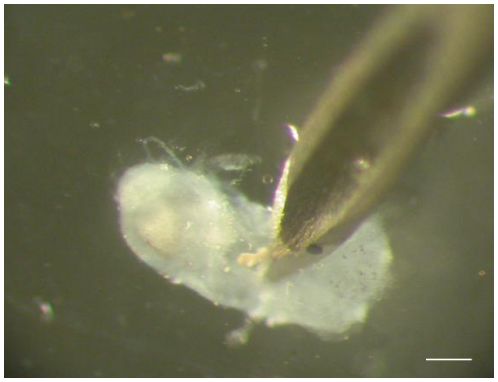

C

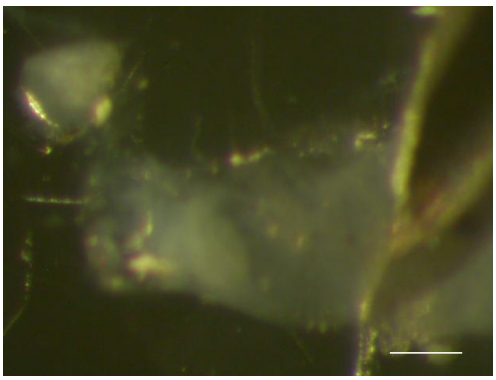

D

Figure 15. HF dissection

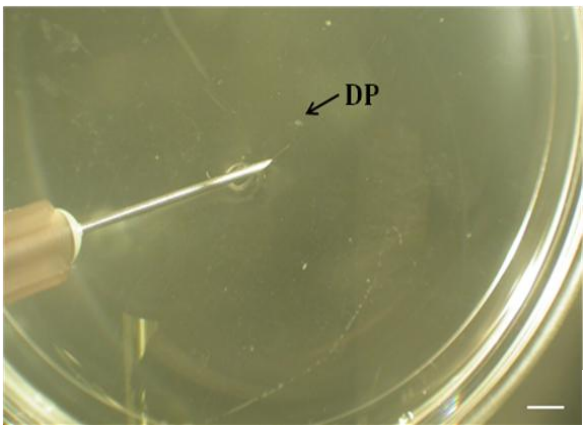

E

The isolated HF (**A**, scale bar=100µm) is cut at the level of the sebaceous gland. Pressure is applied using a needle at the base of the follicle and the hair shaft is pushed out of the DS. This leaves the follicular DP attached to the DS (**B**, scale bar=100µm). A slit is cut along the DS and the DS is manipulated to expose the DP this is cut along the base to leave the DP and DS separated (**C** and **D**, scale bar=100µm). On separation the DP and DS are transferred to different dishes. Once in the dish a scratch is put longitudinally through the DP to help to the DP attach to the dish and promote cell migration (**E**, scale bar=1mm). Similarly with the DS a scratch is put through to attach the DS to the dish and promote cell migration.

2.4 Maintenance of primary cultures

Once cell proliferation was established, the pieces of skin were discarded (in the case of DFs) and the medium was refreshed every 2-3 days, phenol red free DMEM for DFs, DP, and DS and K-SFM for EKs. Cell growth was checked every other day and the cells were passaged and transferred to T75 culture flask, at ratio 1:3 (DF, DP, and DS) or 1:2 (EK), when the confluence was 70%.

2.5 Human cell lines

Two experimental human keratinocyte cell lines, NCTC 2544 and HaCat, were used (data not shown). Both were grown in phenol red free DMEM supplemented with 10% FCS, L-glutamine (10mM), penicillin/streptomycin (100U/ml and 100µg/ml) and amphotericin B (250µl/ml). Human prostate cancer cell lines PC3 and DU145, provided by Dr. Giulio Fracasso of the Department of Pathology of Verona University, Italy) were used as positive control in some experiments (PC3 for the mRNA expression of 5α-reductase 1 and DU145 for 5α-reductase 2, see section *3.1*) and growth with RPMI-1640 (Invitrogen) supplemented with 5% fetal calf serum (FBS) and L-glutamine (2 mM).

2.6 Growth medium

To culture cells, DFs and DS were incubated in phenol red free DMEM supplemented with 10% FCS, L-glutamine (10mM), penicillin/streptomycin (100U/ml and 100µg/ml) and amphotericin B (250µl/ml). Keratinocytes were routinely cultured in K-SFM EGF/BPE supplemented with L-glutamine (10mM), penicillin/streptomycin (100U/ml and 100µg/ml) and amphotericin B (250µl/ml).

2.7 Passaging of cells

Once all cells reached 70% of cell confluence, they were passaged by trypsinization. The growth medium was removed and the cells were washed 3 times with PBS. Cells were incubated at 37°C for 3 min after adding 1-2 ml of trypsin/EDTA for 5 min. Following incubation, the culture flask was gently tapped for a better dissociation of cells from the plastic surface. Medium supplemented with 10% FCS was added to each flask to block the action of the trypsin. The cells were centrifuged at 1,200 x *g* for 5 min and then re-seeded into new culture flasks at ratio of 1:2 (EK) or 1:3 (DF, DP and DS). If not used immediately, cells were frozen in liquid nitrogen.

2.8 Freezing, thawing and re-seeding of cells

Cells were stored in liquid nitrogen once they had reached passage P2. Following trypsinisation, cells were centrifuged at 1,200 x *g* for 5 min. The cell supernatant was then discarded and the cell pellet re-suspended in 1ml DMEM or KSF with 20% FCS and 10% dimethylsulfoxide (DMSO). This was transferred into a criovial and frozen at -20°C for at least 1h, left at -80°C overnight and then stored in liquid nitrogen. If required, cells were thawed by removing from liquid nitrogen and quickly immersing in a water bath at 37°C until only a little piece of ice remained. Cells were then transferred in T75 culture flask and 10-12 ml fresh growth medium were added. After 24 hours, when cells had adhered to the flask, the medium was changed.

2.9 Cell counting

After trypsinization, cells were counted by using a Neubauer haemocytometer. Cell suspension (20 µl) was pipetted into each grid of a haemocytometer. The number of cells was counted within the four boxes of the grid. The total number was divided by four and multiplied per 10^4

obtaining number of cells per ml of suspension. Then, the total number of cells could be calculated.

2.10 Experimental growth medium

To perform experiments where the cells were treated with steroids, all cells were incubated in phenol red free and serum free medium. Phenol red and serum free DMEM was supplemented with L-glutamine (10mM), penicillin/streptomycin (100U/ml and 100µg/ml) and amphotericin B (250µl/ml) for DF, and EPILIFE CF/PRF (Invitrogen) was supplemented with L-glutamine (10mM), penicillin/streptomycin (100U/ml and 100µg/ml) and amphotericin B (250µl/ml) for EK.

2.11 Positive control

cDNA of human adrenal gland, liver, ovary, placenta and the human prostate cancer cell lines DU145 and PC3 were used as positive controls and to verify quality and specificity of primers for genes of interest as described in the following table 1.

cDNA	Target gene
Adrenal gland	P450scc and P450c17
Liver	OATP2B1
Ovary	P450arom
Placenta	STS
DU145	5α-reductase 2
PC3	5α-reductase 1

Table 1. Tissues used as positive control for RT-PCR reactions.

2.12 Total RNA extraction

The total RNA was extracted from whole skin biopsies and HF with TRIzol and from cultured cells with the column method.

2.12.1 RNA extraction by TRIzol

Total RNA was extracted from human skin biopsies (5 x 5 mm) and HFs (n=21 per donor) using TRIzol® reagent (Invitrogen) according to the manufacturer's instructions. Each sample of either skin biopsies or HFs was homogenized in 1 ml of TRIzol® Reagent per 50-100 mg of tissue using a mortar and pestle for skin and a bead-beater for HFs. Then, each homogenized sample was incubated for 5 min at 15-30°C to permit the complete dissociation of nucleoprotein complexes. Chloroform (200 µl per 1 ml of TRIzol® Reagent) was added to the homogenates. The tubes were shaken vigorously by hand for 15 s, incubated for 2-3 min at room temperature for 2-3 min and centrifuged at 12,000 x *g* for 15 minutes at 4°C. Following centrifugation, the mixture was separated into a lower red phase, an interphase and a colorless upper aqueous phase. The RNA remains exclusively in the aqueous phase. The aqueous phase was transferred to a fresh tube and 500 µl of isopropanol was added to each tube to precipitate the RNA. The tubes were incubated at -20°C for at least 2 h. After incubation, the samples were centrifuged at 12,000 x *g* for 15 min at 4°C. The supernatants were carefully removed and the RNA pellets were washed twice by adding 500 µl of 70% ethanol and centrifuging at 7,500 x *g* for 15 min at 4°C. The RNA pellets were dried inside the chemical hood for about 5-10 min and re-dissolved in 20-30 µl of nuclease-free H_2O. Then, the total RNA extracted was successively purified by using RNeasy® Mini Kit (QIAGEN) according to the manufacturer's instructions by starting from the step 2 as described in section *2.12.2*. In this case, total RNA was adjusted to 100 µl with RNase free water and then to a final volume of 700 µl by adding 350 µl of

Buffer RLT/ß-mercaptoethanol and 250 µl of ethanol. The RNA samples were stored at -80°C.

2.12.2 Total RNA extraction by column

Total RNA was extracted from the cultured cells using a protocol based on the RNeasy® Mini Kit Isolation System (QIAGEN) according to the manufacturer's instructions.

Up to 1 x 10^6 cells were disrupted by adding directly 600 µl Buffer RLT (previously mixed with ß-mercaptoethanol) to the cell culture dish or flask. The lysate was collected in a microcentrifuge tube and homogenized by vortexing. One volume of 70% ethanol was then added to the lysate, creating conditions that promote selective binding of RNA to the RNeasy membrane. The sample was then applied to the RNeasy Mini column placed in a 2 ml collection tube and centrifuged for 15 s at 10,000 rpm at RT. The flow-through was discarded and total RNA was bound to the membrane. Buffer RPE (500 µl) was added to the RNeasy column. Then, sample was centrifuged for 15 s at 10,000 rpm at RT to wash the column membrane. The flow-through was discarded. Subsequently, another 500 µl of Buffer RPE was added to the RNeasy column. The sample was centrifuged for 2 min at 10,000 rpm at RT to wash the spin column membrane. The flow-through was discarded. The RNeasy column was placed in a new 2 ml collection tube and centrifuged at full speed for 1 min. The RNeasy column was placed in a new 1.5 ml collection tube. RNase-free water (30 µl) was added directly to the column membrane. The sample was centrifuged for 1 min at 10,000 rpm to elute the RNA. To obtain a higher RNA concentration, the previous step was repeated using the eluate. RNA was stored at – 80 °C before use.

2. 13 Quantification and quality control of total RNA

The concentration of total RNA was measured by using NanoDrop (CELBIO) or NanoVue (GE Healthcare Life Sciences at Skin Centre of University of Bradford, Bradford, UK) spectrophotometer which also gives an evaluation of the purity of the RNA according to the following optical density (O.D.) ratios:

$$\frac{O.D._{260}}{O.D._{280}} \geq 1.8 \quad \text{and} \quad \frac{O.D._{260}}{O.D._{230}} \geq 2$$

In particular, high quality RNA is a key factor for microarray. For this reason, once total the RNA was extracted from the samples, its integrity was analyzed using Agilent 2100 Bioanalyzer at Centro MicroCribi, Dipartimento A. Vallisneri, Padova, Italy. The RNA integrity number (RIN) was analyzed by using 200 ng/µl of total RNA. Only RNA with (RIN) ≥ 7 was used for microarray.

2.14 DNase treatment

To eliminate any possible contamination of DNA, total RNA was treated by using Deoxyribonuclease I, Amplification Grade (Invitrogen).
To a microcentrifuge tube on ice the following were added:

Component	Amount
RNA sample	1 µg
10X DNase I Reaction Buffer	1 µl
DNase I, Amp Grade	1 U/µl 1 µl
DEPC-treated water	to 10 µl

Table 2. DNase treatment mix.

Each tube was incubated for 15 min at room temperature. Then, 1 µl of 25 mM EDTA was added to inactivate the DNase I. The tubes were heated for 10 min at 65°C. Following this final step, each RNA sample was then reverse transcribed before amplification.

2.15 Reverse transcription of total RNA

Reverse transcription of total RNA was performed using either ThermoScript™ RT-PCR system (Invitrogen) or ImProm-II Reverse Transcription System (Promega) according to the manufacturer's instructions.

2.15.1 ThermoScript™ RT-PCR system (Invitrogen)

The ThermoScript™ RT-PCR System is designed for the sensitive, reproducible detection and analysis of RNA molecules in a two-step process. Two micrograms of the purified total RNA was mixed with Mix I reaction (see table 3), denatured by incubating at 65°C for 5 min and then placed on ice for 5 min. Then, 8 µl of Mix II (see table 4) was added to each sample. The samples were incubated at 25°C for 10 min, 55°C for 45 min and 85°C for 5 min. Then, 1 µl of Rnase H (2 U/µl) was added and the mix was incubated at 37°C for 20 min. The cDNA reactions were either stored at -20°C or used for PCR immediately.

Mix I reaction

Component	Amount
Random hexamers (50ng/µl)	1 µl
Total RNA	1 µl
dNTP Mix (10 mM)	2 µg
dNTP Mix (10 mM)	2 µl
DEPC-Treated Water	to 12 µl

Table 3. First mix reaction.

Mix II reaction

Component	Amount
cDNA Synthesis Buffer (5X)	4 µl
DTT (0.1 M)	1 µl
RNaseOUT (40 U/µl)	1 µl
ThermoScript RT (15 U/µl)	1 µl
DEPC-Treated Water	1 µl

Table 4. Second mix reaction.

2.15.2 ImProm-II Reverse Transcription System (Promega)

cDNA was synthesised according to the manufacturer's instructions. Briefly, 1 µg of the purified total RNA was mixed with Mix I reaction (see table 5), denatured by incubating at 70°C for 5 min and then placed on ice for 5 min. After cooling, 15 µl of Mix II (see table 6) was added to each sample. The samples were incubated at 25°C for 5 min, 42°C for 60 min and 70°C for 15

min. The cDNA synthesis reactions were stored at -20°C or used for PCR immediately.

Mix I reaction

Component	Amount
Random hexamers (500µg/ml)	1 µl
Total RNA	1µg
Nuclease-free Water	to 5 µl

Table 5. First mix reaction.

Mix II reaction

Component	Amount
ImProm-II™ Reaction Buffer (5X)	4 µl
$MgCl_2$ (25 mM)	2.4 µl
dNTP Mix (10 mM)	1 µl
Recombinant RNasin® Ribonuclease Inhibitor (40U/µl)	0.5 µl
ImProm-II™ Reverse Transcriptase	1 µl
Nuclease-free Water	to 15 µl

Table 6. Second mix reaction.

2.16 DNA Amplification by Polymerase Chain Reaction (PCR)

PCR is a method used to amplify a specific region of a DNA strand. Biotherm Taq polymerase (Società Italiana Chimici, SIC, Rome, Italy) was used for the PCR amplifications. BioTherm™ Taq DNA Polymerase exhibits deoxynucleotidyl transferase activity, which frequently results in the addition of extra adenines at the 3'-end of PCR products. This property allows easy and efficient ligation of PCR products in the cloning vectors (see section *2.20*). Total cDNA (usually corresponding to 100 ng of total RNA) was amplified by PCR containing a mix reaction (see table 7) to a final volume of

25 µl. For each PCR, a negative control was prepared by replacing the cDNA solution with sterile water to check for cross-contamination. PCR products for each gene of interest were sequenced to confirm amplicon identity. In addition, to check whether the PCR generated the anticipated DNA fragment, 10 µl of each product was analyzed by agarose gel electrophoresis (see section *2.23*). For cloning of the amplified PCR products, DNA fragments of interest were excised from the gel and isolated as described in section *2.17*. The PCR reactions were stored at -20°C.

Mix reaction

Component	Amount
Buffer Biotherm 10X	1X
$MgCl_2$ (50 mM)	1.5 – 2 mM
dNTPs Mix (10 mM)	0.2 mM
Forward primer (10 µM)	0.2 µM
Reverse primer (10 µM)	0.2 µM
Taq Biotherm (U/µl)	1.25 U
cDNA	100 ng
Nuclease free water	to 25 µl

Table 7. PCR mix reaction.

Steps of reaction

Repeat	Step	Time	Temperature
1	Inizialization	2 min	95 °C
40	Denaturation	30 s	95 °C
	Annealing	30 s	variable (see table10)
	Extension	variable (see table10)	72 °C
1	Final extension	20 min	72 °C
1	Final hold	2 min	10 °C

Table 8. PCR conditions.

Each cDNA sample was amplified using specific forward and reverse primers that were derived from mRNA sequences contained in the NCBI database (www.ncbi.nlm.nih.gov). These primers (see table 9) were designed to cross exon/exon boundaries of coding regions in order to prevent co-amplification of genomic DNA, which may compromise assay specificity and dynamic range. β-actin was used as housekeeping gene to verify the quality of cDNA synthesis.

Primer		Sequence	Position*	Accension number
STS-5	sense	5'-ACCCTCATCTACTTCACAT-3'	1206→1224	J04964
STS-2	antisense	5'-GTCCATGTTGCTAGTGGGCT-3'	1409→1390	J04964
Q-scc-hum-1	sense	5'-AAGACTTCACCCCATCTCCGTGAC-3'	1199→1222	M14565
Q-scc-RH-2	antisense	5'-ACCCCAGCCAAAGCCCAAGT-3'	1418→1399	M14565
Q-c17-hum-1	sense	5'-CAATGAGAAGGAGTGGCACCA-3'	1263→1283	NM_000102
Q-c17-hum-2	antisense	5'-CTTTGAAAGAGTCGATCAGAAAGAC-3'	1531→1507	NM_000102
Q-Aro-hum-1	sense	5'-GAATCGGGCTATGTGGACGTGTTG-3'	590→613	Y07508
Q-Aro-hum-2	antisense	5'-AGATGTCTGGTTTGATGAGGAGAG-3'	749→726	Y07508
5α-red-1-F	sense	5'-CATGTTCCTCGTCCACTACG-3'	457→476	NM_001047
5α-red-1-R	antisense	5'-GATGCTCTTTTGCTCTACCAG-3'	899→879	NM_001047
5α-red-2-F	sense	5'-CCTCTTCTGCCTACATTACTTCC3'	326→348	NM_000348
5α-red-2-R	antisense	5'-CCAGAAACATACGTAAACAAGCC-3'	643→620	NM_000348
OATP-B5	sense	5'-AGCTGTCTGTCGCTACTAC-3'	2086→2104	AB026256
OATP-B8	antisense	5'-CCCAAGACAGCTCACACTC-3'	2319→2301	AB026256
ERα	sense	5'-CAGACATGAGAGCTGCCAAC-3'	1945 →1162	M12674
ERα	antisense	5'-CCAAGAGCAAGTTAGGAGCA-3'	15321 →1504	M12674
ERß	sense	5'-TCCCTGGTGTGAAGCAAGATC-3'	1610 →1590	AB006589
ERß	antisense	5'-CGCCGGTTTTTATCGATTGT-3'	1868 →1849	AB006589
AR	sense	5'-AAGAGGAACAGCAGCCTTCACA-3'	789→810	BC132975.1
AR	antisense	5'-ATGGGGCAGCTGAGTCATCCT-3'	941→921	BC132975.1
ß-actin-1	sense	5'-CACCAACTGGGACGACATGGAG-3'	303→324	BC013380
ß-actin-2	antisense	5'-GGCCTGGATGGCCACGTACAT-3'	409→469	BC013380

Table 9. Forward and reverse primers used for RT-PCR reactions. *Nucleotide position in the reported sequence.

Target Gene	Primers	Size bp	[Mg++]	Annealing (°C)	Extension (s)
STS	STS-5 STS-2	204	1.5 mM	56	20
P450c17	Q-c17-hum-1 Q-c17-hum-2	269	1.5 mM	60	25
P450scc	Q-scc-hum-1 Q-scc-RH-2	220	1.5 mM	60	25
P450arom	Q-Aro-hum-1 Q-Aro-hum-2	160	1.5 mM	60	20
5α-reductase 1	5red-1-F 5red-1-R	443	1.5 mM	58	30
5α-reductase 2	5red-2-F 5red-2-R	318	1.5 mM	58	30
OATP2B1	OATP-B5 OATP-B8	234	1.5 mM	58	20
ERα Taylor *et al.* (2001)	Erα-F Erα-R	381	1.5 mM	60	30
ERß Mesiano *et al.* (2002)	ERß-F ERß-R	279	1.5 mM	60	30
AR	AR-F AR-R	153	1.5 mM	64	15
β-actin	Q-Beta-1 Q-Beta-2	187	1.5 mM	60	15

Table 10. Target genes, primers and RT-PCR conditions.

2.17 DNA extraction from agarose gels

Fifty microlitres of the PCR products were run on a 1% agarose gel (see section *2.23*) and the desired fragments were cut out from the gel under UV light. Then, the gel slices were purified with Zymoclean Gel DNA Recovery Kit™ (ZYMO RESEARCH), as described in the manufacturer's manual.
The DNA fragment of interest was excised from the agarose gel using a razor blade and transferred into a 1.5 ml microcentrifuge tube. Three volumes of ADB buffer were added to each volume of agarose excised from the gel (e.g. for 100 µl (mg) of agarose gel slice add 300 µl of ADB). The sample was incubated at 50°C for 5-10 minutes until the gel slice was completely dissolved. To help dissolve the gel, the tube was vortexed every 2–3 min during the incubation. The melted agarose solution was transferred into a Zymo-Spin™ Column in a collection tube and centrifuged at ≥10,000 x *g* for 30 sec. The flow-through was discarded, 200 µl of wash buffer was added to the column and centrifuged at ≥10,000 x *g* for 30 sec. The flow-through was discarded and the wash step was repeated. DNase free water (12 µl) was added directly to the column matrix. The column was then placed into a 1.5 ml tube and centrifuged at ≥10,000 x *g* for 60 sec to elute DNA. The sample was stored at -20°C.

2.18 PCR Product Clean-Up by ExoSAP-IT®

When a single band was visualized on the agarose gel, it was purified by ExoSAP-IT® (ExonucleaseI/Shrimp Alcaline Phosphatase Method) of USB Corporation. The PCR product was mixed with 2 µl of Exosap-IT in a final volume of 5 µl. Then, the reaction was carried out as follow:

Degradation of primers and nucleotides	37°C	for	15 min
Enzyme inactivation	80°C	for	15 min
Hold final	4°C	for	10 min

Following hold final, 2 µl (3.2 pmol) of specific primer was added to the DNA sample for sequencing.

2.19 DNA sequencing

DNA sequencing was performed by BMR Genomics (Padova, Italy). For this purpose a mix containing the specific primer (3.2 pmol) and the required amount of purified DNA was prepared. The mix was dried at 65°C and then delivered to BMR for sequencing.

2.20 Cloning

2.20.1 Ligation

The DNA fragments were ligated into pGEM®-T Easy vector using the pGEM®-T Easy vector system (Promega), according to the manufacturer´s instruction manual. The appropriate amount of DNA fragments to include in the ligation reaction was calculated by the following equation:

$$\frac{\text{ng of vector} \times \text{kb size of insert}}{\text{kb size of vector}} \times \text{insert:vector molar ratio} = \text{ng of insert}$$

The reaction is usually settled as follow:

Component	Amount
2X rapid ligation buffer, T4 DNA ligase	5 µl
pGEM®-T Easy vector (50 ng)	1 µl
PCR product	X µl
T4 DNA ligase (3 U/ µl)	1 µl
Nuclease-free water	to 10 µl

Table 11. Ligation mix.

The reaction was incubated at 4°C overnight and then used to transform chemically competent bacteria (Promega, JM109 Cat.# L2001).

2.20.2 Bacterial transformation

To obtain transgenic bacteria, DNA plasmids from the ligation step were transferred into competent *E. coli* cells (JM109 from Promega) by heat shock induced transformation.
Briefly, competent cells were thawed on ice, mixed with 2 µl of the ligation reaction and incubated on ice for approximately 30 min. The suspension was then heated to 42°C for 30-40 s.
Subsequently the suspension was incubated on ice for 1 min; 250 µl of S.O.C. medium (see appendix 3) were added and the sample was shaken at 37°C for 1 h. The ampicillin LB-Agar plates were prepared with 80 µl of X-Gal (20 mg/ml) and 100 µl of the inductor IPTG (0.1 M) and equilibrated at RT. Subsequently, 50 µl and 100 µl of the transformation culture were plated onto LB-plates that were incubated at 37°C overnight. Bacteria carrying a plasmid without the insert possess a functional ß-galactosidase gene and produce blue colonies due to the X-Gal reaction. In contrast, bacteria containing a plasmid with the insert of interest have a disrupted β-galactosidase gene and produce white colonies (as described in the Technical Manual, Promega).

2.20.3 Identification of positive colonies by PCR reaction

Single white colonies were picked from the plates with pipette tips. The single colony present on the tip was streaked onto a fresh replicate LB-plate and also added to the PCR Mix I (see table 12). The PCR tubes were incubated at 98°C for 10 min to destroy the bacterial cells. Then the PCR mix II (see table 13), containing the Taq polymerase, was added.
The reaction was performed as described in table 14.

PCR Mix I

Component	Amount
10X buffer reaction	2 µl
$MgCl_2$ (50 µM)	1 µl
dNTPs (10mM)	0.6 µl
Biotherm Taq (1.25 U)	0.2 µl
Nuclease-free water	to 10 µl

Table 12. PCR first mix.

PCR Mix II

Component	Amount
Primer Forward (10µM)	0.6 µl
Primer Reverse (10µM)	0.6 µl
Nuclease-free water	to 20 µl

Table 13. PCR second mix.

Steps of reaction

Repeat	Step	Time	Temperature
1	Inizialization	2 min	95 °C
35	Denaturation	45s	95 °C
	Annealing	1min 10sec	55°C
	Extension	2 min	72 °C
1	Final extension	20 min	72 °C
1	Final hold	2 min	10 °C

Table 14. PCR conditions.

2.21 Purification of plasmidic DNA (miniprep)

Plasmidic DNA that contained the insert of interest was purified by plasmid minipreparation using high pure plasmid isolation kit (Roche) according to the manufacturer's instructions. Briefly, single cell colonies were cultured in 5 ml of LB-medium supplemented with 50 µg/ml ampicillin, and incubated on a shaker (200 rpm) at 37°C for 16 h. The bacteria were separated from the medium by centrifugation of 5 ml of each culture into 2 ml tubes at ≥10,000 x *g* for 1 min. The pellets were chemically treated to separate the bacterial chromosomal DNA and proteins from the plasmid DNA. This was eluted with 30 µl of nuclease-free water and then further characterized by sequencing (see section *2.19*).

2.22 Quantitative Real-Time Polymerase Chain Reaction (qRT-PCR)

2.22.1 Absolute quantification

Reverse transcriptase reactions were carried out with 2 µg of total RNA combined with random primers and ThermoScript™ RT-PCR System (see section *2.15.1*). To create the standard curves for absolute qRT-PCR, sequenced PCR products were cloned into the pGEM-T Easy vector (see section *2.20*). The copy numbers of the plasmid DNA templates were calculated according to the plasmid molecular weight and then converted into copy numbers on the basis of Avogadro's number.

Serial dilutions of 10^8–10^2 plasmids/µl were used to generate the calibration curves. qRT-PCR analysis was performed on the same RNA derived from the skin (see appendix 5) and HF (see appendix 6) samples used for RT-PCR. All samples were analyzed in triplicate in 25 µl volume using qPCR Master Mix Plus No ROX kit (Eurogentec).

PCR Mix

Component	Amount
Reaction Buffer 10X No Rox	2.5 µl
$MgCl_2$ (50 mM)	1.5 µl
dNTPs (10mM)	0.5 µl
Primer forward	0.5 µl
Primer reverse	0.5 µl
SYBR Green I	0.75 µl
Taq Hot Goldstar	0.125 µl
cDNA	x µl (see the note *)
Nuclease free water	to 25 µl

Table 15. qRT-PCR mix.

* 4µl of plasmid for standard curves
2 µl of cDNA per each sample (200 ng of total RNA)
nuclease free water as negative control

PCR reactions were performed with the Rotor Gene 6000 (Corbett) at Cutech Padova, Italy. Real-time PCR conditions were optimized after trying various times and temperatures for each cycling step as well as by establishing the concentrations of $MgCl_2$ (3 mM - 6 mM), forward and reverse primers (0.2 µM) and temperature of annealing (56°C – 60°C).
The reaction conditions were performed as described in table 16.

Steps of reaction

Repeat	Step	Time	Temperature
1	Taq activation	10 min	95 °C
40	Denaturation	30s	95 °C
	Annealing /Exstension	variable (see table10)	variable (see table10)
1	Final hold	2 min	10 °C

Table 16. qRT-PCR conditions.

Threshold values for threshold cycle (C_t) determination were generated automatically by the Rotor Gene 6000 Series software 7.1. Specificity of the reaction was checked by analysis of the melting curve of the final amplified product (Figure 29). The results were reported as expression, after normalization, of the transcript amount with respect to the reference gene (ß-actin).

2.22.2 Relative quantification

The relative qRT-PCR for mRNA was performed with the QuantiTect SYBR Green PCR Kit (QIAGEN) and the iQ Real-Time PCR Systems (Bio-Rad) at Centre for Skin Sciences, University of Bradford, UK. PCR predesigned primers (QIAGEN) (table 19) were used according to the conditions shown in table 18.

PCR Mix

Component	Amount
PCR Master Mix	12.5 µl
QantiTect primer assay	2.5 µl
cDNA	1 µl
Nuclease free water	to 25 µl

Table 17. qRT-PCR mix.

Steps of reaction

Repeat	Step	Time	Temperature
1	Taq activation	15 min	95 °C
40	Denaturation	1 min	95 °C
	Annealing	30 sec	58 °C
	Extension	20 sec	72 °C

Table 18. qRT-PCR conditions.

For each gene of interest, qRT-PCR was performed in triplicate. Differences between samples and controls were calculated using the REST 2009 V2.0.13 software (QIAGEN) based on the *Ct* ($^{\Delta\Delta}Ct$) equitation method and normalized to the corresponding reference gene, GADPH values.

Primer	Gene Symbol	Accession numer	Amplicon length
Hs_TXNIP_1_SG QuantiTect Primer Assay	*TXNIP*	NM_006472	109 bp
Hs_LMNB1_1_SG QuantiTect Primer Assay	*LMNB1*	NM_005573	79 bp
Hs_ANGPTL4_1_SG QuantiTect Primer Assay	*ANGPTL4*	NM_016109	89 bp
Hs_CXCL1_1_SG QuantiTect Primer Assay	*CXCL1*	NM_001511	120 bp
Hs_GAPDH_2_SG QuantiTect Primer Assay	*GAPDH*	NM_002046	119 bp

Table 19. PCR predesigned primers (QIAGEN).

2.23 Agarose gel electrophoresis

DNA samples, obtained from the miniprep and PCR reactions, were analyzed by agarose gel electrophoresis. According to their presumptive size, samples were loaded on 1-1.5% agarose gel in TAE 1X containing ethidium bromide or GelRed™ (Biotium, SIC) both diluted 1:20,000. The resulting bands were photographed in a UV chamber supplemented with a camera.

2.24 DNA Microarray Gene Expression (Two-Color)

Agilent Technologies DNA microarray was used in this work and in particular on the whole genome with 4x44K array slides (Figure 16). The microarray experiment was carried out using total RNA extracted from primary keratinocytes and individual HFs. For the cells, "Two-Color Microarray-Based Gene Expression Analysis" (Agilent Technologies, USA) was used, as shown in figure 17. In contrast, RNA extracted from HFs was analyzed by Miltenyi Biotec, in Germany. In this case, the experiment was performed using protocol "One-Color" (Agilent Technologies, USA) and only the Cy3-labeled sample was produced and hybridized.

In addition, the scanning slide was performed on an Agilent G2565BA microarray scanner of Prof. Giovanni Abatangelo of Dipartimento di Biologia Vallisneri, Padova, Italy.

Only the two color method is described below. Regarding the one color procedure, the results and the analysis data will be reported in Results (see section *3.4.6*) and Discussion (see section *4.3.2*).

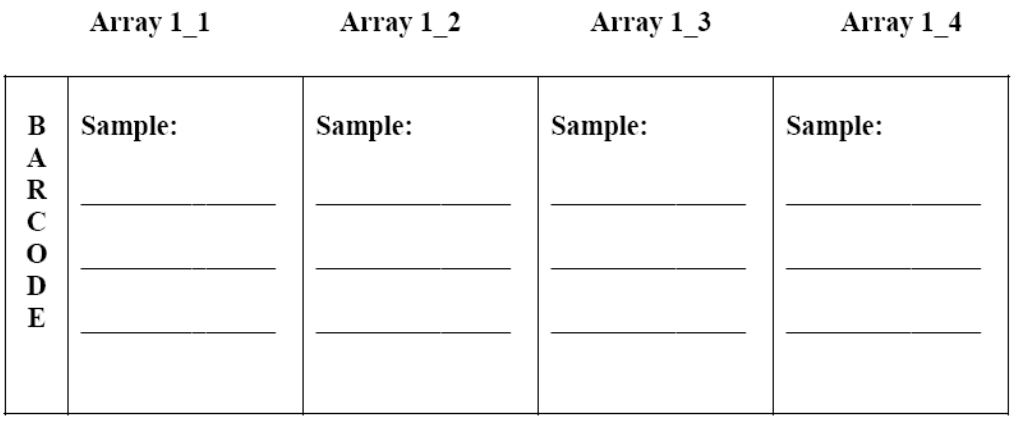

Figure 16. Agilent 4x44K array slide

The images are adapted from Two-Color Microarray-Based Gene Expression Analysis Quick Amp Labeling manual.

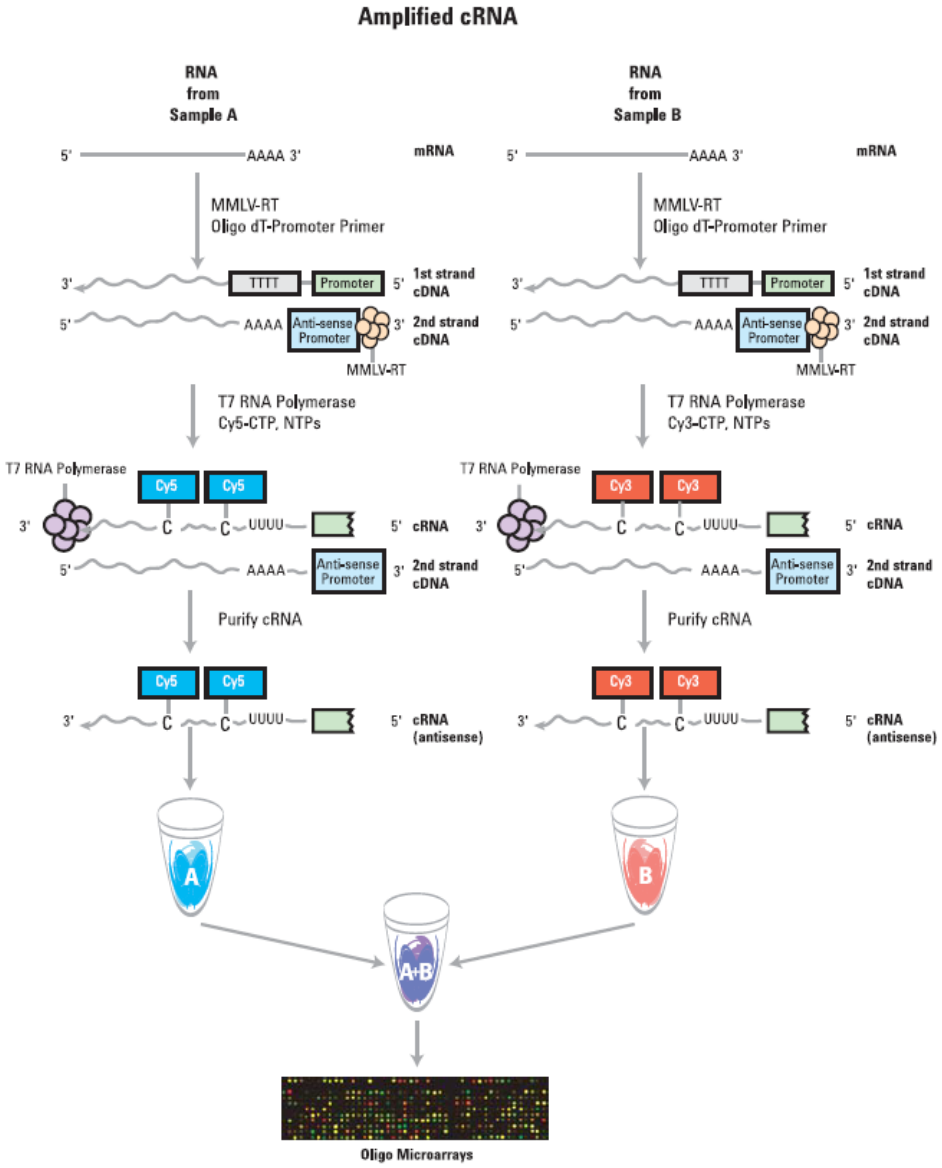

Figure 17. Schematic of amplified cRNA procedure

Generation of cRNA for a two-color microarray experiment is shown. When one-color microarray experiments are performed, only the Cy3-labeled "B" sample is produced and hybridized.

2.24.1 Quantity and Quality assessment of template RNA

The integrity of the RNA was determined using the Agilent 2100 bioanalyzer at MicroCribi of Dipartimento di Biologia Vallisneri of Padova, as described in section *2.13*. For the assessment of total RNA quality, the Agilent 2100 Expert Software automatically provided a RNA Integrity Number (RIN). Only RNA with RIN ≥ 7 was used.

2.24.2 Preparation of Spike A Mix and Spike B Mix

First of all, three dilutions of Spike A Mix and Spike B Mix were prepared for the starting sample ranges of total RNA, as shown in table 20. The first dilution of the Agilent Spike Mix (A or B) was stored for up to 2 months at –80°C. On the other hand, the second and third dilution tubes were discarded after use.

Starting amount of RNA	Serial dilution			Spike A or Spike B Mix volume to be used
Total RNA	First	Second	Third	
201-2000 ng	1:20	1:40	1:4	2 µl

Table 20. Dilutions of Spike A Mix for cyanine 3 and Spike B Mix for cyanine 5 labeling.

2.24.3 Preparation of labeling reaction

A starting sample of 500 ng of total RNA was added to a 1.5 ml microcentrifuge tube in an volume of 8.3 µl. Successively, 1.2 µl of T7 Promoter Primer and 2 µl Spike A Mix/cyanine 3-CTP or Spike B Mix/cyanine 5-CTP dyes were added, as shown in table 21.

RNA volume	Dilute Spike A (or B) Mix amounts	T7 promoter primer	Total volume
8.3 µl	2 µl	1.2 µl	11.5 µl

Table 21. Template (RNA Spike A or B Mix) and T7 Promoter Primer Mix.

Each sample was incubated at 65°C for 10 min to denaturate the primer and the template. After that, the reactions were placed on ice for 5 min.

2.24.4 Synthesis of cDNA double strand and labeling of cRNA

The template was mixed with 8.5 µl of the cDNA Master Mix (table 22). The samples were incubated at 40°C for 2 h, 65°C for 15 min and then placed on ice for 5 min. Successively, the components listed in table 23 were mixed in the order indicated for the Transcription Master Mix at room temperature. The Transcription Master Mix (60µl) was added to each sample tube, gently mixed by pipetting and incubated at 40°C for 2 h.

Components	Vomume per reaction
5X first strand buffer	4 µl
0.1M DTT	2 µl
10mM dNTP mix	1 µl
MMLV-RT	1 µl
RNase OUT	0.5 µl
Total volume	8.5 µl

Table 22. cDNA Master Mix.

Components	Vomume per reaction
Nuclease free water	15.3 µl
4X transcription buffer	20 µl
0.1M DTT	6 µl
NTP mix	8 µl
50% PEG	6.4 µl
RNase OUT	0.5 µl
Inorganic pyrophosphatase	0.6 µl
T7 RNA Polymerase	0.8 µl
Cyanine 3-CTP or cyanine 5-CTP	2.4 µl
Total volume	60 µl

Table 23. Transcription Master Mix.

2.24.5 Purification of labeled/amplified RNA

Qiagen's RNeasy mini spin columns (see section *2.12.2*) were used for the purification of the amplified cRNA samples.

2.24.6 Quantification of cRNA

cRNA was quantitated using a NanoDrop Spectrophotometer (CELBIO). Absorbance ratios 260/280 nm and 260/230 nm were measured to check a good quality (≥ 2) of samples. In addition, cyanine 3 or cyanine 5 dye concentration (pmol/µl) was measured and the specific activity of each reaction was determined as follow:

(Concentration of Cy3 or Cy5/Concentration of cRNA)* 1000 = pmol Cy3 or Cy5 per µg cRNA

2.24.7 Hybridization

For every sample, each of the components indicated in table 24 were added to a 1.5 ml free microfuge tube, mixed thoroughly but gently. Successively, samples were incubated at 60°C for 30 min to fragment the RNA.

Components	Vomume/Mass 4x44k
Cyanine 3-labeled, linearly amplified cRNA	825ng
Cyanine 5-labeled, linearly amplified cRNA	825ng
10X blocking agent	11 µl
Nuclease free water	bring volume to 52.8 µl
25X fragmentation buffer	2.2 µl
Total volume	55 µl

Table 24. Fragmentation mix for 4x44K microarrays.

Then, a 2x GEx Hybridization Buffer HI-RPM was added to the 4x44K array format at the appropriate volume to stop the fragmentation reaction. See table 25.

	Volume per hybridization
Components	**4x44k**
cRNA from fragmentation mix	55µl
2x GEx hybridization buffer HI-RPM	55µl

Table 25. Hybridization mix.

Tubes were briefly centrifuged for 1 min at RT at 13,000 rpm to drive the sample off the walls and lid and to aid in the reduction of bubbles. Successively, samples were placed on ice and loaded immediately onto the gasket well by dispensing the volume of hybridization sample (see table 26).

	Volume per hybridization
Components	**4x44k**
Volume prepared	110 µl
Hybridization sample volume	110 µl

Table 26. Hybridization.

The assembled "sandwich slide" was placed in a hybridization rotator set to rotate at 10 rpm. The hybridization was performed at 65°C for 17 h.

2.24.8 Washing of the microarray slide

The washing equipment was previously cleaned with milliQ water and sterilized at 200°C and Gene Expression Wash Buffer 2 was prewarmed at 37°C the night before washing arrays were performed.
First of all, the sandwich slide was disassembled in Gene Expression Wash Buffer 1 (dish 1). Successively, it was washed by following the conditions as indicated in table 27.

	Dish	Wash Buffer	Temperature	Time
Disassembly	1	GE Wash Buffer 1	Room temperature	-
1st wash	1	GE Wash Buffer 1	Room temperature	1 min
2nd wash	3	GE Wash Buffer 2	37°C	1 min

Table 27. Wash conditions.

2.24.9 Scanning, Feature Extraction and Microarray data analysis

The microarray slide was immediately scanned to minimize the impact of environmental oxidants on signal intensities. Feature extraction was carried out by using GE2-v5_95_Feb07 Software. Successively, analysis data was performed with TM4 package, TIGR MIDAS (Microarray Data Analysis System) software and Microsoft Excel. HFs data files were analyzed using the Rosetta Resolvera gene expression data analysis system (Rosetta Biosoftware).The functional grouping was performed by the Miltenyi Biotec team.

2.25 Migration of dermal fibroblasts and keratinocytes following mechanical wounding *in vitro*

To analyze the effect of steroid hormones on fibroblasts and keratinocytes, cell migration was assessed by scratch wound assay *in vitro* (Morales *et al*., 1995; Basu *et al*., 2001). DFs and EKs between passage 3-5 and cell line of human keratinocytes NCTC 2544 were seeded in 35mm dishes at a density of 50,000 cells per dish. Two ml of DMEM with 10% FCS was used for fibroblasts and both keratinocytes cell lines; while KSF was used for primary keratinocytes. Cells were incubated at 37°C until confluent. Then, the cells were mechanically wounded along the diameter of the dish according to a pre-designed template as previously described (Stevenson *et al*., 2009)(Figure 19A) by using a sterile p1000 tip. The medium was removed and the cells were washed three times with PBS to eliminate unattached cells. Two millilitres of fresh phenol red and serum free medium with each steroid, DHEA-S (10µM), TST (50nM) and E2 (1nM), was added to the wounded cells. Inhibitors of aromatase (Arimidex, 100nM) and of STS (STX64, 100nM) were included to determine the conversion of androgen to E2 (Figure 20 and 21). 10µg/ml mitomycin C (MMC) was included in the migration assay to block proliferation. Migration of cells was analyzed at five fixed time points

between 4 and 48 hours. In each dish the distance between the wound edges was measured using the graticule eyepiece 12.5x and the objective 10x of an inverted Leitz microscope at 6 fixed points (3mm apart) along the length of the wound according to a standardized template (Figure 19B). Photographs were also taken of the central part of the wound at each time points using a Nikon Coolpix 4500 camera. Measurements were made at x125 magnification (eyepiece x12.5 & objective x10). The average distance between the wound edges for each individual group (derived from a total of 18 measurements) was calculated for the different time points and from this the mean migratory distance (G) for each time point was ascertained by a stage micrometer (table 28). The stage micrometer (Figure 18) consists of 100 divisions (1 mm) that are equal to 8.8 divisions of the eyepiece graticule x12.5 using the x10 objective. Each mean migratory distance (G) was multiplied by 1/8.8 mm that is the length of one single division of eyepiece graticule. Then, the mean migratory distance from the graticule reading was converted to a distance in micrometers (μm).

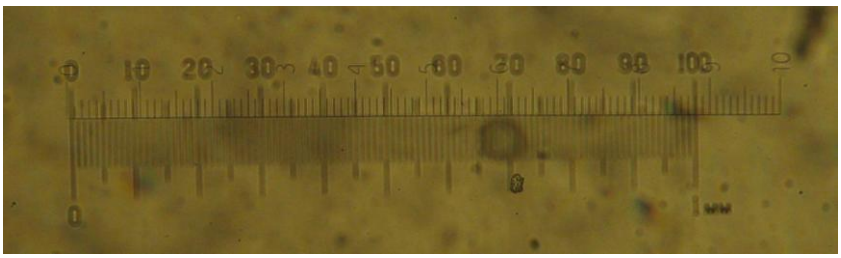

Figure 18. Stage micrometer Graticule LTD Tonbridge, Kent England 100 x 0.01 = 1 mm

The stage micrometer consists of 100 divisions (1 mm) that are equal to 8.8 divisions of the eyepiece graticule x12.5 using the x10 objective.

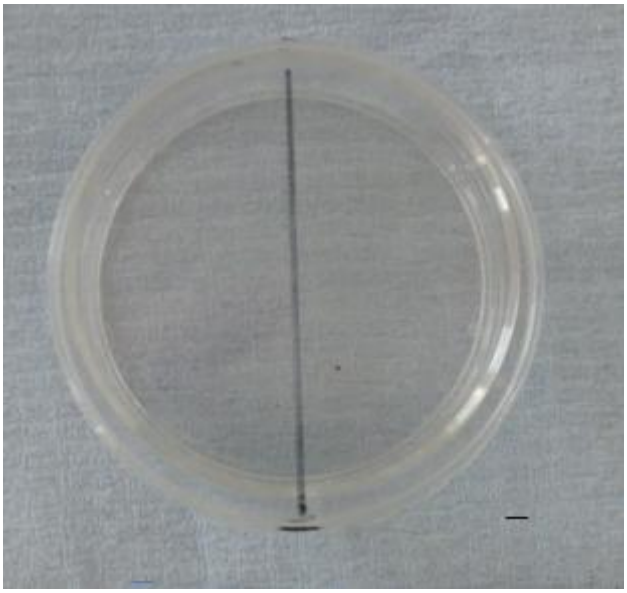

A

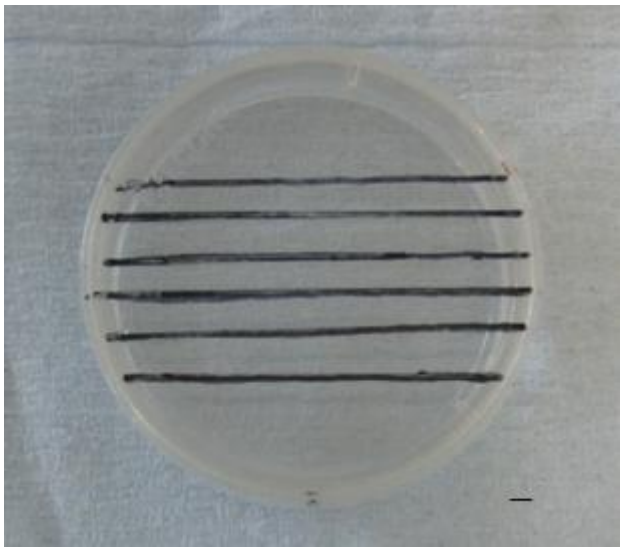

B

Figure 19. Templates used in migration assay

Cells were mechanically wounded according to a pre-designed template (A). A further template (B) was used to ensure that the distance between the wound edges was measured at fixed points in each time point. Scale bar = 1 mm.

dish	point	0 hours	4 hours	8 hours	12 hours	24 hours	48 hours
	1_1	5.1	4.9	4.8	4.7	4.2	3.8
	1_2	4.4	4.3	4.3	4.0	3.7	3.2
	1_3	4.6	4.5	4.4	4.3	3.8	3.2
	1_4	4.3	4.3	4.2	4.0	3.5	3.0
	1_5	4.3	4.1	4.1	4.1	3.7	3.2
1	1_6	4.9	4.8	4.7	4.6	4.1	3.7
	2_1	6.0	5.7	5.6	5.4	5.0	4.7
	2_2	3.8	3.7	3.6	3.5	3.2	2.9
	2_3	4.0	3.9	3.8	3.7	3.1	2.8
	2_4	3.5	3.5	3.4	3.3	3.0	2.6
	2_5	4.0	3.9	3.9	3.8	3.5	3.0
2	2_6	3.1	3.0	2.9	2.7	2.4	2.1
	3_1	4.3	4.3	4.3	4.2	3.8	3.4
	3_2	4.7	4.6	4.5	4.4	4.0	3.6
	3_3	4.9	4.8	4.6	4.5	4.0	3.7
	3_4	6.5	6.4	6.3	6.2	5.7	5.2
	3_5	4.5	4.4	4.3	4.2	3.9	3.5
3	3_6	4.7	4.6	4.5	4.4	4.0	3.7
average		4.5	4.4	4.3	4.2	3.8	3.4
migration distance graticule (G)		N/A	0.1	0.2	0.3	0.7	1.1
migration micrometres		N/A	12	23	34	80	125

Table 28. Migration assay and measured distances.

The distance between the wound edges was measured at six fixed points in triplicate dishes. Measurements were made at x125 magnification (eyepiece x12.5 & objective x10). The average distance was then calculated at the different time points and from this mean migratory distance (G) for each time point was ascertained by comparison with a stage micrometer and expresses in µm. N/A: not applicable.

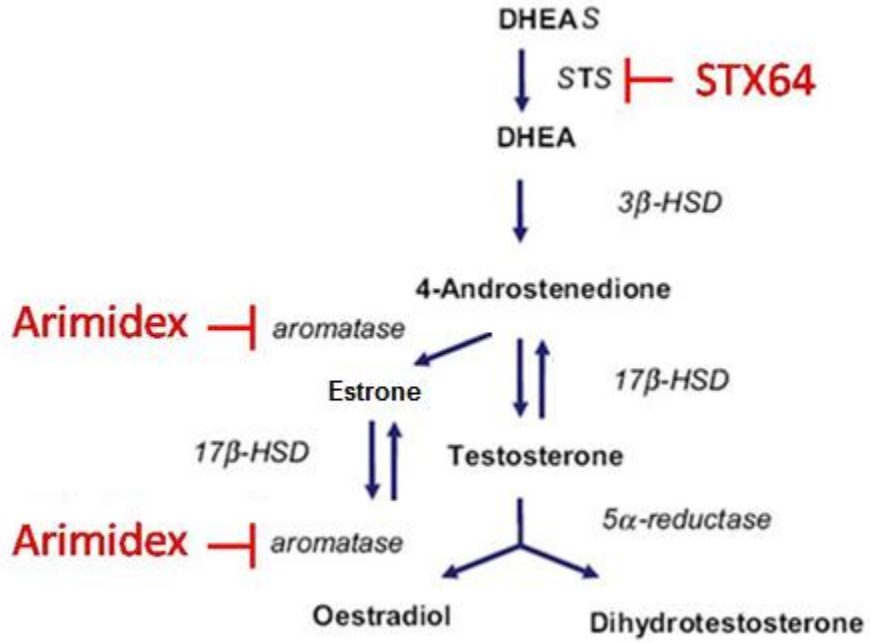

Figure 20. Estrogen and androgen synthesis

The image displays the formation of estrogen and androgen from the steroids precursor DHEA-S. The activity of specific enzymes gives rise to the synthesis of active sex steroid hormones. STS is the enzyme that catalyzes the conversion of DHEA-S to the un-conjugated form DHEA. Aromatase catalyzes the conversion of androgen to estrogen. The STS inhibitor (STX64) and the aromatase inhibitor (arimidex) are in red.

n.	Treatment
1	Vehicle Control
2	DHEA-S
3	DHEA-S + STX
4	DHEA
5	DHEA + Arimidex
6	TST + Arimidex
7	TST
8	E2
9	STX
10	Arimidex

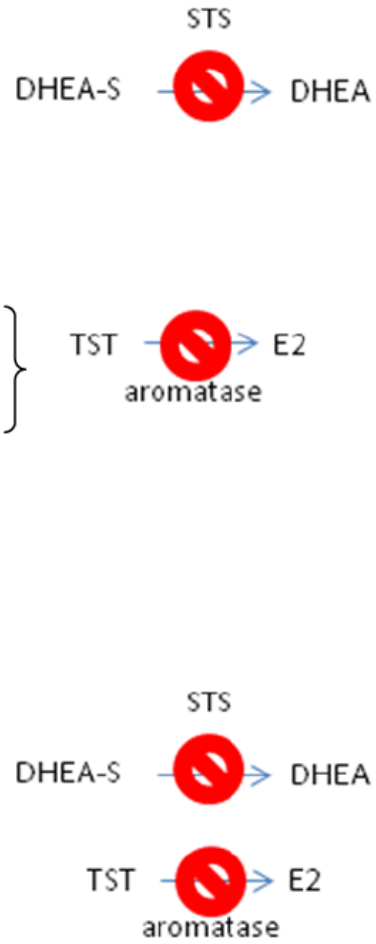

Figure 21. Schematic image of the steroid treatments used for the scratch wound assay *in vitro*. Migration of human DFs and EKs was analyzed at five fixed time points between 4 and 48 hours by the incubation with different steroids. **(1)** Vehicle Control (ETOH 0.0001%), **(2)** DHEA-S (10 M), **(4)** DHEA (10 M), **(7)** TST (50nM), **(8)** and E2 (1 nM). In addition, the inhibitor of **(5,6,10)** aromatase (Arimidex) and that of **(3,9)** STS (STX64) were included to determine the conversion of androgen to E2.

2.26 Assay of aromatase activity

To investigate the aromatase activity in cultured skin cells, the tritiated water assay was used (Lephart and Simpson, 1991). In particular, tritiated androstenedione (Androst-4-ene-3,17-dione, [1β-3H(N)]; C19H2602, 286.4 FW) (NEN Perkin Elmer) was added to fibroblasts and keratinocytes.

DFs were seeded either into 12-well plates at a density of $1x10^4$ in 1ml normal growth media for dexamethasone assay or into six-well plates at a density of $1x10^5$ per well in 2mL normal growth media for the mechanical wound assay. EKs were seeded into six-well plates at a density of $1x10^5$ per well in 2ml normal growth media for both dexamethasone assay and mechanical wound assay. Cells were grown to confluence before changing to their specific experimental medium. After three washes with PBS, cells were incubated with 1 ml of fresh specific serum free medium supplemented with either ETOH (0.0001%) or dexamethasone (250nM) for 24 hours at 37°C. Then the cells were washed 3 times with PBS and incubated with 1 ml of fresh serum free medium supplemented with 0.5μCi of tritiated androstenedione ([1β-3H]-Androstenedione) for 2 hours at 37˚C. During the mechanical wound assay, after scratching, cells were washed 3 times with PBS and incubated with 1 ml of fresh serum free medium supplemented with 0.5μCi of tritiated androstenedione ([1β-3H]-Androstenedione) for 2 hours and 24 hours at 37˚C. Following this period, 500 μl of chloroform was added to halt the reaction and the supernatant centrifuged for 5 min at 6,000 rpm three times sequentially. Then, 500 μl of activated charcoal was added to remove unmetabolized steroids and the supernatant was centrifuged for a futher 5 min at 6,000 rpm. Samples (500 μl) were added with scintillation fluid, mixed well and then analyzed with scintillation counter. Results were expressed as disintegrations per minute (d.p.m.). Then, the cell layer was dissolved in RIPA buffer (Sigma) and the proteins were measured using the DC Protein assay (see section *2.27*). Results were expressed as nmol/mg cell protein. All experiments were performed on triplicate wells.

2.27 Protein extraction and quantification

The protein quantification was performed using the DC Protein Assay (Bio Rad), a colorimetric assay for protein concentration following detergent solubilization. The reaction is similar to the well-documented Lowry assay (Lowry *et al*., 1951). The cell layer was dissolved with 200 µl RIPA buffer (Sigma) supplemented with 4 µl protease inhibitor cocktail (Sigma) for 5 min on ice. Then, the cell lysate was placed in a 1.5 ml tube and centrifuged at ≥10,000 x *g* for 5 min. The resultant supernatant, which contained the solubilised cellular protein, was transferred to a clean tube, and used for the protein quantification or frozen at -80 °C until further use. For the protein quantification, 5 µl of either the resultant supernatant or the protein standard (see appendix 4) was added to the appropriate well on a 96 well plate in triplicate. Reagent A' (25 µl) and B (200 µl) (see appendix 4) were added to every well. The plate was shaken for 15 min using a plate shaker and then, was placed into a plate reader (Dynex MRX) that measured each sample absorbance at 750 nm. The calibration curve and the noted absorbance of the protein samples were used to ascertain the protein concentration of each of the cell extract samples.

2.28 Statistical analysis

All data were presented as donor mean ± SEM. The difference between individual means was analysed using the paired and unpaired Student's *t*-test. A p-value of less than 0.05 was considered significant (*), 0.01 very significant (**) and 0.001 extremely significant (***). Software GraphPad Prism 5 was used to obtained statistical values and graphs.

3. Results

3.1 RT-PCR analysis for mRNA expression of steroidogenic proteins in human skin

A preliminary analysis was carried out to investigate the expression of seven genes encoding the following steroidogenic proteins: P450arom, P450scc, P450c17, STS, OATP2B1, 5α-reductase 1 and 5α-reductase 2. Human skin biopsies, individual isolated HFs, cultured DFs, and cultured EKs were used for RNA extraction (see section *2.12*), cDNA synthesis (see section *2.15*) and identification of the genes of interest (see section *2.16*). The identity of the mRNA was confirmed by size using gel electrophoresis, and the analysis of the nucleotide product sequence by NCBI BLAST bl2seq (http://blast.ncbi.nlm.nih.gov).

To ascertain the specificity of the primer pairs, human tissue derived from glands or cell lines known to express the genes of interest were used as positive controls: adrenal gland for P450scc and P450c17, ovary for P450arom, liver for OATP2B1, placenta for STS, and the prostate cancer cell lines PC3 and DU145 for 5α-reductase 1 and 5α-reductase 2, respectively. RT-PCR was performed using primers specific for the housekeeping gene ß-actin. The detection of this gene indicated that the cDNA was of good quality for the efficiency of RT-PCR analysis. The amplification products from all samples corresponded to the expected size of ß-actin (187 bp) (data not shown).

In the negative control, in which the template cDNA was excluded from the reaction mix, no PCR products were present, demonstrating that no DNA contamination occurred in the reaction mix.

The expression of the seven target genes was investigated in whole human skin biopsies (see appendix 5), HFs (see appendix 6), DFs (see appendix 8), and EKs (see appendix 7 and 8). All samples produced PCR products of the

expected size for P450scc, P450c17, STS and 5α-reductase 1 (Figures 22,23,25,27). The mRNA expression of 5α-reductase 2 was detected only in HF (Figure 23). EK did not produce the transcript of P450arom (data not shown) and DF did not express OATP2B1 (data not shown). The results indicated that human skin expresses genes encoding proteins involved in steroidogenesis.

3.2 Expression of mRNA for ER and AR in human skin

The biological action of estrogens and androgens can be mediated by steroid binding to specific receptors, the estrogen receptors ERα and ERß, and the androgen receptor AR. In the present study, the mRNA expression of ERα, ERß, and AR was investigated in human cultured DFs (see appendix 8) and EKs (see appendix 7 and 8) derived from female and male healthy donors. The analysis was performed also in HFs derived from female non-balding fronto-temporal scalp (see appendix 6). ERα and ERß were expressed in cultured keratinocytes as well as in DFs. In particular, EK showed to strongly express ERß compared to ERα (Figure 28). In contrast, ERα was detected to be more highly expressed than ERß in DF (Figure 26). Differences in ER expression have been demonstrated also in human scalp HFs (Figure 24) which strongly expressed ERß in comparison with ERα. All the above also demonstrated AR expression (Figures 24,26,28). This study has confirmed that human skin and cultured cells express ERs and AR providing evidence for their involvement in the genomic signaling pathways of sex steroids.

Figure 22. The expression of steroidogenic genes in human skin

The PCR products were separated by 1.5% agarose gel electrophoresis and visualized with ethidium bromide staining. **(L)** DNA ladder (100bp), **(1-4)** lanes with the expression of P450scc in skin biopsies (n=4 individuals), **(+)** as positive control: human adrenal gland for P450scc and P450c17, human ovary for P450arom, human liver for OATP2B1, human placenta for STS, human prostate cancer cell line PC3 for 5α-reductase 1 and human prostate cancer cell line DU145 for 5α-reductase 2, **(-)** negative control wherein cDNA was omitted from the PCR reaction. The expected amplicon size for P450scc is 220bp, for P450c17 is 269bp, for P450arom is 160bp, for STS is 204bp, for OATP2B1 is 234bp, for 5α-reductase 1 is 443bp.

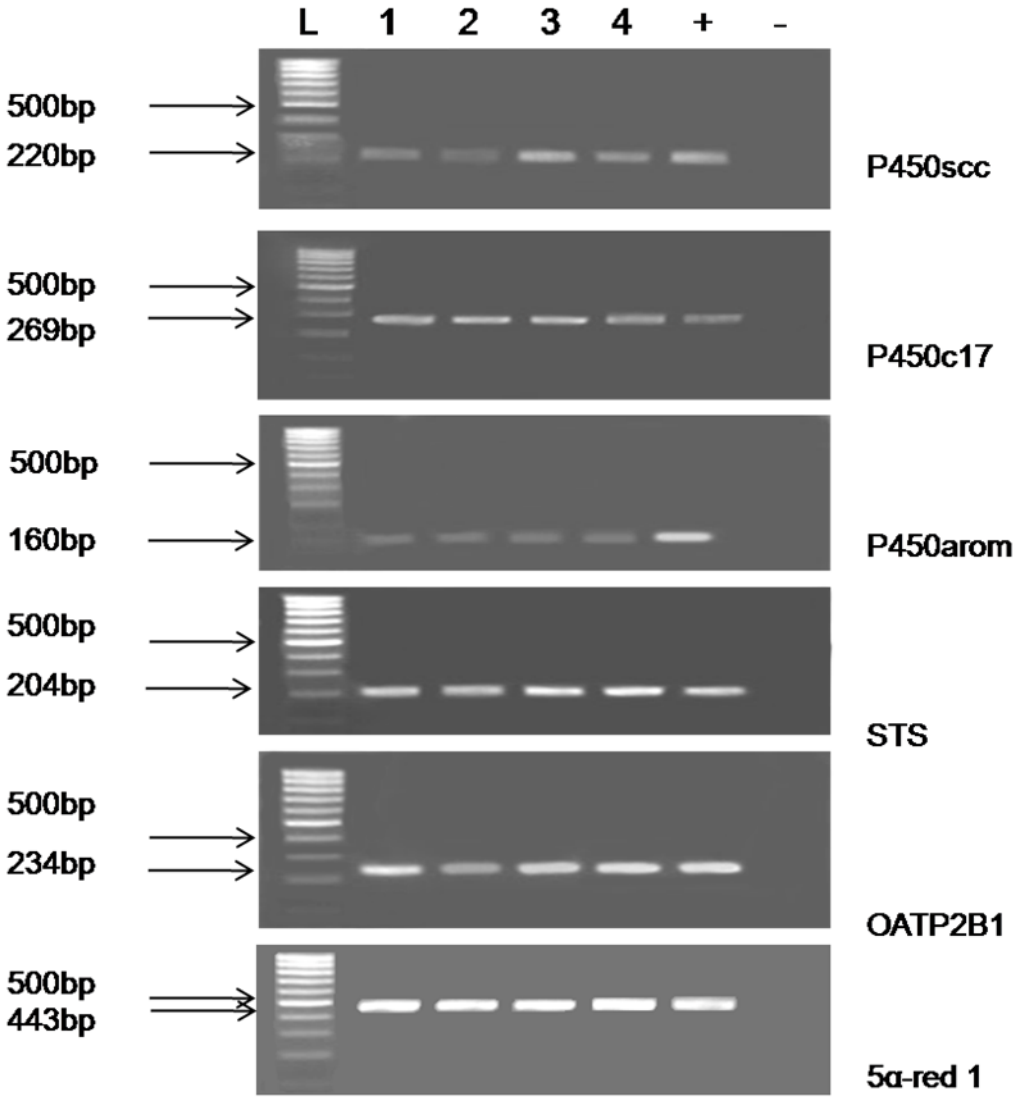

Figure 23. The expression of steroidogenic genes in human HF

The PCR products were separated by 1.5% agarose gel electrophoresis and visualized with ethidium bromide staining. **(L)** DNA ladder (100bp), **(1-5)** lanes with the expression of P450scc in HFs (n=5 individuals), **(+)** as positive control: human adrenal gland for P450scc and P450c17, human ovary for P450arom, human liver for OATP2B1, human placenta for STS, human prostate cancer cell line PC3 for 5α-reductase 1 and human prostate cancer cell line DU145 for 5α-reductase 2, **(-)** negative control wherein cDNA was omitted from the PCR reaction. The expected amplicon size for P450scc is 220bp, for P450c17 is 269bp, for P450arom is 160bp, for STS is 204bp, for OATP2B1 is 234bp, for 5α-reductase 1 is 443bp, and for 5α-reductase 2 is 318bp.

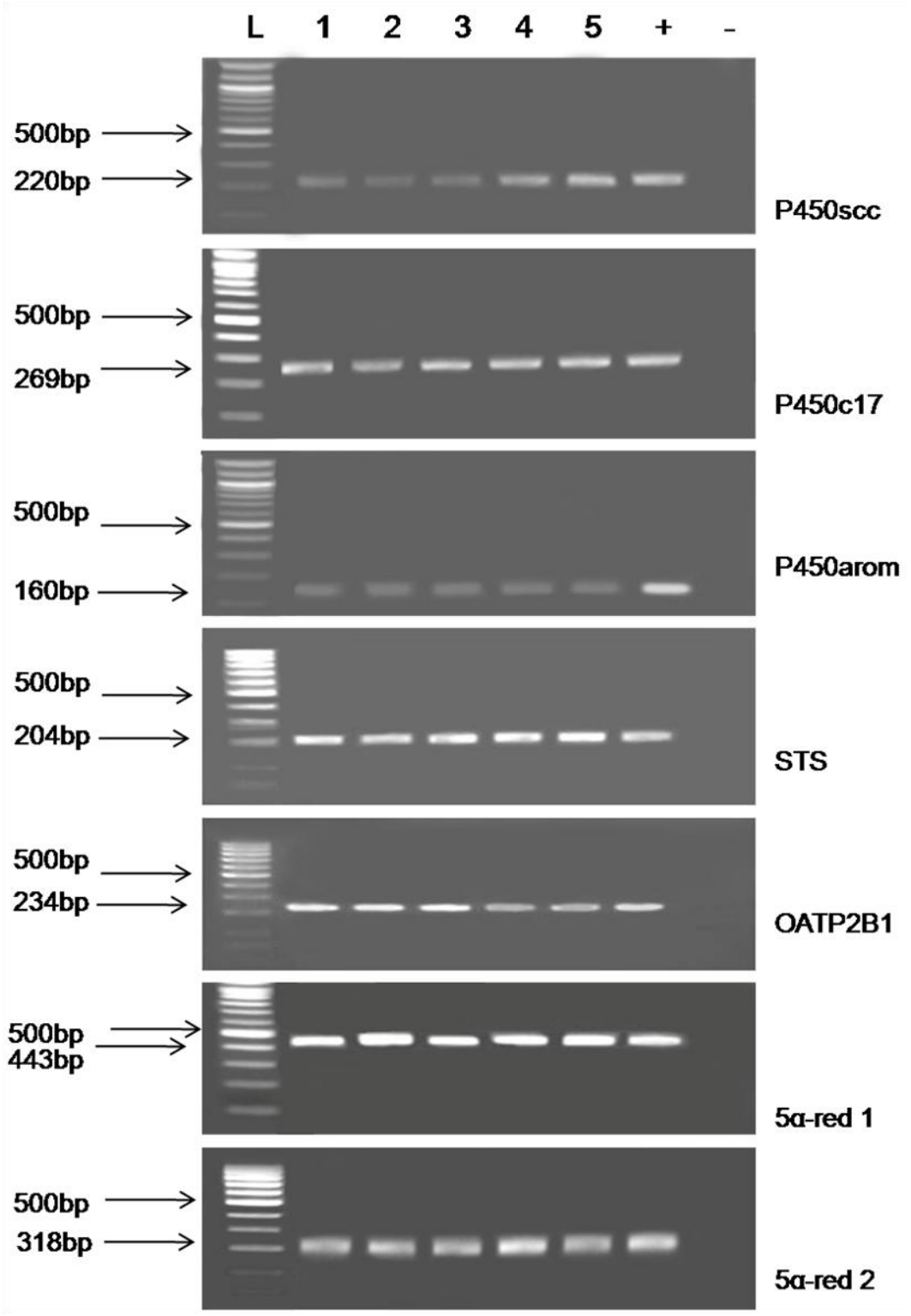
L
1
2
3
4
5
+
-
500bp
220bp
P450scc
500bp
269bp
P450c17
500bp
160bp
P450arom
500bp
204bp
STS
500bp
234bp
OATP2B1
500bp
443bp
5α-red 1
500bp
318bp
5α-red 2

Figure 24. The expression of AR and ERs in human HF

The PCR products were separated by 1.5% agarose gel electrophoresis and visualized with ethidium bromide staining. **(L)** DNA ladder (100bp), **(1-5)** lanes with the expression of P450scc in HFs (n=5 individuals), **(-)** negative control wherein cDNA was omitted from the PCR reaction. The expected amplicon size for AR is 152bp, for ERα is 381bp, and for ERß is 279bp.

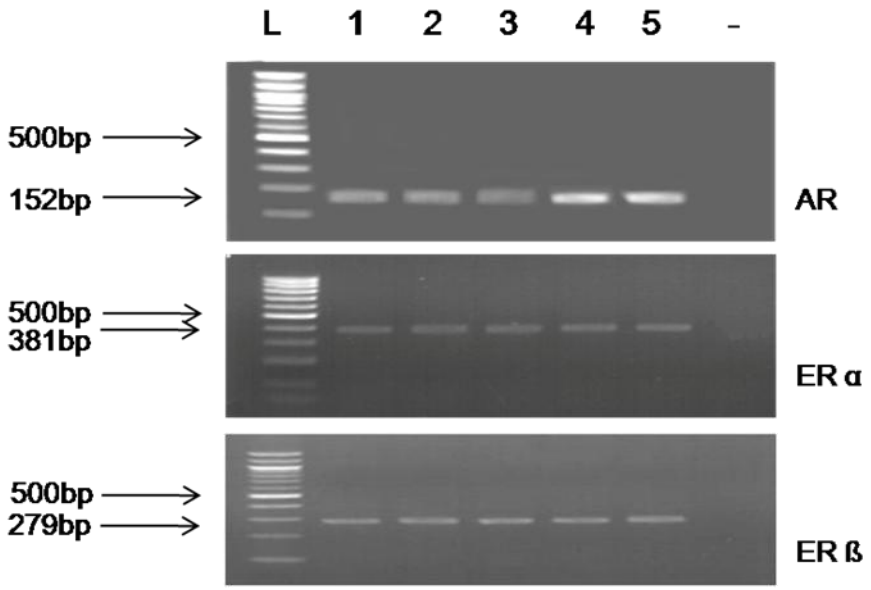

Figure 25. The expression of steroidogenic genes in human DFs

The PCR products were separated by 1.5% agarose gel electrophoresis and visualized with ethidium bromide staining. **(L)** DNA ladder (100bp), **(1-8)** lanes with the expression of P450scc in DFs (n=8 individuals), **(+)** as positive control: human adrenal gland for P450scc and P450c17, human ovary for P450arom, human liver for OATP2B1, human placenta for STS, human prostate cancer cell line PC3 for 5α-reductase 1 and human prostate cancer cell line DU145 for 5α-reductase 2, **(-)** negative control wherein cDNA was omitted from the PCR reaction. The expected amplicon size for P450scc is 220bp, for P450c17 is 269bp, for P450arom is 160bp, for STS is 204bp, and for 5α-reductase 1 is 443bp,

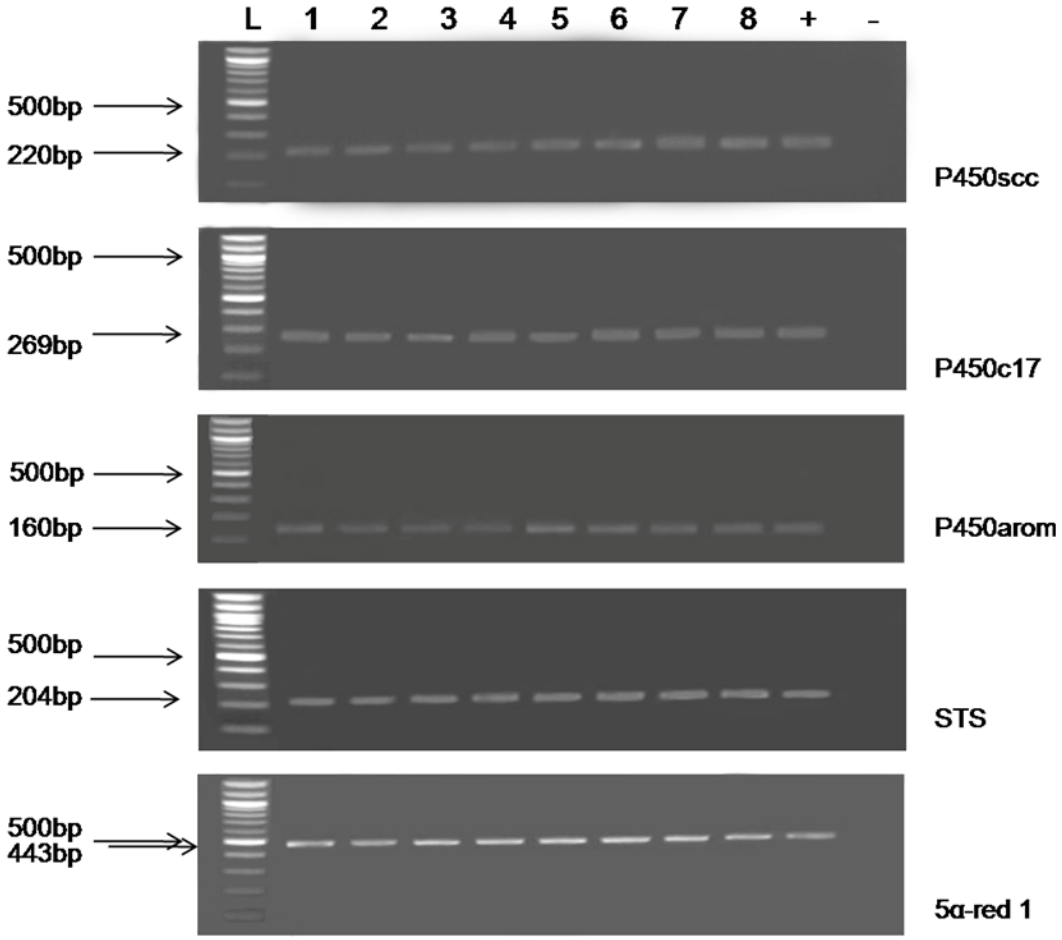

Figure 26. The expression of AR and ERs in human DFs

The PCR products were separated by 1.5% agarose gel electrophoresis and visualized with ethidium bromide staining. **(L)** DNA ladder (100bp), **(1-8)** lanes with the expression of P450scc in DFs (n=8 individuals), **(-)** negative control wherein cDNA was omitted from the PCR reaction. The expected amplicon size for AR is 152bp, for ERα is 381bp, and for ERß is 279bp.

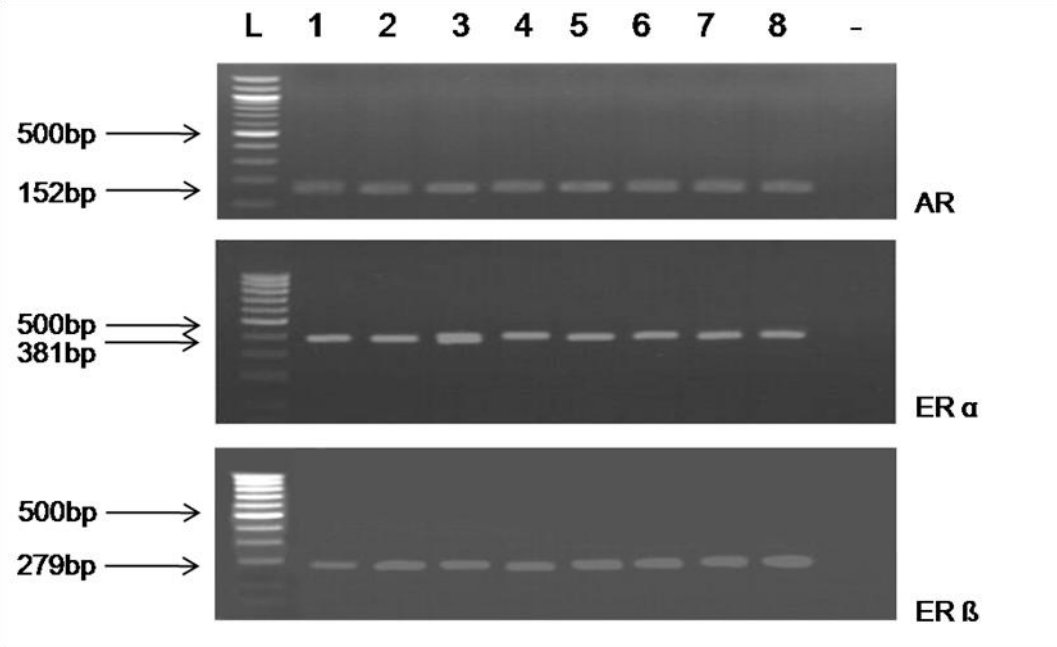

Figure 27. The expression of steroidogenic genes in human EKs

The PCR products were separated by 1.5% agarose gel electrophoresis and visualized with ethidium bromide staining. **(L)** DNA ladder (100bp), **(1-8)** lanes with the expression of P450scc in EKs (n=8 individuals), **(+)** as positive control: human adrenal gland for P450scc and P450c17, human ovary for P450arom, human liver for OATP2B1, human placenta for STS, human prostate cancer cell line PC3 for 5α-reductase 1 and human prostate cancer cell line DU145 for 5α-reductase 2, **(-)** negative control wherein cDNA was omitted from the PCR reaction. The expected amplicon size for P450scc is 220bp, for P450c17 is 269bp, for STS is 204bp, for OATP2B1 is 234bp, and for 5α-reductase 1 is 443bp.

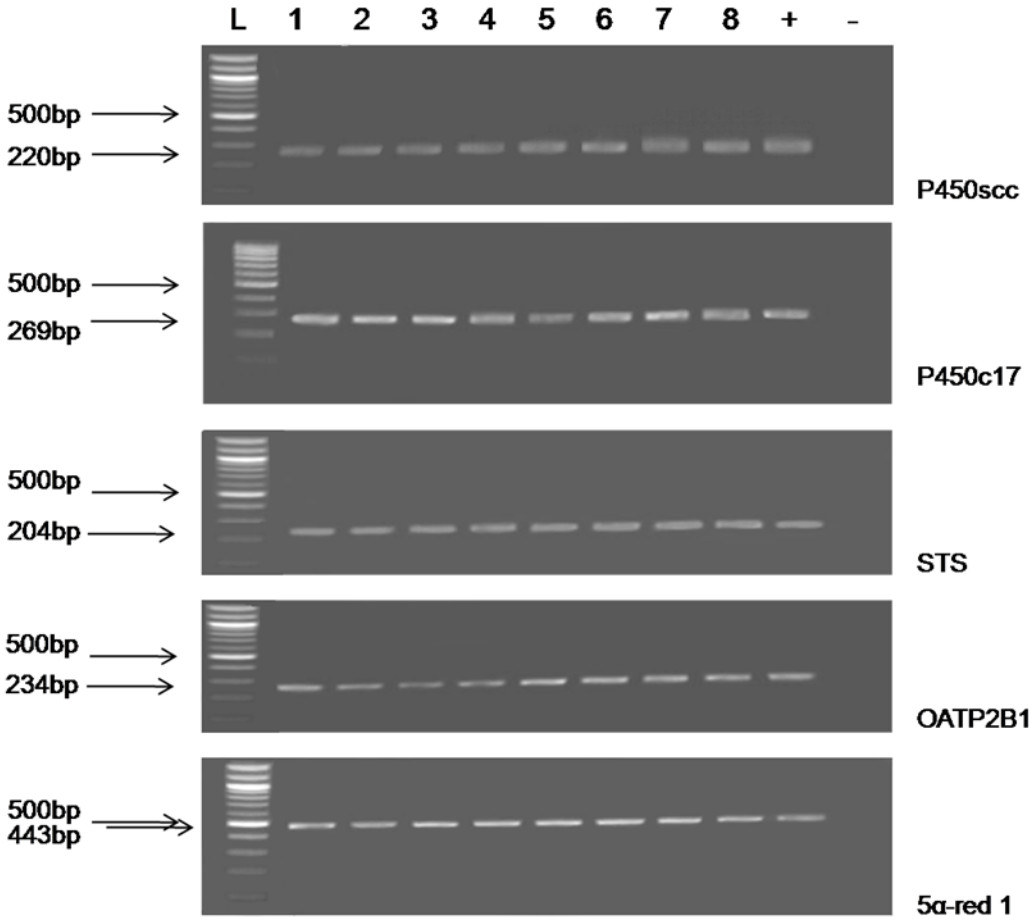

Figure 28. The expression of AR and ERs in human EKs

The PCR products were separated by 1.5% agarose gel electrophoresis and visualized with ethidium bromide staining. **(L)** DNA ladder (100bp), **(1-8)** lanes with the expression of P450scc in EKs (n=8 individuals), **(-)** negative control wherein cDNA was omitted from the PCR reaction. The expected amplicon size for AR is 152bp, for ERα is 381bp, and for ERß is 279bp.

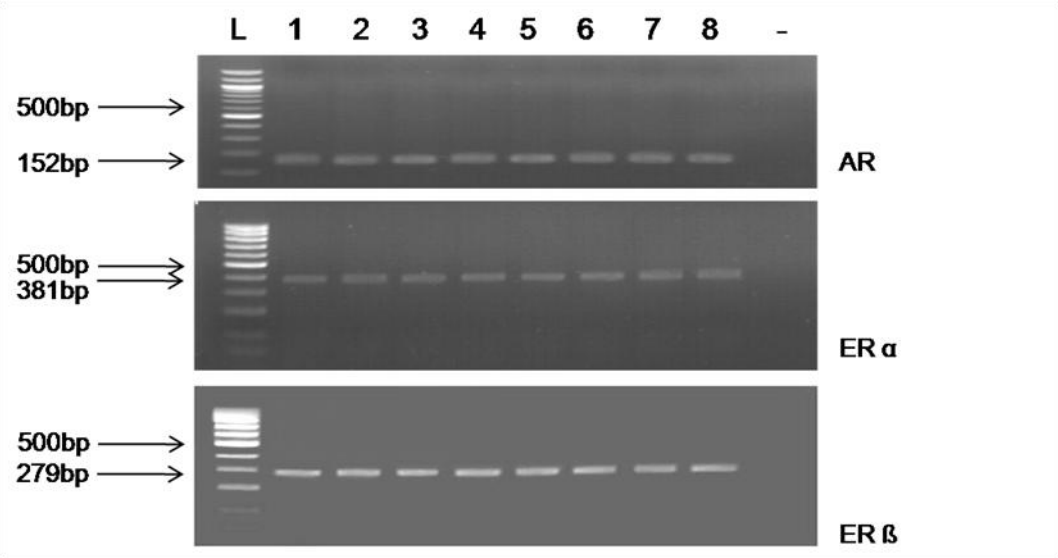

3.3 Absolute qRT-PCR on human skin and hair follicles

3.3.1 Optimization and validation of qRT-PCR

The reactions were optimized by using RT-PCR protocol to evaluate the most specific annealing temperature, between 56°C and 60°C (see table 10), of the primer pairs for all seven transcripts, that were analyzed by non quantitative RT-PCR (see section *3.1*), as well as for the housekeeping gene ß-actin mRNA, used as an internal control. The concentration of $MgCl_2$ was established by testing between 3mM and 6mM. Gel agarose electrophoresis analysis suggested a concentration of 3mM as the optimal concentration to amplify all of the target transcripts. The specificity of the real-time amplicons was determined by analysis of amplification profiles and melting curves (Figure

29). Primer dimers and non-specific products were not detected. Samples were also analyzed on agarose gel (data not shown).

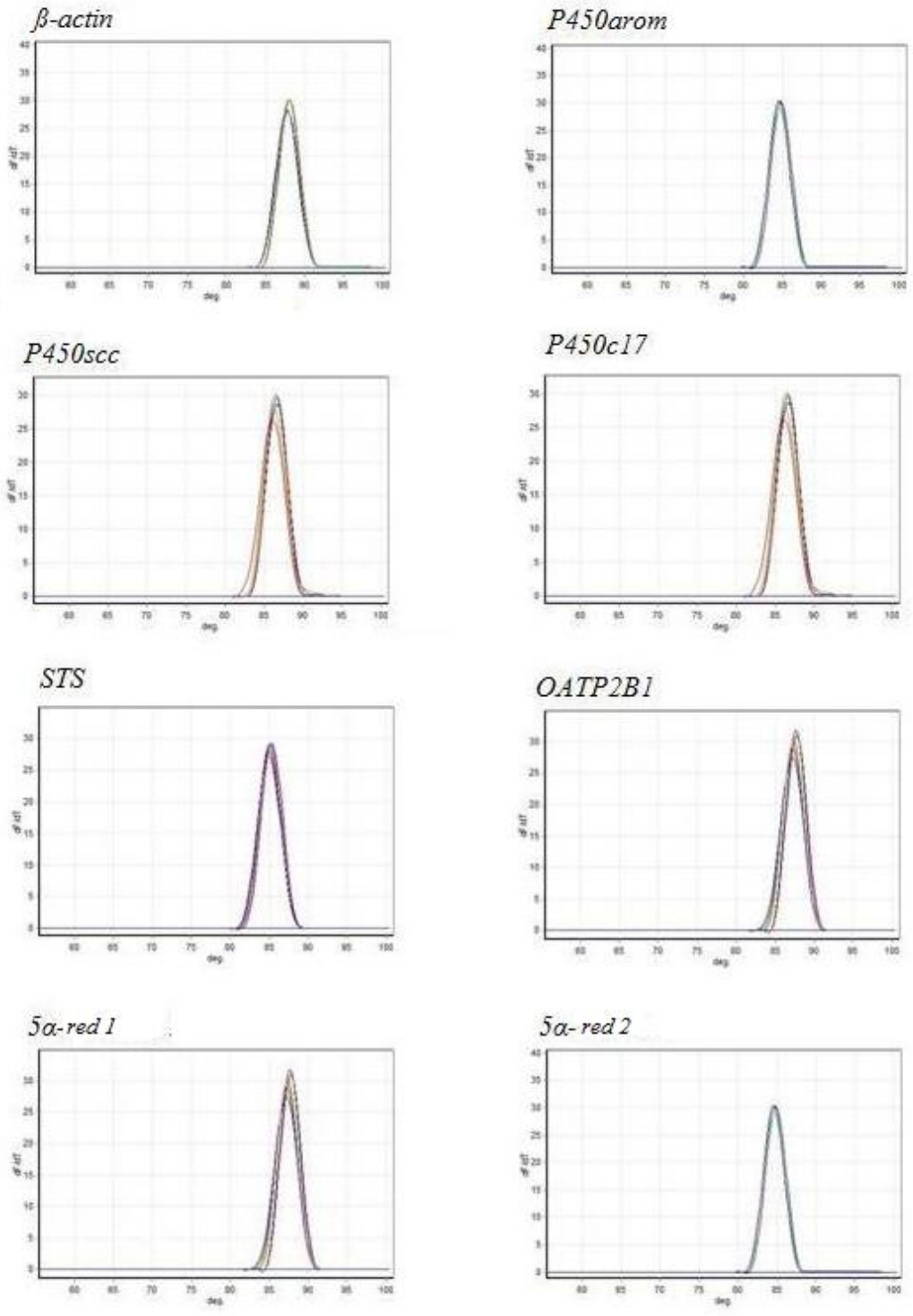

Figure 29. Melting curves of real time reactions

The images indicated that primer dimers and non-specific products were not detected in all reactions of all seven target genes as well as the housekeeping gene, ß-actin.

The absolute amount of target nucleic acid was determined using external standards. Eight standard curves of known copy numbers were used: seven for the transcripts of interest and one for the internal control. The C_t value of the target was compared with the standard curve, allowing calculation of the initial amount of the target by the formula:

$$\text{Efficiency} = 10^{(-1/\text{slope})} - 1$$

Mathematically, it takes 3.32 cycles for a 100% efficient PCR amplification to increase the number of template molecules 10 fold (23.32 = 10) in any given sample. Standard curves provide information about the PCR assay. The slope of the line is a measure of the assay efficiency. Slopes of every reaction were detected between -3.2 and -3.3 (around 100% efficient) as acceptable.
The R^2, a measure of the performance of the assay and the coefficient of correlation between the data generated and the results expected under ideal conditions, was around 0.99 for each reaction. This means that >99% of the data matched the hypothesis that the given standards formed a standard curve.

3.3.2 Quantification of mRNA expression

The analysis was carried out on human non-hairy skin biopsies (n=4) (see appendix 5) derived from female face and abdomen and female scalp HFs (n=5) (see appendix 6) to investigate the level of mRNA expression of the seven genes of interest: P450arom, P450scc, P450c17, STS, OATP2B1, 5α-reductase 1 and 2. The results are expressed as copies per reaction in logarithmic scale.
The skin samples (Figures 30,32,33) expressed all the genes of interest with the exception of 5α-reductase 2. In particular, the expression of the 5α-reductase 1 transcript was the highest whereas aromatase revealed the lowest level of expression.

HFs (Figures 31,32,33) expressed all genes with 5α-reductase 1 the highest transcript detected. In contrast to the whole skin biopsies, individual analysis showed the expression of the 5α-reductase 2. However, aromatase was again the transcript expressed at the lowest level with respect to all the other genes of interest.

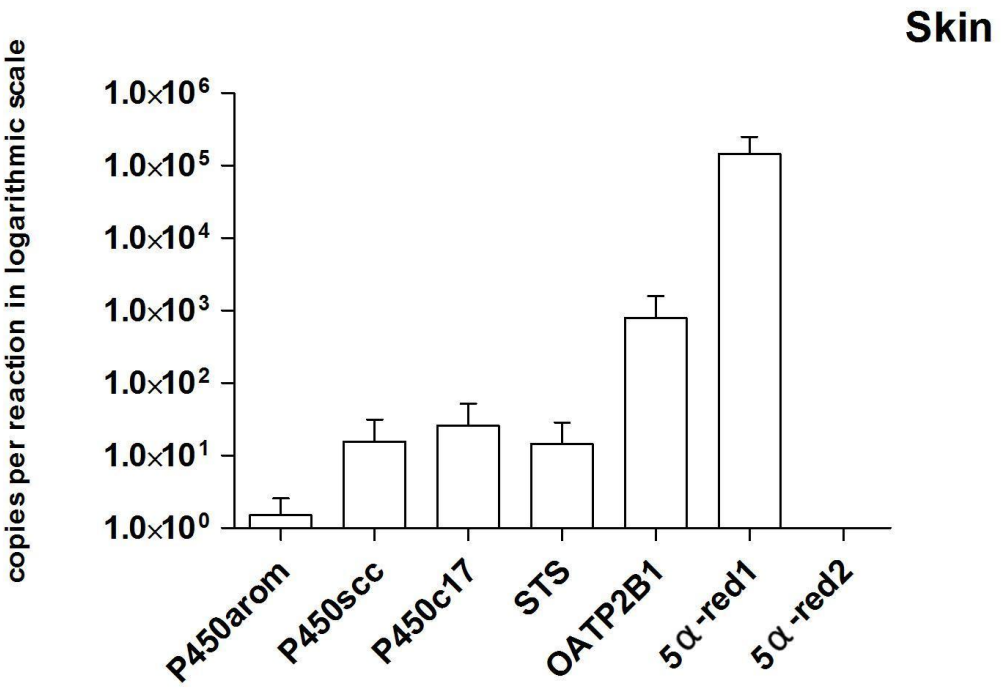

Figure 30. mRNA expression of steroidogenic genes in human skin

The absolute quantification of mRNA expression of P450arom, P450scc, P450c17, STS, OATP2B1, 5α-reductase 1 and 5α-reductase 2 in skin biopsies (n=4). Results are expressed as copies per reaction in logarithmic scale. Messenger RNA levels are presented after correction for individual ß-actin levels (data not shown) and as the mean ± SEM of individual biopsies.

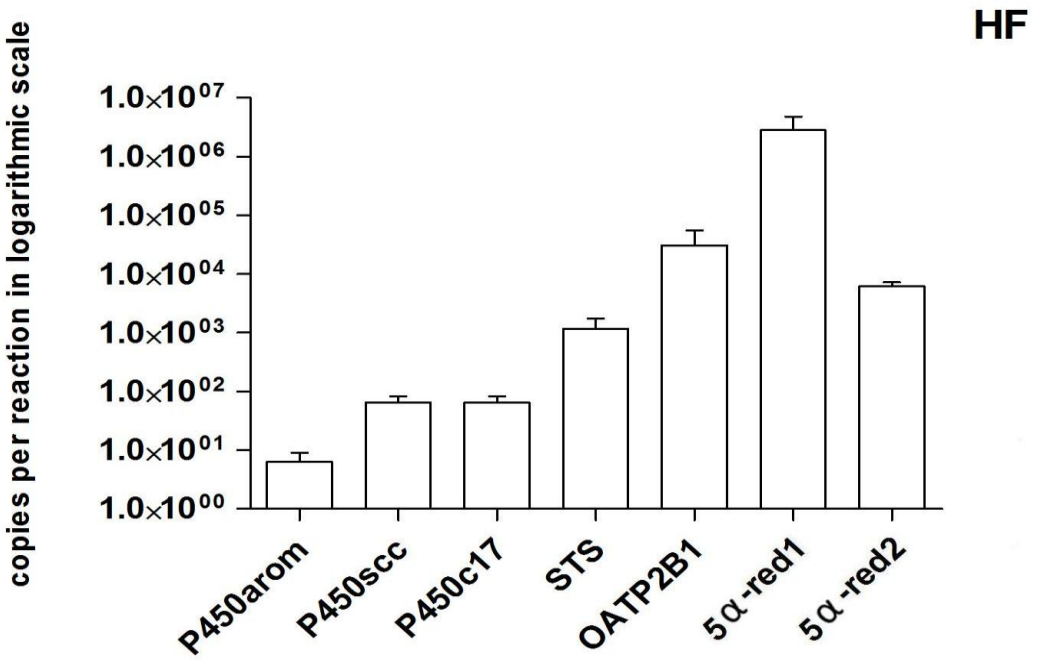

Figure 31. mRNA expression of steroidogenic genes in human HFs

The absolute quantification of mRNA expression of P450arom, P450scc, P450c17, STS, OATP2B1, 5α-reductase 1 and 5α-reductase 2 in isolated human HFs (n=5). Results are expressed as copies per reaction in logarithmic scale. Messenger RNA levels are presented after correction for individual ß-actin levels (data not shown) and as the mean ± SEM of individuals.

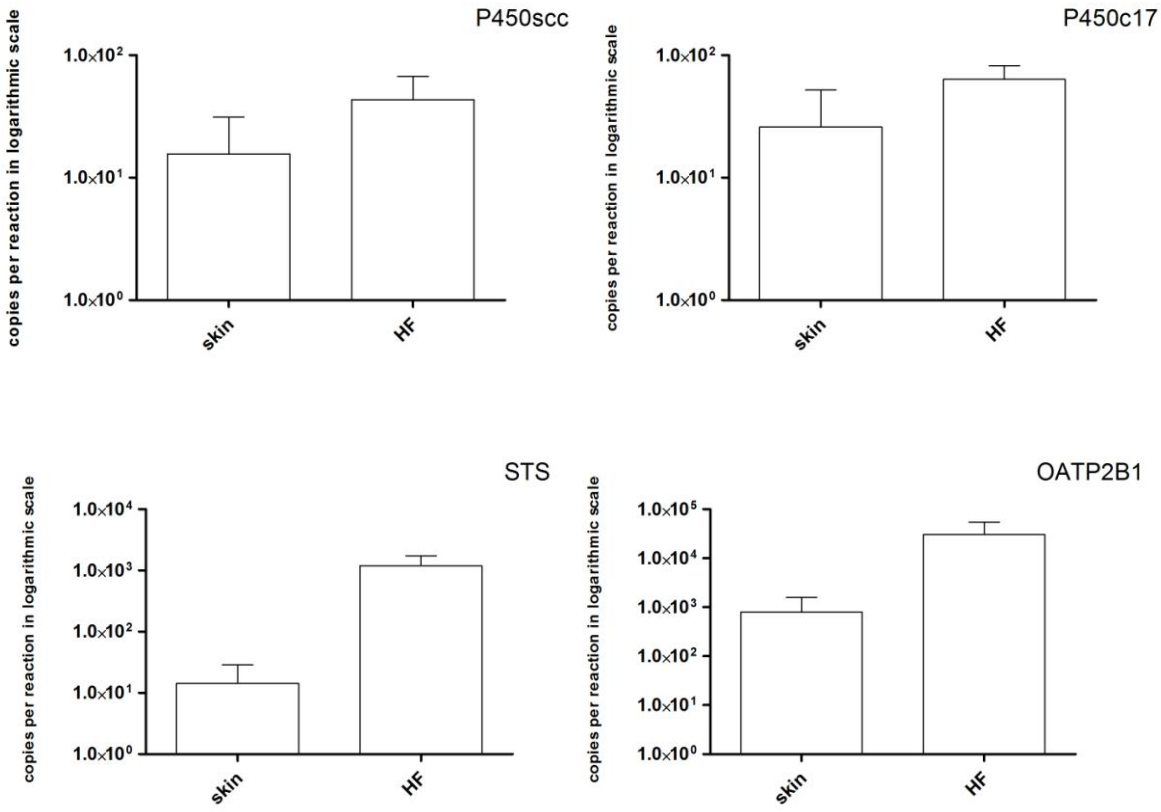

Figure 32. A comparison of mRNA expression of P450scc, P450c17, STS and OATP2B1 in whole skin and individual HF

Results are expressed as copies per reaction in logarithmic scale. Messenger RNA levels are presented after correction for individual ß-actin levels (data not shown) and as the mean ±SEM (skin n=4; HF n=5).

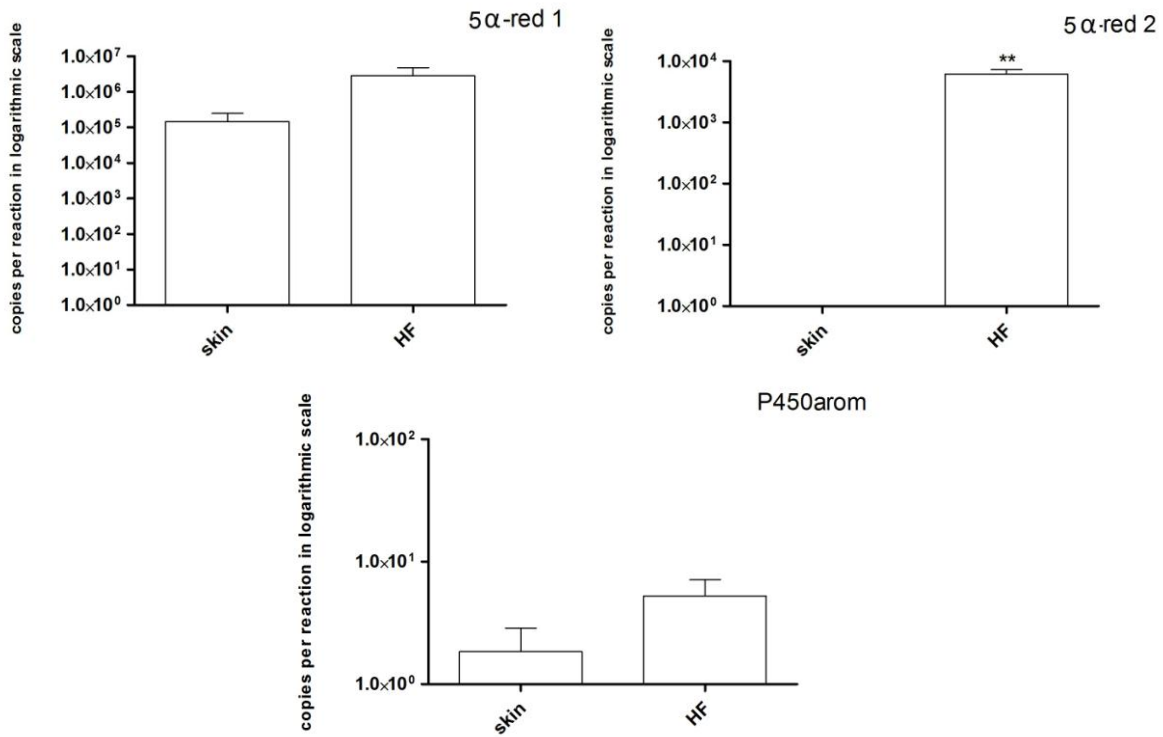

Figure 33. A comparison of mRNA expression of 5α-reductase 1, 5α-reductase 2 and P450arom in skin and HF

Results are expressed as copies per reaction in logarithmic scale. Messenger RNA levels are presented after correction for individual ß-actin levels (data not shown) and as the mean ± SEM. (skin n=4; HF n=5) (Student's *t* test, **p<0.01).

3.4 Microarray analysis of the effects of steroid hormones on gene expression

Gene array analysis was carried out to identify the differential expression of genes on human HFs isolated from female frontotemporal scalp (see appendix 6) and primary female facial EKs (see appendix 7) after steroid treatment. Three different hormones were used: DHEA-S (10µM), TST (50nM) and E2 (1nM), and HFs and cells were incubated for 24h as described in section *2.10*.

The aim of this experiment was to investigate the effects of the precursor, DHEA-S, and two metabolites, a biologically active androgen (TST) and a biologically active estrogen (E2).

3.4.1 RNA quality control after steroid treatment

After 24h of steroid incubation, total RNA was extracted from each sample as described in section *2.12.2*. RNA was analyzed by Agilent 2100 Bioanalyzer to determine RNA integrity. The results of single analyzed sample were described as an electropherogram and a virtual image identical to that of a standard agarose gel (Figure 34). Only the samples with an optimal quality of RNA and with RIN≥7 were used. Excellent quality of RNA is detected when the bands of 28S and 18S rRNAs are well separated and their correspondent peaks are in good evidence.

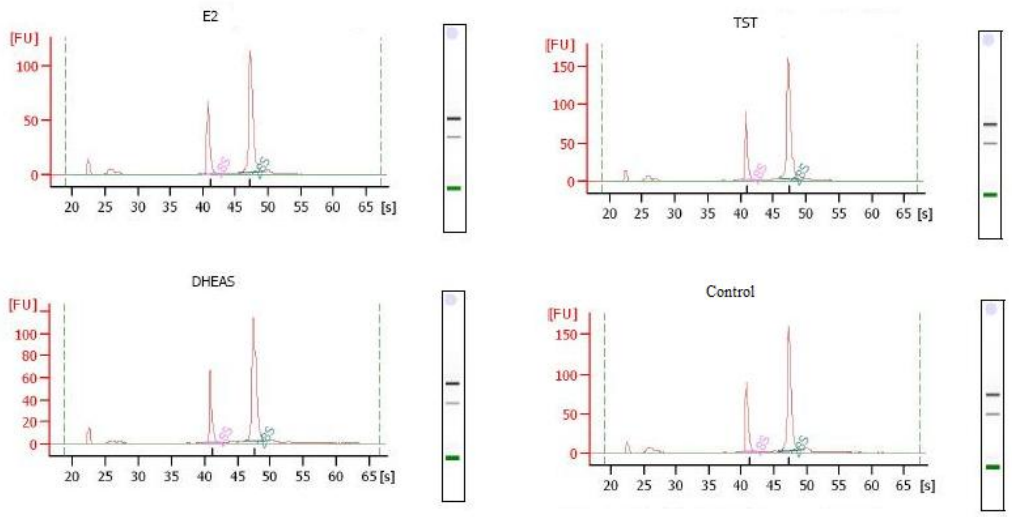

Figure 34. Electropherogram and virtual gel of quality of RNA analyzed by Agilent 2100 Bioanalyzer

The green band corresponds to an internal standard. Two highest peaks of electropherogram correspond to 18S and 28S, from left. Axis y describes the fluorescence (FU) while axis x the nucleotide size (s).

3.4.2 Gene array

Once the quality of RNA for all samples was analyzed and samples were selected, gene array procedure was carried out as described in *2.24*. For each single examined sample, three different steroid treatments and one for vehicle were performed as indicated in the following table:

n.	RNA
1	E2
2	TST
3	DHEA-S
4	Vehicle

Table 29. Three different steroid treatments as well as vehicle were performed.

The analysis consisted of two color array for EKs and one color for HFs, as following described.

3.4.3 Gene Array two color on keratinocytes

For initial amplification and then for incorporation of cyanine (see tables 30,31,32,33), 500 ng of total RNA was used. Hybridization was performed using 825 ng of each labeled cRNA. Samples were labeled with Cy5 and the control with Cy3. Replicates (n=2) were performed by dye swap to get a better selection of significant variation of gene expression.

Sample	cRNA (ng/µl)	Cy3 (pmol/µl)	Cy5 (pmol/µl)	Incorporation (fmol/µl)
E2	265.21	-	7.0184	26.5
TST	295.54	-	5.8552	20
DHEA-S	290.01	-	5.1872	18
Control	271.85	-	7.0029	26
Control	219.51	3.2006	-	15
TST	166.97	2.3303	-	13.9

Table 30. Quantification of cRNA and incorporation of cyanine Cy3 (green) and Cy5 (red) for sample of EKs (sample n. 3, see appendix 7).

Copies of hybridization of cRNA Sample vs. control		
n.	**Sample**	**Control**
1	E2	Control
2	TST	Control
3	DHEA-S	Control
4	TST	Control

Table 31. Copies of hybridization of cRNA on 4x44k for sample of EKs (sample n. 3, see appendix 7).

Sample	cRNA (ng/µl)	Cy3 (pmol/ µl)	Cy5 (pmol/ µl)	Incorporation (fmol/µl)
E2	143.32	2.6139	-	18.24
TST	205.14	3.6284	-	17.69
DHEA-S	181.43	2.9296	-	16.20
Control	167.25	2.3804	-	14.23
Control	166.20	-	4.2885	25.8
DHEA-S	284.20	-	5.2170	18.36

Table 32. Quantification of cRNA and incorporation of cyanine Cy3 (green) and Cy5 (red) for sample of EKs (sample n. 4, see appendix 7).

Copies of hybridization of cRNA Sample vs. control		
n.	**Sample**	**Control**
1	E2	Control
2	TST	Control
3	DHEA-S	Control
4	DHEA-S	Control

Table 33. Copies of hybridization of cRNA on 4x44k for sample of EKs (sample n. 4, see appendix 7).

3.4.4 Gene Array one color on hair follicle

One µg of each RNA amplified sample was labeled with Cy3. The results of incorporation were optimal as shown in tables 34 and 35. Then, 1.65 µg of cRNA was hybridized on 4x44k. Comparison between the sample and control was performed by using Microsoft Excel (table 37) to get the fold ratio change of up- or down-regulation.

Sample	cRNA (ng/µl)	Cy3 (pmol/µl)	Incorporation (fmol/µl)
E2	165.08	1.56	9
TST	183.13	1.73	9
DHEA-S	172.64	1.73	10
Control	173.15	1.75	10

Table 34. Quantification of cRNA and incorporation of cyanine Cy3 (green) of HFs (sample n. 5, see appendix 6).

Copies of cRNA Sample vs. Control		
n.	**Sample**	**Control**
1	E2	Control
2	TST	Control
3	DHEA-S	Control

Table 35. Copies of comparison between sample and control for sample of HFs (sample n. 5, see appendix 6).

3.4.5 Scanning and analysis of microarray data of epidermal keratinocytes

Feature extraction was carried out by using GE2-v5_95_Feb07 Software and the normalization of data was performed automatically. Data were shown as M *vs*. A plot with $\log_{10}$ (sample/control) on y axys (M) and $\log_{10}$ (sample x control) on x axis (A) (Figure 35A). The confirmation of the data distribution was performed by using Microsoft Excel as shown in figure 35B by taking as example E2 *vs.* Control. This analysis was carried out for each array and sample. Successively, the analysis was carried on by converting $\log_{10}$ratio to $\log_2$ as shown in Figure 36. Analysis was finally carried out on 44,000 genes by selecting those significant according to specific rules of Agilent Technologies (www.genomics.agilent.com). Only data with an abosolute value of Cy3 and Cy5 intensity ≥ 200 were considered. TM4 package and TIGR MIDAS Software were used for this selection by Low intensity filter of 200 and Slice analysis with a data population of 500 genes and a standard deviation of 2 (Figure 37 and 38). Successively, data were elaborated by Microsoft Excel.

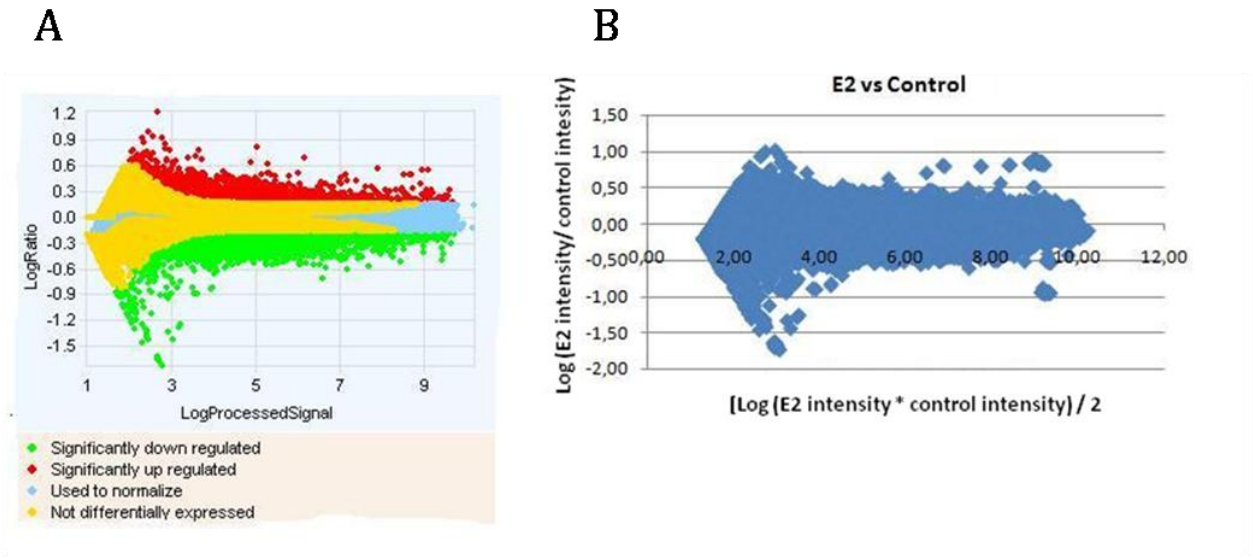

Figure 35. Example of M *vs.* A plot of data distribution of gene array analysis

Data are expressed as $\log_{10}$ (E2/Control) on y axis and [$\log_{10}$ (E2*Control)]/2 on x axis. A) M *vs.* A plot got by feature extraction. B) M *vs.* A plot for confirmation and designed by Microsoft Excel.

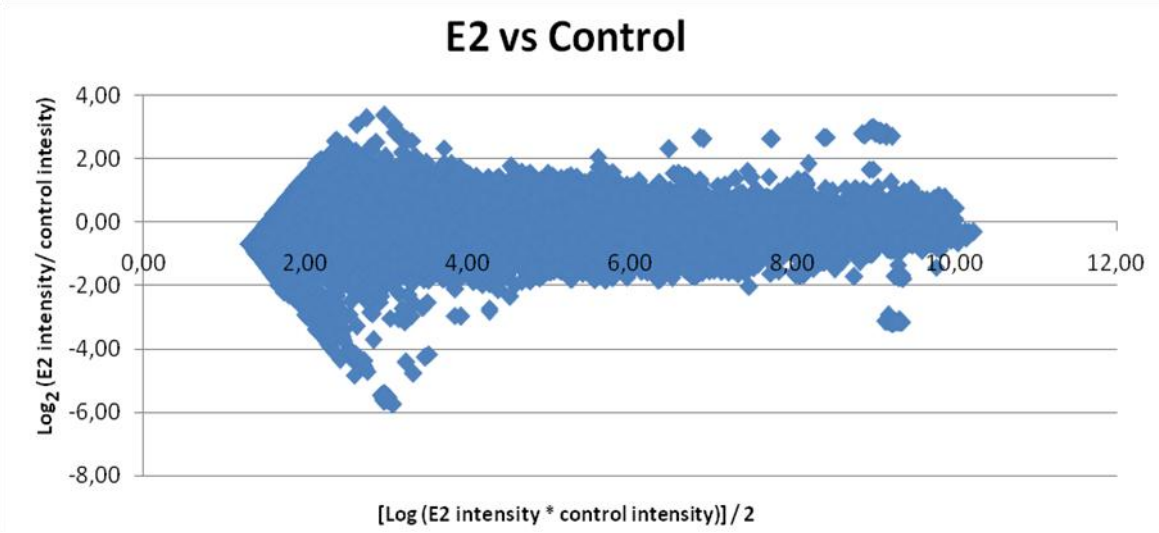

Figure 36. Example of data distribution by using log_2(E2/Control) on y axis

Data are expressed as log_2 (E2/Control) on y axis and [log_{10} (E2*Control)]/2 on x axis. B) in a M *vs.* A plot using Microsoft Excel.

3.4.6 Interpretation of microarray results

The annotation and functional grouping of differentially regulated genes of EKs and HFs were performed by Miltenyi Biotec team (Bergisch Gladbach, Germany). In the functional grouping analysis, information was derived from databases for gene function in order to find common features among the genes sharing similar expression characteristics. The annotations used were derived from Gene Ontology (GO) which provides information on molecular function, as well as various pathway resources for information on involvement in biological signaling pathways.

Then, the interpretation of functionally grouping was determined the by fold change cut off of 2.5. Moreover, the ratio of intensity of down-regulated genes was inverted to control *vs*. sample and indicated with a minus sign. A summary of up- and down-regulated genes was obtained for each steroid treatment (see tables 36 and 37).

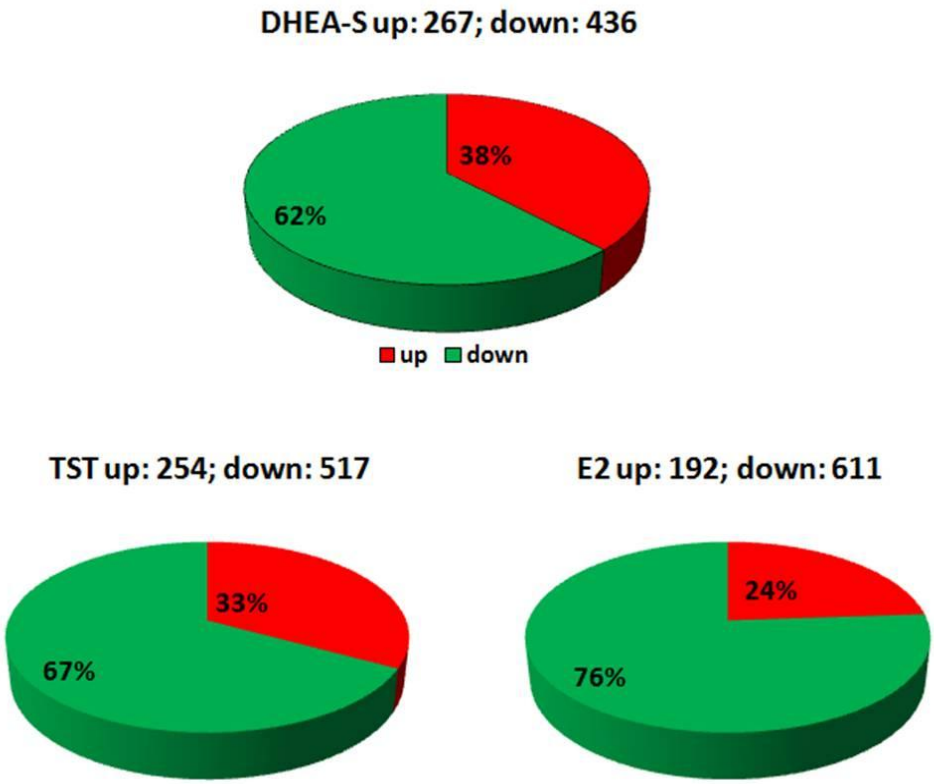

Figure 37. Up- and down-regulation of mRNA in EKs

The graphs display the global modulations of mRNA by DHEA-S, TST and E2 in human EKs. Genes in red are up-regulated and genes in green are down-regulated. The image shows the number and the percentage of up- and down-regulations for each steroid treatment.

Function	Gene	Description	Up or down		
			DHEA-S	TST	E2
Transcription					
	TXNIP	thioredoxin interacting protein	↑	↑	↑
	OTX1	orthodenticle homeobox 1	-	-	-
	EGR1	early growth response 1	-	-	↓
Cell differantiation	ANGPTL4	angiopoietin-like 4	↑	↑	↑
	TXNIP	thioredoxin interacting protein	↑	↑	↑
	EGR1	early growth response 1	↑	-	-
	BMP1	bone morphogenetic protein 1	-	-	↓
	MMP14	matrix metallopeptidase 14	-	-	↓
	AQP3	aquaporin 3	-	-	↓
Cell proliferation	CXCL1	chemokine (C-X-C motif) ligand 1	↑	↑	↑
	FSCN1	fascin homolog 1, actin-bundling protein	-	-	↓
	GNAI2	guanine nucleotide binding protein (G protein)	-	-	↓
	KRT16	keratin 16	-	-	↓
	MMP14	matrix metallopeptidase 14	-	-	↓
Inflammation					
	CXCL1		↑	↑	↑
Cytoskeleton					
	CXCL1	chemokine (C-X-C motif) ligand 1	↑	↑	↑
	ENC1	ectodermal-neural cortex	↑	-	↑
	LMNB1	lamin B1	↑	↑	↑
	KRT6L	keratin 79	-	-	↓
	K6HF	keratin 75	-	-	↓
	KRT6E	keratin 6A	-	-	↓
	KRT16	keratin 16	-	-	↓
	KRT13	keratin 13	-	-	↓
	KRT33A	keratin 33A	-	-	↓
Extracellular matrix	ANGPTL4	angiopoietin-like 4	↑	↑	↑
	TINAGL1	tubulointerstitial nephritis antigen-like 1	-	-	↓
	MMP14	matrix metallopeptidase 14	-	-	↓
	KRT77	keratin 77	-	↓	-

Table 36. Genes up (↑) or down (↓) regulated by 10µM DHEA-S, 50nM TST and 1nM E2 (FD>2.5) in human EKs. (-, unchanged).

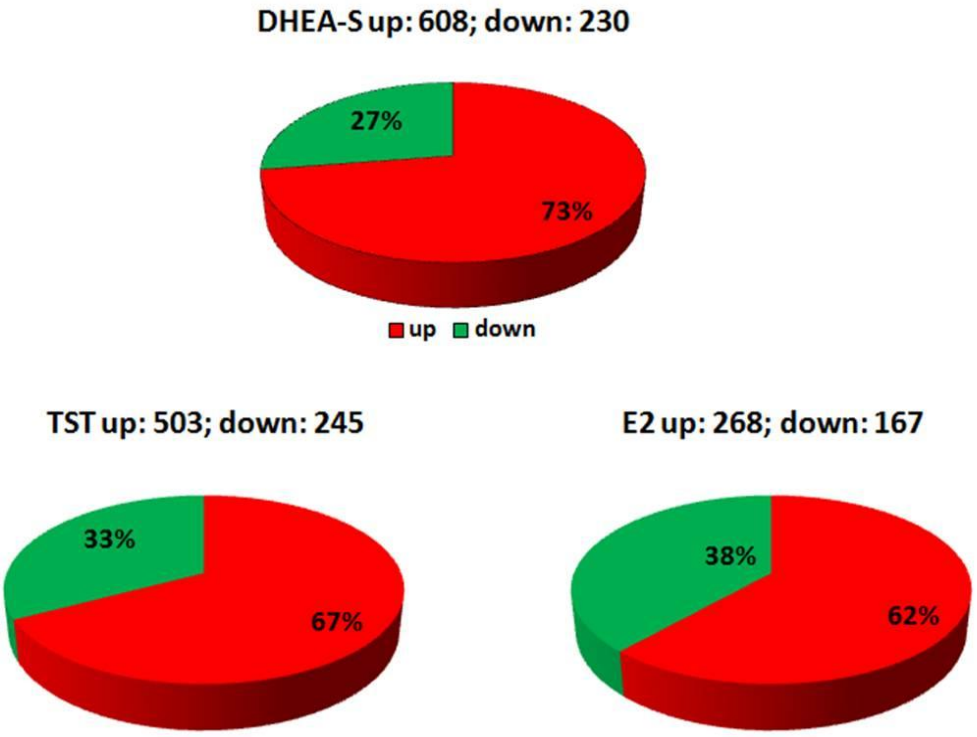

Figure 38. Up- and down-regulation of mRNA in HF

The graphs display the global modulations of mRNA by DHEA-S, TST and E2 in human HF. Genes in red are up-regulated and genes in green are down-regulated. The image shows the number and the percentage of up- and down-regulations per each steroid treatment.

Function	Gene	Description	Up or down		
			DHEA-S	TST	E2
Cell cycle					
	BTG4	B-cell translocation gene 4	-	-	↑
	TUBB1	tubulin, beta 1	-	-	↑
	FMN2	formin 2	-	-	↑
	SLC5A8	solute carrier family 5 (iodide transporter), 8	↑	-	-
	PRM2	protamine 2	↓	-	-
	ARHGAP20	Rho GTPase activating protein 20	↓	-	-
Cell proliferation					
	HNF4A	hepatocyte nuclear factor 4, α	-	↓	↑
	BTG4	B-cell translocation gene 4	-	-	↑
	CNTFR	ciliary neurotrophic factor receptor	-	-	↑
	FSHB	follicle stimulating hormone, beta polypeptide	-	-	↑
	NOX1	NADPH oxidase 1	-	-	↑
	RARB	retinoic acid receptor, beta	-	-	↑
	CXCL5	chemokine (C-X-C motif) ligand 5	-	-	↑
	TNFRSF17	tumor necrosis factor receptor superfamily, 17	↓	-	-
	THPO	thrombopoietin	-	-	↓
	INSL4	insulin-like 4 (placenta)	-	-	↓
Cell death					
	GFRAL	GDNF family receptor α like	-	-	↑
	ALB	albumin	-	-	↑
	PRKCE	protein kinase C, epsilon	-	-	↑
	VNN1	vanin 1	-	-	↑
	SFRP5	secreted frizzled-related protein 5	-	-	↑
	KRT20	keratin 20	-	-	↑
	RARB	retinoic acid receptor, beta	-	-	↑
	C14ORF153	chromosome 14 open reading frame 153	-	-	↑
	SLC5A8	solute carrier family 5 (iodide transporter), 8	-	↓	-
Cell differantiation					
	LOR	loricrin	↑	↑	-
	BTG4	B-cell translocation gene 4	-	-	↑
	MYH11	myosin, heavy chain 11, smooth muscle	-	-	↑
	ALS2	amyotrophic lateral sclerosis 2 (juvenile)	-	-	↑
	VNN1	vanin 1	-	-	↑
	SFRP5	secreted frizzled-related protein 5	-	-	↑
	RARB	retinoic acid receptor, beta	-	-	↑
	LEP	leptin	-	-	↑
	AK094175	tropomyosin 1 (α)	-	↑	-
	ADAM12	ADAM metallopeptidase domain 12	-	-	↓
	CRP	C-reactive protein, pentraxin-related	-	-	↓
	PRM2	protamine 2	-	↓	-
Migration					
	DNAH11	dynein, axonemal, heavy chain 11	↑	↑	↑
	X03757	ATPase, Na+/K+ transporting, α 1 polypeptide	↑	-	-
	VNN1	vanin 1	-	-	↑
	NOX1	NADPH oxidase 1	-	-	↑
	SAA1	serum amyloid A1;serum amyloid A2	-	-	↑
	ATP1A2	ATPase, Na+/K+ transporting, α 2 (+) polypeptide	-	↑	-
	ITGA5	integrin, α 5 (fibronectin receptor, α polypeptide)	-	↑	-
	AK094175	tropomyosin 1 (α)	-	↑	-
	GDF2	growth differentiation factor 2	-	↓	-

Table 37. Genes up (↑) or down (↓) regulated by 10µM DHEA-S, 50nM TST and 1nM E2 (FD>2.5) in human HF. (-, unchanged).

3.4.7 Analysis of differentially expressed genes by relative qRT-PCR in epidermal keratinocytes

In order to confirm the differential expression of genes that were identified by microarray technology, four genes were selected for validation by relative real time PCR.

3.4.7.1 *CXCL1* (chemokine (C-X-C motif) ligand 1)

In the present study, all three steroids determined up-regulation of *CXCL1* mRNA (table 36). The qRT-PCR confirmed the results with significantly higher expression for E2 and DHEA-S (Figure 39).

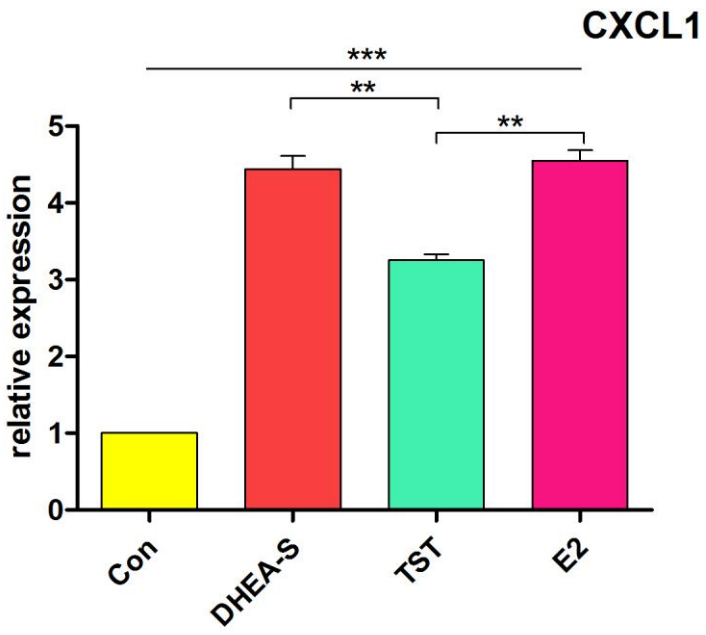

Figure 39. Relative mRNA expression of *CXCL1* in cultured human keratinocytes in response to incubation with steroid hormones

mRNA expression was investigated in response to vehicle control ETOH 0.0001% (Con, yellow), 10 µM dehydroepiandrosterone-sulphate (DHEA-S, red), 50 nM testosterone (TST, blue) and 1 nM 17ß-estradiol (E2, pink). Messenger RNA levels are presented after correction for individual GAPDH levels (data not shown) and as the mean ± SEM. (***P<0.001; Student's *t*-test; n=3).

3.4.7.2 *ANGPTL4* (angiopoietin-like 4)

In the present study, the gene array analysis detected up-regulation of *ANGPTL4* mRNA with all three steroids (table 36). The qRT-PCR confirmed the results with significant higher stimulation for DHEA-S and E2 compared to the Control and the TST treatment (Figure 40).

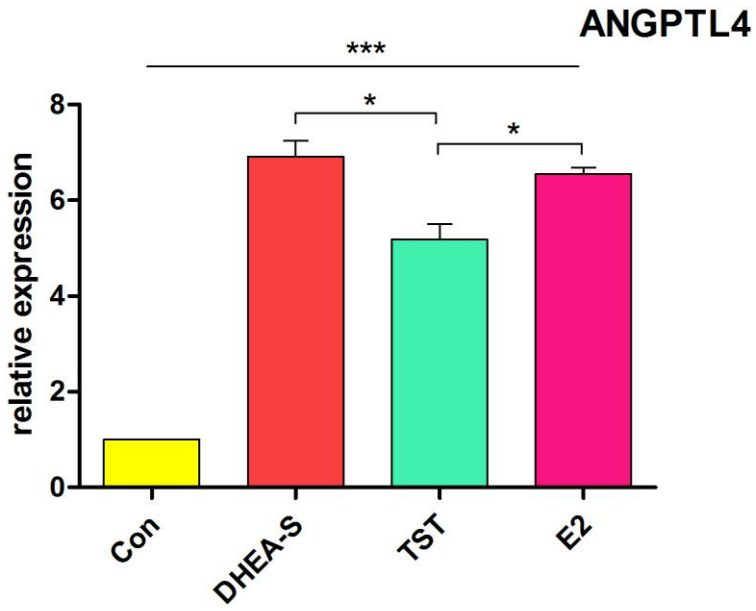

Figure 40. Relative mRNA expression of ANPTL4 in cultured human keratinocytes in response to incubation with steroid hormones

mRNA expression was investigated in response to vehicle control ETOH 0.0001% (Con, yellow), 10 µM dehydroepiandrosterone-sulphate (DHEA-S, red), 50 nM testosterone (TST, blue) and 1 nM 17ß-estradiol (E2, pink). Messenger RNA levels are presented after correction for individual GAPDH levels (data not shown) and as the mean ± SEM. (***P<0.001; Student's *t*-test; n=3).

3.4.7.3 TXNPI (thioredoxin interacting protein)

The gene array analysis of the present study showed up-regulation of *TXNIP* mRNA in presence of all three steroids (table 36). The qRT-PCR confirmed that result with a significant higher stimulation by DHEA-S and E2 compared to TST (Figure 41).

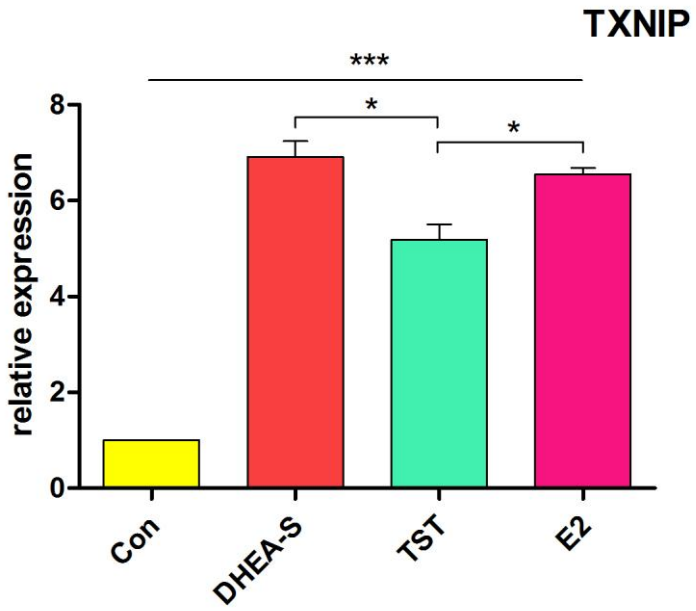

Figure 41. Relative mRNA expression of *TXNIP* in cultured human keratinocytes in response to incubation with steroid hormones

mRNA expression was investigated in response to vehicle control ETOH 0.0001% (Con, yellow), 10 µM dehydroepiandrosterone-sulphate (DHEA-S, red), 50 nM testosterone (TST, blue) and 1 nM 17ß-estradiol (E2, pink). Messenger RNA levels are presented after correction for individual GAPDH levels (data not shown) and as the mean ± SEM. (***P<0.001; Student's *t*-test; n=3).

3.4.7.4 *LMNB1* (lamin B1)

In the present study, the mRNA expression of *LMNB1* was detected up-regulated by DHEA-S, TST and E2 in the gene array analysis (table 36). The qRT-PCR analysis revealed the up-regulation in all three treatments with significant higher expression for DHEA-S and E2 compared to the Control and TST (Figure 42).

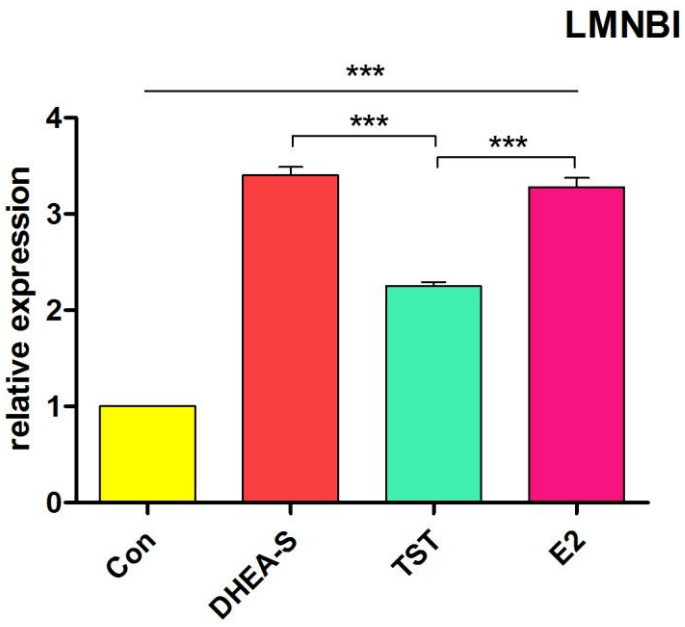

Figure 42. Relative mRNA expression of *LMNB1* in cultured human keratinocytes in response to incubation with steroid hormones

mRNA expression was investigated in response to vehicle control ETOH 0.0001% (Con, yellow), 10 µM dehydroepiandrosterone-sulphate (DHEA-S, red), 50 nM testosterone (TST, blue) and 1 nM 17ß-estradiol (E2, pink). Messenger RNA levels are presented after correction for individual GAPDH levels (data not shown) and as the mean ± SEM. (***P<0.001; Student's *t*-test; n=3).

3.5 Scratch wound assay

A scratch wound assay was used to assess the migration of DFs and EKs in response to incubation with DHEA-S, DHEA, E2 or TST and the ability of the cells to metabolise these steroids was assessed by including inhibitors of aromatase (Arimidex) and of STS (STX64).

3.5.1 Establishment and maintenance of cultured human dermal fibroblasts and epidermal keratinocytes

DFs and EKs were established from scalp skin biopsies as described in section *2.3*. In particular, the migration/proliferation of DFs was usually evident after 7-10 days and the cells had the typical bipolar spindle shaped morphology of DFs (Figure 50). EKs and DFs had usually reached confluence by 4 weeks at which time they were subcultured into T75 flasks. For each of the samples obtained, primary cultures were established, and DFs and EKs grew well during early culture and throughout experimentation.

3.5.2 Mitomycin C (MMC) does not affect migration of cells

Mitomycin C (MMC) was included in the assay to block cell proliferation establishing that the effect of steroids on migration was not due to an increase in proliferation. The addition of MMC to the cells incubated with either vehicle control or the different steroids did not affect the rate of migration of either DFs (Figure 43) or Eks (Figure 44).

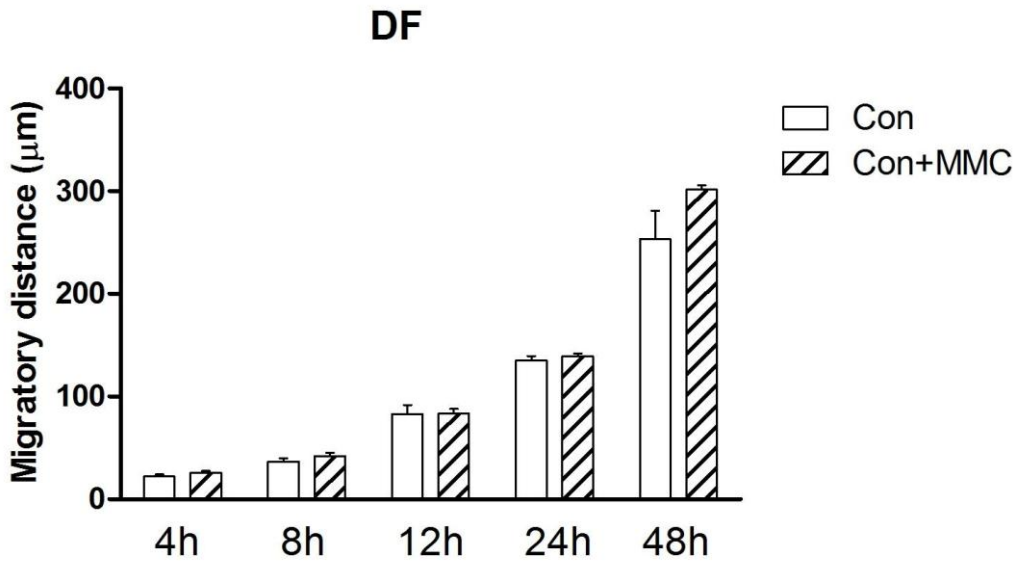

Figure 43. The addition of Mytomycin C does not alter the migration of human DFs cultured *in vitro*

Human female facial DFs were cultured with vehicle control (ETOH 0.0001%) in the presence (Con + MMC) or absence (Con) of 10 μg/ml Mitomycin C (MMC) to block the effects of proliferation and determine the true migration rate. Six points per dish were assessed and each point was performed in triplicate dishes for each cell line at five fixed time points (between 4 and 48 hours). Data are expressed as donor mean (n=5) ± SEM.

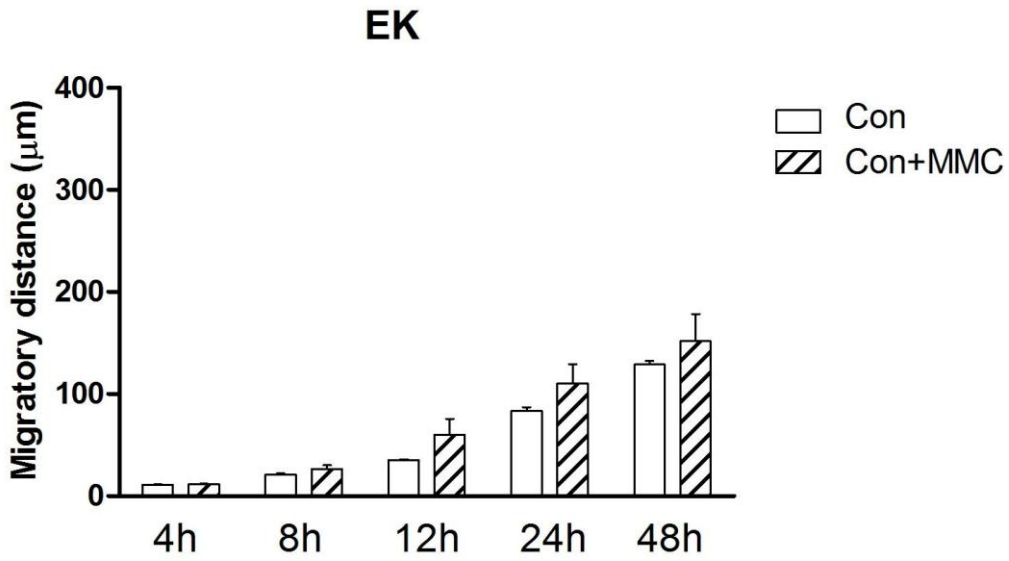

Figure 44. The addition of Mytomycin C does not alter the migration of human EKs cultured *in vitro*

Human female facial EKs were cultured with vehicle control (ETOH 0.0001%) in the presence (Con + MMC) or absence (Con) of 10 μg/ml Mitomycin C (MMC) to block the effects of proliferation and determine the true migration rate. Six points per dish were assessed and each point was performed in triplicate dishes for each cell line at five fixed time points (between 4 and 48 hours). Data are expressed as donor mean (n=3) ± SEM.

3.5.3 Migration of cultured cells in response to steroids following mechanical wounding *in vitro*

The scratch wound assay was performed on female facial DFs (Figure 50) and EKs (Figure 56) as described in section *2.25*.

3.5.3.1 Migration of cultured human dermal fibroblasts in response to androgens and estrogens

The migration of human DFs (n=5) was analyzed at five fixed time points between 4 and 48 hours following incubation with different steroids: vehicle control (ETOH 0.0001%), DHEA-S (10 μM), DHEA (10 μM), TST (50nM), and E2 (1 nM). In addition, the aromatase inhibitor (Arimidex) (100nM) and the STS inhibitor (STX64) (100nM) were included in additional cultures either alone, or in combination with DHEA and TST (Arimidex) or DHEA-S (STX64) to determine whether androgens are metabolised to E2. All steroids stimulated DF migration (Figures 45,46,47,48,49). In particular, a significant increase of migration was seen in the presence of E2 at 8h ($p<0.05$), 12h ($p<0.01$), 24h ($p<0.001$) and 48h ($p<0.01$). DFs also showed significant acceleration in migration in response to DHEA at 4h ($p<0.05$), 8h ($p<0.01$), 12h ($p<0.01$), 24h ($p<0.001$) and 48h ($p<0.001$). The stimulation of migration by DHEA-S was also significant at 4h ($p<0.05$), 8h ($p<0.01$), 12h ($p<0.01$), and 24h ($p<0.001$). In contrast, the cells did not show any significant increase in migration in response to TST. In addition, incubation with inhibitors of steroidogenic enzymes revealed that the effect of DHEA was reversed in the presence of Arimidex at 8h ($p<0.05$), 12h ($p<0.05$), 24h ($p<0.001$), and 48 h ($p<0.01$) and the effect of DHEA-S was impaired with STX64 at 8h ($p<0.05$), 12h ($p<0.01$), and 24h ($p<0.001$).

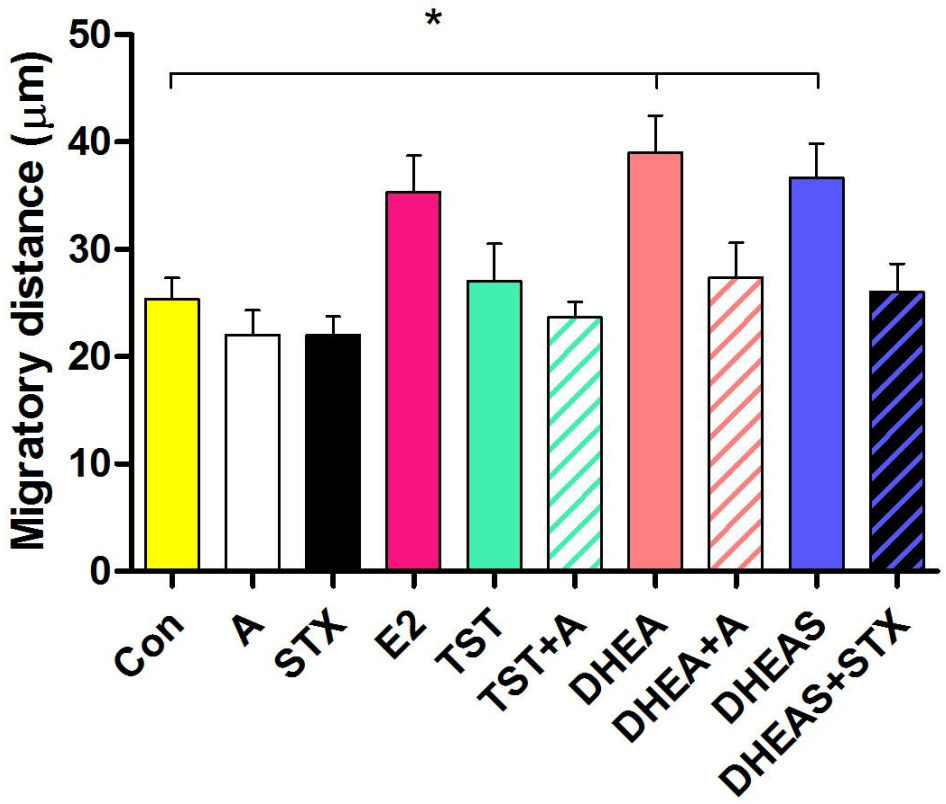

Figure 45. Migration of human dermal fibroblasts in the presence of androgens and estrogens at 4h following wounding *in vitro*

A scratch wound assay was used to measure the migration of cultured dermal fibroblasts (n=5) in response to E2 (1nM), (pink); TST (50nM), (green); DHEA (10μM), (red); DHEA-S (10μM), (dark blue); TST plus an aromatase inhibitor (green hatched); DHEA plus an aromatase inhibitor (red hatched) and DHEA-S plus a STS inhibitor (dark blue hatched). The control is labeled in yellow, the aromatase inhibitor alone (A) in white and the STS inhibitor alone (STX) in black. Six points per dish were assessed and each point was performed in triplicate dishes for each cell line. Data presented as patient mean ± SEM. *,$p<0.05$; Student's *t* test.

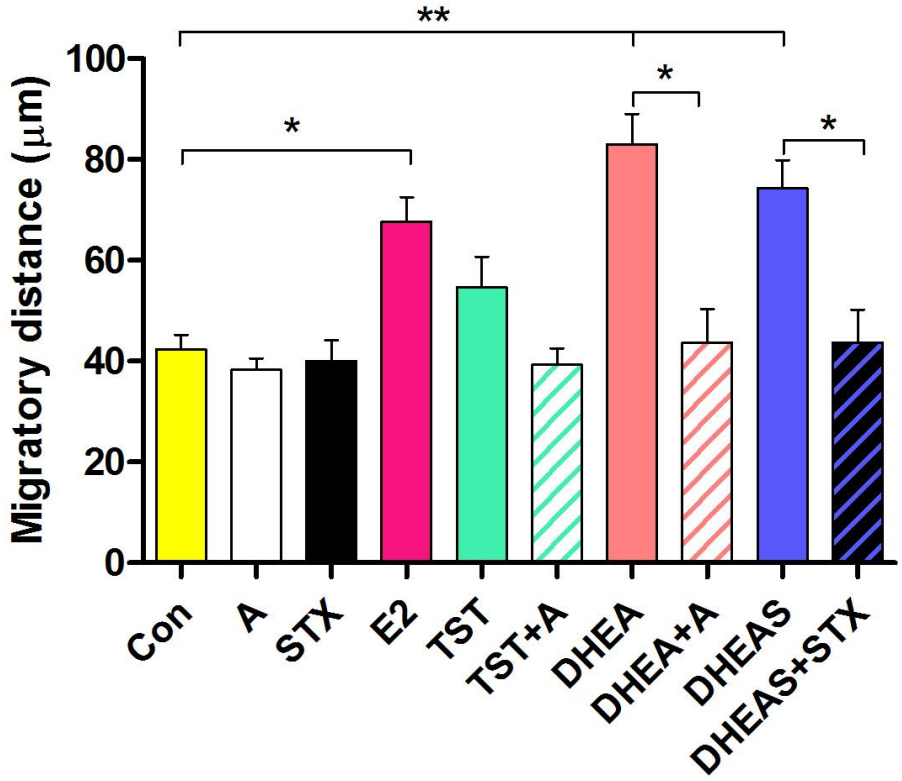

Figure 46. Migration of human dermal fibroblasts in the presence of androgens and estrogens at 8h following wounding *in vitro*

A scratch wound assay was used to measure the migration of cultured dermal fibroblasts (n=5) in response to E2 (1nM), (pink); TST (50nM), (green); DHEA (10μM), (red); DHEA-S (10μM), (dark blue); TST plus an aromatase inhibitor (green hatched); DHEA plus an aromatase inhibitor (red hatched) and DHEA-S plus a STS inhibitor (dark blue hatched). The control is labeled in yellow, the aromatase inhibitor alone (A) in white and the STS inhibitor alone (STX) in black. Six points per dish were assessed and each point was performed in triplicate dishes for each cell line. Data presented as patient mean ± SEM. *,$p<0.05$; **,$p<0.01$; Student's *t* test.

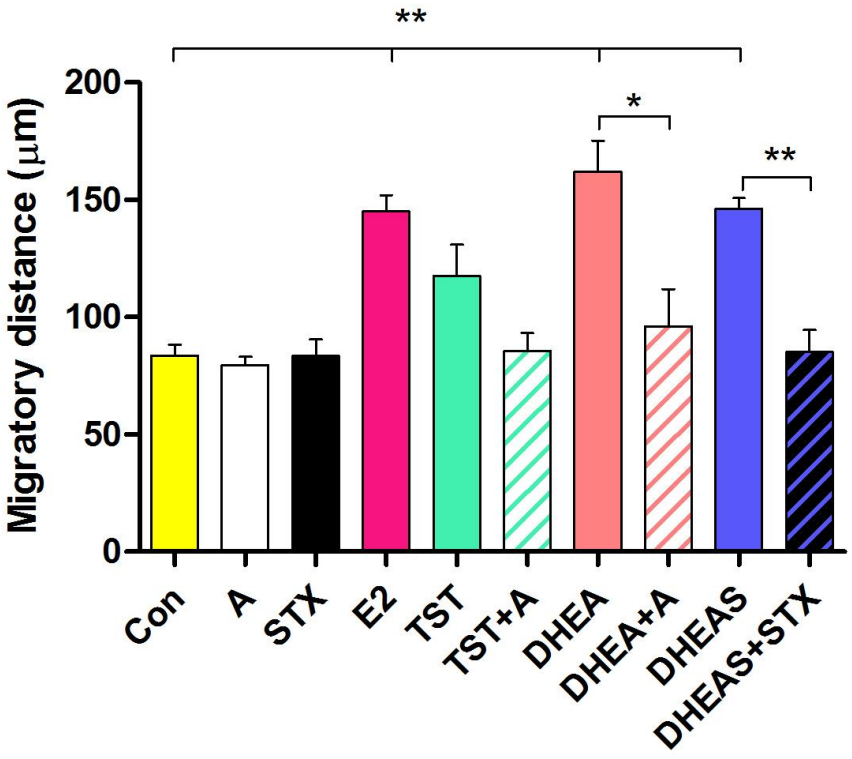

Figure 47. Migration of human dermal fibroblasts in the presence of androgens and estrogens at 12h following wounding *in vitro*

A scratch wound assay was used to measure the migration of cultured dermal fibroblasts (n=5) in response to E2 (1nM), (pink); TST (50nM), (green); DHEA (10μM), (red); DHEA-S (10μM), (dark blue); TST plus an aromatase inhibitor (green hatched); DHEA plus an aromatase inhibitor (red hatched) and DHEA-S plus a STS inhibitor (dark blue hatched). The control is labeled in yellow, the aromatase inhibitor alone (A) in white and the STS inhibitor alone (STX) in black. Six points per dish were assessed and each point was performed in triplicate dishes for each cell line. Data presented as patient mean ± SEM. *,$p<0.05$; **,$p<0.01$; Student's *t* test.

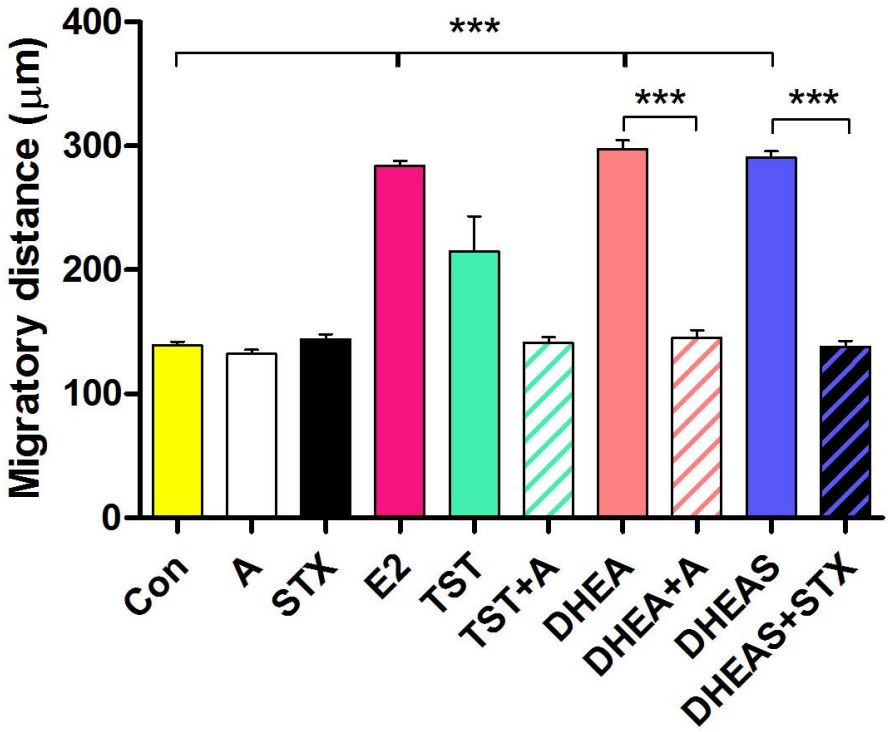

Figure 48. Migration of human dermal fibroblasts in the presence of androgens and estrogens at 24h following wounding *in vitro*

A scratch wound assay was used to measure the migration of cultured dermal fibroblasts (n=5) in response to E2 (1nM), (pink); TST (50nM), (green); DHEA (10μM), (red); DHEA-S (10μM), (dark blue); TST plus an aromatase inhibitor (green hatched); DHEA plus an aromatase inhibitor (red hatched) and DHEA-S plus a STS inhibitor (dark blue hatched). The control is labeled in yellow, the aromatase inhibitor alone (A) in white and the STS inhibitor alone (STX) in black. Six points per dish were assessed and each point was performed in triplicate dishes for each cell line. Data presented as patient mean ± SEM. ***,$p<0.001$; Student's *t* test.

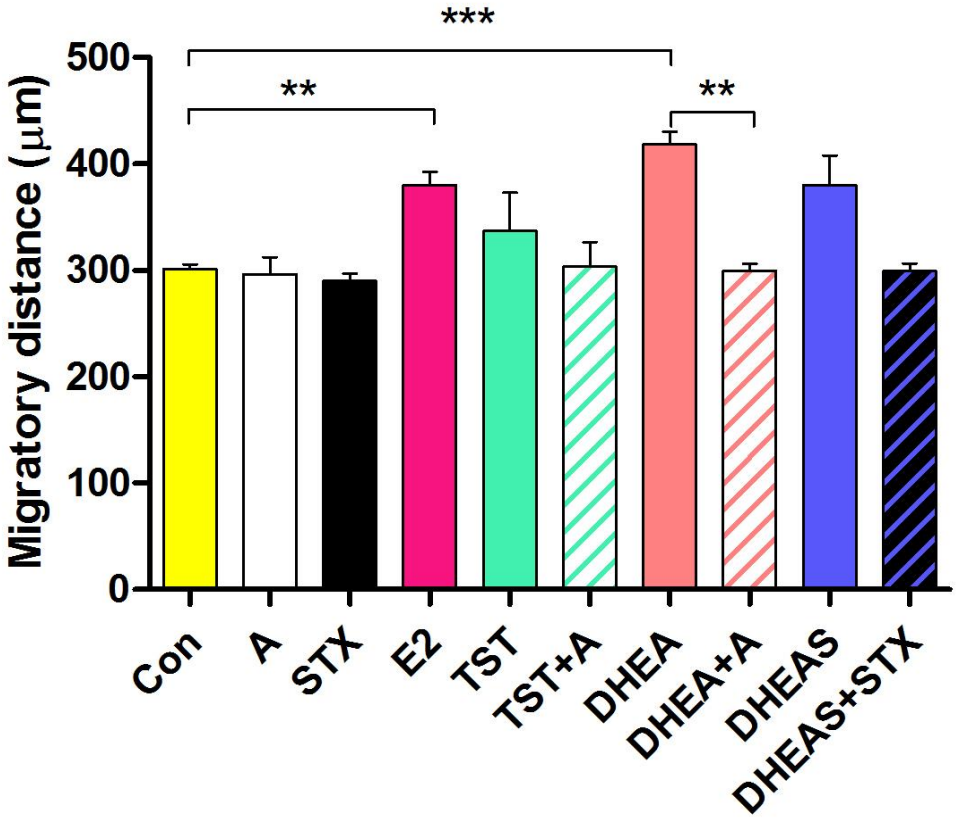

Figure 49. Migration of human dermal fibroblasts in the presence of androgens and estrogens at 48h following wounding *in vitro*

A scratch wound assay was used to measure the migration of cultured dermal fibroblasts (n=5) in response to E2 (1nM), (pink); TST (50nM), (green); DHEA (10μM), (red); DHEA-S (10μM), (dark blue); TST plus an aromatase inhibitor (green hatched); DHEA plus an aromatase inhibitor (red hatched) and DHEA-S plus a STS inhibitor (dark blue hatched). The control is labeled in yellow, the aromatase inhibitor alone (A) in white and the STS inhibitor alone (STX) in black. Six points per dish were assessed and each point was performed in triplicate dishes for each cell line. Data presented as patient mean ± SEM. **,$p<0.01$; ***,$p<0.001$; Student's *t* test.

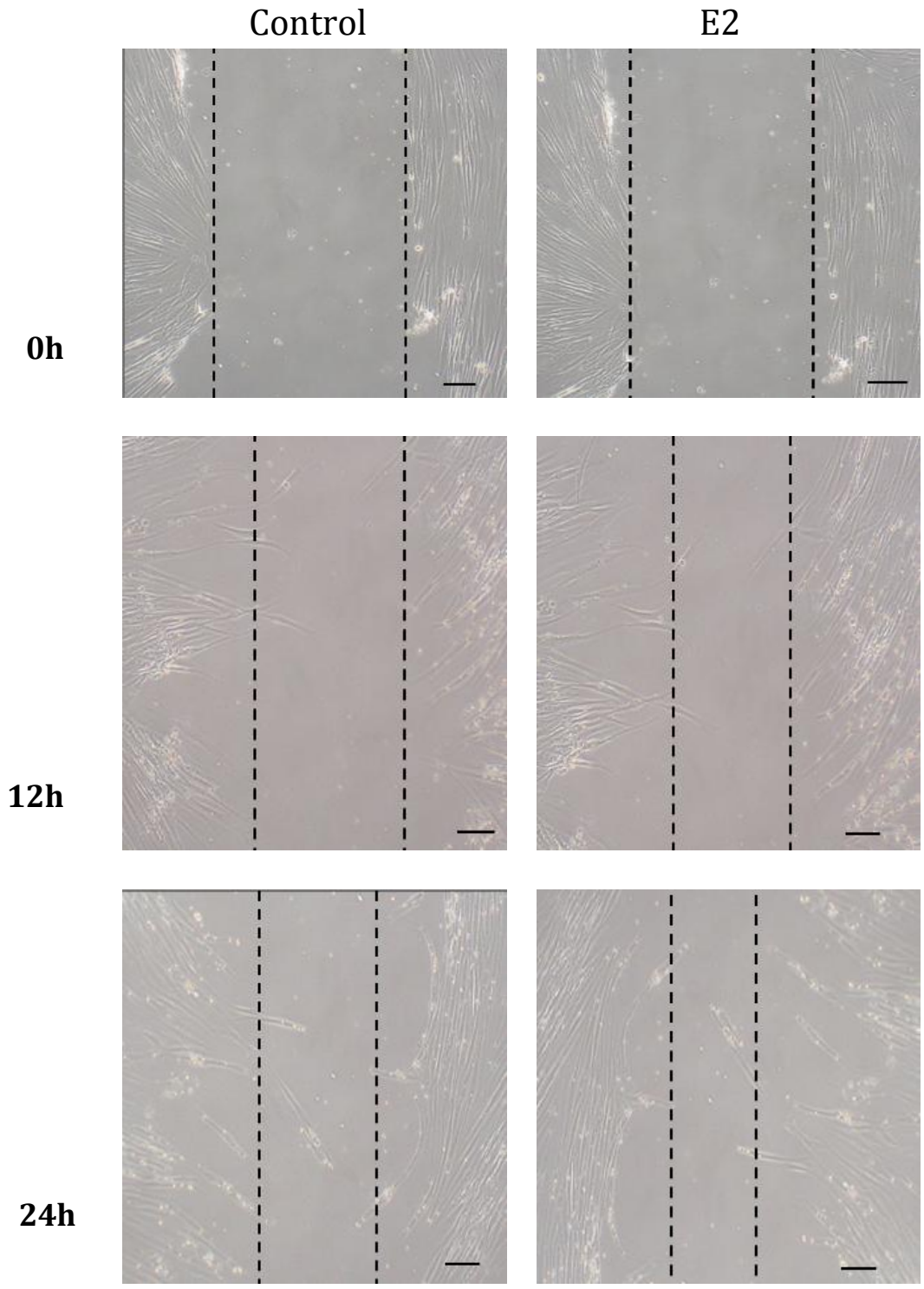

Figure 50. Migration of cultured human DFs in the presence of 17ß-estradiol

A scratch wound assay was used to measure the migration of cultured human female facial DFs. Representative time points at 0, 12 and 24h images of wounded cultures of Control and E2 in presence of mitomycin C (10 µg/ml). Black dotted lines represent the scratch gap. Scale bar = 100 µm.

3.5.3.2 Migration of cultured human epidermal keratinocytes in response to androgens and estrogens

The migration of human EKs (n= 3) was analyzed at five fixed time points between 4 and 48 hours following incubation with different steroids: vehicle control (ETOH 0.0001%), DHEA-S (10 µM), DHEA (10 µM), TST (50nM), and E2 (1 nM). In addition, the inhibitor of aromatase (Arimidex) (100nM) and that of STS (STX64) (100nM) were included in additional cultures either alone, or in combination with DHEA and TST (Arimidex) or DHEA-S (STX64) to determine the conversion of androgen to E2. All steroids stimulated cell migration (Figures 51,52,53,54,55). In particular, a significant increase of migration was seen with E2 at 4h($p<0.01$), 8h ($p<0.05$), 12h ($p<0.01$), 24h ($p<0.01$) and 48h ($p<0.01$). EKs showed also significant acceleration in response to DHEA at 4h ($p<0.01$), 12h ($p<0.05$), 24h ($p<0.01$) and 48h ($p<0.01$). The stimulation of migration by DHEA-S was significant at 4h($p<0.01$), 12h ($p<0.01$), 24h ($p<0.05$) and 48h ($p<0.01$). In contrast, the cells showed partial but not significant increase only at later time points in migration in response to TST. In addition, inhibitors of steroidogenic enzymes revealed that the effect of TST was significantly blocked in the presence of Arimidex at 24h ($p<0.01$) and 48h ($p<0.05$). Arimidex reversed also the effect of DHEA at 8h ($p<0.05$), 12h ($p<0.05$), 24h ($p<0.001$), and 48h ($p<0.01$) (Figures 52,53,54,55). The effect of DHEA-S was impaired with STX64 at 8h ($p<0.05$), 12h ($p<0.01$), and 24h ($p<0.001$).

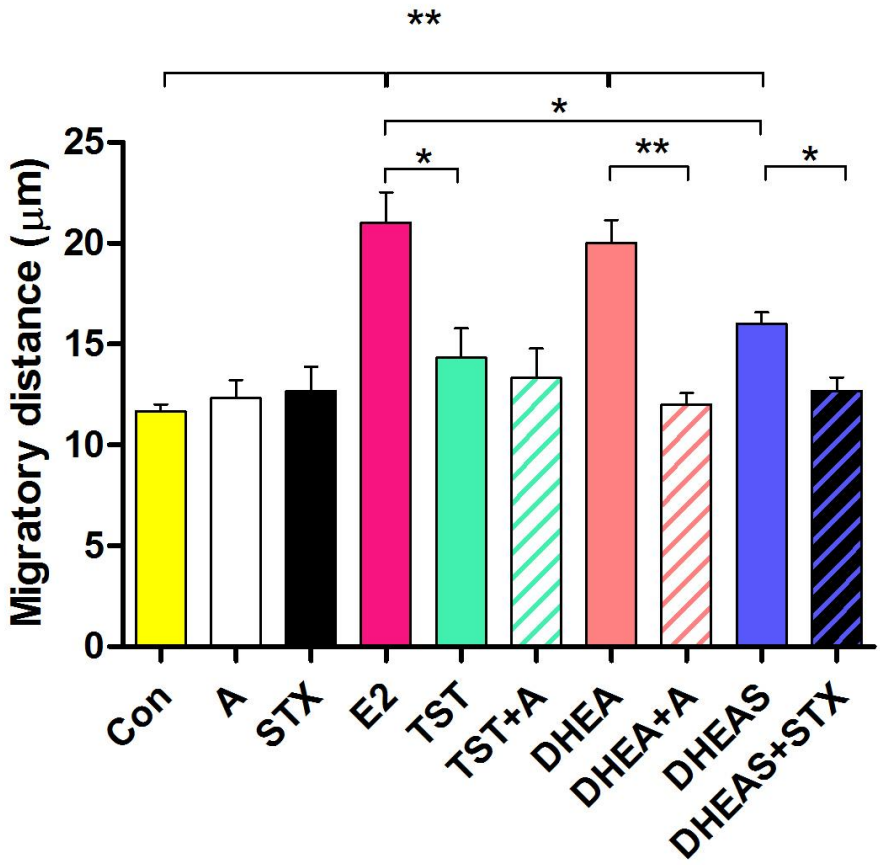

Figure 51. Migration of human epidermal keratinocytes in the presence of androgens and estrogens at 4h following wounding *in vitro*

A scratch wound assay was used to measure the migration of cultured epidermal keratinocystes (n=3) in response to E2 (1nM), (pink); TST (50nM), (green); DHEA (10μM), (red); DHEA-S (10μM), (dark blue); TST plus an aromatase inhibitor (green hatched); DHEA plus an aromatase inhibitor (red hatched) and DHEA-S plus a STS inhibitor (dark blue hatched). The control is labeled in yellow, the aromatase inhibitor alone (A) in white and the STS inhibitor alone (STX) in black. Six points per dish were assessed and each point was performed in triplicate dishes for each cell line. Data presented as patient mean ± SEM. *,$p<0.05$; **,$p<0.01$; Student's *t* test.

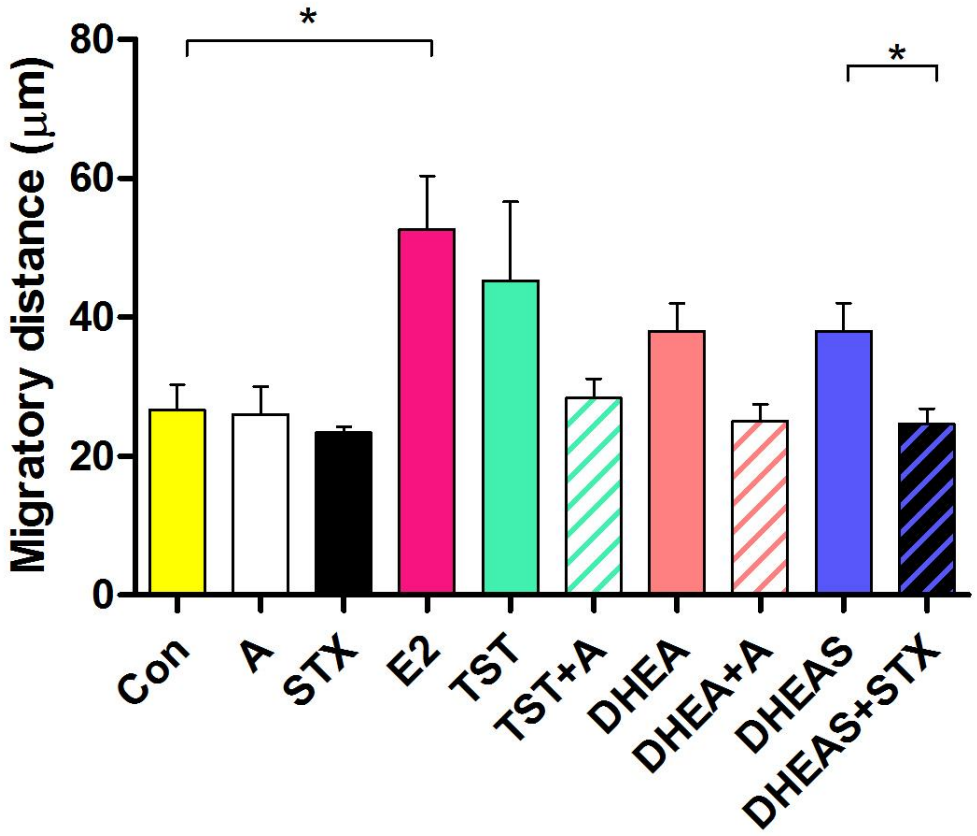

Figure 52. Migration of human epidermal keratinocytes in the presence of androgens and estrogens at 8h following wounding *in vitro*

A scratch wound assay was used to measure the migration of cultured epidermal keratinocystes (n=3) in response to E2 (1nM), (pink); TST (50nM), (green); DHEA (10μM), (red); DHEA-S (10μM), (dark blue); TST plus an aromatase inhibitor (green hatched); DHEA plus an aromatase inhibitor (red hatched) and DHEA-S plus a STS inhibitor (dark blue hatched). The control is labeled in yellow, the aromatase inhibitor alone (A) in white and the STS inhibitor alone (STX) in black. Six points per dish were assessed and each point was performed in triplicate dishes for each cell line. Data presented as patient mean ± SEM. *, $p<0.05$; Student's *t* test.

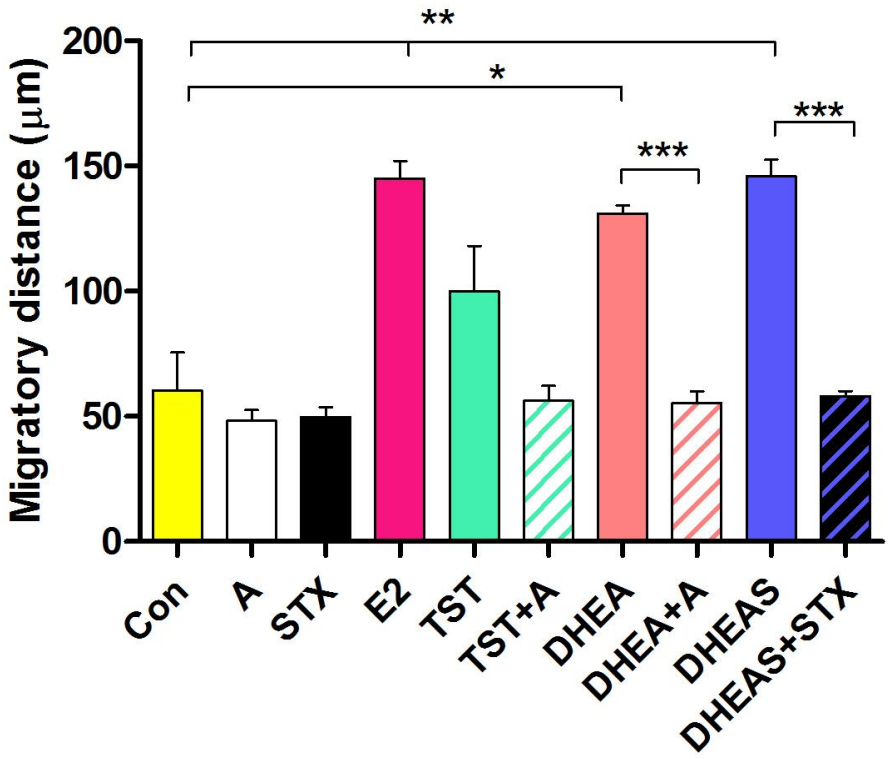

Figure 53. Migration of human epidermal keratinocytes in the presence of androgens and estrogens at 12h following wounding *in vitro*

A scratch wound assay was used to measure the migration of cultured epidermal keratinocystes (n=3) in response to E2 (1nM), (pink); TST (50nM), (green); DHEA (10μM), (red); DHEA-S (10μM), (dark blue); TST plus an aromatase inhibitor (green hatched); DHEA plus an aromatase inhibitor (red hatched) and DHEA-S plus a STS inhibitor (dark blue hatched). The control is labeled in yellow, the aromatase inhibitor alone (A) in white and the STS inhibitor alone (STX) in black. Six points per dish were assessed and each point was performed in triplicate dishes for each cell line. Data presented as patient mean ± SEM. *,$p<0.05$; **,$p<0.01$; ***,$p<0.001$; Student's *t* test.

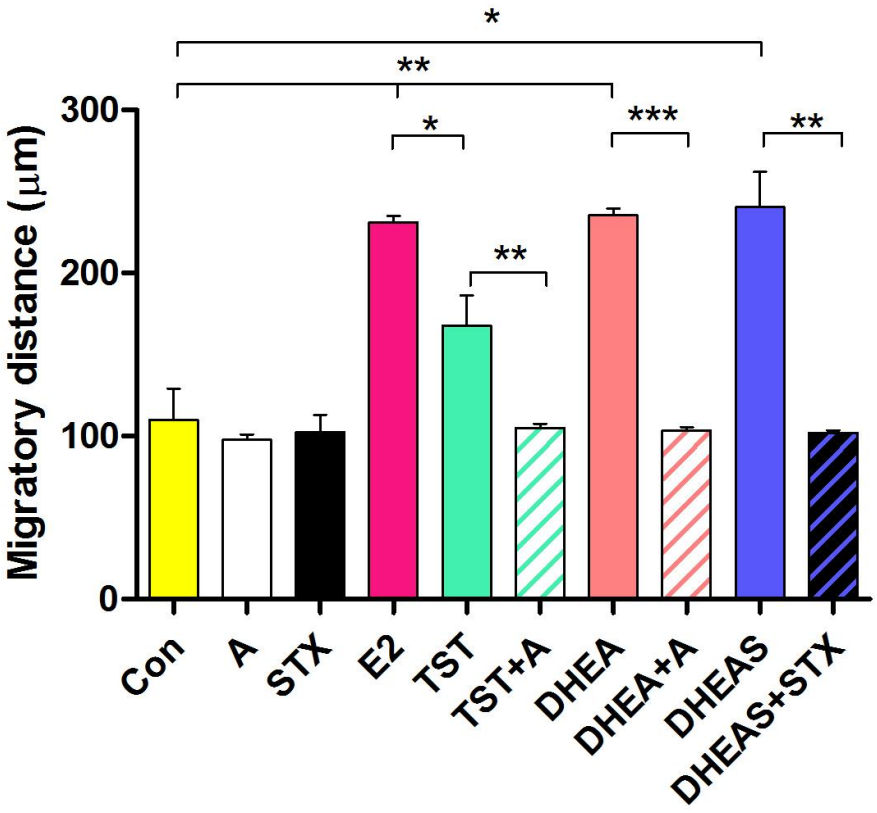

Figure 54. Migration of human epidermal keratinocytes in the presence of androgens and estrogens at 24h following wounding *in vitro*

A scratch wound assay was used to measure the migration of cultured epidermal keratinocystes (n=3) in response to E2 (1nM), (pink); TST (50nM), (green); DHEA (10μM), (red); DHEA-S (10μM), (dark blue); TST plus an aromatase inhibitor (green hatched); DHEA plus an aromatase inhibitor (red hatched) and DHEA-S plus a STS inhibitor (dark blue hatched). The control is labeled in yellow, the aromatase inhibitor alone (A) in white and the STS inhibitor alone (STX) in black. Six points per dish were assessed and each point was performed in triplicate dishes for each cell line. Data presented as patient mean ± SEM. *,$p<0.05$; **,$p<0.01$; ***,$p<0.001$; Student's *t* test.

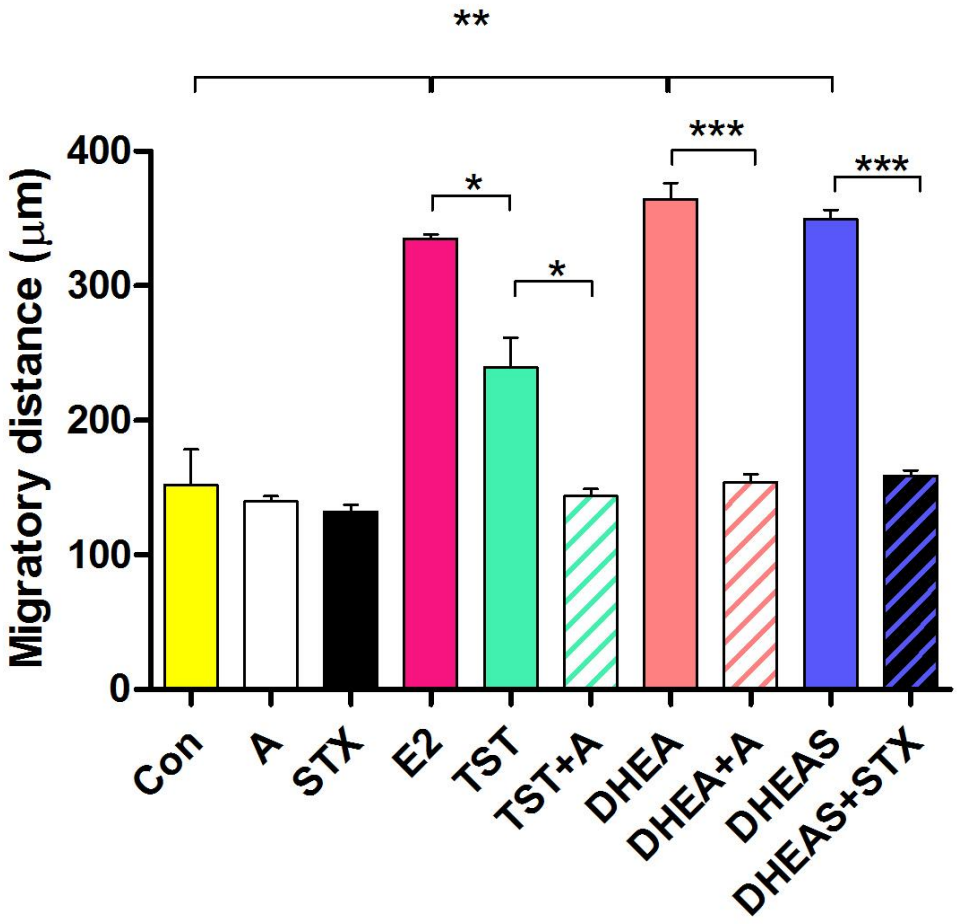

Figure 55. Migration of human epidermal keratinocytes in the presence of androgens and estrogens at 48h following wounding *in vitro*

A scratch wound assay was used to measure the migration of cultured epidermal keratinocystes (n=3) in response to E2 (1nM), (pink); TST (50nM), (green); DHEA (10μM), (red); DHEA-S (10μM), (dark blue); TST plus an aromatase inhibitor (green hatched); DHEA plus an aromatase inhibitor (red hatched) and DHEA-S plus a STS inhibitor (dark blue hatched). The control is labeled in yellow, the aromatase inhibitor alone (A) in white and the STS inhibitor alone (STX) in black. Six points per dish were assessed and each point was performed in triplicate dishes for each cell line. Data presented as patient mean ± SEM. *,$p<0.05$; **,$p<0.01$; ***,$p<0.001$; Student's *t* test.

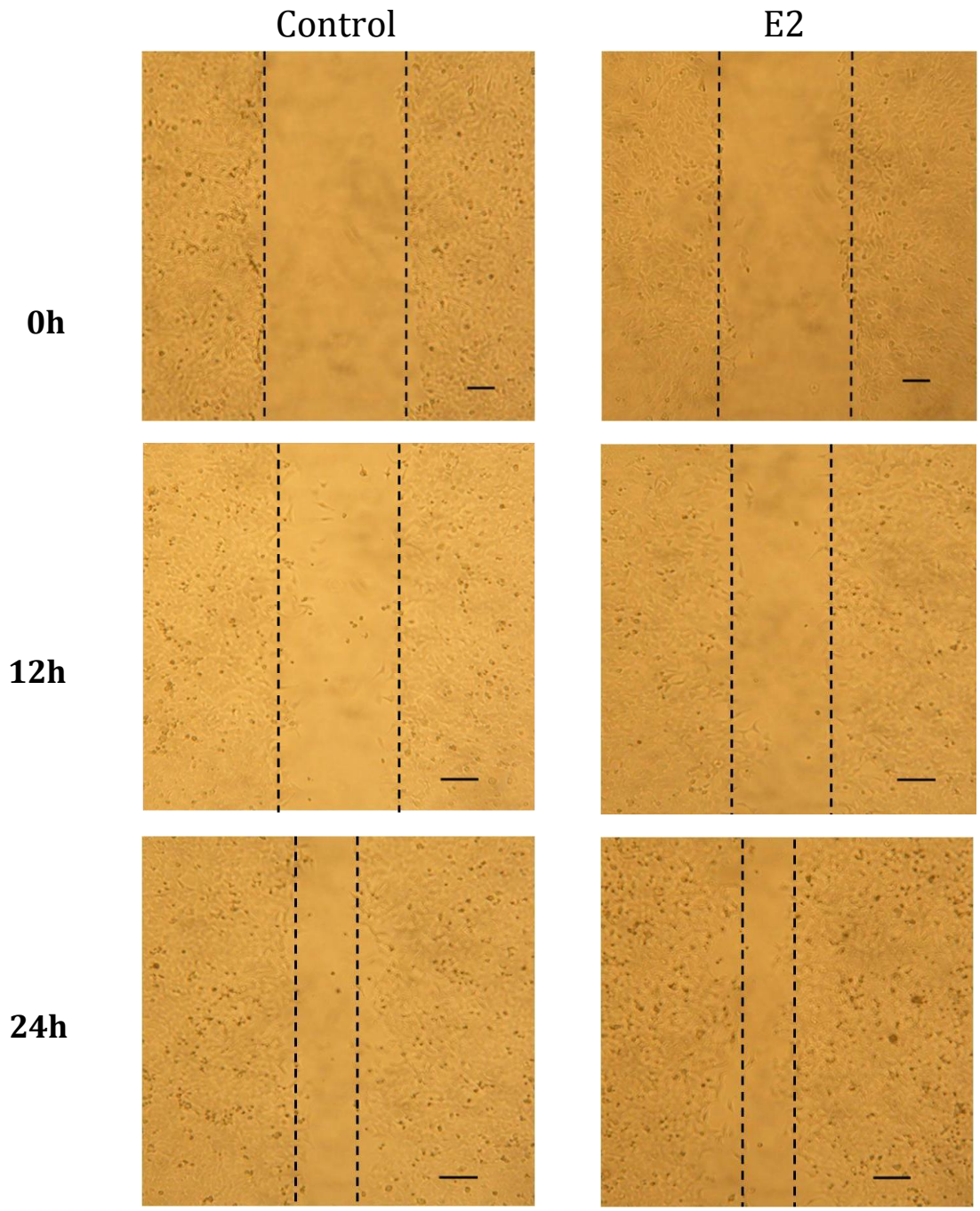

Figure 56. Migration of cultured human EKs in the presence of 17ß-estradiol

A scratch wound assay was used to measure the migration of cultured human female facial EKs. Representative time points at 0, 12 and 24h images of wounded cultures of Control and E2 in presence of mitomycin C (10 µg/ml). Black dotted lines represent the scratch gap. Scale bar = 100 µm.

3.6 The effect of Dexamethasone on aromatase activity and mRNA expression in cultured human dermal fibroblasts and epidermal keratinocytes

The aromatase activity of cultured human DFs and EKs was assessed by the tritiated water assay as described in section *2.26*. Cells were incubated in experimental medium (see section *2.10*) supplemented with either ETOH (0.0001%) or dexamethasone (250 nM) for 24 hours at 37˚C. Then cells were incubated 2h with 0.5µCi of tritiated androstenedione ([1β^{3}H]-Androstenedione). All experiments were performed in triplicate.

3.6.1 Dexamethasone increases aromatase activity in cultured human dermal fibroblasts

A ^{3}H-Androstenedione assay was used to assess the effect of dexamethasone (DEX) on the activity of aromatase by human DFs derived from female face (n=5), male face (n=1), breast (n=1) and female abdomen (n=1) (see appendix 8). The incubation with DEX showed a significant ($p<0.01$) increase in the enzymatic activity only in DFs established from female (Figure 57) and male (Figure 58) face samples when compared to the control. In contrast, the cells established from breast skin (Figure 59) and abdominal skin (Figure 60) did not show an increase of the aromatase activity.

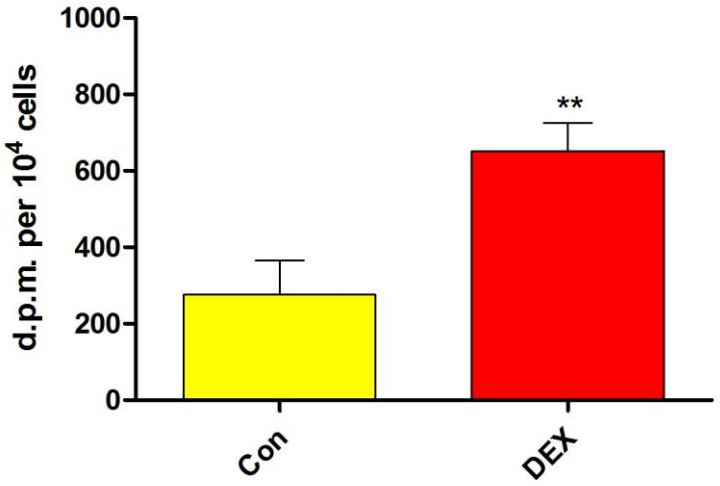

Figure 57. Dexamethasone increases the aromatase activity of human female facial DFs in vitro

A ^{3}H-Androstenedione assay was used to measure the activity of aromatase by human female facial DFs (n=5) cultured in the presence (red) or absence (yellow) of dexamethasone (DEX). Cells were established from female facial skin (n=5). Data are presented as donor mean ± SEM. **, p<0.01 Student's *t* test.

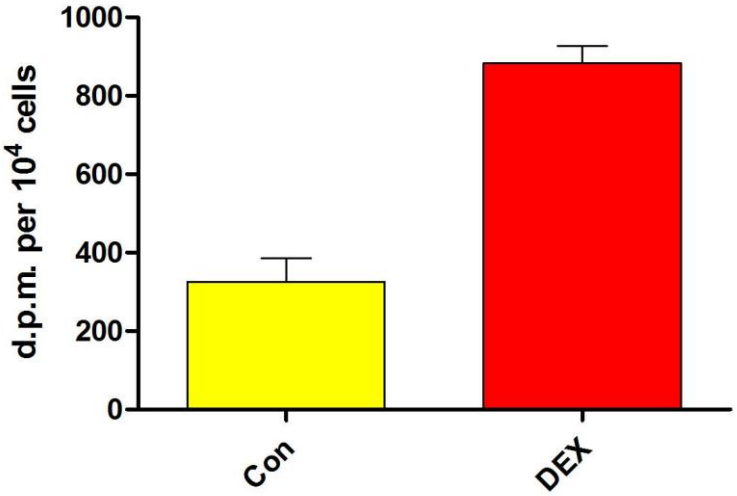

Figure 58. Dexamethasone increases the aromatase activity of human male facial DFs in *vitro*

A ^{3}H-Androstenedione assay was used to measure the activity of aromatase by human male facial DFs cultured in the presence (red) or absence (yellow) of dexamethasone (DEX). Cells were established from male facial skin (n=1). Data are presented as mean of triplicate dishes ± SEM.

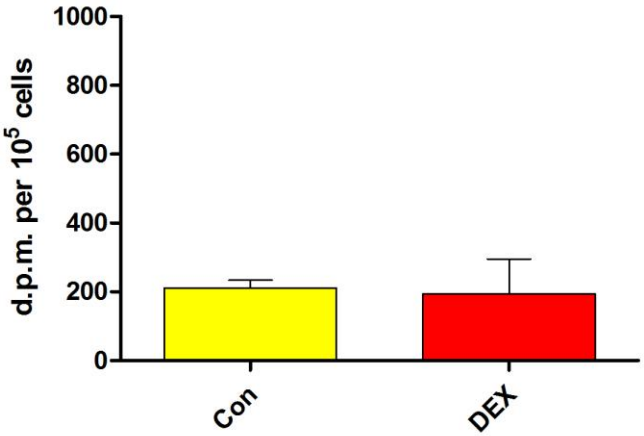

Figure 59. Dexamethasone does not alter the aromatase activity of human breast DFs in *vitro*

A ^{3}H-Androstenedione assay was used to measure the activity of aromatase by human breast DFs cultured in the presence (red) or absence (yellow) of dexamethasone (DEX). Cells were established from breast skin (n=1). Data are presented as mean of triplicate dishes ± SEM.

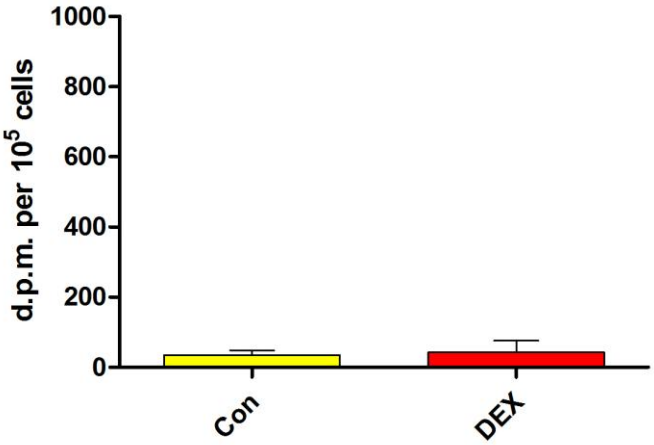

Figure 60. Dexamethasone does not the aromatase activity of human female abdominal dermal fibroblasts *in vitro*

A ^{3}H-Androstenedione assay was used to measure the activity of aromatase by human female abdominal DFs cultured in the presence (red) or absence (yellow) of dexamethasone (DEX). Cells were established from female abdominal skin (n=1). Data are presented as mean of triplicate dishes ± SEM.

Site	Sex	Aromatase activity control (10^2 nmol/mg protein)	Aromatase activity dexamethasone (250 nmol/l) (10^2 nmol/mg protein)
Face	F	79	689
Face	F	44	1146
Face	F	565	1311
Face	F	180	291
Face	F	549	483
Face	M	322	1240
Abdomen	F	77	75
Breast	F	422	352

Table 38. Effect of DEX on aromatase activity in cultured DFs after 24h. F: female; M: male.

3.6.2 Dexamethasone does not alter aromatase activity in epidermal keratinocytes

A ^{3}H-Androstenedione assay was used to assess the effect of dexamethasone (DEX) on the activity of aromatase by human female (n=3) and male (n=1) facial EKs (see appendix 8). The incubation with DEX did not significantly increase the activity compared to the control in any of the samples (Figures 61 and 62).

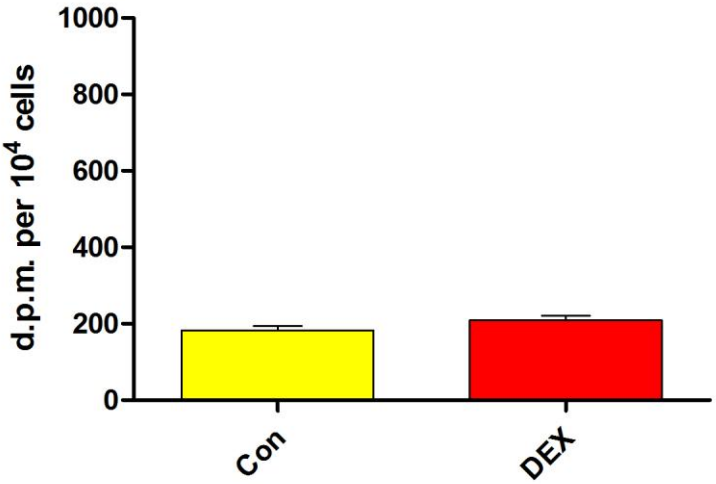

Figure 61. Dexamethasone does not alter the activity of aromatase of human female facial EKs *in vitro*

A ^{3}H-Androstenedione assay was used to measure the activity of aromatase by human female facial EKS cultured in the presence (red) or absence (green) of dexamethasone (DEX). Cells were established from female facial skin (n=3). Data are presented as donor mean ± SEM.

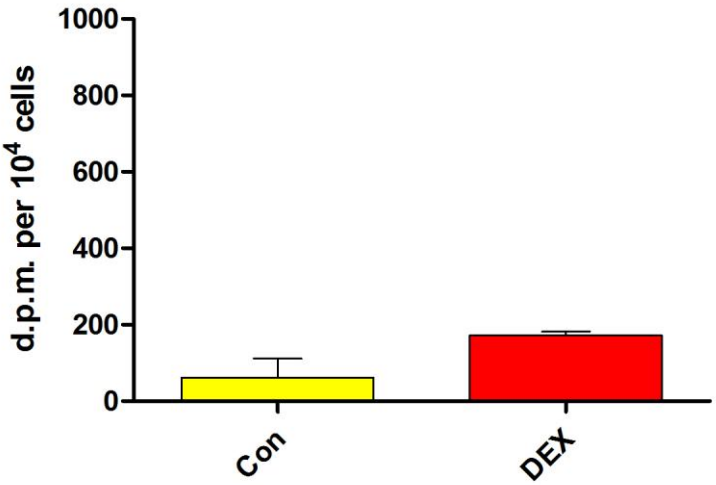

Figure 62. Dexamethasone does not alter the aromatase activity of human male facial EKs *in vitro*

A ^{3}H-Androstenedione assay was used to measure the activity of aromatase by human male facial EKs cultured in the presence (red) or absence (green) of dexamethasone (DEX). Cells were established from male facial skin (n=1). Data are presented as mean of triplicate dishes ± SEM.

Site	Sex	Aromatase activity control (10^2 nmol /mg protein)	Aromatase activity dexamethasone (250 nmol/l) (10^2 nmol /mg protein)
Face	F	10	15
Face	F	7	15
Face	F	65	53
Face	M	18	44

Table 39. Effect of DEX on aromatase activity in cultured EKs. F: female; M: male.

3.7 The effect of Dexamethasone on mRNA expression of aromatase in cultured human fibroblasts and epidermal keratinocytes

The mRNA expression of aromatase was investigated by relative qRT-PCR (see section *2.22.2*). Cells were incubated with either ETOH (0.0001%) or dexamethasone (250 nM) for 24h and then the total RNA was extracted as described in section *2.12.2*.

3.7.1 Up-regulation of the mRNA expression of aromatase by dexamethasone in dermal fibroblasts

The mRNA expression of aromatase was investigated by relative qRT-PCR after 24h of incubation with DEX. DFs derived from female (n=5) and male (n=1) face, breast (n=1) and female abdomen (n=1) (see appendix 8). The treatment with DEX increased the mRNA expression in facial (Figures 63 and 64) and abdominal (Figure 66) cells compared with the control. In contrast, DEX had not effect on the fibroblasts established from breast (Figure 65).

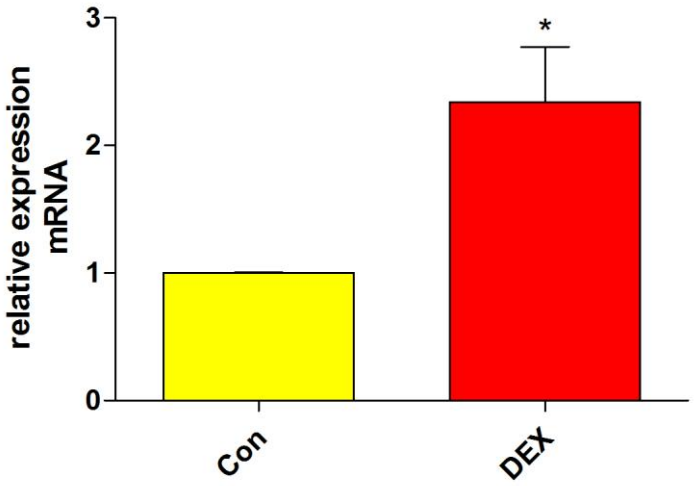

Figure 63. Dexamethasone increases mRNA expression of aromatase after 24 hours in female facial DFs. The relative qRT-PCR assay was used to analyzed the mRNA expression of aromatase of cultured human female facial DFs (n=5) following 24 hours of incubation with DEX (250 nM) *in vitro*. Data presented as donor mean ± SEM. *p<0.05; Student's *t* test.

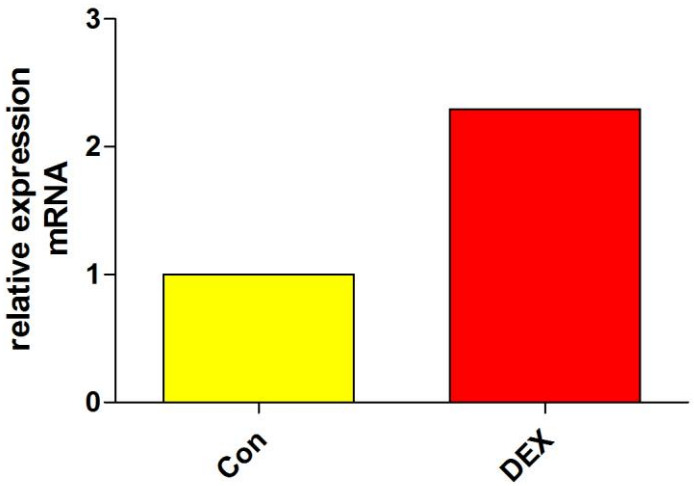

Figure 64. Dexamethasone increases mRNA expression of aromatase after 24 hours in male facial DFs

The relative qRT-PCR assay was used to analyzed the mRNA expression of aromatase of cultured human male facial DFs (n=1) following 24 hours of incubation with DEX (250 nM) *in vitro*. Data presented as donor as mean of triplicate measurements.

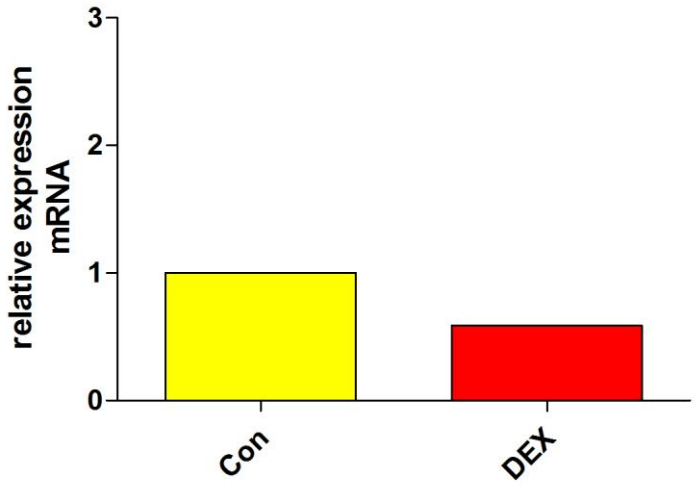

Figure 65. Dexamethasone does not increase mRNA expression of aromatase after 24 hours in breast DFs

The relative qRT-PCR assay was used to analyzed the mRNA expression of aromatase of cultured human breast DFs (n=1) following 24 hours of incubation with DEX (250 nM) *in vitro*. Data presented as mean of triplicate measurements.

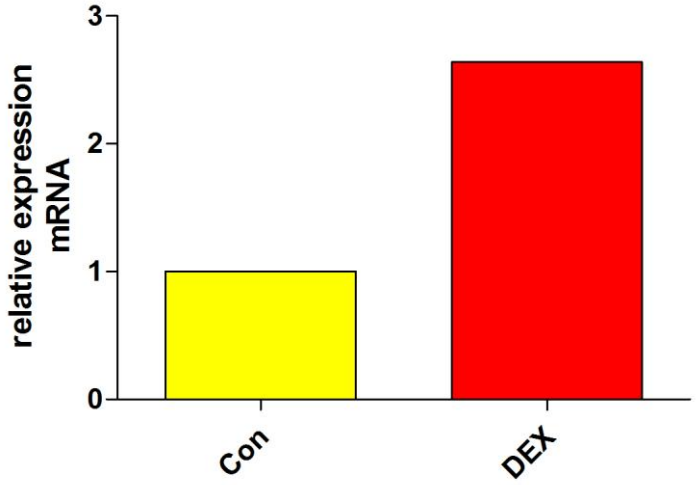

Figure 66. Dexamethasone increases mRNA expression of aromatase after 24 hours in female abdominal DFs

The relative qRT-PCR assay was used to analyzed the mRNA expression of aromatase of cultured human female abdominal DFs (n=1) following 24 hours of incubation with DEX (250 nM) *in vitro*. Data presented as donor as mean of triplicate measurements.

3.7.2 Up-regulation of the mRNA expression of aromatase by dexamethasone in epidermal keratinocytes

The mRNA expression of aromatase was investigated by relative qRT-PCR after 24h of incubation with DEX. EKs were derived from female (n=3) and male (n=1) face (see appendix 8). The treatment with DEX significantly ($p<0.01$) increased the mRNA expression in the cells established from female donors (Figure 67). In contrast, DEX had not effect on the keratinocytes established from the male facial sample (Figure 68).

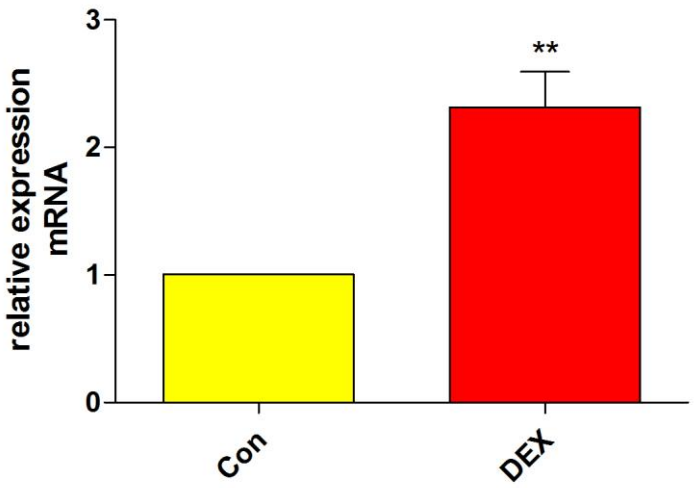

Figure 67. Dexamethasone increase mRNA expression of aromatase after 24 hours in female facial EKs The relative qRT-PCR assay was used to analyzed the mRNA expression of aromatase of cultured human female facial EKs (n=3) following 24 hours of incubation with DEX (250 nM) *in vitro*. Data presented as donor mean ± SEM. **, $p<0.01$ Student's *t* test.

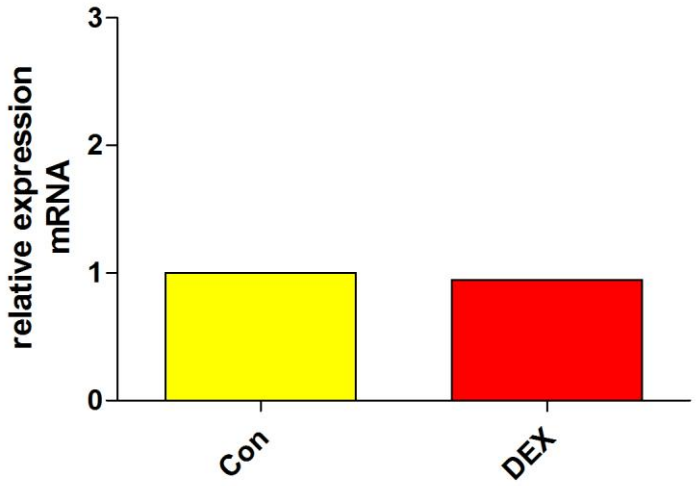

Figure 68. Dexamethasone does not increase mRNA expression of aromatase after 24 hours in male facial EKs

The relative qRT-PCR assay was used to analyzed the mRNA expression of aromatase of cultured human male facial EKs (n=1) following 24 hours of incubation with DEX (250 nM) *in vitro*. Data presented as donor mean of triplicate measurements.

3.8 The effect of mechanical wounding on the aromatase activity of cultured human fibroblasts and epidermal keratinocytes

Aromatase activity as measured by the tritiated assay (see section *2.26*) was quantited after the mechanical wounding of monolayers of DFs and EKs. The analysis was performed by the incubation of cells with 0.5 µCi of [1β^{3}H]-Androstenedione for 2 and 24h.

3.8.1 Mechanical wounding does not alter the aromatase activity of dermal fibroblasts at 2h

^{3}H-Androstenedione was used to assess the effect of mechanical wounding on the aromatase activity by human DFs derived from female (n=5) and male (n=1) face, breast (n=1) and female abdomen (n=1) (see appendix 8). The

mechanical wounding did not increase the activity in any group of samples after 2h (Figures 69,70,71,72).

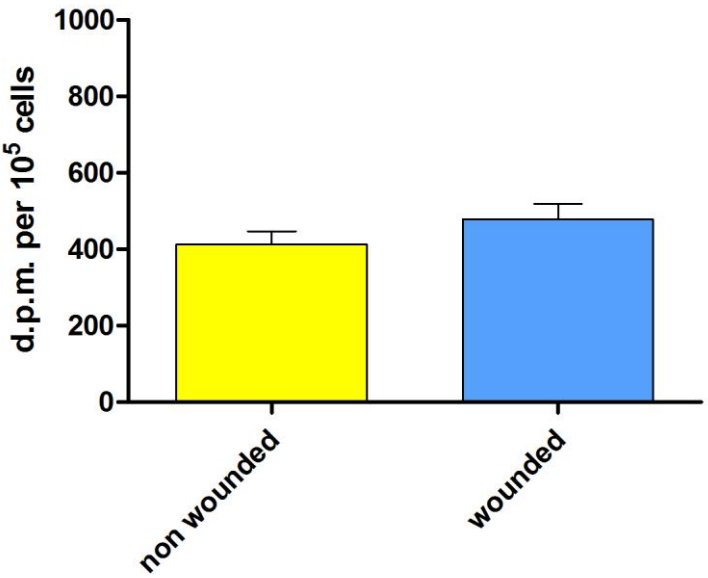

Figure 69. *In vitro* wounded female facial DFs do not alter aromatase activity after 2 hours

The tritiated water assay was used to measure the activity of aromatase of cultured human female facial DFs (n=5) following wounding *in vitro* after 2 hours. Data presented as donor mean ± SEM.

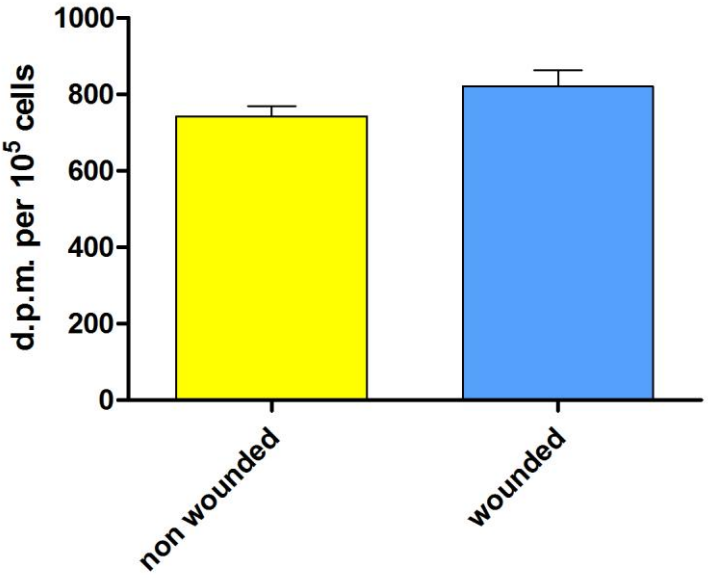

Figure 70. *In vitro* wounded male facial DFs do not alter aromatase activity after 2 hours

The tritiated water assay was used to measure the activity of aromatase of cultured human male facial DFs (n=1) following wounding *in vitro* after 2 hours. Data are presented as mean of triplicate dishes ± SEM.

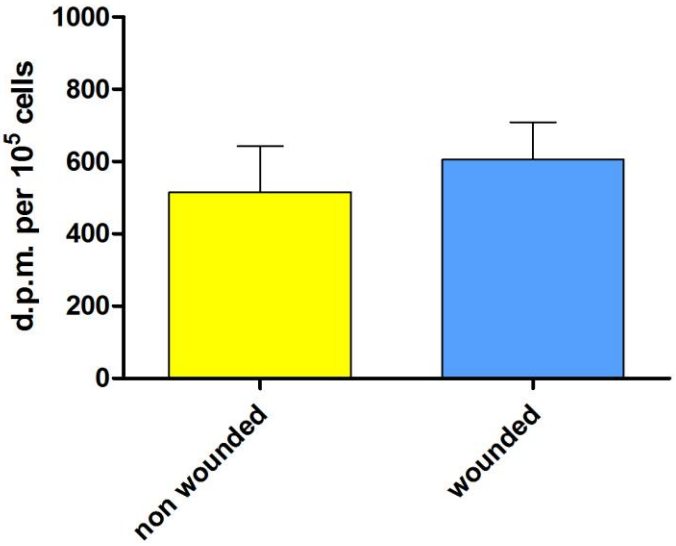

Figure 71. *In vitro* wounded breast DFs do not alter aromatase activity after 2 hours

The tritiated water assay was used to measure the activity of aromatase of cultured human breast DFs (n=1) following wounding *in vitro* after 2 hours. Data are presented as mean of triplicate dishes ± SEM.

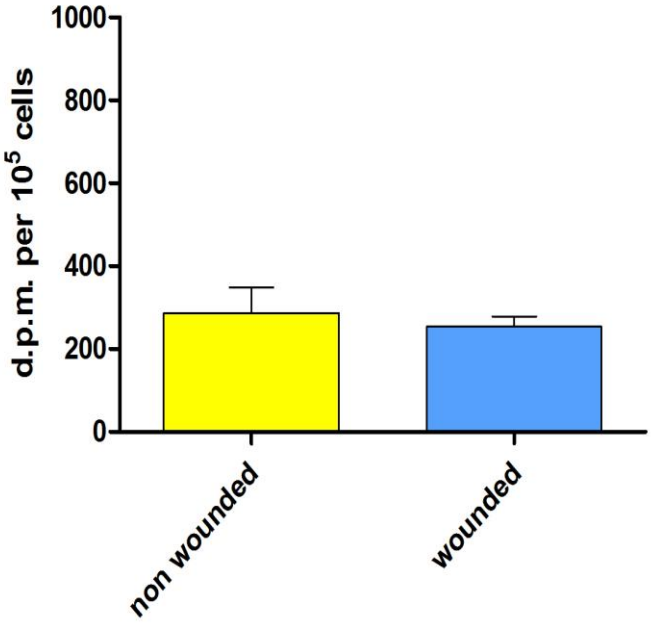

Figure 72. *In vitro* wounded female abdominal DFs do not alter aromatase activity after 2 hours

The tritiated water assay was used to measure the activity of aromatase of cultured human female abdominal DFs (n=1) following wounding *in vitro* after 2 hours. Data are presented as mean of triplicate dishes ± SEM.

3.8.2 Mechanical wounding does not alter the aromatase activity of dermal fibroblasts at 24h

^{3}H-Androstenedione was used to assess the effect of mechanical wounding on the aromatase activity by human DFs derived from female (n=5) and male (n=1) face, breast (n=1) and female abdomen (n=1) (see appendix 8). The mechanical wounding didn't increase the activity in any group of samples after 24h (Figure 73,74,75,76).

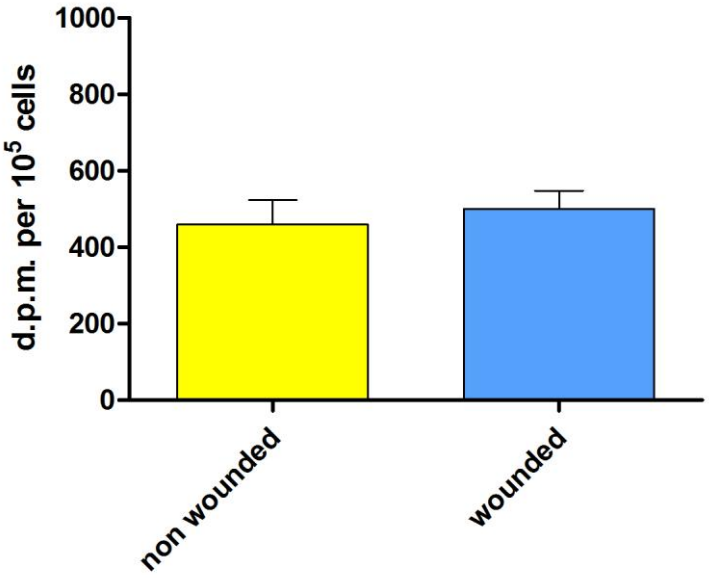

Figure 73. *In vitro* wounded female facial DFs do not alter aromatase activity after 24 hours

The tritiated water assay was used to measure the activity of aromatase of cultured human female facial DFs (n=5) following wounding *in vitro* after 24 hours. Data presented as donor mean ± SEM.

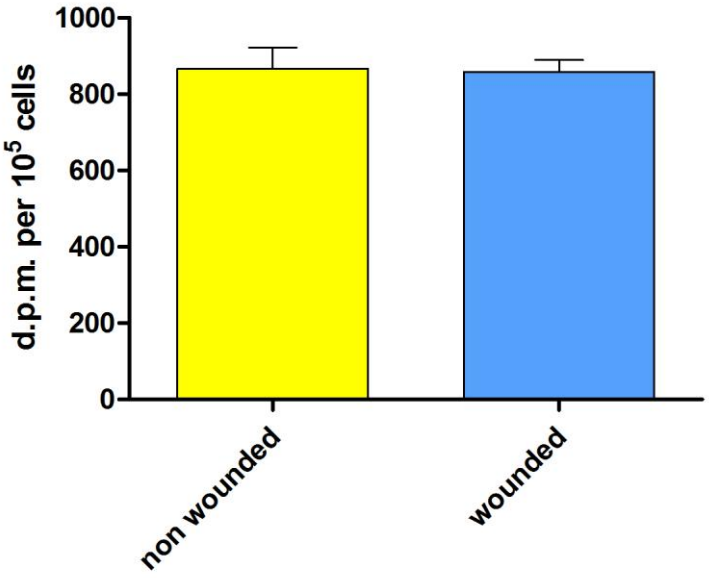

Figure 74. *In vitro* wounded male facial DFs do not alter aromatase activity after 24 hours

The tritiated water assay was used to measure the activity of aromatase of cultured human male facial DFs (n=1) following wounding *in vitro* after 24 hours. Data are presented as mean of triplicate dishes ± SEM.

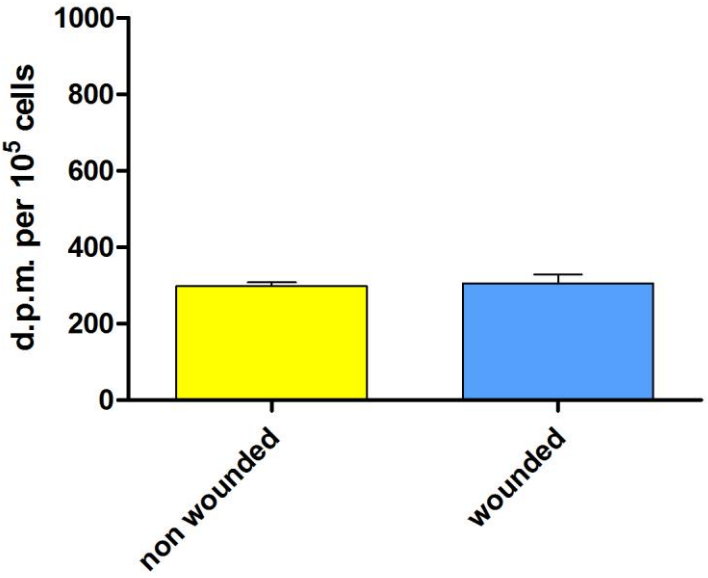

Figure 75. *In vitro* wounded breast DFs do not alter aromatase activity after 24 hours
The tritiated water assay was used to measure the activity of aromatase of cultured human breast DFs (n=1) following wounding *in vitro* after 24 hours. Data are presented as mean of triplicate dishes ± SEM.

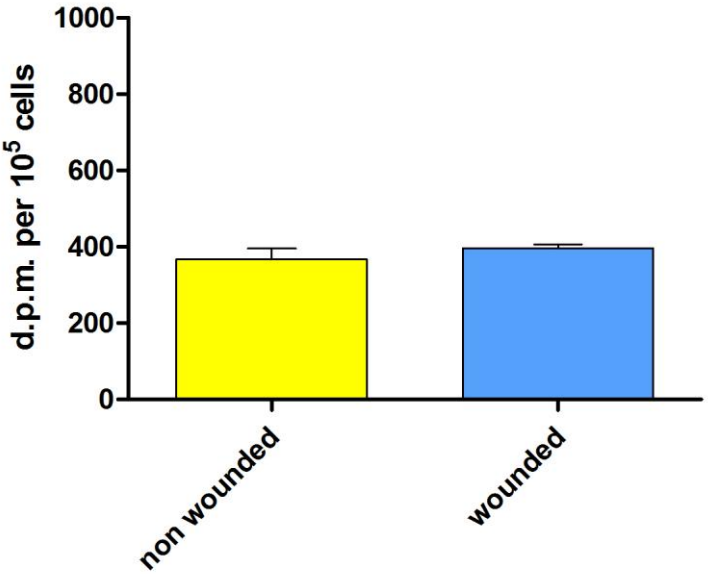

Figure 76. *In vitro* wounded female abdominal DFs do not alter aromatase activity after 24 hours
The tritiated water assay was used to measure the activity of aromatase of cultured human female abdominal DFs (n=1) following wounding *in vitro* after 24 hours. Data are presented as mean of triplicate dishes ± SEM.

Site	Sex	Aromatase activity non wounded (10^2 nmol /mg protein)	Aromatase activity wounded 24h (10^2 nmol /mg protein)
Face	F 47	609	411
Face	F 63	275	146
Face	F 2	516	258
Face	F 55	533	350
Face	F 3	417	230
Face	M 70	945	505
Abdomen	F 42	516	201
Breast	F 17	448	333

Table 40. Effect of mechanical wounding on aromatase activity in cultured DFs after 24h. F: female; M: male.

3.8.3 Mechanical wounding increases the aromatase activity of epidermal keratinocytes

^{3}H-Androstenedione was used to assess the effect of mechanical wounding on the aromatase activity by human EKs derived from female facial skin (n=3) (see appendix 8). The mechanically wounded keratinocytes showed an increase in aromatase activity after 24h ($p<0.01$) (Figure 78).

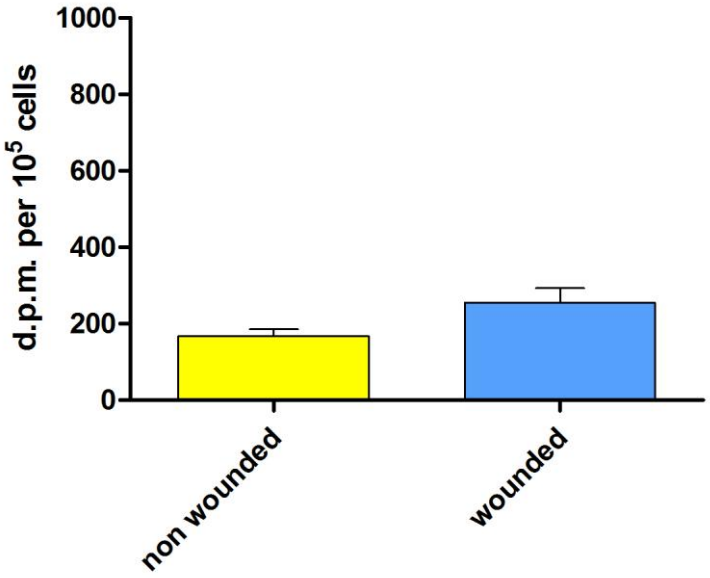

Figure 77. *In vitro* wounded female facial EKs do not alter aromatase activity after 2 hours. The tritiated water assay was used to measure the activity of aromatase of cultured human female facial EKs (n=3) following wounding *in vitro* after 2 hours. Data presented as donor mean ± SEM.

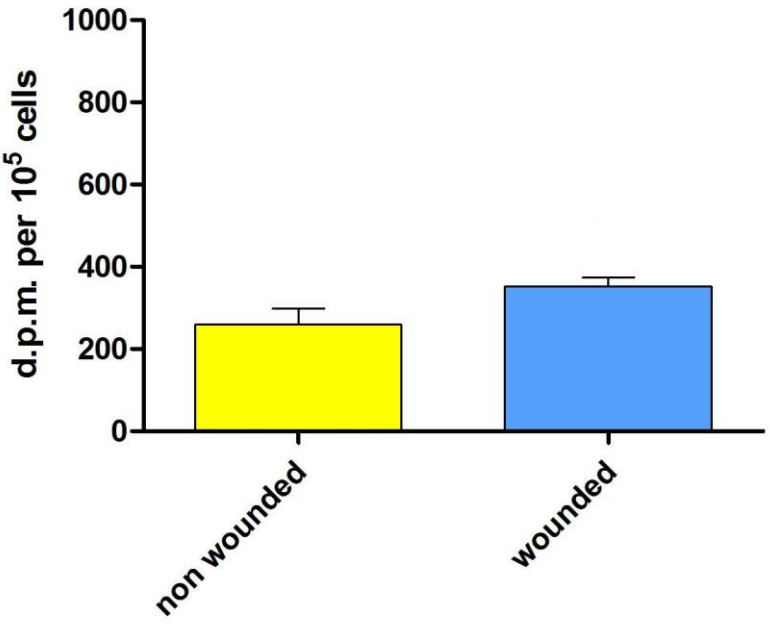

Figure 78. *In vitro* wounded female facial EKs increase aromatase activity after 24 hours. The tritiated water assay was used to measure the activity of aromatase of cultured human female facial EKs (n=3) following wounding *in vitro* after 24 hours. Data presented as donor mean ± SEM.

Site	Sex	Aromatase activity non wounded (10^2 nmol /mg protein)	Aromatase activity wounded 24h (10^2 nmol /mg protein)
Face	F	122	506
Face	F	200	598
Face	F	359	336

Table 41. Effect of mechanical wounding on aromatase activity in cultured EKs after 24h. F: female; M: male.

3.9 Up-regulation of the mRNA expression of aromatase by mechanically wounding in human cultured cells

The mRNA expression of aromatase was investigated by relative qRT-PCR (see section *2.22.2*) to assess the effect of wounding on DFs and EKs. The analysis was performed by the incubation of cells with 0.5µCi of [1β^{3}H]-Androstenedione for 24h. Then the total RNA was extracted as described in section *2.12.2*.

3.9.1 Up-regulation of the mRNA expression of aromatase by mechanically wounding in dermal fibroblasts

The mRNA expression of aromatase was investigated by relative qRT-PCR to assess the effect of mechanical wounding on human DFs. The cells derived from female (n=5) and male (n=1) face, breast (n=1) and female abdomen (n=1) (see appendix 8). The mechanical wounding increased the mRNA expression in cells derived from female face samples (Figure 79) and from breast sample (Figure 81) after 24h. In contrast, the fibroblasts established

from the male face sample (Figure 80) as well as the abdominal (Figure 82) skin didn't show an up-regulation compared with the non wounded cells.

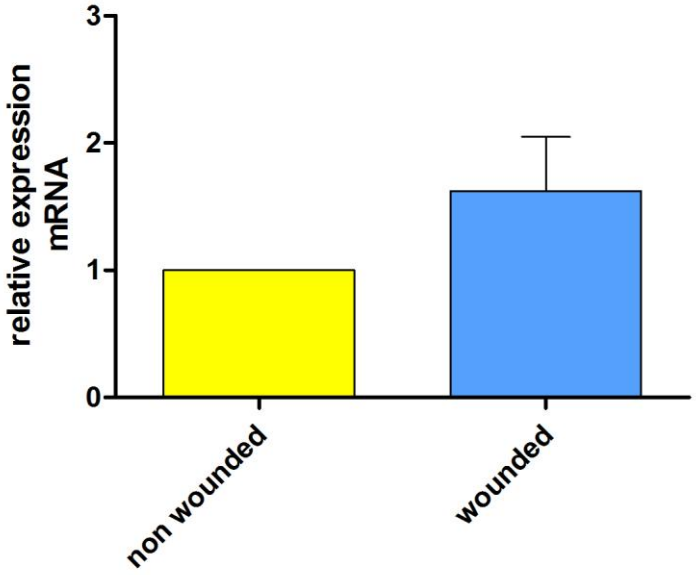

Figure 79. *In vitro* wounded female facial DFs increase mRNA expression of aromatase after 24 hours

The relative qRT-PCR assay was used to analyzed the mRNA expression of aromatase of cultured human female facial DFs (n=5) following wounding *in vitro* after 24 hours. Data presented as donor mean ± SEM.

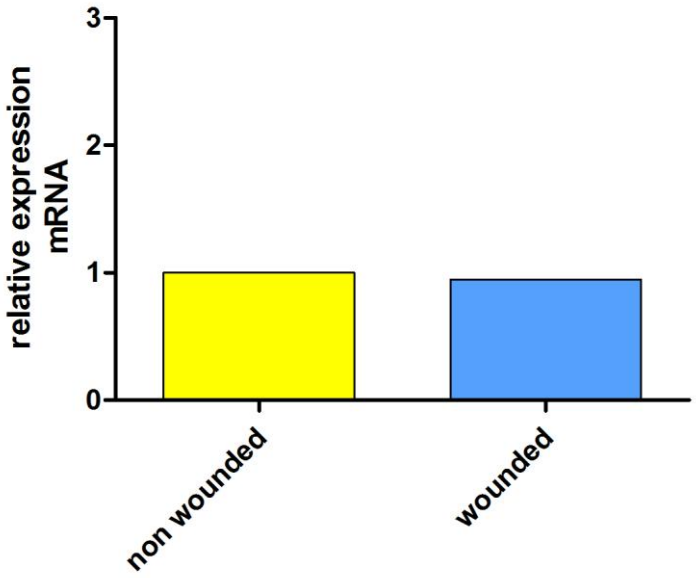

Figure 80. *In vitro* wounded male facial DFs does not increase mRNA expression of aromatase after 24 hours

The tritiated water assay was used to analyzed the mRNA expression of aromatase of cultured human male facial DFs (n=1) following wounding *in vitro* after 24 hours. Data presented as donor mean of triplicate measurements.

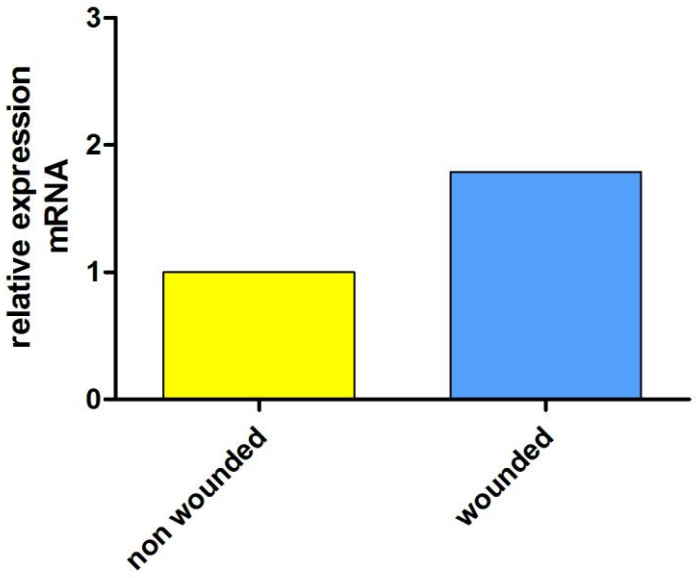

Figure 81. *In vitro* wounded breast DFs increase mRNA expression of aromatase after 24 hours. The tritiated water assay was used to analyzed the mRNA expression of aromatase of cultured human breast DFs (n=1) following wounding *in vitro* after 24 hours. Data presented as donor mean of triplicate measurements.

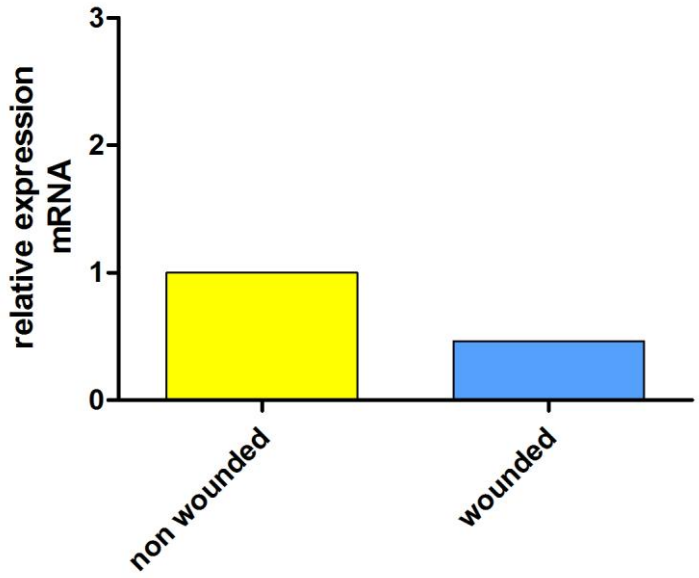

Figure 82. *In vitro* wounded female abdominal DFs does not increase mRNA expression of aromatase after 24 hours

The tritiated water assay was used to analyzed the mRNA expression of aromatase of cultured human female abdominal DFs (n=1) following wounding *in vitro* after 24 hours. Data presented as donor mean of triplicate measurements.

3.9.2 Up-regulation of the mRNA expression of aromatase by mechanically wounding in epidermal keratinocytes

The mRNA expression of aromatase was investigated by relative qRT-PCR to assess the affect of mechanical wounding on human EKs. The cells derived from female face (n=3) (see appendix 8). The mechanical wounding increased the mRNA expression after 24h (Figure 83).

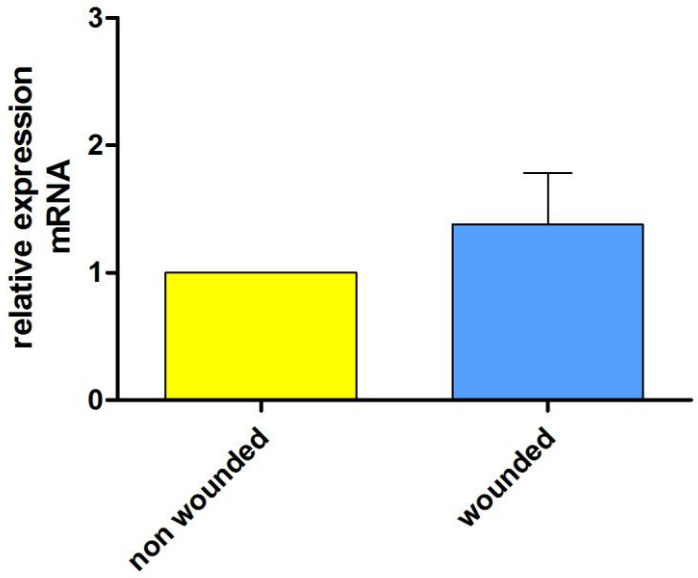

Figure 83. *In vitro* wounded female facial EKs increase mRNA expression of aromatase after 24 hours

The relative qRT-PCR assay was used to analyzed the mRNA expression of aromatase of cultured human female facial EKs (n=3) following wounding *in vitro* after 24 hours. Data presented as donor mean ± SEM.

4. Discussion

The aim of this study was to determine whether human skin expresses the enzymes required for the local biosynthesis of active sex steroid hormones. In addition, the *in vitro* effect of androgens or estrogens on enzyme expression was explored using isolated human HFs and cultured DFs and EKs. DFs and EKs were established from tissue explants of human facial, abdominal and breast skin. Both cell types grew well in culture and maintained their normal morphology and growth characteristics. Both cell types displayed the ability to migrate in a scratch wound assay when cultured in serum-free or growth factor-free, phenol red-free medium for up to 48 hours. This was important as the presence of serum in the medium can confound the evaluation of the effect of steroids on DF migration because serum contains growth factors in unknown and variable concentrations. The absence of serum ensures that the only growth factors present are those that are secreted by the cells (Carroll and Koch, 2003). Previous studies have shown that DFs (Stevenson *et al*., 2009) and epidermal keratinocytes (Thornton M.J., personal communication) maintain normal growth and characteristics in absence of serum for up to 48 hours. Phenol-red free medium was also used in this study as the pH indicator phenol-red has been shown to have weak estrogenic properties. Indeed, Berthois *et al*. (1986), demonstrated that phenol-red binds to the estrogen receptor of human MCF-7 breast cancer cells and stimulates cell proliferation although, the binding affinity of phenol-red is only 0.001% that of estradiol. They suggested that this might occur as phenol-red bears a structural resemblance to non-steroidal estrogens. However, a more recent report has questioned the results of this initial study and suggested that the inclusion of phenol-red does not affect estradiol binding or cell growth in a number of estrogen responsive cell lines (Moreno-Cuevas and Sirbasku, 2000).

4.1 RT-PCR analysis of steroidogenic proteins mRNAs in human skin

To understand the steroid hormone interactions that might occur in human skin, the expression of seven genes encoding steroidogenic proteins, six enzymes (P450scc, P450c17, P450arom, steroid sulfatase and 5α-reductase1 and 2) and one carrier protein (OATP2B1) was assessed in human skin biopsies, cultured DFs and EKs derived from female and male healthy donors. The analysis was performed also in HFs derived from female non-balding fronto-temporal scalp. The results demonstrated that human skin expresses genes encoding proteins that are involved in both paracrine and intracrine pathways of steroidogenesis. In particular, the presence of the P450 side chain cleavage system (P450scc) was documented in all samples delineating the steroidogenic pathway upstream from DHEA. In fact, the cytochrome P450scc is the initiating enzyme for steroidogenesis and converts cholesterol to pregnenolone. The gene expression and activity of P450scc provides evidence to support the concept of *de novo* production of steroids from cholesterol in human skin (Thiboutot *et al*., 2003). By contrast, P450c17 is the qualitative regulator of steroidogenesis. The presence or absence of the activity of P450c17 directs pregnenolone towards its final metabolic pathway (Miller *et al*., 1997). Previous studies have demonstrated the expression of P450c17 enzyme in human sebocytes (Thiboutot *et al*., 2003) and EKs (Hannen *et al*., 2010). In addition, the present study has provided evidence that human DFs and HFs express the enzyme required for the synthesis of the androgenic prohormones dehydroepiandrosterone and androstenedione (Figure 5). However, these prohormones can be converted into more potent androgens like testosterone and dihydrotestosterone (Figure 5). Androgens have several functions in human skin, such as sebaceous gland growth, differentiation and sebum production, regulation of the hair cycle in some regions, epidermal barrier homeostasis and rate of wound healing. The endogenous 5α-reductase activity of human follicular DP cells, from either beard or scalp hair, is stronger than that of dermal fibroblasts (Liu and

Yamauchi, 2008). In addition, it has been detected that TST synthesized in cultured human SZ95 sebocytes is derived mainly from DHEA (Chen *et al.,* 2010). The conversion of TST to 5α-DHT can be catalyzed by 5α-reductase type 1 or type 2. To further clarify the molecular mechanisms responsible for steroidogenesis in human skin and HFs, the present study presented evidence that human skin, including cultured EKs and DFs, and HFs all express endogenous 5α-reductase mRNA. However, only the HF expressed 5α-reductase 2. It has previously been reported that 5α-reductase 2 is predominantly expressed in male genital tissues and mutations are known to cause a severe virilization disorder in affected males (Steers, 2001). In contrast, the role of the type 1-enzyme in normal male androgen physiology is unclear (Thomas *et al*., 2008). However, studies using specific inhibitors of 5α-reductase 1 (LY306089) and 5α-reductase 2 (finasteride) showed that the type 2 isoform is predominant in skin of normal men, normal women, and hirsute patients (Mestayer *et al.,* 1996). The absolute real-time PCR analysis of the present study revealed that 5α-reductase 1 was the most highly expressed enzyme in both skin (Figure 22) and HFs (Figure 23) amongst all genes investigated. Previous studies have revealed that both men and women with androgenetic alopecia have higher levels of androgen receptors and 5α-reductase 1 and 5α-reductase 2 in HFs derived from the frontal scalp compared to the occipital scalp, whereas higher levels of the aromatase enzyme were found in occipital follicles (Sawaya and Price, 1997). These differences in levels of steroid-converting enzymes may account for the different clinical presentations of androgenetic alopecia in women and men. In addition, the expression of mRNA for OATP2B1 was analyzed for the first time in HFs from female scalp (Figure 23) and in cultured EKs from female facial skin (Figure 27). The OATP2B1 transporter has been detected in the hepatocyte basolateral membrane (König *et al*., 2000; Kullak-Ublick *et al.,* 2001), the basal membrane of the placental syncytiotrophoblast (St-Pierre *et al.*, 2002), the apical membrane of small intestinal epithelial cells (Kobayashi *et al*., 2003; Englund *et al.,* 2006), in the myoepithelial cells of the mammary gland (Pizzagalli *et al.,* 2003) and in the kidney (Tamai *et al*., 2000) and

(König *et al*., 2000), brain (Sugiyama *et al*., 2001; Steckelbroeck *et al*., 2004), and heart (Grube *et al.,* 2006). However the expression pattern in skin has not been analyzed greatly (Tamai *et al*., 2000; Schiffer *et al*., 2003). In the present study it was demonstrated that whole skin (Figure 22), EKs (Figure 27) and HFs (Figure 23) all express mRNA for OATP2B1. In contrast, the expression of mRNA for OATP2B1 was not demonstrated in cultured DFs (Figure 25). Previous findings have shown the expression of the protein in DFs derived from neonatal foreskin by immunolocalization (Schiffer *et al*., 2003). The results may support the possible correlation in distinct skin cells between OATP2B1 and STS, the enzyme responsible for the hydrolysis of the inactive steroid conjugates into active hormones (Reed *et al*., 2005). Since OATP2B1 has been suggested to be one of the membrane transporter proteins implicated in the uptake of steroid sulfates through the cell membrane, recent studies have focused on the correlation between the OATP2B1 and STS expression levels in patients with hormone dependent cancer, such as breast cancer, in order to investigate the potential prognostic value of both proteins. In particular, the inhibition of STS activity in skin has been reported to be a potential new treatment strategy for a number of skin disorders, including hirsutism, androgen-dependent alopecia, acne and psoriasis (Reed *et al.,* 2008). All the data indicate that keratinocytes express OATP-mediated uptake of sulfated steroids as well as STS (Figure 27), which is necessary for their conversion to the precursors of active androgens and/or estrogens. Further investigations are required to assess the prognostic and diagnostic value of this mechanism. Collectively, the analysis of mRNAs expression corroborated previous studies that described human skin as a both hormone target tissue and an endocrine gland (Zouboulis, 2004).

4.2 Expression of mRNA for ER and AR in human cultured dermal fibroblasts, cultured epidermal keratinocytes, and hair follicles

The biological action of estrogens and androgens can be mediated by the steroids binding to their specific receptors, the estrogen receptors ERα and ERß, and the androgen receptor AR, which all belong to the nuclear receptor superfamily, a family of ligand-regulated transcription factors. Indeed, the main function of the steroid receptor is to act as a DNA-binding transcription factor that regulates gene expression. In the present study, the mRNA expression of ERα, ERß, and AR was investigated in human cultured DFs and EKs derived from female and male healthy donors. The analysis was performed also in HFs derived from female non-balding fronto-temporal scalp. Previous immunohistochemistry analysis has showed that human scalp EKs expressed ERß but not ERα *in situ* (Thornton *et al*., 2003). In addition, it has been shown using RT-PCR, that ERß and not ERα mRNA was expressed by human cultured foreskin EKs (Kanda and Watanabe, 2003). In contrast, this study has demonstrated that both ERα and ERß are expressed in cultured keratinocytes (Figure 28) as well as in DFs (Figure 26). In particular, EKs demonstrated a stronger expression of ERß when compared to ERα. In contrast, expression of mRNA for ERα was detected at higher levels than ERß in DF. Differences in estrogen receptor expression have also been demonstrated in human HFs (Figure 24) that have exhibit strong expression of ERß when compared with ERα. On the other hand, all the samples expressed the AR. This investigation confirms previous studies indicating that human skin expresses ERs and AR and suggesting that they may be locally involved in the genomic mechanism of action of sex steroids.

4.3 Microarray analysis of steroids effects on gene expression

In order to further investigate the influence of androgens and estrogens on the mechanism of steroid metabolism in human skin, a gene array analysis was performed on the whole transcriptome of human HFs and primary EKs after steroid treatment. Three different hormones were used for a 24h of incubation: DHEA-S (10µM), TST (50nM) and E2 (1nM). EKs were established from human female facial skin and HFs were micro-dissected from female fronto-temporal scalp.

4.3.1 Gene Array of keratinocytes

Recently, Calvo *et al.* (2008) explored for the first time the changes in the pangenomic profile induced in human skin in women treated with DHEA applied locally. Their results strongly suggested the possibility that DHEA could exert an anti-aging effect on human skin through the stimulation of collagen biosynthesis increasing the expression of several members of the collagen family, and by increasing the proliferation and differentiation of keratinocytes. In the present study, the global mRNA expression profiling revealed changes in the expression of a large number of genes. In particular, there was a significant up-regulation of genes involved in inflammation, cell proliferation, differentiation and structural functions. The analysis was focused on four genes upregulated in the presence of all three steroids investigated:

CXCL1, a member of the alpha-chemokine family, expressed in normal human epidermis, has been demonstrated to be involved in the wound healing process of human burn wounds, especially during the inflammatory phase, re-epithelialisation and angiogenic processes (Engelhardt *et al.*, 1998). In particular, *CXCL1* has been shown to participate in the stimulation of keratinocyte proliferation (Zaja-Milatovic and Richmond, 2008). Cytokines

and chemokines promote inflammation and angiogenesis, facilitate the passage of leukocytes from the circulation into the tissue and contribute to the regulation of epithelialisation (Rennekampff *et al*., 1997). It appears conceivable that chemokines could be exploited therapeutically as major adjuvant to stimulate wound healing. Recent studies have revealed that sex hormones manifest a variety of biological and immunological effects in the skin (Gilliver *et al*., 2003; Shah and Maibach, 2001). However, these findings have indicated the contrasting contributions made by sex steroid hormones to the regulation of cutaneous repair processes. The administration of E2, either systemically or topically, has been shown to reverse the fundamental repair defects observed in postmenopausal women (Gilliver and Ashcroft, 2007). Estrogen *in vitro* down-regulates the production of the neutrophil, type 1 T cell and macrophage-attracting chemokines, CXCL8 and CXCL10 in human foreskin keratinocytes (Kanda and Watanabe, 2005). In addition, estrogen accelerates the production of the cutaneous wound healing stimulating cytokine, GM-CSF, in murine keratinocytes (Kanda and Watanabe, 2005) and the production of the growth factors bFGF and TGF-beta1 in murine fibroblasts (Ashcroft *et al*., 1997; Fujimoto *et al*., 1997), and can lead to the enhancement of wound re-innervation, re-epithelialisation and granulation tissue formation (Barrientos, et al., 2008; Przybylski, 2009; Douglas, 2010). However, Gilliver and colleagues (2010) have reported that E2 markedly delays wound re-epithelialisation in castrated male mice. Regarding DHEA, the local injection of the steroid precursor accelerates impaired healing in an ageing mouse model acting through the ER (Mills *et al*., 2005). On the other hand, DHT prolongs inflammation, reduces deposition of extracellular matrix in wounds, and reduces the rate of wound healing (Kanda and Watanabe, 2005).

In this study, DHEA, TST and E2 all stimulated the expression of the chemokine CXCL1 in human facial female EKs (Figure 39). However, the influence of sex steroids on the expression of the gene *CXCL1* still remains poorly investigated. Recently, Brown *et al*. (2010) showed that E2 signaling regulates brain proinflammatory cytokine and chemokines levels through

ERs using an *in vivo* lipopolysaccharide (LPS) model of systemic inflammation in ovariectomized (OVX) and OVX E2-treated (OVX_E2) mice (Qin *et al*., 2007). In particular, they showed that CXCL1 protein concentrations were significantly increased at 24 h in ERαKO and ERßKO mice from both OVX and OVX_E2-treated groups. However, there were no significant changes in sham (0h) ERKO mice compared with sham WT mice. These findings suggest that E2 can act by dependent and/or independent roles for ERs. Further studies are necessary to understand the role of chemokines and how E2 might influence their functions as proinflammatory mediators, making them therapeutic targets. On the other hand, Nadiminty *et al*., (2010a) showed that *CXCL1* mRNA expression is up-regulated in the LNCaP prostate cancer cell line by NF-kB2/p52, a transcription factor involved in inflammation and cell survival (Zhang *et al*., 2004). The over-expression of NF-kappaB2/p52 protects androgen sensitive LNCaP cells from apoptotic cell death and cell cycle arrest induced by androgen-deprivation (Nadiminty *et al*., 2008). In addition, NF-kappaB/p52 can activate the AR in prostate cancer cells such as LNCap (Nadiminty *et al.,* 2010b). Since, prostate cancer initiation and progression are dependent on the AR (Mimeault and Batra, 2006), NF-kappaB/p52 can induce the progression of prostate cancer. With respect to cancer, chemokines are being studied for both their role in tumor biology and as promising immunotherapy candidates (Dubinett *et al*., 2010). Many human cancers possess a complex chemokine network that may influence the leukocyte infiltration, angiogenesis, tumor cell growth, survival and migration (Balkwill, 2003). Collectively these results suggest that the manipulation of the chemokine network could have therapeutic potential in malignant diseases. In particular, further investigations are required to verify the role of androgens and estrogens and their pathway of signaling regarding the regulation of CXCL1 gene expression and protein activity providing beneficial therapies for skin syndromes.

ANGPTL4, a member of the angiopoietin/angiopoietin like gene family, a direct glucocorticoid receptor target, has been shown to participate in

glucocorticoid-regulated triglyceride metabolism (Koliwad *et al*., 2009) and in the inhibition of the proliferation and tubule formation of endothelial cells (Ito *et al*., 2003). It is a protein inhibitor of lipoprotein lipase, synthesized and secreted during fasting, when circulating glucocorticoid levels are physiologically increased. Treatment with the synthetic glucocorticoid dexamethasone has been shown to increase *Angptl4* mRNA levels in primary hepatocytes and adipocytes (2-3-fold) and in the liver and white adipose tissue of mice (approximately 4-fold) (Koliwad *et al*., 2009). In addition, *in vitro* experiments using purified recombinant angiopoietin-related protein (ARP4) revealed that ARP4 markedly inhibited the proliferation, chemotaxis and tubule formation of endothelial cells (Ito *et al*., 2003).

In the present study, the presence of either DHEA, TST or E2 determined the up-regulation of ANGPTL4 mRNA expression in human female facial EKs (Figure 40). Interestingly, recent studies have demonstrated an unpredicted role for angiopoietin like 4 in wound healing and in particular in the migration of EKs by an interaction with integrins using the *in vitro* scratch wound assay (Goh *et al*., 2010). Collectively, these findings provide a novel control of wound healing via ANGPTL4-dependent regulation of cell-matrix communication and suggest an important role for androgens and estrogens in cell-matrix communication during angiogenesis, cancer metastasis and wound healing. Since the effect of sex steroid hormones has been explored extensively in both human and animal models, the identification of their target genes can provide a better understanding of their role and potential implications in wound healing.

TXNIP (Thioredoxin-interactin protein) is a protein localized to the basal layer of normal human epidermis. Champliaud *et al*. (2003) showed that TXNIP is highly expressed in the upper epidermal layers in the proliferative epidermis of patients with psoriasis. Moreover, they demonstrated that TXNIP is involved in the differentiation of epidermal cells (Champliaud *et al*., 2003). Northern blot analysis has showed strong bands in murine heart, lung, thymus, kidney, spleen, testis, and muscle (Junn *et al*., 2000). In addition,

Champliaud *et al*. (2003) have detected the protein in human normal and pathological cutaneous tissue as well as in cultured keratinocytes. These results suggest that TXNIP may have a role in epithelial tissues in regulating the transition of transient amplifying cells to suprabasal differentiating cells. In the present study, the presence of either DHEA, TST or E2 determined the up-regulation of *TXNIP* mRNA expression in human female facial EKs (Figure 41). Given the known role of TXNIP in differentiation of keratinocytes, it is a potential therapeutic candidate for the sex steroid-treatment of cutaneous impaired wound healing and psoriasis. In addition, there is evidence that E2 has a critical role in murine Txn pathway suggesting that Txnip has an important function in the rodent uterus and fertility (Deroo *et al*., 2004). Although the mouse Txnip promoters contain half-estrogen response elements (AGGTCA) and several SP1 sites, which have been shown to synergize with the ER, the mechanism of regulation of Txnip by estrogen remains unclear, given that Txnip promoter does not contains a canonical ERE (Bloomfield *et al*., 2003). Additionally, it remains to be determined by what mechanism the androgens and estrogens regulate the expression of human *TXNIP*.

LMNB1 **(Lamin B1)**, a protein of the nuclear lamina, has been suggested to have important roles in the morphogenesis of the nucleus and in cell differentiation (Dahl *et al*., 2008). In normal skin, the expression level of lamin B diminishes when moving from the basal cells to the granular cells of the epidermis (Oguchi *et al*., 2002). In this study, DHEA, TST and E2 all stimulated the expression of LMNB1 in human facial female EKs (Figure 42). Given the important role of LMB1 in cell differentiation, the stimulation and regulation of its gene expression by sex steroids may have implications in disorders of the epidermis. In particular, lamin expression has been shown to depend on the differentiation and transformation of the human epidermis. There is some indication that LMNB1 has a reduced expression in the basal cell layer of the epidermis overlying squamous cell carcinoma (SCC) compared with normal skin (Oguchi *et al*., 2002; Tilli *et al*., 2003). Since there

is no previous evidence for interactions between androgens and/or estrogen and LMB1 gene/protein expression, it would be interesting to investigate the potential mechanism via either genomic or non-genomic pathways of the sex steroid actions and establish whether LMB1 might be a direct target of sex steroids.

4.3.2 Gene array of hair follicles

Recent studies suggest that the androgen-driven alteration to the autocrine and paracrine factors produced by scalp DP cells may be a key to androgen-potentiated balding. Kwack *et al*. (2008) have screened dihydrotestosterone regulated genes in balding DP cells and found that dickkopf 1 (*DKK-1*), a potent inhibitor of the Wnt pathway (Krupnik *et al*., 1999; Fedi *et al*., 1999), is one of the most up-regulated genes. On the other hand, in the present study a pangenomic analysis was performed on the whole transcriptome of human non-balding scalp HFs following exposure to androgens or estrogens *in vitro*. The global mRNA expression profile revealed changes in the expression of a large number of genes. In particular, the grouping analysis using a cut off of the FD (2.5) revealed a significant modulation by E2 (table 37). The assessment showed that there is a weak correlation among the data obtained with all three different steroids compared to the analysis on keratinocytes (table 36). These results could be related to a more complex anatomy and biology of the isolated HF compared to the individual keratinocytes cultured *in vitro*. In addition, the expression of key steroidogenic enzymes such as STS, 5α-reductase and aromatase, and the ERs and AR, provide further evidence for the formation and action of active androgens and estrogens in human HFs. Although steroid hormones have important modulatory effects on the HF, the mechanisms by which they regulate human hair growth are still poorly understood. Thornton and colleagues (2006) have demonstrated that aromatase activity was stimulated in both frontal scalp and beard DP cell cultures by dexamethasone. This provides a basis for action of estradiol produced locally by autocrine or paracrine mechanisms. It has been known

that estrogens profoundly alter the hair cycle by binding to locally expressed high-affinity ERs (Ohnemus *et al*., 2006). Further investigations regarding estrogen-mediated signaling could potentially provide endocrinological-based therapies for common hair growth disorders. On the other hand, androgens are also important regulators of human HFs. In particular, the response to androgens varies with the body site (Randall, 2008). Androgens play an important role within the HF altering the mesenchyme-epithelial cell interactions, changing the length of hair growth cycle, the DP size, and keratinocyte and melanocyte activity (Randall, 2008). A greater understanding of the mechanisms of androgen action in HFs should improve therapies for poorly controlled hair disorders like alopecia and hirsutism. In this study, incubation of HFs with sex steroids demonstrated the modulation of genes involved in cell proliferation, migration, differentiation, and apoptosis. An interesting change was the up-regulation of *LOR*, a major protein component of the cornified cell envelope found in terminally differentiated epidermal cells (Rogers and Koike, 2009). Mutations in this gene are associated with Vohwinkel's syndrome and progressive symmetric erythrokeratoderma, both inherited skin diseases (Candi *et al*., 1995). It is pertinent to note that the binding of a loricrin antibody to the developing cortex was observed in an immunochemical study on the wool follicle (Jones and Rogers, 2005). In addition, the expression of loricrin has been found in the hair peg, IRS and ORS (Akiyama *et al*., 2002) indicating an important role in HF development. The mRNA expression of *LOR* (loricrin) was up-regulated by DHEA-S and TST in the female frontotemporal scalp HFs. Given the important role of loricrin in the epidermis, it may be a potential target of sex steroids in regulating keratinocytes differentiation of the hair shaft and controlling hair growth (Schneider *et al.,* 2009). It has been known that androgens are one of the main regulators of human HFs, changing small vellus follicles into larger intermediate and terminal hairs (Paus, 2007). It has been also reported that the response to androgens varies with the body site as it is specific to the HF itself. Normally around puberty, androgens stimulate axillary and pubic hair in both sexes, while later they may also

inhibit scalp hair growth in men causing androgenetic alopecia (Randall, 2008). The hypothesis of androgen action on the HF, proposed by Randall *et al*. (1991), focuses on the DP wherein androgens may bind AR and then modulate the gene expression of regulatory factors which influence other target cells. In particular, the role of androgens in female pattern hair loss (FPHL) is less clear than in male balding. The authors appear to agree with the concept that the relative importance of estrogen in normal female scalp hair follicle function and in FPHL pathogenesis remains widely underestimated and may even exceed that of androgens (Langan and Paus, 2010). Moreover, FPHL has been described in a patient with complete androgen insensitivity syndrome suggesting that mechanisms other than direct androgen action contribute to this common form of hair loss in women (Cousen and Messenger, 2010). A greater understanding of the mechanisms of androgen and estrogen action in HFs should provide improved therapies for poorly controlled hair disorders like hirsutism and alopecia in both sexes. The purpose of this study was to explore the list of genes that are relevant to hair growth in general. The global analysis and in particular the expression pattern of *LOR* suggest that androgens and estrogens may be relevant to the development of HF. Future studies are needed for the validation of the data obtained with the array analysis. Moreover, functional assays may assess the potential role of sex steroids in regulating important aspects of HF biology.

4.4 Migration of cultured cells in response to steroids following mechanical wounding in vitro

Cells have the ability to move in their environment. Cell movement has afforded the accomplishment of complex integrated functions, starting from tissue and organ development or renewal to immune surveillance and wound healing (Simoncini *et al*., 2006). Cell movement and migration depend on the modification of the spatial organization of actin fibers within the cell and their relationship with membrane anchoring filaments such as integrins and

focal adhesion complexes (Sheetz, 2001), which allows cell movement in the extracellular environment (Pollard and Borisy, 2003). The activation of actin-binding, proteins induces actin depolymerization and reassembly toward the cell membrane to form cortical actin complexes. These complexes sustain the formation of molecular bridges between actin, integrins, and focal adhesion complexes at specialized cell membrane sites such as ruffles and pseudopodia (Tsukita and Yonemura, 1999; Chen *et al*., 2001). The scratch wound assay (Soderholm and Heald, 2005; Yarrow *et al*., 2004) is a recognized method of assessing migration and has been used in wound healing assays for cultured fibroblasts, keratinocytes, and endothelial cells (Stevenson *et al*., 2009; Goh *et al*., 2010; Morales *et al*., 1995). Different methods have been described for producing the scratch wound and assessing cell migration. Previous studies have investigated cell migration by recording the time until wound closure (Basu, *et al.,* 2001), or by using photographic images to measure the distance between the wound edges at random points (Morales, *et al*., 1995). In this study, as previously described (Stevenson *et al*., 2009), a standardized wound was produced along the diameter of a cell culture dish. The distance between the wound edges was measured at the same position along the length of the wound at each time point, thus providing an accurate measurement of cell migration.

4.4.1 Migration of cultured dermal fibroblasts

In previous studies, it has been demonstrated that *in vitro* DF migration is affected by age (Ashcroft *et al*., 1995), growth factors (Barrientos *et al*., 2008), and steroid hormones and estrogen agonists or estrogen antagonists (E2, DHEA, specific ERα and ERß agonists, tamoxifen or raloxifene) (Stevenson *et al.,* 2009). In the present study, DF migration was investigated after wounding *in vitro* in the presence of androgens and estrogen (DHEA, DHEA-S, TST or E2), an inhibitor of aromatase (Arimidex) and an inhibitor of STS (STX64). DFs were established from tissues explants of human female facial skin. The cell migration was analyzed at five fixed time points between

4 and 48 hours in the presence of different steroids DHEA-S (10μM), DHEA (10μM), TST (50nM), and E2 (1nM) or the vehicle control (ETOH 0.0001%). E2, DHEA and DHEA-S all had a significant effect on accelerating cell migration, but the migration of cells incubated with TST was not significantly different from the migration of cells incubated with the vehicle control (see section *3.5.3.1*). This stimulation was seen during the time period investigated. The significant increase in response to E2 was seen after 8h and then the difference in the migratory rate remained significantly higher than the control. On the other hand, the cells showed a significant response at an earlier time point (4 hours) when incubated with either DHEA or DHEA-S, which remained significantly higher than the control. The presence of early (4 and 8 hours) and late (48 hours) effects suggests that both non-genomic and genomic pathways may be activated and that a greater response is initiated via the non-genomic pathway. It has been known that estrogens are powerful regulators of cell movement during embryonic development as well as in adult organisms (Simoncini *et al*., 2006). On the other hand, estrogen-induced cell migration is the base for progression and metastasis of hormone-sensitive cancers (Chen *et al*., 2001). For all of these reasons, understanding the mechanistic basis through which estrogens control the interaction between the cell and the extracellular environment gives rise to important biological and medical implications. Previous studies demonstrated that estrogens enhance endothelial proliferation at sites of vascular injury, promoting endothelial recovery after structural damage (Broucher *et al*., 2001). This has been related to the activation of both long-term, genomic actions as well as rapid, presumably non-genomic signaling by estrogens (Mendelsohn and Karas, 1999; Simoncini and Genazzani, 2003; Arnal *et al*., 2004), although no mechanistic explanation has been presented. Further studies will be required to determine whether the estrogen-signaling pathway is common also for G protein-regulated proteins. A similar effect in DFs may explain the great early response to DHEA and DHEA-S. Both these steroids are weak androgens produced primarily by the adrenal gland. Although their plasma concentrations by far exceed those of any other

adrenal product, their physiological roles have not yet been determined. In plasma, where the major portion of these hormones is present in the sulfate form, it is possible that DHEA-S serves as a reservoir for DHEA (Leowattana, 2001) since various tissues have been shown to contain STS. Recently, Stevenson *et al*. (2009) have investigated the effect of E2 and DHEA on human DFs using an *in vitro* wound assay. Both the steroids significantly accelerated cell migration and increased DNA synthesis. All data suggest that the effect of DHEA and DHEA-S, following conversion to estrogen, have significant effects on human fibroblasts, the key mesenchymal cell involved in the wound healing process. Further understanding of the mechanisms involved may have important implications for the management of age-related impaired wound healing. On the other hand, few studies have examined gonadal androgens and wound healing. In contrast to the beneficial effects of estrogen, most of the recent evidence suggests that androgens have a negative effect on wound repair. Increased testosterone levels are associated with delayed wound healing in elderly men. Elderly men also heal more slowly than elderly women (Gilliver *et al*., 2007). However, patients in catabolic states (e.g., as a result of severe burn injury) may experience beneficial effects from anabolic steroids, such as testosterone (Demling and Orgill, 2000). The present study also explored the effect of testosterone on human DFs. The response to this androgen was lower and not significant compared to the other steroids that were investigated. However, the TST effect was reversed in presence of Arimidex, suggesting a putative conversion of TST to estradiol by aromatase (see section *3.5.3.1*). Androgens, like estrogens, are thought to exert their influence on all the different phases of wound repair. They are associated with an enhanced inflammatory response (Gilliver *et al*., 2007). Inflammation can contribute to delayed wound healing by leading to increased proteolytic destruction of collagen and fibronectin. However, their administration also influences the remodelling phase of wound healing by increasing collagen deposition. An intricate balance between the synthesis and degradation of collagen characterizes the remodelling phase. Matrix metalloproteinases play a role in this androgenic

effect. Androgen receptors have been demonstrated to negatively regulate MMP-1 expression, possibly reducing proteolytic action on the forming matrix and tipping the balance toward increased collagen deposition of the wound (Schneikert *et al*., 1996).

Current knowledge on androgens and their mechanism of action is associated with negative and positive effects on aging and repair processes. Further investigations are needed to determine the role of androgens. In addition, the present study revealed that the effect of DHEA and TST was reversed in the presence of Arimidex, suggesting the requirement of aromatization of androgen to estrogen by aromatase. The effect of DHEA-S was impaired in presence of STX64 indicating the importance of STS activity for the conversion of DHEA-S to the un-conjugated form. However, the effect of aromatase and aromatase inhibition in the wound healing process has yet to be fully defined. The delayed healing of cutaneous wounds in aged individuals may in part reflect the decline in circulating levels of DHEA and estrogens. The beneficial response on wound healing that DHEA exerts may be blocked by aromatase inhibition. Based on animal models, aromatase inhibitors may adversely affect cutaneous wound healing in the acute setting (Howgate *et al*., 2009). So far, there have been no clinical trials investigating the adverse affect of aromatase inhibitors on the process of cutaneous wound healing in humans. Further studies are necessary to assess the mechanisms involved that may have important implications for the management of age-related impaired wound healing.

4.4.2 Migration of cultured epidermal keratinocytes

In the present study, the effect of estrogens and androgens on the migration of cultured human EKs after wounding *in vitro* was investigated. Cell migration was analyzed at five fixed time points between 4 and 48 hours following the incubation with different steroids DHEA-S (10µM), DHEA (10µM), TST (50nM), and E2 (1nM) or the vehicle control (ETOH 0.0001%). In particular, it was demonstrated that E2, DHEA and DHEA-S had a

significant effect on accelerating cell migration. The significant increase in response to E2, DHEA and DHEA-S all was seen after 4h and then the difference in the migratory rate remained significantly higher than the control (see section *3.5.3.2*). It has been known that estrogen affects proliferation and migration of different skin components, thus influencing the wound healing processes. A recent study has investigated and confirmed the beneficial effects of estrogen on the migration of the human keratinocyte cell line NCTC 2544 between 5 and 24h using the scratch wound assay (Merlo *et al.,* 2009). This suggests that estrogen positively modulates *in vitro* wound healing by accelerating cell migration within a few hours of treatment. On the other hand, Gilliver *et al*. (2009) revealed that DHT retarded the *in vitro* migration of murine EKs in a monolayer following scratch wounding. In contrast, the present study revealed an increase of EK migration in presence of TST. This stimulation was significantly higher than the incubation with Arimidex after 24 and 48 hours. Previous studies have demonstrated that DHT retarded the *in vitro* migration of rat EKs following scratch wounding (Gilliver *et al*., 2009). In particular, since the *in vivo* effects of DHT were not apparently shared with testosterone, this suggests that epithelialisation may potentially be improved through selective prevention of DHT biosynthesis, rather than total androgen blockade. In contrast, in the present study, the results suggest that EK migration may be accelerated with TST. In particular, this acceleration was determined at the late time points (24 and 48 hours). Interestingly, although TST did not significantly increase keratinocyte migration, its effect was significantly inhibited by an aromatase inhibitor (Arimidex). However, since there was also a significant difference between the effect of E2 and TST (in the absence of an aromatase inhibitor) on cell migration (see section *3.5.3.2*), it is unlikely that TST is fully aromatized to E2. Since the activity of aromatase has not been well described previously in human female EKs, the mRNA expression and activity of P450arom were also explored in the present study as described in section *4.5.2* which also supports the possibility of aromatization of androgens to estrogens. The effect of DHEA-S was impaired in the presence of STX64 showing the

importance of STS activity for the conversion of DHEA-S to the un-conjugated form. This also supports the beneficial effect of the precursor of steroids on wound healing in an animal model (Gilliver *et al*., 2007). The conversion of DHEA-S and DHEA locally to downstream steroid hormones leads to estrogenic and/or androgenic effects which may be important in age-related skin homeostasis, and which would avoid systemic adverse effects related to estrogen. In fact, it has been demonstrated that DHEA accelerated impaired healing in an impaired healing animal model by the local conversion of DHEA to estrogen, acting through the estrogen receptor (Mills *et al*., 2005). Since DHEA accelerates keratinocyte migration, its exogenous application may be applicable to the treatment of human impaired wound healing states.

The presence of early (4 hours) and late (48 hours) effects in DF and EK migration, suggests that both non genomic and genomic pathways might be activated. A previous study has demonstrated the *in vitro* stimulation of human endothelial cell migration in response to E2 via the non-genomic activation of membrane-associated ERα, which leads to actin cytoskeleton remodelling (Simoncini *et al*., 2005). A similar effect in DFs and EKs may explain the early increase in cell migration. Recent advances in this field suggest the hypothesis that the balance between transcriptional and non-transcriptional ER actions is physiologically important (Simoncini and Genazzani, 2003). The non transcriptional effects result from the recruitment of different pathways, including novel membrane receptors and interactions of nuclear steroid receptors with membrane and cytoplasmic signaling molecules such as adapter proteins (Boonyaratanakornkit and Edwards, 2007), G proteins, ion channels, and protein kinases (such as mitogen-activated protein kinases—MAPK, or phosphatidylinositol-3 kinase—PI3K) (Simoncini *et al*., 2003). A better definition of receptor mechanisms involved in mediating activation of non-genomic signaling pathways is important improve the understanding of the biology of steroid hormones. In order to differentiate between non-genomic and genomic pathways, DFs and EKS

could be cultured in the presence of specific ER agonists or antagonists. Recent studies have reported that tamoxifen and raloxifene accelerate cutaneous wound healing in ovariectomized mice that were used as an age-associated impaired wound healing model (Hardman *et al*., 2008) and that they also stimulate proliferation in a scratch wound assay of cultured human female abdominal DFs (Stevenson *et al*., 2009). Moreover, studies employing protein kinase signaling inhibitors and dominant negative mutants of signaling pathway components have revealed that extranuclear functions of AR and ERs involve functional and direct interactions with components of the Src/Shc/ERK signaling pathways (Kousteni *et al.,* 2001). In addition, an alternative to investigate the extranuclear mode of action of androgens and estrogens is a novel class of mechanism-specific pharmacotherapeutic agents called ANGELS (Activators of Non-Genotropic Estrogen-Like Signaling). These are a new class of drug which have been shown to selectively activate estrogen regulated cytosolic protein kinase pathways in bone without activating classical ERs (Moggs *et al*., 2003; Manolagas *et al.,* 2004). The mechanism of binding and action of DHEA is also important. Recent evidence suggests high affinity binding of DHEA to G protein-coupled membrane receptors in neuronal-like PC12 rat pheochromocytoma cells, initiating signaling pathways comprising phosphorylation of Src and PKCα/β, activation of CREB and NFκB and up-regulation of the ratio anti-apoptotic/pro-apoptotic Bcl-2 family proteins, favoring cell survival (Charalampopoulos *et al.*, 2004; Charalampopoulos *et al*., 2006a; Charalampopoulos *et al*., 2006b). Furthermore, membrane G protein-coupled receptors, exerting high specificity for DHEA, have been described in bovine aortic endothelial cells (BAEC) and primary human umbilical vein endothelial cells (HUVEC) (Liu *et al*., 2007; Charalampopoulos *et al*., 2008). Recently, Alexaki *et al*. (2009), have reported a protective effect of DHEA, on the human keratinocytes cell line HaCaT, through activation of G-proteins and regulation of Bcl-2 family proteins, mitochondrial disruption and caspase 9 cleavage, favoring survival. The results suggest the activation of non-genomic signaling via DHEA. A greater understanding of DHEA signalling in DFs and

EKs may help develop wound healing therapies, without the risks of estrogen treatment, which will be of particular benefit to the elderly and patients with impaired wound healing.

4.5 The effect of Dexamethasone mRNA expression and enzyme activity of aromatase in cultured human dermal fibroblasts and epidermal keratinocytes

The expression of aromatase, the enzyme required for the conversion of androgen to estrogen, has been previously reported in human skin (Chen *et al.,* 2002). In the present study, the mRNA expression of P450arom was investigated by non quantitative RT-PCR as described in section *3.1*. The expression of mRNA for CYP19 in EKs was not determined although it was clearly demonstrated to be present in DFs (Figure 25). To confirm these data, the aromatase enzyme activity was investigated in cultured EKs and DFs using the tritiated water assay (Lephart and Simpson, 1991). A large number of studies support the importance of local estrogen biosynthesis in human skin. In a previous report, it has been found that forskolin (FSK) synergistically induces aromatase expression in a dexamethasone (DEX) dependent manner in a human osteoblastic cell line, SV-HFO (Watanabe *et al*., 2005). In addition, Thornton *et al.* (2006) demonstrated the stimulation of aromatase mRNA and enzyme activity by dexamethasone in human follicular DP cell cultures. These observations provide evidence for the selective action of estradiol produced locally by autocrine or paracrine mechanisms. In the present study, it was investigated whether EKs and DFs express aromatase activity. In addition, the cells were treated with DEX to explore the effect on mRNA expression and activity of the P450arom enzyme.

4.5.1 The effect of Dexamethasone on mRNA expression and enzyme activity of aromatase in cultured human dermal fibroblasts

DFs were established from tissues explants of human female and male facial skin and female abdominal and breast skin. The incubation with DEX stimulated a significant increase in enzymatic activity only in DFs established from female (Figure 57) and male (Figure 58) facial skin when compared to the control. In contrast, the cells established from breast skin and abdominal skin did not show any increase in the enzyme activity. In addition, the results of relative qRT-PCR suggested that the amount of CYP19 gene transcript was up-regulated by DEX in DFs derived from face and abdomen. Aromatase activity has been reported in human DFs cultured from both genital and non-genital skin (Svenstrup *et al*., 1990) and human fibroblasts from adipose tissue (Rink *et al*., 1996). These observations provide evidence for the biosynthesis of estradiol via aromatase in human DFs. Additionally, the data obtained in the present study support the mRNA expression of CYP19 and the enzyme activity in DFs established from female and male skin. Moreover, the up-regulation of aromatase by the facial and abdominal cells in response to DEX supports the local estrogen production in cells in the presence of a glucocorticoid. However, the mechanisms regulating aromatase expression by DEX in DFs is not really clear. In a previous study (Harada, 1992), cDNA of human DEX-treated fibroblasts was isolated by the PCR method including the rapid amplification of cDNA ends (RACE) protocol (Chenchik *et al.,* 1996). All 5'-fragments obtained from fibroblast aromatase cDNA contained a unique sequence in the region encoded by exon 1. A unique sequence was also deduced for the region between exons 1 and 2 of the placental aromatase gene from its cDNA, indicating that this region is used as an exon 1 by alternative splicing in skin fibroblasts. Tissue-specific use of multiple exons 1 in the splicing of aromatase transcripts has been demonstrated by the mRNAs obtained from various tissues (Bulun *et al.*, 2004). Watanabe *et al*., (2004) showed that the expression of aromatase activity and gene

transcripts were stimulated by DEX in the human fetal osteoblastic cell line, SV-HFO. They reported the first evidence of an osteoblastic cell line which predominantly uses promoter I.4 to drive aromatase expression. These data elucidated the mechanisms regulating local estrogen synthesis in human osteoblasts.

4.5.2 The effect of Dexamethasone on mRNA expression and enzyme activity of aromatase in cultured epidermal keratinocytes

The aromatase expression in human EKs is still unclear. The only evidence of aromatase activity in EKs has been detected by the $^{3}H_2O$ assay using cells established from foreskin (Hughes *et al*., 1997). In addition, Cheng and colleagues (2006) have demonstrated the aromatase expression in normal oral keratinocytes as well as differentiated oral SCC. Since aromatase catalyzes the conversion of androgen to oestrogen, its gene expression and enzyme activity in EKs and the local estrogen synthesis play an important role in the physiological conditions and in the growth of epidermis. In this study, EKs were established from tissues explants of human female and male facial skin. EKs were incubated with DEX for 24h. Previous studies showed that the mRNA expression and enzyme activity of aromatase are stimulated by DEX in human DFs (Berkovitz *et al*., 1989; see section *3.6.1*) in human follicular DP cell cultures (Thornton *et al.* 2006). In the present study, the incubation with DEX did not alter the activity in EKs established from all samples when compared to the control. However, the results of relative qRT-PCR suggested that the amount of CYP19 gene transcript was up-regulated by DEX. These observations indicate possible local synthesis of estradiol via aromatase in EK from human female and male facial skin. The common coding region of aromatase mRNA was detected in the human oral keratinocytes with variations in exon 1 expression among the individual samples (Cheng *et al*., 2006). Since the CYP19 gene regulatory region contains distinct promoters regulated in a tissue- or signaling pathway-specific manner (Bulun *et al*., 2004), the aromatase expression at the

common coding region and at the various exon Is (Simpson *et al*., 2002), and the mechanisms regulating aromatase expression by DEX in human EKs remains to be determined.

4.6 The effect of mechanical wounding on the aromatase activity of cultured human fibroblasts and epidermal keratinocytes

The conversion of DHEA locally to downstream steroid hormones leads to estrogenic and/or androgenic effects which may be important in age-related skin homeostasis. It has been thought that the delayed healing of cutaneous wounds in aged individuals may in part reflect the decline in circulating levels of DHEA and estrogens. The beneficial response on wound healing that DHEA and estrogen exert may be blocked by aromatase inhibition (Howgate *et al*., 2009). In particular, in postmenopausal women, the decline of sex steroids production impairs the efficiency of skin repair mechanisms. A series of clinical studies has identified estrogens as being endogenous enhancers of the healing processes (Brincat *et al*., 2005). The administration of E2, either systemically or topically, has been shown to reverse the fundamental repair defects observed in postmenopausal women. In contrast, androgenic species retard repair and interfere with the accumulation of the structural proteins that reconstitute the damaged dermis (Gilliver and Ashcroft, 2007). Since estrogens may promote wound healing, in the present study it was investigated whether the aromatase activity and mRNA expression were modulated in cultured skin cells in response to mechanical wounding.

4.6.1 Mechanical wounding does not alter the aromatase activity of cultured human dermal fibroblasts

The aromatase activity was measured by the tritiated assay to assess the effect of wounding on DFs at 2 and 24h. DFs were established from tissues explants of human female and male facial skin, and female abdominal and breast skin. The analysis revealed that the enzyme activity was not induced in the scratch wound assay in any group of samples after either 2h (see section *3.8.1*) or 24h (see section *3.8.2*) following mechanical wounding, although the migration assay of cultured human female facial DFs after wounding *in vitro* (see section *4.4.1*) suggested the local estrogen formation through aromatization. However, the investigation using relative qRT-PCR, revealed an increase in mRNA expression only in the female facial (Figure 79) and breast (Figure 81) DFs after 24h. Since the basal mRNA expression (see section *3.1*) and the basal enzyme activity of aromatase (see section *3.7.1*) were detected in DFs, the beneficial effect of DHEA (-S) on DF migration after scratching may indicate the local conversion to E2. It has demonstrated that DHEA accelerated impaired healing in mice through aromatisation to estrogen, acting through the estrogen receptor (Mills *et al*., 2005). However, the human DF migration did not show significant acceleration in presence of either TST or Arimidex (see section *3.5.3.1*). Moreover, a previous study showed that DHT retards the *in vitro* migration of rat EKs following scratch wounding. By contrast, it failed to influence the migratory and proliferative properties of rat DFs, suggesting that its primary inhibitory effect is upon re-epithelialization (Gilliver *et al*., 2009). Taken together, these data suggest that it would be helpful to investigate whether and how DHEA (-S) may modulate aromatase expression and/or activity as a mechanism for producing more E2.

4.6.2 Mechanical wounding increases the aromatase activity of epidermal keratinocytes

Aromatase activity was measured by the tritiated assay to assess the effect of wounding on EKs at 2 and 24h. EKs (n=3) were established from tissues explants of human female facial skin. The analysis revealed that the mechanically wounded keratinocytes showed a increase in aromatase activity at 24h compared to the non-wounded cells. These results were also supported by the analysis of mRNA expression using relative qRT-PCR. These findings indicate that both aromatase mRNA expression and enzyme activity are induced by the *in vitro* scratch wound assay, suggesting that factors secreted by wounded keratinocytes that stimulate proliferation and migration also stimulate aromatase activity providing evidence for a role for local estrogen formation in EK during skin repair. Both the modulation of the expression of chemokines and angiogenic genes (see section *4.3.1*) and the stimulation of EK migration (see section *4.4.2*) in response to sex steroids, suggest that estrogens and androgens may regulate EKs functions. Since the beneficial response on wound healing that DHEA and estrogen exert was blocked by an aromatase inhibitor (see section *3.5.3.2*), the activity of this enzyme in wounded EKs may have implications for the wound healing process through the conversion of androgen to estrogen. EK play a key role in wound healing and a recent study showed that estrogen amodulates not only migration, but also the proliferation of a human keratinocyte cell line NCTC 2544 (Merlo *et al*., 2009). Collectively, these results appear particularly valuable in view of the increasing interest toward approaches, including aromatase targeting, for regenerative wound healing.

4.7 Conclusions and future perspectives

Sex steroids play a fundamental role in the development of sexually dimorphic characteristics essential for reproduction. In recent years, the interest of researchers has been particularly focused on the role of androgens and estrogens in pathological conditions such as neoplasia, vascular disease and osteoporosis (Ashcroft and Ashworth, 2003). In addition, the skin appears to act as an endocrine organ target and a source of active sexual hormones. In particular, important structural and functional skin alterations may occur in post-menopausal women (Shah and Maibach, 2001; Calvo *et al*., 2008). These skin changes can be related to altered hormonal profiles. Indeed, the reduction of human adrenal DHEA-S levels during aging results in a remarkable decline in the production of androgens and estrogens in peripheral target tissues, which could be involved in the pathogenesis of age-related diseases such as insulin resistance and obesity (Labrie, 2004). This decrease is thought to be related also to the pathogenesis of some age-related skin conditions (El-Alfy *et al*., 2010). *In vivo* studies have demonstrated the importance of estrogen in both skin homeostasis and wound healing (Ashcroft *et al*., 1999), but little is known about the molecular and cellular responses of the individual cell types. The present study showed that human skin, and individual cultured DFs and EKs, and HFs express the key steroidogenic proteins required for the local synthesis and action of active sex steroid hormones. Androgens and estrogens have been shown to significantly modulate genes with roles in wound healing, skin aging and cancer in cultured EKs. The effect of sex steroids on the transcriptome of human HFs showed a weak correlation between the data obtained with three different steroids (DHEA-S, TST and E2) compared to the analysis on keratinocytes. These results could be related to the more complex anatomy and biology of the isolated HF compared to the individual keratinocytes grown *in vitro*. The analysis on the HF needs future validation of the data obtained with the array technology. The modulation of *LOR* will be explored using relative qRT-PCR to confirm the down-regulation in presence of DHEA-

S. In addition this study has shown that androgens and estrogens accelerate DF and EK migration following mechanical wounding of cell monolayers *in vitro.* The results of the cell migration assay support a previous study investigating the effects of estrogen on cultured human DFs (Stevenson *et al*., 2009). However, in current study the inhibition of aromatase which blocks the stimulatory effect of DHEA and TST on both DF and EK migration provides evidence for a requirement for aromatisation of androgens to estrogen. To confirm this hypothesis, DFs and EKs have been shown to express mRNA and enzyme activity of the necessary enzyme (aromatase) required for conversion of androgens to estradiol. In addition, the inhibition of STS reversed the stimulatory effect of DHEA-S on cell migration in both DFs and EKs. In particular, the preliminary analysis using non quantitative RT-PCR did not revealed the expression of the transporter OATP2B1 in human DFs. However, several OATPs, such as OATP-A, OATP-B, OATP-C, OATP-8, and OATP-E (Hagenbuch and Meier, 2003) and two members of the organic anion transporter (OAT) family, OAT-3 and OAT-4, can mediate the cellular uptake of steroid conjugates in the kidney, liver, brain, and placenta (Cha *et al*. 2000, 2001). Schiffer *et al*. (2003) have detected only the expression of mRNA of OATP-B, OATP-D and OATP-E in human DFs and EKS from foreskin. Future studies will need to investigate the expression of all these transporters in both DFs and EKs obtained from human female face, abdomen and breast. The migration assay also revealed additional valuable evidence of a more effective stimulation in presence of both DHEA and DHEA-S than TST. Since the conversion of androgens to estrogens is catalyzed by aromatase as the final step in the steroidogenic pathway and TST is the direct substrate for aromatase (Figure 5), a further understanding of DHEA signalling is required to help develop wound healing therapies. Recent evidence suggests that in some tissues DHEA may have also direst actions, independent of AR and ERs (Williams *et al.,* 2004). However, the effect of DHEA on DF and EK migration in the presence or absence of an inhibitor of aromatase may suggest that DHEA is metabolised to E2. On the other hand, the presence of early (4 hours) and late (48 hours) effects in DF

and EK migration, suggests that both non genomic and genomic pathways might be activated. Future analysis using ER and AR antagonists will help to understand further the mechanism of signalling of sex steroid hormones and providing development of potential therapies that specifically affect non-genomic action alone or even both modes of action with applications in various areas such as skin repair. Interestingly, there were differences in the modulation of aromatase activity between different anatomical sites, sex and type of human skin cells in response to DEX and following mechanical wounding *in vitro*. Since primary cultures were established from skin obtained during routine plastic surgical procedures, there is a limitation to the samples available. A further interesting comparison would be related to the potential difference between men and women.

Collectively, the results obtained in this study suggest that sex steroids may appear particularly valuable in view of the increasing interest toward approaches for regenerative wound healing. Further studies are necessary to investigate the effect of sex steroids on wound healing *in vivo* in order to formulate better targeted strategies for improving skin repair. In particular, with its low toxicity and large availability and acceptability for use even in males, topical applications of DHEA could provide a potential treatment for wound healing. Further studies are necessary to investigate the effect of sex steroids on wound healing *in vivo* in order to formulate better targeted strategies for improving skin repair.

Bibliography

Adamson R., (2009). Role of macrophages in normal wound healing: an overview. J. Wound Care, 18(8):349-51.

Agar N. and Young A.R., (2005). Melanogenesis: a photoprotective response to DNA damage? Mutat. Res., 571(1-2):121-32.

Akiyama M., Matsuo I., Shimizu H., (2002). Formation of cornified cell envelope in human hair follicle development. Br. J. Dermatol., 146(6):968-76.

Alexaki V.I., Charalampopoulos I., Panayotopoulou M., Kampa M., Gravanis A., Castanas E., (2009). Dehydroepiandrosterone protects human keratinocytes against apoptosis through membrane binding sites. Exp. Cell. Res., 315(13): 2275-83.

Ankrom M.A., Patterson J.A., d'Avis P.Y., Vetter U.K., Blackman M.R., Sponseller P.D., Tayback M., Robey P.G., Shapiro J.R., Fedarko N.S., (1998). Age-related changes in human oestrogen receptor alpha function and levels in osteoblasts. Biochem. J., 333 (Pt 3): 787-94.

Arnal J.F., Gourdy P., Elhage R., Garmy-Susini B., Delmas E., Brouchet L., Castano C., Barreira Y., Couloumiers J.C., Prats H., Prats A.C., Bayard F., (2004). Estrogens and atherosclerosis. Eur. J. Endocrinol., 150(2):113-7.

Ashcroft G.S. and Ashworth J.J., (2003). Potential role of estrogens in wound healing. Am. J. Clin. Dermatol., 4(11):737-43.

Ashcroft G.S., Dodsworth J., van Boxtel E., Tarnuzzer R.W., Horan M.A., Schultz G.S., Ferguson M.W., (1997). Estrogen accelerates cutaneous wound healing associated with an increase in TGF-beta1 levels. Nat. Med., 3(11):1209-15.

Ashcroft G.S., Greenwell-Wild T., Horan M.A., Wahl S.M., Ferguson M.W., (1999). Topical estrogen accelerates cutaneous wound healing in aged humans associated with an altered inflammatory response. Am. J. Pathol. 155(4):1137-46.

Ashcroft G.S., Horan M.A., Ferguson M.W., (1995). The effects of ageing on cutaneous wound healing in mammals. J. Anat., 187 (Pt 1):1-26.

Auger F.A., Lacroix D., Germain L., (2009). Skin substitutes and wound healing. Skin Pharmacol. Physiol., 22(2):94-102.

Balkwill F., (2003). Chemokine biology in cancer. Semin. Immunol., 15(1):49-55.

Barrientos S., Stojadinovic O., Golinko M.S., Brem H., Tomic-Canic M., (2008). Growth factors and cytokines in wound healing. Wound Repair Regen., 16(5):585-601.

Basu A., Kligman L.H., Samulewicz S.J., Howe C.C., (2001). Impaired wound healing in mice deficient in a matricellular protein SPARC (osteonectin, BM-40). BMC Cell Biol., 2: 15.

Beanes S.R., Dang C., Soo C., Ting K., (2003). Skin repair and scar formation: the central role of TGF-beta. Expert. Rev. Mol. Med., 5(8):1-22.

Berkovitz G.D., Bisat T., Carter K.M., (1989). Aromatase activity in microsomal preparations of human genital skin fibroblasts: influence of glucocorticoids. J. Steroid Biochem., 33(3):341-7.

Berthois Y., Katzenellenbogen J.A., Katzenellenbogen B.S., (1986). Phenol red in tissue culture media is a weak estrogen: implications concerning the study of estrogen-responsive cells in culture. Proc. Natl. Acad. Sci. U. S. A., 83(8):2496-500.

Bienová M., Kucerová R., Fiurásková M., Hajdúch M., Kolář Z., (2005). Androgenetic alopecia and current methods of treatment. Acta Dermatovenerol. Alp. Panonica Adriat., 14(1):5-8.

Bikle D.D., (2010). Vitamin D and the skin. J. Bone Miner Metab., 28(2):117-30.

Birch M.P., Lalla S.C., Messenger A.G., (2002). Female pattern hair loss. Clin Exp. Dermatol., 27(5):383-88.

Bloomfield K.L., Osborne S.A., Kennedy D.D., Clarke F.M., Tonissen K.F., (2003). Thioredoxin-mediated redox control of the transcription factor Sp1 and regulation of the thioredoxin gene promoter. Gene, 319:107-16.

Boonyaratanakornkit V. and Edwards D.P., (2007). Receptor mechanisms mediating non-genomic actions of sex steroids. Semin. Reprod. Med., 25(3):139-53.

Bossen C. and Schneider P., (2006). BAFF, APRIL and their receptors: structure, function and signaling. Semin. Immunol., 18(5):263-75.

Botchkarev V.A. and Paus R., (2003). Molecular biology of hair morphogenesis: development and cycling. J. Exp. Zool. B. Mol. Dev. Evol., 298(1):164-80.

Boucher A., Kharfi A., Al-Akoum M., Bossù P., Akoum A., (2001). Cycle-dependent expression of interleukin-1 receptor type II in the human endometrium. Biol. Reprod., 65(3):890-8.

Boulais N. and Misery L., (2007). Merkel cells. J. Am. Acad. Dermatol., 57(1):147-65.

Brincat M.P., Baron Y.M., Galea R., (2005). Estrogens and the skin. Climacteric., 8(2):110-23.

Brown C.M., Mulcahey T.A., Filipek N.C., Wise P.M., (2010). Production of proinflammatory cytokines and chemokines during neuroinflammation: novel roles for estrogen receptors alpha and beta. Endocrinology, 151(10):4916-25.

Bulun S.E., Takayama K., Suzuki T., Sasano H., Yilmaz B., Sebastian S., (2004). Organization of the human aromatase p450 (CYP19) gene. Semin. Reprod. Med., 22(1):5-9.

Calvin M., (2000). Oestrogens and wound healing. Maturitas, 34(3): 195-210.

Calvo E., Luu-The V., Morissette J., Martel C., Labrie C., Bernard B., Bernerd F., Deloche C., Chaussade V., Leclaire J., Labrie F., (2008). Pangenomic changes induced by DHEA in the skin of postmenopausal women. J. Steroid. Biochem. Mol. Biol., 112(4-5):186-93.

Candi E., Melino G., Mei G., Tarcsa E., Chung S.I., Marekov L.N., Steinert P.M., (1995) Biochemical, structural, and transglutaminase substrate properties of human loricrin, the major epidermal cornified cell envelope protein. J. Biol. Chem., 270(44):26382-90.

Carroll L.A. and Koch R.J., (2003). Heparin stimulates production of bFGF and TGF-beta 1 by human normal, keloid, and fetal dermal fibroblasts. Med. Sci. Monit., 9(3):BR97-108.

Cha S.H., Sekine T., Fukushima J.I., Kanai Y., Kobayashi Y., Goya T. and Endou H., (2001). Identification and characterization of human organic anion transporter 3 expressing predominantly in the kidney. Molecular Pharmacology, 59:1277–1286.

Cha S.H., Sekine T., Kusuhara H., Yu E., Kim J.Y., Kim D.K., Sugiyama Y., Kanai Y. and Endou H., (2000). Molecular cloning and characterization of multispecific organic anion transporter 4 expressed in the placenta. Journal of Biological Chemistry, 275:4507–4512.

Chabab A., Sultan C., Fenart O., Descomps B., (1986). Stimulation of aromatase activity by dihydrotestosterone in human skin fibroblasts. J. Steroid. Biochem., 25(1):165-9.

Champion R.H., (1970). An introduction to the biology of the skin. Oxford, Blackwell Scientific.

Champliaud M.F., Viel A., Baden H.P., (2003). The expression of vitamin D-upregulated protein 1 in skin and its interaction with sciellin in cultured keratinocytes. J. Invest. Dermatol.,121(4):781-5.

Charalampopoulos I., Alexaki V.I., Lazaridis I., Dermitzaki E., Avlonitis N., Tsatsanis C., Calogeropoulou T., Margioris A.N., Castanas E. and Gravanis A., (2006a). G protein-associated, specific membrane binding sites mediate the neuroprotective effect of Dehydroepiandrosterone. FASEB J., 20:577–579.

Charalampopoulos I., Alexaki V.I., Tsatsanis C., Minas V., Dermitzaki E., Lasaridis I., Vardouli L., Stournaras C., Margioris A.N., Castanas E. and Gravanis A., (2006b). Neurosteroids as endogenous inhibitors of neuronal cell apoptosis in aging. Ann. N. Y. Acad. Sci., 1088:139–152.

Charalampopoulos I., Remboutsika E., Margioris A.N. and Gravanis A., (2008). Neurosteroids as modulators of neurogenesis and neuronal survival. Trends. Endocrinol. Metab., 19:300–307.

Charalampopoulos I., Tsatsanis C., Dermitzaki E., Alexaki V.I., Castanas E., Margioris A.N. and Gravanis A., (2004). Dehydroepiandrosterone and allopregnanolone protect sympathoadrenal medulla cells against apoptosis via antiapoptotic Bcl-2 proteins. Proc. Natl. Acad. Sci. U. S. A., 101:8209–8214.

Chen K.S. and DeLuca H.F., (1994). Isolation and characterization of a novel cDNA from HL-60 cells treated with 1,25-dihydroxyvitamin D-3. Biochim. Biophys. Acta., 1219(1):26-32.

Chen W., Thiboutot D., Zouboulis C.C., (2002). Cutaneous androgen metabolism: basic research and clinical perspectives. J. Invest. Dermatol., 119: 992-1007.

Chen W., Tsai S.J., Sheu H.M., Tsai J.C., Zouboulis C.C., (2010). Testosterone synthesized in cultured human SZ95 sebocytes derives mainly from dehydroepiandrosterone. Exp Dermatol. 2010 May;19(5):470-2.

Chen W., Zouboulis C.C., Fritsch M., Blume-Peytavi U., Kodelja V., Goerdt S., Luu-The V., Orfanos C.E., (1998). Evidence of heterogeneity and quantitative differences of the type 1 5α-reductase expression in cultured human skin cells. Evidence of its presence in melanocytes. J. Invest. Dermatol., 110: 84-89.

Chen Y., Clegg N.J. and Scher H.I., (2009). Antiandrogens and androgen depleting therapies in prostate cancer: novel agents for an established target. Lancet. Oncol., 10(10): 981–991.

Chen Z., Fadiel A., Feng Y., Ohtani K., Rutherford T., Naftolin F., (2001). Ovarian epithelial carcinoma tyrosine phosphorylation, cell proliferation, and ezrin translocation are stimulated by interleukin 1alpha and epidermal growth factor. Cancer, 92(12):3068-75.

Chenchik A., Diachenko L., Moqadam F., Tarabykin V., Lukyanov S., Siebert P.D., (1996). Full-length cDNA cloning and determination of mRNA 5' and 3' ends by amplification of adaptor-ligated cDNA. Biotechniques, 21(3):526-34.

Cheng Y.S., Mues G., Wood D., Ding J., (2006). Aromatase expression in normal human oral keratinocytes and oral squamous cell carcinoma. Arch. Oral Biol., 51(7):612-20.

Chu D.H., Haake A.R., Holbrook K., Loomis C.A., (2003). The structure and development of skin. See Freedberg *et al*. (2003), 58–88.

Clark R.A.F. and Henson P.M., (1988). The Molecular and cellular biology of wound repair, Plenum Press.

Cotsarelis G., (2006). Gene expression profiling gets to the root of human hair follicle stem cells. J. Clin. Invest., 116: 19-22.

Cousen P. and Messenger A., (2010). Female pattern hair loss in complete androgen insensitivity syndrome. Br. J. Dermatol., 162(5):1135-7.

Dahl K.N., Ribeiro A.J., Lammerding J., (2008). Nuclear shape, mechanics, and mechanotransduction. Circ. Res., 102(11):1307-18.

Demling R.H. and Orgill D.P., (2000). The anticatabolic and wound healing effects of the testosterone analog oxandrolone after severe burn injury. J. Crit. Care., 15: 12-17.

Deroo B.J., Hewitt S.C., Peddada S.D., Korach K.S., (2004). Estradiol regulates the thioredoxin antioxidant system in the mouse uterus. Endocrinology, 145(12):5485-92.

Desmouliere A., Chaponnier C., Gabbiani G., (2005). Tissue repair, contraction, and the myofibroblast. Wound Repair Regen., 13(1): 7-12.

Douglas H.E., (2010). TGF-ß in wound healing: a review. J. Wound Care, 19(9):403-6.

Dubinett SM, Lee JM, Sharma S, Mulé JJ. Chemokines: can effector cells be redirected to the site of the tumor? Cancer J. 2010 Jul-Aug;16(4):325-35.

El-Alfy M., Deloche C., Azzi L., Bernard B.A., Bernerd F., Coutet J., Chaussade V., Martel C., Leclaire J., Labrie F., (2010). Skin responses to topical dehydroepiandrosterone: implications in antiageing treatment? Br. J. Dermatol., 163(5):968-76.

Elias P.M., Feingold K.R., Fluhr J.W., (2003). Skin as an organ of protection. See Freedberg *et al*., (2003), 107–18.

Eming S.A., Brachvogel B, Odorisio T, Koch M., (2007, a). Regulation of angiogenesis: wound healing as a model. Prog. Histochem. Cytochem., 42(3):115-70

Eming S.A., Krieg T., Davidson J.M., (2007, b). Inflammation in wound repair: molecular and cellular mechanisms. J. Invest. Dermatol., 127(3):514-25.

Engelhardt E., Toksoy A., Goebeler M., Debus S., Bröcker E.B., Gillitzer R., (1998). Chemokines IL-8, GROalpha, MCP-1, IP-10, and Mig are sequentially and differentially expressed during phase-specific infiltration of leukocyte subsets in human wound healing. Am. J. Pathol., 153(6):1849-60.

Englund G., Rorsmana F., Rönnblom A., Karlbomc U., Lazorovab L., Gråsjö J., Kindmarka A. and Arturssonb P., (2006). Regional levels of drug transporters along the human intestinal tract: coexpression of ABC and SLC transporters and comparison with Caco-2 cells. Eur. J. Pharm. Sci., 29:(3–4):269–277.

Fedi P., Bafico A., Nieto Soria A., Burgess W.H., Miki T., Bottaro D.P., Kraus M.H., Aaronson S.A., (1999). Isolation and biochemical characterization of the human Dkk-1 homologue, a novel inhibitor of mammalian Wnt signaling. J. Biol. Chem., 274(27):19465-72.

Fistarol S.K., Itin P.H., (2010). Disorders of pigmentation. J. Dtsch. Dermatol. Ges., 8(3):187-201.

Foradori C.D., Weiser M.J., Handa R.J., (2008). Non-genomic actions of androgens. Front. Neuroendocrinol., 29(2):169-81.

Freedberg I.M., Eisen A.Z., Wolff K., Austen F.K., Goldsmith L.A., Katz S.I., eds., (2003). Fitzpatrick's Dermatology in General Medicine. New York: McGraw-Hill.

Fritsch M., Orfanos C.E., Zouboulis C.C., (2001). Sebocytes are the key regulators of androgen homeostasis in human skin. J. Invest. Dermatol., 116(5):793-800.

Fujimoto J., Hori M., Ichigo S. and Tamaya T., (1997). Ovarian steroids regulate the expression of basic fibroblast growth factor and its mRNA in fibroblasts derived from uterine endometrium. Ann. Clin. Biochem., 34:91–96.

Ghalbzouri A., Hensbergen P., Gibbs S., Kempenaar J., van der Schors R., Ponec M., (2004). Fibroblasts facilitate re-epithelialization in wounded human skin equivalents. Lab.. Invest., 84(1):102-12.

Gill S.E. and Parks W.C., (2008). Metalloproteinases and their inhibitors: regulators of wound healing. Int. J. Biochem. Cell Biol., 40(6-7):1334-47.

Gilliver S.C. and Ashcroft G.S., (2007). Sex steroids and cutaneous wound healing: the contrasting influences of estrogens and androgens. Climacteric., 10(4):276-88.

Gilliver S.C., Ashworth J.J., Ashcroft G.S., (2007). The hormonal regulation of cutaneous wound healing. Clin. Dermatol., 25: 56-62.

Gilliver S.C., Ruckshanthi J.P., Hardman M.J., Zeef L.A., Ashcroft G.S., (2009). 5alpha-dihydrotestosterone (DHT) retards wound closure by inhibiting re-epithelialization. J. Pathol., 217(1):73-82.

Gilliver S.C., Wu F. and Ashcroft G.S., (2003). Regulatory roles of androgens in cutaneous wound healing. Thromb Haemost, 90:978–985.

Gilliver S.C., Emmerson E., Campbell L., Chambon P., Hardman M.J., Ashcroft G.S., (2010). 17beta-estradiol inhibits wound healing in male mice via estrogen receptor-alpha. Am. J. Pathol., 176(6):2707-21.

Goh Y.Y., Pal M., Chong H.C., Zhu P., Tan M.J., Punugu L., Lam C.R., Yau Y.H., Tan C.K., Huang R.L., Tan S.M., Tang M.B., Ding J.L., Kersten S., Tan N.S., (2010). Angiopoietin-like 4 interacts with integrins beta1 and beta5 to modulate keratinocyte migration. Am. J. Pathol., 177(6):2791-803.

Goldsmith L., (1983). Biochemistry and physiology of the skin. New York, Oxford University Press.

Goldsmith L.A., (1991). Physiology, biochemistry, and molecular biology of the skin. New York; Oxford, Oxford University Press.

Goss P.E., Clark R.M., Ambus U., Weizel H.A., Wadden N.A., Crump M., Walde D., Tye L.M., De Coster R., Bruynseels J., (1995). Phase II study of vorozole (R83842), a new aromatase inhibitor, in postmenopausal women with advanced breast cancer in progression on tamoxifen. Clin. Cancer. Res. 1:287–294.

Gras M.P., Laâbi Y., Linares-Cruz G., Blondel M.O., Rigaut J.P., Brouet J.C., Leca G., Haguenauer-Tsapis R., Tsapis A., (1995). BCMAp: an integral membrane protein in the Golgi apparatus of human mature B lymphocytes. Int. Immunol., 7(7):1093-106.

Green S., Walter P., Kumar V., Krust A., Bornert J. M., Argos P., Chambon P. (1986). Human oestrogen receptor cDNA: sequence, expression and homology to v-erb-A. Nature, 320:134–9.

Grube M., Köck K., Oswald S., Draber K., Meissner K., Eckel L., Böhm M., Felix S.B., Vogelgesang S., Jedlitschky G., Siegmund W., Warzok R. and Kroemer H.K., (2006). Organic anion transporting polypeptide 2B1 is a high-affinity transporter for atorvastatin and is expressed in the human heart. Clin. Pharmacol. Ther., 80(6):607–620.

Guyton A.C. and Hall J.E. (1996). Textbook of medical physiology. Philadelphia; London, Saunders.

Hagenbuch B. and Meier P.J., (2003). The superfamily of organic anion transporting polypeptides. Biochimica et Biophysica Acta (BBA)—Biomembranes, 1609:1–18.

Hamilton W.J., Boyd J.D., *et al*. (1972). Hamilton, Boyd and Mossman's human embryology : prenatal development of form and function. Cambridge, Heffer.

Hannen R.F., Michael A.E., Jaulim A., Bhogal R., Burrin J.M., Philpott M.P., (2010). Steroid synthesis by primary human keratinocytes; implications for skin disease. Biochem. Biophys. Res. Commun. [Epub ahead of print].

Harada N.A., (1992). A unique aromatase (P-450AROM) mRNA formed by alternative use of tissue-specific exons 1 in human skin fibroblasts. Biochem. Biophys. Res. Commun, 189(2):1001-7.

Hardman M.J., Emmerson E., Campbell L., Ashcroft G.S., (2008). Selective estrogen receptor modulators accelerate cutaneous wound healing in ovariectomized female mice. Endocrinology, 149: 551–557.

Hauffa B., Hiort O., (2011). P450 side-chain cleavage deficiency - a rare cause of congenital adrenal hyperplasia. Endocr. Dev., 20:54-62.

Hodgins M.B., Murad S., Simpson N.B., (1985). A search for variation in hair follicle androgen metabolism which might be linked to male pattern baldness. Br. J. Dermatol., 113: 794.

Hoffmann R., (2003). Steroidogenic isoenzymes in human hair and their potential role in androgenetic alopecia. Dermatology, 206: 85-95.

Hoffmann R., Rot A., Niiyama S., Billich A., (2001). Steroid sulfatase in the human hair follicle concentrates in the dermal papilla. J. Invest. Dermatol., 117(6):1342-8.

Howgate D.J., Gamie Z., Panteliadis P., Bhalla A., Mantalaris A., Tsiridis E., (2009). The potential adverse effects of aromatase inhibitors on wound healing: in vitro and in vivo evidence. Expert Opin.. Drug Saf., 8(5):523-35.

Hughes S.V., Robinson E., Bland R., Lewis H.M., Stewart P.M., Hewison M., (1997). 1,25-dihydroxyvitamin D3 regulates estrogen metabolism in cultured keratinocytes. Endocrinology, 138(9):3711-8.

Itami S., Kurata S., Takayasu S., (1990). 5 alpha-reductase activity in cultured human dermal papilla cells from beard compared with reticular dermal fibroblasts. J. Invest. Dermatol.., 94(1):150-2

Itami S., Sonoda T., Kurata S. and Takayasu S., (1994). Mechanism of action of androgen in hair follicles. Journal of Dermatological Science, 7(1):S98-S103.

Ito Y., Oike Y., Yasunaga K., Hamada K., Miyata K., Matsumoto S., Sugano S., Tanihara H., Masuho Y., Suda T., (2003). Inhibition of angiogenesis and vascular leakiness by angiopoietin-related protein 4. Cancer Res., 63: 6651-6657.

Jesse R.L., Loesser K., Eich D.M., Qian Y.Z., Hess M.L., Nestler J.E., (1995). Dehydroepiandrosterone inhibits human platelet aggregation in vitro and in vivo. Ann. N.Y. Acad. Sci., 774: 281-90.

Jones L.N. and Rogers G.E., (2005). Protein expression in developing wool fibre cuticle cells. Proceedings 11th International Wool Research Conference. Leeds: Fundamental, Wool Science, 108.

Junn E., Han S.H., Im J.Y., Yang Y., Cho E.W., Um H.D., Kim D.K., Lee K.W., Han P.L., Rhee S.G., Choi I., (2000). Vitamin D3 up-regulated protein 1 mediates oxidative stress via suppressing the thioredoxin function. J. Immunol., 164(12):6287-95.

Kadekaro A.L., Kanto H., Kavanagh R., Abdel-Malek Z.A., (2003). Significance of the melanocortin 1 receptor in regulating human melanocyte pigmentation, proliferation, and survival. Ann. N.Y. Acad. Sci., 994:359-65.

Kanda N. and Watanabe S., (2003). 17beta-estradiol inhibits oxidative stress-induced apoptosis in keratinocytes by promoting Bcl-2 expression. J. Invest. Dermatol., 121(6): 1500-9.

Kanda N. and Watanabe S., (2005). Regulatory roles of sex hormones in cutaneous biology and immunology. J. Dermatol. Sci., 38(1):1-7.

Kanitakis J., Vassileva S., *et al*. (1998). Diagnostic immunohistochemistry of the skin : an illustrated text. London, Chapman & Hall Medical.

Karrer-Voegeli S., Rey F., Reymond M.J., Meuwly J.Y., Gaillard R.C., Gomez F., (2009). Androgen dependence of hirsutism, acne, and alopecia in women: retrospective analysis of 228 patients investigated for hyperandrogenism. Medicine (Baltimore), 88(1):32-45.

Klinge C.M., (2001). Estrogen receptor interaction with estrogen response elements. Nucleic Acids Res., 29(14):2905-19.

Kobayashi D., Nozawa T., Imai K., Nezu J., Tsuji A. and Tamai I., (2003). Involvement of human organic anion transporting polypeptide OATP-B (SLC21A9) in pH-dependent transport across intestinal apical membrane. J. Pharmacol. Exp. Ther., 306(2):703–708.

Koliwad S.K., Kuo T., Shipp L.E., Gray N.E., Backhed F., So A.Y., Farese R.V. Jr., Wang J.C., (2009). Angiopoietin-like 4 (ANGPTL4, fasting-induced adipose factor) is a direct glucocorticoid receptor target and participates in glucocorticoid-regulated triglyceride metabolism. J. Biol. Chem., 284(38):25593-601.

Kollias N., (1995). The physical basis of skin color and its evaluation. Clin. Dermatol., 13:361–67.

König J., Cui Y., Nies A.T. and Keppler D., (2000). A novel human organic anion transporting polypeptide localized to the basolateral hepatocyte membrane. Am. J. Physiol. Gastrointest. Liver Physiol., 278(1):G156–G164.

Kousteni S., Bellido T., Plotkin L.I., O'Brien C.A., Bodenner D.L., Han L., Han K., DiGregorio G.B., Katzenellenbogen J.A., Katzenellenbogen B.S., Roberson P.K., Weinstein R.S., Jilka R.L., Manolagas S.C., (2001). Nongenotropic, Sex-nonspecific signaling through the estrogen or androgen receptors: dissociation from transcriptional activity. Cell, 104:719–730.

Krause K. and Foitzik K., (2006). Biology of the hair follicle: the basics. Semin. Cutan. Med. Surg., 25(1):2-10.

Krupnik V.E., Sharp J.D., Jiang C., Robison K., Chickering T.W., Amaravadi L., Brown D.E., Guyot D., Mays G., Leiby K., Chang B., Duong T., Goodearl A.D., Gearing D.P., Sokol S.Y., McCarthy S.A., (1999). Functional and structural diversity of the human Dickkopf gene family. Gene, 238(2):301-13.

Kullak-Ublick G.A., Ismair M.G., Stieger B., Landmann L., Huber R., Pizzagalli F., Fattinger K., Meier P.J. and Hagenbuch B., (2001). Organic anion-transporting polypeptide B (OATP-B) and its functional comparison with three other OATPs of human liver. Gastroenterology, 120:(2):525–533.

Kwack M.H., Sung Y.K., Chung E.J., Im S.U., Ahn J.S., Kim M.K., Kim J.C., (2008). Dihydrotestosterone-inducible dickkopf 1 from balding dermal papilla cells causes apoptosis in follicular keratinocytes. J. Invest. Dermatol., 128(2):262-9.

Labrie F., (2004). Adrenal androgens and intracrinology. Semin. Reprod. Med., 22(4):299-309.

Labrie F., (2010). DHEA, important source of sex steroids in men and even more in women. Prog. Brain Res., 182:97-148.

Labrie F., Bélanger A., Luu-The V., Labrie C., Simard J., Cusan L., Gomez J.L., Candas B., (1998). DHEA and the intracrine formation of androgens and estrogens in peripheral target tissues: its role during aging. Steroids, 63(5-6):322-8.

Labrie F., Luu-The V., Bélanger A., Lin S.X., Simard J., Pelletier G., Labrie C., (2005). Is dehydroepiandrosterone a hormone? J. Endocrinol., 187(2):169-96.

Labrie F., Luu-the V., Labrie C., Bélanger A., Simard J., Lin S-X and Pelletier G., (2003). Endocrine and intracrine sources of androgens in women: inhibition of breast cancer and other roles of androgens and their precursor dehydroepiandrosterone. Endocrine Reviews, 24: 152–182.

Langan E.A. and Paus R., (2010). Female pattern hair loss: beyond an androgenic aetiology? Br. J. Dermatol., 163(5):1140-1.

Leowattana W., (2001). DHEA(S): the fountain of youth. J. Med. Assoc. Thai., 84 Suppl 2:S605-12.

Lephart E.D. and Simpson E.R., (1991). Assay of aromatase activity. Methods Enzymol., 206: 477–483.

Liegibel U.M., Sommer U., Boercsoek I., Hilscher U., Bierhaus A., Schweikert H.U., Nawroth P., Kasperk C., (2003). Androgen receptor isoforms AR-A and AR-B display functional differences in cultured human bone cells and genital skin fibroblasts. Steroids, 68(14):1179-87.

Liu D., Si H., Reynolds K.A., Zhen W., Jia Z. and Dillon J.S., (2007). Dehydroepiandrosterone protects vascular endothelial cells against apoptosis through a Galphai protein-dependent activation of phosphatidylinositol 3-kinase/Akt and regulation of antiapoptotic Bcl-2 expression. Endocrinology, 148:3068–3076.

Liu S. and Yamauchi H., (2008). Different patterns of 5alpha-reductase expression, cellular distribution, and testosterone metabolism in human follicular dermal papilla cells. Biochem. Biophys. Res. Commun. 368(4):858-64.

Lowry O.H., Rosebrough N.J., Farr A.L., Randall R.J., (1951). Protein measurement with the Folin phenol reagent. J. Biol. Chem., 193(1):265-75.

Lubahn D.B., Joseph D.R., Sullivan P.M., Willard H.F., French F.S., Wilson E.M., (1988). Cloning of human androgen receptor complementary DNA and localization to the X chromosome. Science, 240(4850):327-30.

Luu-The V., Bélanger A., Labrie F., (2008). Androgen biosynthetic pathways in the human prostate. Best Pract. Res. Clin. Endocrinol. Metab., 22(2):207-21.

Lynn B., (1991). Cutaneous sensation. See Goldsmith (1991), 779–815.

Manolagas S.C., Kousteni S., Chen J.R., Schuller M., Plotkin L., Bellido T., (2004). Kinase-mediated transcription, activators of nongenotropic estrogen-like signaling (ANGELS), and osteoporosis: a different perspective on the HRT dilemma. Kidney Int Suppl., 91:S41-9.

Marks R. 1991. Mechanical properties of the skin. See Goldsmith, (1991).

Matthews J. and Gustafsson J.A., (2003). Estrogen signaling: a subtle balance between ER alpha and ER beta. Mol. Interv., 3(5):281-92.

McClellan K.J. and Markham A., (1999). Finasteride: a review of its use in male pattern hair loss. Drugs, 57(1):111-26.

Mendelsohn M.E. and Karas R.H., (1999). The protective effects of estrogen on the cardiovascular system. N. Engl. J. Med., 340(23):1801-11.

Merlo S., Frasca G., Canonico P.L., Sortino M.A., (2009). Differential involvement of estrogen receptor alpha and estrogen receptor beta in the healing promoting effect of estrogen in human keratinocytes. J. Endocrinol., 200(2):189-97.

Mesiano S., Chan E.G., Fitter J.T., Kwek K., Yeo G., Smith R., (2002). Progesterone withdrawal and estrogen activation in human parturition are coordinated by progesterone receptor A expression. J. Clin. Endocrinol. Metab., 87:2924–2930.

Mestayer C., Berthaut I., Portois M.C., Wright F., Kuttenn F., Mowszowicz I., Mauvais-Jarvis P., (1996). Predominant expression of 5 alpha-reductase type 1 in pubic skin from normal subjects and hirsute patients. J. Clin. Endocrinol. Metab., 81(5):1989-93.

Midwood K.S., Williams L.V., Schwarzbauer J.E., (2004). Tissue repair and the dynamics of the extracellular matrix. Int. J. Biochem. Cell Biol., 36(6):1031-7.

Miller W.L., (1988). Molecular biology of steroid hormone synthesis. Endocr. Rev., 9: 295-318.

Miller W.L., Auchus R.J., Geller D.H., (1997). The regulation of 17,20 lyase activity. Steroids, 62(1):133-42.

Mills S.J., Ashworth J.J., Gilliver S.C., Hardman M.J., Ashcroft G.S., (2005). The sex steroid precursor DHEA accelerates cutaneous wound healing via the estrogen receptors. J. Invest. Dermatol., 125(5):1053-62.

Mimeault M. and Batra S.K., (2006). Recent advances on multiple tumorigenic cascades involved in prostatic cancer progression and targeting therapies. Carcinogenesis, 27(1):1-22.

Moggs J.G., Deavall D.G., Orphanides G., (2003). Sex steroids, ANGELS and osteoporosis. Bioessays, 25(3):195-9.

Morales D.E., McGowan K.A., Grant D.S., Maheshwari S., Bhartiya D., Cid M.C., Kleinman H.K., Schnaper H.W., (1995). Estrogen promotes angiogenic activity in human umbilical vein endothelial cells in vitro and in a murine model. Circulation, 91(3): 755-63.

Moreno-Cuevas J.E. and Sirbasku D.A., (2000). Estrogen mitogenic action. III. is phenol red a "red herring"? In Vitro Cell Dev. Biol. Anim., 36(7):447-64.

Morgan B.A., (2006). Upending the hair follicle. Nat. Genet., 38(3):273-4.

Nagase H. and Woessner J.F., (1999). Matrix metalloproteinases. J. Biol. Chem., 274(31): 21491-4.

Nadiminty N., Chun .JY., Lou W., Lin X., Gao A.C., (2008). NF-kappaB2/p52 enhances androgen-independent growth of human LNCaP cells via protection from apoptotic cell death and cell cycle arrest induced by androgen-deprivation. Prostate, 68(16):1725-33.

Nadiminty N., Dutt S., Tepper C., Gao A.C., (2010a). Microarray analysis reveals potential target genes of NF-kappaB2/p52 in LNCaP prostate cancer cells. Prostate, 70(3):276-87.

Nadiminty N., Lou W., Sun M., Chen J., Yue J., Kung H.J., Evans C.P., Zhou Q., Gao A.C., (2010b). Aberrant activation of the androgen receptor by NF-kappaB2/p52 in prostate cancer cells. Cancer Res., 70(8):3309-19.

Nelson L., (2005). The role of oestrogens in skin.

Németh A.H., Gallen I.W., Crocker M., Levy E., Maher E., (2002). Klinefelter-like phenotype and primary infertility in a male with a paracentric Xq inversion. J. Med. Genet., 39(6):E28.

Nestle F.O., Di Meglio P., Qin J.Z., Nickoloff B.J., (2009). Skin immune sentinels in health and disease. Nat. Rev. Immunol., 9(10):679-91.

Oguchi M., Sagara J., Matsumoto K., Saida T., Taniguchi S., (2002). Expression of lamins depends on epidermal differentiation and transformation. Br. J. Dermatol., 147(5):853-8.

Oh D.M. and Phillips T.J., (2006). Sex Hormones and Wound Healing. Wounds, 18 (1): 8–18.

Ohnemus U., Uenalan M., Inzunza J., Gustafsson J.A., Paus R., (2006). The hair follicle as an estrogen target and source. Endocr. Rev., 27(6):677-706.

Ohyama M., (2007). Hair follicle bulge: a fascinating reservoir of epithelial stem cells. J. Dermatol. Sci., 46(2):81-9.

Pandey A.V. and Miller W.L., (2005). Regulation of 17,20 lyase activity by cytochrome b5 and by serine phosphorylation of P450c17. J. Biol. Chem., 280(14):13265-71.

Parker K.L. and Schimmer B.P., (1997). Steroidogenic factor 1: A key determinant of endocrine development and function. Endocrine Rev., 18: 361–377.

Paus R., (2007). Frontiers in the (neuro-)endocrine controls of hair growth. J. Investig. Dermatol. Symp. Proc., 12(2):20-2.

Payne A.H. and Hales D.B., (2004). Overview of steroidogenic enzymes in the pathway from cholesterol to active steroid hormones. Endocr. Rev. 25:947–970.

Pelletier G. and Ren L., (2004). Localization of sex steroid receptors in human skin. Histol. Histopathol., 19(2): 629-36.

Pierce G.F., Mustoe T.A., Altrock B.W., Deuel T.F., Thomason A., (1991). Role of platelet-derived growth factor in wound healing. J. Cell Biochem., 45(4): 319-26.

Pizzagalli F., Varga Z., Huber R.D., Folkers G., Meier P.J. and St-Pierre M.V., (2003). Identification of steroid sulfate transport processes in the human mammary gland. J. Clin. Endocrinol. Metab., 88(8):3902–3912.

Pollard T.D. and Borisy G.G., (2003). Cellular motility driven by assembly and disassembly of actin filaments. Cell, 112(4):453-65.

Proksch E., Brandner J.M., Jensen J.M., (2008). The skin: an indispensable barrier. Exp Dermatol., 17(12):1063-72.

Przybylski M., (2009). A review of the current research on the role of bFGF and VEGF in angiogenesis. J. Wound Care, 18(12):516-9.

Qin L., Wu X., Block M.L., Liu Y., Breese G.R., Hong J.S., Knapp D.J., Crews F.T., (2007). Systemic LPS causes chronic neuroinflammation and progressive neurodegeneration. Glia, 55:453–462.

Ralph M. Tru¨eb, (2002). Molecular mechanisms of androgenetic alopecia. Experimental Gerontology, 37 981–990.

Randall V.A., (2008). Androgens and hair growth. Dermatol. Ther., 21(5):314-28.

Randall V.A., Thornton M.J., Hamada K., Redfern C.P.F., Nutbrown M. and Ebling F.J.G., (1991). Androgens and the hair follicle: cultured human dermal papilla cells as a model system. Ann. N. Y. Acad. Sci., 642:355–375.

Reed M.J., Purohit A., Woo L.W., Newman S.P., Potter B.V., (2005). Steroid sulfatase: molecular biology, regulation, and inhibition. Endocr. Rev., 26(2):171-202.

Reed M.J., Purohit A., Woo L.W.L., Potter B.V.L., (2008). Steroid sulfatase inhibitors for the tropical treatment of skin disorders. Drugs Fut., 33(7): 597.

Rennekampff H.O., Hansbrough J.F., Woods V. Jr., Doré C., Kiessig V., Schröder J.M., (1997). Role of melanoma growth stimulatory activity (MGSA/gro) on keratinocyte function in wound healing. Arch. Dermatol. Res., 289: 204-212.

Rink J.D., Simpson E.R., Barnard J.J., Bulun S.E., (1996). Cellular characterization of adipose tissue from various body sites of women. J. Clin. Endocrinol. Metab., 81(7):2443-7.

Risau W., (1997). Mechanisms of angiogenesis. Nature, 386(6626):671-4.

Rogers G. and Koike K., (2009). Laser capture microscopy in a study of expression of structural proteins in the cuticle cells of human hair. Exp. Dermatol., 18(6):541-7.

Samson M., Labrie F., Luu-The V., (2005). Inhibition of human-type 1 3beta-hydroxysteroid deshydrogenase/Delta(5)-Delta(4)-isomerase expression using siRNA. J. Steroid. Biochem. Mol. Biol., 94(1-3):253-7.

Sanderson J.T., (2006). The steroid hormone biosynthesis pathway as a target for endocrine-disrupting chemicals. Toxicol. Sci., 94(1):3-21.

Santoro M.M. and Gaudino G., (2005). Cellular and molecular facets of keratinocyte reepithelization during wound healing. Exp. Cell Res., 304(1): 274-86.

Sato T., Kirimura Y., Mori Y., (1997). The co-culture of dermal fibroblasts with human epidermal keratinocytes induces increased prostaglandin E2 production and cyclooxygenase 2 activity in fibroblasts. J. Invest. Dermatol., 109(3):334-9.

Sawaya M.E. and Price V.H., (1997). Different levels of 5alpha-reductase type I and II, aromatase, and androgen receptor in hair follicles of women and men with androgenetic alopecia. J. Invest. Dermatol., 109:296–300.

Schiffer R., Neis M., Höller D., Rodríguez F., Geier A., Gartung C., Lammert F., Dreuw A., Zwadlo-Klarwasser G., Merk H., Jugert F., Baron J.M., (2003). Active influx transport is mediated by members of the organic anion transporting polypeptide family in human epidermal keratinocytes. J. Invest. Dermatol., 120(2):285-91.

Schneider M.R., Schmidt-Ullrich R., Paus R., (2009). The hair follicle as a dynamic miniorgan. Curr. Biol., 19(3):R132-42.

Schneikert J., Peterziel H., Defossez P.A., Klocker H., Launoit Y., Cato A.C., (1996). Androgen receptor-Ets protein interaction is a novel mechanism for steroid hormone-mediated down-modulation of matrix metalloproteinase expression. J. Biol. Chem., 271: 23907-23913.

Shah M.G. and Maibach H.I., (2001). Estrogen and skin. An overview. Am. J. Clin. Dermatol., 2(3):143-50.

Shea C.R and Parrish J.A., (1991). Nonionizing radiation and the skin. See Goldsmith (1991), 910–27.

Sheetz M.P., (2001). Cell control by membrane-cytoskeleton adhesion. Nat. Rev. Mol. Cell. Biol., 2(5):392-6.

Shephard P., Martin G., Smola-Hess S., Brunner G., Krieg T., Smola H., (2004). Myofibroblast differentiation is induced in keratinocyte-fibroblast co-cultures and is antagonistically regulated by endogenous transforming growth factor-beta and interleukin-1. Am. J Pathol., 164(6):2055-66.

Shibasaki M. and Crandall C.G., (2010). Mechanisms and controllers of eccrine sweating in humans. Front. Biosci. (Schol. Ed.), 2:685-96.

Simard J., Ricketts M.L., Gingras S., Soucy P., Feltus F.A., Melner M.H., (2005). Molecular biology of the 3beta-hydroxysteroid dehydrogenase/delta5-delta4 isomerase gene family. Endocr. Rev., 26(4):525-82.

Simoncini T. and Genazzani A.R., (2003). Non-genomic actions of sex steroid hormones. Eur. J. Endocrinol., 148(3):281-92.

Simoncini T., Scorticati C., Mannella P., Fadiel A.,. Giretti M.S, Fu X.D., Baldacci C., Garibaldi S., Caruso A., Fornari L., Naftolin F. and Genazzani A.R., (2006). Estrogen Receptor αInteracts with Gα13 to Drive Actin Remodeling and Endothelial Cell Migration via the RhoA/Rho Kinase/Moesin Pathway. Mol. Endocrinol., 20 (8): 1756-1771.

Soderholm J. and Heald R., (2005). Scratch n' screen for inhibitors of cell migration. Chem. Biol., 12(3):263-5.

Sparkes R.S., Klisak I., Miller W.L., (1991). Regional mapping of genes encoding human steroidogenic enzymes: P450scc to 15q23-q24, adrenodoxin to 11q22; adrenodoxin reductase to 17q24-q25; and P450c17 to 10q24-q25. DNA Cell Biol., 10(5):359-65.

Spearman RIC, (1977). Hair follicle development, cyclical changes and hair form. In: Jarrett A (ed) The physiology and pathophysiology of the skin, vol 4 (The hair follicle). Academic Press, New York, 1255–1292.

Stadelmann W.K., Digenis A.G., Tobin G.R., (1998). Physiology and healing dynamics of chronic cutaneous wounds. Am. J. Surg., 176(2A Suppl):26S-38S.

Stanway S.J., Delavault P., Purohit A., Woo L.W., Thurieau C., Potter B.V., Reed M.J., (2007). Steroid sulfatase: a new target for the endocrine therapy of breast cancer. Oncologist., 12(4):370-4.

Steers W.D., (2001). 5alpha-reductase activity in the prostate. Urology, 58(6 Suppl 1):17-24.

Steckelbroeck S., Nassen A., Ugele B., Ludwig M., Watzka M., Reissinger A., Clusmann H., Lutjohann D., Siekmann L., Klingmuller D. and Hans V.H., (2004). Steroid sulfatase (STS) expression in the human temporal lobe: enzyme activity, mRNA expression and immunohistochemistry study. J. Neurochem., 89(2):403–417.

Stevenson S., Sharpe D.T., Thornton M.J., (2009). Effects of oestrogen agonists on human dermal fibroblasts in an in vitro wounding assay. Exp. Dermatol., 18(11):988-90.

Stoitzner P., Sparber F., Tripp C.H., (2010). Langerhans cells as targets for immunotherapy against skin cancer. Immunol Cell Biol., 88(4):431-7.

St-Pierre M.V., Ugele B., Hagenbuch B., Meier P.J. and Stallmach T., (2002). Characterization of an anion-transporting polypeptide (OATP-B) in human placenta. J. Clin. Endocrinol. Metab., 87(4):1856–1863.

Sugiyama D., Kusuhara H., Shitara Y., Abe T., Meier P.J., Semine T., Envou H., Suzuki H. and Sugiyama Y., (2001). Characterization of the efflux transport of 17beta-estradiol-D-17beta-glucuronide from the brain across the blood–brain barrier. J. Pharmacol. Exp. Ther., 298(1):316–322.

Svenstrup B., Brünner N., Dombernowsky P., Nøhr I., Micic S., Bennett P., Spang-Thomsen M., (1990). Comparison of the effect of cortisol on aromatase activity and androgen metabolism in two human fibroblast cell lines derived from the same individual. J. Steroid. Biochem., 35(6):679-87.

Szpaderska A., Egozi E.I., Gamelli R.L., DiPietro L.A., (2003). The effect of thrombocytopenia on dermal wound healing. J. Invest. Dermatol., 120:1130–1137.

Takehara K., (2000). Growth regulation of skin fibroblasts. J. Dermatol. Sci., 24(1): S70-7.

Tamai I., Nezu J., Uchino H., Sai Y., Oku A., Shimane M., Tsuji A., (2000). Molecular identification and characterization of novel members of the human organic anion transporter (OATP) family. Biochem. Biophys. Res. Commun., 273(1):251-60.

Taylor A.H., Pringle J.H., Bell S.C., Al-Azzawi F., (2001). Specific inhibition of estrogen receptor alpha function by antisense oligodeoxyribonucleotides. Antisense Nucl. Acid. Drug Dev., 11:219–231.

Taylor S.C., (2002). Skin of color: biology, structure, function, and implications for dermatologic disease. J. Am. Acad. Dermatol., 46:S41–62.

Thiboutot D., Jabara S., McAllister J.M., Sivarajah A., Gilliland K., Cong Z., Clawson G., (2003). Human skin is a steroidogenic tissue: steroidogenic enzymes and cofactors are expressed in epidermis, normal sebocytes, and an immortalized sebocyte cell line (SEB-1). J. Invest. Dermatol., 120(6):905-14.

Thomas L.N., Douglas R.C., Lazier C.B., Too C.K., Rittmaster R.S., Tindall D.J., (2008). Type 1 and type 2 5alpha-reductase expression in the development and progression of prostate cancer. Eur. Urol., 53(2):244-52.

Thomson M., (2003). Does cholesterol use the mitochondrial contact site as a conduit to the steroidogenic pathway? Bioessays, 25(3):252-8.

Thornton M.J., Nelson L.D., Taylor A.H., Birch M.P., Laing I., Messenger A.G., (2006). The modulation of aromatase and estrogen receptor alpha in cultured human dermal papilla cells by dexamethasone: a novel mechanism for selective action of estrogen via estrogen receptor beta? J. Invest. Dermatol., 126(9):2010-8.

Thornton M.J., Taylor A.H., Mulligan K., Al-Azzawi F., Lyon C.C., O'Driscoll J., Messenger A.G., (2003). Estrogen receptor beta (ERb) is the predominant estrogen receptor in human scalp. Exp. Dermatol., 12(2): 181-90.

Tilli C.M., Ramaekers F.C., Broers J.L., Hutchison C.J., Neumann H.A., (2003). Lamin expression in normal human skin, actinic keratosis, squamous cell carcinoma and basal cell carcinoma. Br. J. Dermatol., 148: 102-9.

Tonnesen M.G., Feng X., Clark R.A., (2000). Angiogenesis in wound healing. J. Investig. Dermatol. Symp. Proc., 5(1): 40-6.

Trüeb R.M., (2004). Finasteride treatment of patterned hair loss in normoandrogenic postmenopausal women. Dermatology, 209(3):202-7 Swiss Trichology Study Group.

Tsukita S. and Yonemura S., (1999). Cortical actin organization: lessons from ERM (ezrin/radixin/moesin) proteins. J. Biol. Chem., 274(49):34507-10.

Verdier-Sevrain S., Yaar M., Cantatore J., Traish A., Gilchrest B.A., (2004). Estradiol induces proliferation of keratinocytes via a receptor mediated mechanism. Faseb J., 18(11): 1252-4.

Watanabe M., Ohno S., Nakajin S., (2005). Forskolin and dexamethasone synergistically induce aromatase (CYP19) expression in the human osteoblastic cell line SV-HFO. Eur. J. Endocrinol., 152(4):619-24.

Watanabe M., Simpson E.R., Pathirage N., Nakajin S., Clyne C.D., (2004). Aromatase expression in the human fetal osteoblastic cell line SV-HFO. J. Mol. Endocrinol, 32(2):533-45.

Welboren W.J., Stunnenberg H.G., Sweep F.C., Span P.N., (2007). Identifying estrogen receptor target genes. Mol. Oncol., 1(2):138-43.

Williams M.R., Dawood T., Ling S., Dai A., Lew R., Myles K., Funder J.W., Sudhir K., Komesaroff P.A., (2004). Dehydroepiandrosterone increases endothelial cell proliferation in vitro and improves endothelial function in vivo by mechanisms independent of androgen and estrogen receptors. J. Clin. Endocrinol. Metab., 89(9): 4708-15.

Williams M.R., Ling S., Hashimura K., Dai A., Li H., Liu J.P., Funder J.W., Sudhir K., Komesaroff P.A., (2002). Dehydroepiandrosterone inhibits human vascular smooth muscle cell proliferation independent of ARs and ERs. J. Clin. Endocrinol. Metab., 87(1): 176-81.

Wilson C.M. and McPhaul M.J., (1996). A and B forms of the androgen receptor are expressed in a variety of human tissues. Mol. Cell Endocrinol., 120(1):51-7.

Wood E.J. and Bladon P.T., (1985). The Human Skin. London, Edward Arnold.

Xin S., Liu W., Cheng B., (2009). Biological effects of estrogen on capillary vessel formation in wound healing. Zhongguo Xiu Fu Chong Jian Wai Ke Za Zhi., 23(12):1502-5. [Abstract].

Yarrow J.C., Perlman Z.E., Westwood N.J., Mitchison T.J., (2004). A high-throughput cell migration assay using scratch wound healing, a comparison of image-based readout methods. BMC Biotechnol., 4:21.

Zaja-Milatovic S. and Richmond A., (2008). CXC chemokines and their receptors: a case for a significant biological role in cutaneous wound healing. Histol. Histopathol., 23(11):1399-407.

Zhang J., Xu L.G., Han K.J., Shu H.B., (2004). Identification of a ZU5 and death domain-containing inhibitor of NF-kappaB. J. Biol. Chem., 279(17):17819-25.

Zouboulis C.C., (2000). Human skin: an independent peripheral endocrin organ. Horm. Res., 54: 230-242.

Zouboulis C.C., (2004). The human skin as a hormone target and an endocrine gland, Horm., 3:9-26.

Appendices

Appendix 1. Reagents for RNA extraction

(1) Extraction by TRIzol

- TRIzol (Invitrogen)
- Chloroform
- Isopropanol
- 70% ethanol
- Rnase free water

(2) Extraction by column

- ß-mercaptoethanol
- 95% ethanol
- RLT lysis buffer (QIAGEN)
- RPE wash buffer (QIAGEN)
- Rnase free Water

Appendix 2. Reagents for DNA extraction from agarose gel

- Agarose gel loading dye (6x): 30% glycerol, 0.2% bromophenol blue, 0.2% xylene cyanol
- PBS: 7.5 mM Na_2HPO_4; 2.5 mM NaH_2PO_4; 145 mM NaCl
- TAE-buffer (10X): 400mM Tris-Acetate; 11.4 ml glacial acetic acid; 10mM EDTA
- ADB buffer (ZYMO RESEARCH)
- DNA Wash buffer (ZYMO RESEARCH)
- Nuclease free water

Appendix 3. Reagents for Cloning

- LB broth medium (Sigma)

  Tryptone (pancreatic digest of casein) 10 g/L; Yeast extract 5 g/L; NaCl 5 g/L

- LB Agar medium (Sigma)

  Tryptone (pancreatic digest of casein) 10 g/L; Yeast extract 5 g/L; NaCl 5 g/L;

  Agar 15 g/L

- S.O.C. medium (Invitrogen)

  2% tryptone; 0.5% yeast extract; 10 mM sodium chloride; 2.5 mM potassium chloride; 10 mM magnesium chloride; 10 mM magnesium sulfate; 20 mM glucose

Appendix 4. Reagents for DC Protein assay

The following were required for the quantification of protein in cell extracts:

(1) Bovine Serum Albumin (BSA) stock solution

- RIPA buffer (Sigma)
  150 mM NaCl; 1.0% IGEPAL® CA-630; 0.5% sodium deoxycholate; 0.1% SDS;
  50 mM Tris pH 8.0
- Bovine Serum Albumin (Sigma) 0.1 g (final concentration of 10 mg/ml)

(2) Protein Standards (Bovine Serum Albumin)

- Blank: 1000 µl RIPA buffer
- 10 µg/ml: 99 µl + 1 µl BSA stock
- 20 µg/ml: 98 µl + 2 µl BSA stock
- 40 µg/ml: 96 µl + 4 µl BSA stock
- 60 µg/ml: 94 µl + 6 µl BSA stock
- 80 µg/ml: 92 µl + 8 µl BSA stock
- 100 µg/ml: 90 µl + 10 µl BSA stock
- 200 µg/ml: 80 µl + 20 µl BSA stock

(3) Reagent A'

- Reagent A (Bio Rad) 2 ml
- Reagent S (Bio Rad) 40 µl

(4) Reagent B

- Reagent B (Bio Rad) 200 µl

Appendix 5. Human skin samples used for RT-PCR

Sample	Skin	Age	Sex
1	Abdominal	35	F
2	Abdominal	38	F
3	Abdominal	N.D.	F
4	Thigh	80	F

Table 42. Skin biopsies supplied by cutech s.r.l. and clinic of Orthopoedic of Padova, Italy. Samples were used for the total RNA extraction and for the investigation of the mRNA expression of steroidogenic genes by RT-PCR. N.D.: not detected.

Appendix 6. Human hair follicle samples used for RT-PCR and gene array expression

Sample	Hair follicle	Age	Sex
1	Frontotemporal scalp	34	F
2	Frontotemporal scalp	55	F
3	Frontotemporal scalp	51	F
4	Frontotemporal scalp	43	F
5	Frontotemporal scalp	40	F

Table 43. HFs (n=21 per donor) supplied by Cutech s.r.l., Padova, Italy. Samples were used for the total RNA extraction and for the investigation of the mRNA expression of steroidogenic genes by RT-PCR. The sample n. 5 was used for the gene expression analysis.

Appendix 7. Human epidermal keratinocytes samples used for gene array expression and RT-PCR analysis

Sample	Keratinocytes	Age	Sex
1	Abdominal	N.D.	F
2	Abdominal	N.D.	F
3	Facial	56	F
4	Facial	38	F

Table 44. Established human primary EKs supplied by cutech s.r.l., Padova, Italy. All samples were used for the total RNA extraction. Only cells established from face were used for the array gene expression and RT-PCR analysis. N.D.: not detected.

Appendix 8. Human skin samples used for RT-PCR, migration assay and analysis of the aromatase activity

Sample	Skin	Age	Sex	Dermal fibroblasts	Epidermal keratinocytes	Dermal sheath cells	Dermal papilla cells
1	Facial	55	F	✓		✓	✓
2	Facial	59	F	✓		✓	✓
3	Facial	N.D.	F	✓	✓	✓	✓
4	Facial	47	F	✓	✓	✓	✓
5	Facial	63	F	✓	✓	✓	✓
6	Facial	40	M	✓	✓		
7	Breast	17	F	✓	✓		
8	Abdominal	42	F	✓	✓		

Table 45. Samples supplied in University of Bradford, UK. All samples were used to establish primary cells and for RT-PCR analysis. N.D.: not detected.